

The Role of Secondary Metabolites in Plant-Associated Microbial Communities

Dissertation

der Mathematisch-Naturwissenschaftlichen Fakultät

der Eberhard Karls Universität Tübingen

zur Erlangung des Grades eines

Doktors der Naturwissenschaften

(Dr. rer. nat.)

vorgelegt von

Franziska Höhn

aus Reutlingen

Tübingen

2024

Gedruckt mit Genehmigung der Mathematisch-Naturwissenschaftlichen Fakultät der
Eberhard Karls Universität Tübingen.

Tag der mündlichen Qualifikation:

19.12.2024

Dekan:

Prof. Dr. Thilo Stehle

1. Berichterstatter/-in:

Prof. Dr. Nadine Ziemert

2. Berichterstatter/-in:

Prof. Dr. Hannes Link

TABLE OF CONTENT

TABLE OF CONTENT	II
ACKNOWLEDGEMENTS	IV
ABSTRACT	VI
ZUSAMMENFASSUNG	VII
ABBREVIATIONS	VIII
THESIS - INTRODUCTION	1
The plant microbiome and its perspective for sustainable agriculture	1
Assembly of the plant microbiome from rhizosphere to phyllosphere.....	2
Microbial secondary metabolites and their potential to shape and stabilize plant microbiomes	
5	
How to investigate microbiome dynamics	8
Synthetic communities as model systems for microbe-microbe interaction research	9
The SynCom as model system to study the role of secondary metabolites in the <i>A. thaliana</i>	
leaf microbiome	10
INFORMATION ON THE MANUSCRIPTS	13
Manuscript 1: Strong Pairwise Interactions do not Drive Interactions in a Plant Leaf	
Associated Microbial Community	13
Manuscript 2: Identifying Potential Community-Driving Metabolites in a Microbial Plant Leaf	
associated community	13
MANUSCRIPT 1	14
Declarations on the Contribution of Co-Authors to the Manuscript.....	14
ABSTRACT	16
INTRODUCTION	16
MATERIALS AND METHODS	19
Microbial strains and SynCom assembly	19
Culture media and conditions	20
Sterile plants and plant spraying.....	20
Correlation network analysis.....	21
Cross streaking experiments	21
Genome mining	22

Pseudobactin identification and purification	22
Deletion Mutant creation.....	22
Pseudobactin interaction studies	23
Amplicon sequencing	24
RESULTS	26
DISCUSSION	35
Data Availability.....	39
REFERENCES.....	40
Acknowledgements	44
Author contribution	44
Competing Interests	45
SUPPLEMENTAL INFORMATION MANUSCRIPT 1	46
MANUSCRIPT 2	74
Declarations on the Contribution of Co-Authors to the Manuscript.....	74
Abstract.....	76
Introduction	76
Materials and Methods	78
Results and Discussion	84
Conclusion	105
Data Availability.....	107
References.....	107
Acknowledgements	113
SUPPLEMENTAL INFORMATION MANUSCRIPT 2	108
THESIS - DISCUSSION	119
The discovery of hub organisms and key metabolites in the SynCom	120
Antimicrobial metabolites might play a subordinate role in the SynCom	130
Limitations and perspectives of the project.....	132
THESIS- CONCLUSION.....	134
THESIS - BIBLIOGRAPHY	XI

ACKNOWLEDGEMENTS

I would love to express my biggest thanks to:

My supervisors Nadine, Heike and Eric for giving me the opportunity to create the present work, being there for me with their great advice and supporting me to become a real microbiologist. Thank you, Nadine, for the great work experience in your group and creating a wonderful group and working atmosphere. Thank you, Heike, for always having an open ear for me and helping me with your great knowledge. Thank you, Eric, for including me in your group and treating me as one of your own students.

The co- authors and collaboration partners

Daniel for his great knowledge and advice in non-targeted metabolomics. Thank you for the amazing collaboration on the project! Detective Chambers for solving the puzzle about the fluorescence of *P. koreensis* and catching pseudobactin. Paolo for measuring my samples and dealing with my mistakes even on his birthday! Vasvi for the help with the beautiful SynCom members and teaching me how to deal with plants. Caner for supporting me (bioinformatics noop) with his informatic skills and handling all my raw data. Elke for the great time we had together while walking through the amplicon sequencing pipeline and preparing a lot of material for me. Maryam for the spontaneous collaboration, the calculation of networks and the fantastic explanations on the science behind them. Hamed for his help with the very accurate data storage in the ARC.

My students Lara for creating the pseudobactin mutant very independently and giving me a great time working in the lab. I really enjoyed the time with you! Marina for helping me with alle the jobs which take to people to finish (which are a lot!). For your strength in dealing with frustration and hard situations (from failing experiments to mental support of PhD students). You are not only a great student I once worked with I rather found an amazing person which I never want to miss in my life. Chiara for taming *Methylobacterium*, which is beautiful but also a drama queen and the very fun time we hand together in the lab. Gina for supporting me during my last experiments and all the repetitions I needed to perform. You have been such a great help for me!

My groups the Ziemertlab for the support and help with any question, for the great working atmosphere and for the fun we had doing all the cool group activities! The group of Heike for the support in the group meeting, the nice chats we had and for inviting and integrating me to group activities. The Kemenlab for the great time I had while working in your labs and for the great support I experienced.

My funder the excellence cluster Controlling Microbes to Fight Infections (CMFI) funded by the DGE. Thank you for the opportunity to work in this fantastic project in which I experienced the possibility to participate with own ideas, a great level of esteem and a modern way of science communication.

And all the people which have accompanied me and which I met along the way of my PhD:

My family which always belief in me, support me and have an open ear for my problems. My parents for letting me know how proud they are no matter what I decide for my life. My grandparents, which have no clue about microbiology but were so interested in my work and always came up with great ideas. My sister for never letting me down and being there for me in situation where no one else was.

Davide for laughing, crying and being angry together. For the constant support and for giving me the feeling to be something special.

My lab family Jens, Alena, Dardan and Yvonne without whom I would have never finished my PhD. Thank you for the great time we had together, for sharing all problems, feelings, advice and gossip! You made the work so much fun, and you really are the best colleges and friends one can find!

My Stuttgarter Roadtrip family for bringing me back to the roots when research frustration was gaining the upper hand over my life. For being so open and tolerant people and for making everyone feeling comfortable around you all. And some of you for bringing me back to life.

All the helpful minds of the 10th floor Thomas for being the good soul of the 10th floor. Without you I wouldn't have finished my degree because I would still be searching a medium component in the chemical room. Aysun for the nice conversations we had and for dealing with all my stuff especially when calling the Personalabteilung was necessary. Andy for always telling a joke and all the ice cream. Herr and Frau Lemaire for the technical lab support.

My childhood friends Ame, Ela, Lu, Maike and Jones for happy free time activity and constantly asking: "What exactly are you doing again?". Special thanks to Maike for the mental support and good advice on how to deal with PhD stress. Especially for the idea of doing deep learning session. And special thanks to Ela for doing deep learning together for such a long time!

Linking Park and Rammstein for helping me set free my frustration on the way back home from failed experiments.

Maneskin for the jamming sessions in the car and making me happy before and after work.

ABSTRACT

Its positive impact on host plants makes the microbiome a promising platform for sustainable agriculture, which is urgently needed. By 2050, global food requirements are expected to increase by 70%, while climate change contributes to challenge crop production. To promote a healthy plant microbiome, develop probiotics and identify biocontrol agents, extensive knowledge about microbiome dynamics is needed. Synthetic communities enable the investigation of such dynamics in a less complex and stable model system. In my PhD project, a synthetic community (SynCom) from the *Arabidopsis thaliana* leaf was used as a model system to investigate microbe-microbe interactions and the role of secondary metabolites in shaping and stabilizing the community with the aim to identify hub organisms and key metabolites. In the first part of my PhD project, co-abundance networks of natural *A. thaliana* microbiomes were compared to *in vitro* interactions of SynCom members. Findings revealed more positive correlations in nature-related networks compared to *in vitro* pairwise interactions. By using pseudobactin as an example of a potent antimicrobial compound detected in pairwise interactions, the impact of such metabolites on the SynCom composition was investigated. Pseudobactin was found to have no effect on the community composition *in planta* although its producer *Pseudomonas koreensis* was highly abundant. It was further found that the strong pairwise inhibitor *Bacillus altitudinis* was a low abundant strain in the community. The findings led to the conclusion that antimicrobials might not give the producer a colonization advantage in the community and might play a subordinate role in a community context. By using a non-targeted metabolomics approach in the second part of the work, the aim was to identify metabolites with the potential to shape the community composition. It was based on the hypothesis that metabolites important for the SynCom are highly present in the community. By comparing single strain samples to SynCom co-cultures, production upregulated and activated compounds in the community were identified. Among them, the vitamin biotin and the cytokinin trans-zeatin were identified in significantly higher concentrations in the community compared to single strain samples. Additionally, biotin showed a growth promotive effect on *Bacillus altitudinis*, suggesting that a metabolite involved in microbe-microbe interactions was successfully identified with the workflow and that cross-feeding might be a driving force of SynCom dynamics. The results of this PhD thesis contribute to the understanding of mechanisms that shape and stabilize synthetic communities and highlight possible strategies for sustainable plant treatments.

ZUSAMMENFASSUNG

Die positiven Eigenschaften des Pflanzenmikrobioms auf ihren Wirt machen es zu einer vielversprechenden Plattform für eine nachhaltige Landwirtschaft. Bis 2050 wird der weltweite Nahrungsmittelbedarf voraussichtlich um 70 % steigen, während der Klimawandel die landwirtschaftliche Produktion erheblich beeinträchtigt. Um ein gesundes Pflanzenmikrobiom zu fördern, Probiotika zu entwickeln und Mikroorganismen sowie chemische Stoffe für Pflanzentherapien zu identifizieren, ist ein umfassendes Verständnis der grundlegenden Dynamiken in Mikrobiomen notwendig. Synthetische Gemeinschaften (SynComs) bieten ein vereinfachtes und stabiles Modellsystem zur Untersuchung dieser Dynamiken.

In der vorliegenden Arbeit wurde eine SynCom aus der Phyllosphäre von *Arabidopsis thaliana* verwendet, um mikrobielle Interaktionen zu identifizieren und den Einfluss von Sekundär-Metaboliten auf solche Interaktionen zu untersuchen. Ziel der Forschung war es, zentrale Organismen und Schlüsselmetabolite zu identifizieren, die an diesen Interaktionen beteiligt sind. Durch den Vergleich von co-abundance-Netzwerken natürlicher *A. thaliana*-Mikrobiom mit *in vitro*-Interaktionen der SynCom-Mitglieder zeigte sich, dass natürliche Netzwerke mehr positive Korrelationen aufweisen als *in vitro*-Paarinteraktionen. Pseudobactin, produziert von *Pseudomonas koreensis*, wurde *in vitro* als antimikrobielles Siderophore identifiziert, zeigte *in planta* jedoch keinen Einfluss auf die Zusammensetzung der SynCom. Ebenso wurde *Bacillus altitudinis* als Inhibitor zahlreicher SynCom-Stämme identifiziert, war jedoch nur in geringer Menge in der Gemeinschaft vertreten. Diese Ergebnisse legen nahe, dass antimikrobielle Substanzen dem Produzenten keinen signifikanten Vorteil bei der Kolonisierung in der SynCom bieten und in der Gemeinschaftsdynamik eine untergeordnete Rolle spielen.

Ein non-targeted metabolomics-Ansatz wurde verwendet, um weitere chemische Stoffe zu identifizieren, die das Potenzial haben, die Zusammensetzung der SynCom zu beeinflussen. Dabei wurde vermutet, dass Metabolite, die in höheren Konzentrationen in SynCom-Co-Kulturen vorkamen als in Kulturen einzelner Stämme, eine wichtige Rolle für die Gemeinschaft spielen könnten. Das Vitamin Biotin und das Cytokinin Trans-Zeatin wurden in signifikant höheren Konzentrationen in der Gemeinschaft gefunden. Biotin förderte das Wachstum von *Bacillus altitudinis*, was darauf hinweist, dass Cross-Feeding eine wesentliche Rolle in der SynCom könnte. Diese Erkenntnisse tragen zum Verständnis der Mechanismen bei, die synthetische Gemeinschaften formen und stabilisieren, und heben mögliche Strategien für nachhaltige Pflanzenbehandlungen hervor.

ABBREVIATIONS

<i>A. thaliana</i>	<i>Arabidopsis thaliana</i>
ADAP chromatogram	automated data analysis pipeline chromatogram
Asp	aspartic acid
ASV	Amplicon sequence variant
BGC	biosynthetic gene cluster
CK /CKs	cytokinin / cytokinins
cor	correlation index
d	days
e.g.	exempli gratia → for example
EPS	exopolysaccharides
ES	External supplements
FA	formic acid
FBMN	feature-based molecular networking
Fig.	figure
fw	forward
HCN	Hydrogen cyanide
HPLC-MS	high-performance liquid chromatography-mass spectrometry
MALDI	matrix-assisted laser desorption/ionization
MeOH	methanol
NA	nutrient agar
NB	nutrient broth
NMR	nuclear magnetic resonance
NRP	non-ribosomal peptide
NRPS	non-ribosomal peptide synthetase
OTU	operational taxonomic unit
p.	page
PCoA	principal coordinate analysis
PCR	polymerase chain reaction
PDA	potato-dextrose agar
PDB	potato-dextrose broth
PK	polyketide
PKS	Polyketide synthase

ppm	parts per million
RiPPs	ribosomally synthesized and post translationally modified peptide
rpm	rounds per minute
RT	room temperature
rt	retention time
rv	reverse
sp.	species
spp.	species (plural)
SynCom	synthetic community
T	timepoint
TFA	trifluoroacetic acid
tZ	trans-zeatin
UHPLC-MS/MS	ultra-high-performance liquid chromatography-tandem mass spectrometry.
USI	universal spectrum identifier
UV	ultraviolet
WT	wild type

THESIS - INTRODUCTION

THE PLANT MICROBIOME AND ITS PERSPECTIVE FOR SUSTAINABLE AGRICULTURE

As the human gut, the skin or soil, plants are colonized by their own microbiome [1-4]. The plant and its colonizing microbes build up a co-evolved ecosystem, acting as a unity. Due to their close relationship, the plant and its microbiome are known as the plant holobiont [5, 6]. Carrying a healthy microbiome has several advantages for the plant. It helps in nutrient acquisition, increases the tolerance to abiotic stress and promotes the plant's resistance to pathogens [7-10]. In return, the microbes have a niche to colonize and can utilize metabolites secreted by the plant [11, 12]. Studies have shown that several members of the microbiome are involved in nitrogen and phosphate fixation, produce specific sugars or enhance nutrient uptake by the plant [5]. Others investigated the tolerance of plants against salinity, drought, heavy-metal stress or temperature changes and found a significant improvement in plant growth in the presence of a healthy microbiome [7]. The improved resistance to pathogens of plants could be related to the production of antimicrobials [13, 14], the competition for space [15] and the stimulation of the host immune system by phytohormone production [16, 17].

The various positive effects of plant colonizers on its host, highlight the plant microbiome as promising platform for plant treatments. Such methods are urgently needed since sustainable agriculture will get more challenging in the future. By 2050 the global food requirement will increase by 70 % due to an increasing world population and the use of biomass for energy and feed industry [18, 19]. At the same time, climate change contributes to challenge farmers to maintain and ensure a seamless food supply. The changing weather conditions including more and longer drought periods, heavy rain falls or increasing temperatures will lead to reduced plant fitness, soil leaching or higher plant disease rates and therefore immense crop losses [19, 20]. Since our impact on the environment is already enormous, sensitive and sustainable ways for plant growth promotion need to be developed. Therefore, the natural plant microbiome is suggested as a platform for sustainable plant treatments [21, 22]. Research efforts have already achieved some successes in engineering the plant microbiome in positive ways. Promising techniques ranging from indirect methods by changing the soil conditions with attractants for the assembly of specific beneficial organisms to direct methods by the introduction of such single organisms or whole communities into the plant microbiome [9, 23]. Great achievements have already been made regarding the use of biocontrol agents to control infections and probiotics to promote plant growth. Successful introduction of single plant-

beneficial microbes or whole communities have been demonstrated using different introduction methods like soil inoculation [24], direct tissue injection [25] or plant spraying [26]. By doing so, a positive effect of biocontrol agents and probiotics on plant growth, photosynthetic activity, root biomass, pathogen resistance and abiotic stress tolerance was observable [22]. Both direct and indirect engineering approaches require great knowledge about beneficial metabolites and beneficial strains for the plant and for its already established microbiome. Since the success of engineering methods depends on the establishment of probiotics or biocontrol agents within the host native microbiome research not only needs to identify beneficial compounds and strains but also needs to understand microbe-host and microbe-microbe interactions within the plant holobiont. Schmitz *et al.* successfully demonstrated the transfer of a synthetic community assembled from the rhizosphere of the desert plant *Indigofera* on tomato plants. By inoculating the vegetable with the synthetic community, they were able to increase the salt tolerance of the plant [27]. The study shows that plant beneficial communities, once they are identified, are promising treatments across different plant species. Nevertheless, other studies showed the challenge related to successful introductions. Biocontrol agents for instance can be outcompeted by the native microbiome. Furthermore, they often are stable only for short periods of time or they are not transmitted to the next generation [22, 28]. To ensure the stability of biocontrol agents and plant beneficial communities in nature over longer periods like a complete season or even up to the next generation, more research on community dynamics is needed. Therefore, a profound understanding of the plant, its microbiome and the interactions going on in the niche is essential. The next chapter describes what is already known about the plant holobiont and were research needs to make further progress.

ASSEMBLY OF THE PLANT MICROBIOME FROM RHIZOSPHERE TO PHYLLOSPHERE

Right from the start as a little seed, the plant carries a microbiome, which is further assembled, shaped and stabilized during growth. One part of the microbiome is obtained vertically by the inheritance of spermosphere microbes [29]. The other part arises by horizontal transfer from the environment. Several extrinsic and intrinsic factors like the soil, climate, genetic variations, the plant immune system, surface structure, microbe-host interactions, and microbe-microbe interaction play crucial roles in shaping the holobiont [30-33]. Significant variations can be seen through the plant microbiome in different compartments. The plant can be divided into soil associated parts, like the rhizosphere or rhizoplane, and areal parts constituting the phyllosphere. Within both the phyllosphere and rhizosphere, organisms colonize surfaces as epiphytic microbiome, and inner compartments of the plant as endophytic communities. As home of multiple kingdoms, the plant holobiont contains representatives of bacteria, fungi and

yeasts, phages and protists [5, 30]. In *Arabidopsis thaliana*, the part harboring the highest diversity of microbes is the rhizosphere. It is colonized by organisms associated with the roots of plants. Therefore, the shape of the rhizosphere is highly dependent on the soil properties [34]. Another strong factor influencing the composition of microbes living in this niche is the rhizosphere effect, which describes the significant effect of root exudates (e.g. sugars, organic acids and plant growth regulators) in shaping the microbiome [5, 35]. The most abundant phyla within the rhizosphere niche are Proteobacteria, Actinobacteria, Acidobacteria and Ascomycota [36-38]. But some phyla very specific for the rhizosphere can also be found, most of them arising from the surrounding soil. Chloroflexi and Planctomycetes are relatively abundant phyla related to the rhizosphere and nearly absent in areal plant compartments [37, 39]. Many organisms from the rhizosphere are involved in decomposing, oxidizing and transforming compounds from the soil. Therefore, the microbial community, not only degrades contaminants but furthermore, supplies nutrients to the plant and interacts with its metabolism [35]. Since the roots are the part of plants mainly responsible for nutrient uptake and compound release, it is not surprising to find organisms contributing to these processes. *Chloroflexi spp.* for instance, are known degraders of contaminants by dechlorination [40, 41]. Members of Planctomycetes are able to oxidize ammonium under anaerobic conditions and therefore play a role in the nitrogen cycle [42].

From the rhizosphere, many bacterial species can spread along the plant during growth and colonize the arial parts (phyllosphere). This can be seen by the high coverage of the same taxa in both habitats. Especially Firmicutes, Actinobacteria and Proteobacteria can be found in both [30]. However, the structures of the rhizosphere and phyllosphere microbiome are altered by the adaption to the niche and therefore differ from each other, especially on genus level [36]. Whereas, the rhizosphere microbiome is highly connected to soil conditions and climate, the phyllosphere community is additionally shaped by environmental factors like wind and radiation [43]. Due to the accessibility and the lower complexity of the phyllosphere microbiome, it gained attention in research. Studies have already shown that the phyllosphere is a promising environment for biocontrol and plant therapies. The microbiome of plant leaves seems to be even more tolerant to fertilization as the rhizosphere microbiome [39]. Therefore, it is worth to dive deeper into the areal parts of the plant and its inhabitants.

A CLOSER LOOK ON THE SURFACE: DYNAMICS SHAPING THE PHYLLOSHERE MICROBIOME

Dependent on the plant species, the leaf is colonized by 10^6 - 10^7 bacterial cells and 10^3 - 10^4 fungi cells per cm^2 often organized in small multi species colonies (micro-colonies) [31]. But the plant leaf surface is a challenging environment for its inhabitants and requires a high level of adaption. J. Leveau describes the processes involved in shaping and stabilizing plant microbiomes as an environment-plant-microbiome triad. He states:

“[...] these processes include 1) the environment to which the plant and its leaves are exposed, 2) the plant genotype and phenotype, and 3) the ability of microbial colonizers to exploit phyllosphere-specific resources, to tolerate or avoid phyllosphere-specific stresses, and to interact with each other and their host.” (J. Leveau, 2019, p. 42) [32]

As J. Leveau describes, studies have shown that the plant genotype and phenotype influence the leaf microbiome [33, 44]. Genetically diseased plants show an altered microbiome composition when compared to their healthy equivalents [32]. And it has been shown that variations within host immune genes can affect the whole fungal leaf microbiome of switchgrass [45]. The genotype also impacts the phenotype of a plant to a certain level. The vein and stomata density for instance is one factor involved in shaping the microbiome composition on the leaves of different tree species suggesting the impact of genotype and phenotype [46]. Leaf veins enable microbial aggregation and therefore are involved in micro-colony formation [47, 48]. Stomata are the portal for organisms entering the inner plant tissue and therefore important for the endophytic microbiome [31].

A second process, J. Leveau is pointing out is the impact of the environment on the phyllosphere. Microorganisms living in this niche not only face drought or rain but are furthermore influenced by wind and radiation like UV light [43]. These circumstances require strategies to deal with the impacts. A common strategy of leaf colonizers against the impact of UV light is the production of light emitting pigments. Typical species of the *A. thaliana* leaf microbiome like the bacteria *Sphingomonas* spp., *Methylobacterium* spp and the yeasts *Dioszegia* spp. or *Rhodotorula* spp. make use of the ability to produce carotenoids as pigments for UV protection [49-52]. To deal with weather and therefore with constant changes from drought to wetness, several microbiome members form biofilms. Abundant phyllosphere colonizers like *Bacillus* spp. and *Pseudomonas* spp. are able to secrete exopolysaccharides for biofilm formation. About 70 % of microbes colonizing the leaves live together in biofilms forming micro-colonies [31]. Of course, not all microbes living in these multi-species colonies are able to produce biofilms. They rather profit by harboring some biofilm builders among them [21, 53, 54]. Biofilms are not only important in protection against environmental factors, they further play a crucial role in successful surface adhesion since the plant leaf is a challenging ground to live on.

The adaption and ability to colonize the leaf surface is the last factor of the environment-plant-microbiome triad discussed by J. Leveau [32]. The cuticle is the highly hydrophobic layer covering the majority of plants. It plays an essential protective role for the plant e.g. as transpiration or radiation barrier. The hydrophobicity is caused by the polymer cutin and waxes, which are the main building blocks [55]. The production of extracellular matrix promotes the attachment of micro-colonies to the waxy ground, giving biofilm producers and inhabitants the necessary advantage for the niche. Another strategy for successfully colonizing the cuticle is

to release biosurfactants. Various *Bacillus* and *Pseudomonas* species are known to produce these amphiphilic compounds, which enable better water diffusion, adhesion, motility and nutrient exchange on the cuticle surface [31, 56, 57]. Microbes from the leaf microbiome are experts in using nutrients available on the leaf or consuming the degradation products of their fellows. The availability of carbon sources is limited on the leaf surface to certain carbohydrates, amino acids, sugar alcohols and organic acids [58, 59]. Therefore, organisms developed own ways to deal with the situation. Widely found members of the Methylobacterium phylum, for instance, are well adapted to the leaf by using methanol as a carbon source, a byproduct released by the plant during cell wall synthesis [48]. Other microbes produce specific compounds involved in the uptake of limited nutrients. Iron chelating siderophores produced by microorganisms are highly abundant in leaf microbiomes, suggesting extensive competition for iron in the niche [12]. Although studies on the iron availability on plant leaves differ in their conclusions about the iron content, it was shown that bacterial siderophores play a role in the growth of epiphytes in the phyllosphere [48, 60]. For siderophores, it is furthermore known that they can be shared within multi species communities and therefore help it to overcome iron starvation [61, 62]. Siderophore-sharing shows that direct microbe-microbe interactions are another important factor within phyllosphere microbiomes. Where so many different species from various kingdoms live together and form micro-colonies, constant interspecies communication and interaction can be expected. Either by cell-cell contact or the secretion of metabolites microbe-microbe interactions shape and stabilize the microbiome [63]. Quorum sensing, for instance, is a common way to communicate within the plant microbiome. It is known to occur between single and multiple species and regulates gene expression for colonization, motility, biofilm formation and virulence [31]. Other secreted molecules like antimicrobials are involved in the permanent competition for space and the protection against pathogenic invaders [64, 65].

In total the plant microbiome is a complex system of interactions with the environment, the host, and fellow microbes. Further research is necessary to fully understand which mechanisms are active in which space or time and especially which processes are needed for minimal but effective probiotics and biocontrol agents. Striking about the above discussed dynamics is the number of interactions based on the production of secondary metabolites (e.g. surfactants, pigments, siderophores and antimicrobials). The compounds might play a key role in community stability on the leaf. Nevertheless, due to the complexity of the microbiome and its interspecies interactions, much remains unknown about the role of secondary metabolites in microbe-microbe interactions on the plant leaf.

MICROBIAL SECONDARY METABOLITES AND THEIR POTENTIAL TO SHAPE AND STABILIZE PLANT MICROBIOMES

In the previous chapter, the so far known dynamics that shape and stabilize the microbiome are discussed. Biosurfactants, siderophores and signaling molecules as well as the inhibition of competitors by antimicrobials are named as important factors for community dynamics. All these compounds are secondary metabolites produced by organisms to survive and adapt to the phyllosphere niche. Their high abundance makes them interesting targets for microbiome research. Secondary metabolites are often known as natural products with important bioactivity for our lives. For example, they find application as antibiotics, chemotherapeutics, herbicides, fungicides or in food and cosmetic industry as emulsifier or flavors [66-71]. But their role in nature often remains in the background. However, knowledge about the natural role of secondary metabolites can help us in many ways e.g. in the search for new natural products, in activation of secondary metabolite production genes, in antimicrobial resistance development and in finding sensitive treatments based on pre- and probiotics [72].

Short excursion into important secondary metabolite classes and their biosynthesis

The biosynthesis genes of secondary metabolites are organized in clusters. For many molecules, this allows a genetically based classification into secondary metabolite classes. The following section provides short insides into main secondary metabolite classes and their biosynthesis.

Non ribosomal peptides (NRPs) are produced by huge modular enzyme complexes called non ribosomal peptide synthetases (NRPSs). Typically, the compounds are assembled from proteinogenic and non-proteinogenic amino acids, which were linked to each other by peptide bonds. A more detailed look on NRPSs and their products can be found in the review of Strieker *et al* [73].

Polyketides (PKs) are compounds produced by polyketide synthases (PKS). These multifunctional enzymes catalyze the decarboxylative condensation between their building blocks similar to the fatty acid assembly. Characteristic building blocks for polyketides belong mainly to the families of acetyl-CoAs as starter and malonyl-CoAs as extender units. For more detailed information about the structure of PKSs and their different types, the review of Risdian *et al.* is recommended [74].

Ribosomally synthesized and posttranslationally modified peptides (RiPPs) are peptides composed of proteinogenic amino acids. The precursor peptide is assembled by the ribosome in the exact order encoded in the biosynthesis genes. Posttranslational modification and cleavage of the leader peptide from the core peptide is a characteristic of RiPPs. To learn more about the structure and different types of RiPPs, see the review of Hudson and Mitchell [75].

Terpenes are a highly diverse group of compounds arising by the fusion of terpene units. The huge variety of terpenes is generated by sequentially acting enzymes, starting with the terpene

cyclase, which is responsible for creating diverse terpene skeletons. The following tailoring steps ensure even more diversity. See the review of Avalos *et al.* for more details about terpenes and their diversity [76].

Additionally, compounds produced by the secondary metabolism can be grouped based on their molecular structure and/or physiological function. This can be especially expedient when investigating structure-function relations, which can give insights into the roles of such compound groups in their environment [77]. The following two groups represent examples for structural and functional secondary metabolite groups, which are mentioned in the context of this PhD thesis.

Betalactones are a structural group of secondary metabolites, characterized by their β -lactone ring. The β -lactone synthase catalyzes the cyclization of a β -hydroxy acid to the actual ring. Lately, a second pathway for the β -lactone ring formation was identified by a thioesterase domain (TE) of NRPS assembly lines, suggesting the involvement of NRPSs in the biosynthesis of some betalactones. Therefore, the classification of β -lactones is not only based on a specific biosynthesis pathway but rather on their ring structure. To read more about β -lactones and their classification see the review of Robinson *et al.* [78].

Siderophores are a functional group of secondary metabolites and characterized by their iron binding ability. They can be produced by specific siderophore biosynthesis genes called NISs (NRPS independent synthetases) but also by enzyme complexes of the NRPS or PKS class. Therefore, their structure is not made up to specific building blocks but varies from amino acids, over acetyl-CoA molecules to citric or succinic acids. Their common property is the chelation of iron making them an own noteworthy class. To read more about the complexity of siderophores, the review of Timofeeva *et al.* is recommended [79].

Genetic knowledge about secondary metabolite synthesis opened a new range of possibilities in secondary metabolite research. Highly conserved regions within secondary metabolite biosynthetic gene clusters enable the classification of known, but also of new discovered secondary metabolites into the existing groups based on the gene similarity [80]. Furthermore, certain classes can be, in parts, related to the function of the metabolites belonging to it. The classes of NRPs, PKs or RiPPs for instance carry a noticeably high number of antibiotics, suggesting that new compounds classified as these have a potential for showing antimicrobial activity [75, 81, 82]. Other classes are directly connected to the function of the metabolite by carrying enzymatic genes specific for the compound's activity. Examples for this are siderophores, which can be identified by the presence of genes for metal dependent transporters [83]. The prediction of biosynthetic gene clusters from the genome sequence and their classification into groups enables the investigation of the biosynthetic potential of organisms and can give already great knowledge about the putative metabolome of a strain. *In situ* genome mining of microbial genomes developed into a promising method for pre-

selection of organisms showing high biosynthetic potential in the quest for new antibiotics, but also for identifying biocontrol agents and probiotics for humans and plants [80]. Since the plant microbiome has a huge potential to produce secondary metabolites they are suspected to take over a key role in such multi-species communities [84].

HOW TO INVESTIGATE MICROBIOME DYNAMICS

The complexity and sensitivity to extrinsic and intrinsic impacts of plant microbiomes make them a challenging environment to study. Therefore, different levels of investigation need to be considered to fully understand the dynamics of the plant microbiome. Understanding the plant as a whole ecosystem includes the naturally occurring interactions shaped by environmental factors and host genetic variations. A deeper look on the organismic level helps to understand shaping and stabilization of plant microbiomes by microbe-microbe / microbe-host interactions. Even deeper, the molecular level gives information about area specific interactions and the underlying metabolites [63]. Only knowledge about all levels gives an overall picture about the plant holobiont and enables promoting the plant efficiently by engineering its microbiome. Researchers use various methods to address interactions observed at different levels. Some common strategies include top-down and bottom-up workflows. Top-down methods use the progress in sequencing techniques like 16S rRNA amplicon sequencing or whole metagenome shotgun sequencing to picture the whole microbiome composition directly from nature [85]. By the use of co-abundance networks, interactions between microbiome members can be investigated based on the generated genetic data [86, 87]. The networks enable conclusions about the impacts on the plant microbiome in natural environments, such as the effects of environmental factors, fertilizers, or soil treatments [43, 88]. Additionally, they help to identify core and hub organisms across different locations and over time [89], ultimately leading to the isolation of potential biocontrol strains or key metabolic products. The challenge lies in identifying key organisms for further investigation, as natural systems have limited potential for manipulation. Such manipulation might be necessary to detect key strains associated with specific conditions. Nevertheless, one has to keep in mind, that correlation networks based on co-abundance are prone to picture abundance dependencies, which might not be based on real microbial interactions since the co- absence of two strains could also be due to the sensitivity to the same environmental factors [90]. Therefore, it can be advantageous to combine the method with bottom-up strategies. Bottom-up methods start by single microbiome strains or metabolites and investigating their interactions with other microbiome members, communities and up to the whole holobiont in nature. Some studies already proved that the bottom-up method can be successful for the identification of relevant interactions in nature by identifying secondary metabolites in pairwise interactions and showing their effect on the composition of the plant

microbiome [60, 91-93]. But the chance is high to follow dead ends since organisms behave differently dependent on growth media and conditions [94]. At the end, a combination of both approaches might be the key to discover the total dynamics of plant microbiomes. A good compromise between using top-down and bottom-up approaches on the same system can be made by breaking down the microbiome to synthetic communities.

SYNTHETIC COMMUNITIES AS MODEL SYSTEMS FOR MICROBE-MICROBE INTERACTION RESEARCH

Due to the huge number of neutral, positive and negative microbe-microbe and microbe-host interactions estimated to take place in parallel, the natural plant microbiome is a complex and challenging ecosystem for research [86] [95]. Therefore, the use of synthetic communities is nowadays a common tool. Synthetic communities are microbial communities assembled from carefully selected microbiome members, which allow the investigation of interactions and microbiome principles in a stable model system. Their stability brings several advantages for microbiome research. It excludes unwanted environmental impacts and helps focusing on microbe-host and microbe-microbe interactions [96]. Synthetic communities can be manipulated by introducing mutants, pathogens or metabolites for investigating their role or impact on the community [97]. And they allow the identification and investigation of traits, which might be overlooked in the complex microbiome [98]. Even though synthetic communities only comprise a small subset of whole microbiomes, and they are not able to display all the underlying principles or make it likely to miss important microbes, they already proved their high potential in the field [63]. Especially as a first step of pre-selecting and pre-analyzing interactions or the effect of pathogens, treatments and environmental impacts, they were successfully used in the past [99, 100]. Correa de Souza *et al.* for instance, used a synthetic microbial community as a system to identify traits leading to a successful plant colonization [101]. Nevertheless, the coverage of naturally occurring principles within synthetic communities is highly dependent on their composition and therefore on the assembly parameters. In general, the higher the microbial richness and the more nature-related microorganisms in synthetic communities are, the more conclusions on whole plant microbiomes can be drawn and verified [102, 103]. Communities, that cover the whole core microbiome and include several strains of the same species are more likely to display natural dynamics [104]. On the other hand, community size is connected to the complexity again and can make downstream analyses, especially in wet lab more challenging. So, the criteria that were used for the assembly of a synthetic community significantly influence the handling and outcome. Several strategies can be applied to assemble synthetic communities. Most studies used taxonomic and composition-based strategies to choose their community members [27, 105, 106]. The underlying idea by using this strategy is to cover the core microbiome, which is

co-occurring in nature under changing environments and therefore represents a stable group of plant colonizers. In the past, the hypothesis that organisms present in high numbers play a major role in microbiomes lead often to the use of composition-based strategies for synthetic community assembly [27]. However, recent studies indicated that the function of an organism is another, if not, the major factor for its importance in microbiomes [107]. Therefore, interactions of microbiome members with each other and the host are more often accounted for the assembly strategies [96, 108, 109]. Correlation networks based on co-abundance of microbiome microbes give insights into the connectivity of certain strains within the community [89]. Genomics, transcriptomics, metabolomics and proteomics can furthermore reveal the potential of organisms for the production of metabolites, and therefore nominate them as promising synthetic community members. The combination of different strategies for community assembly not only improves the approximation to natural microbiomes, but it also opens further fields for research [63, 96]. Synthetic communities can be assembled not only to mimic the natural microbiome and gain knowledge about microbiome dynamics in nature. They can also be assembled based on major functional traits e.g. the degradation of nutrients, the production of siderophores or the secretion of antimicrobials against a certain pathogen and serve as probiotic treatments for plants [110-112]. Their lower complexity and manipulation ability e.g. by the introduction and observation of mutants, are what makes synthetic communities promising as model systems for microbiome research, as probiotics and as biocontrol tools.

THE SYNCOM AS MODEL SYSTEM TO STUDY THE ROLE OF SECONDARY METABOLITES IN THE *A. THALIANA* LEAF MICROBIOME

The synthetic community assembled by the group of Prof. Eric Kemen from native *Arabidopsis thaliana* microbiomes in a common garden experiment [89] is used as a model system for investigating dynamics between microbiome members. Over three years, Almario *et al.*, collected samples of *A. thaliana*, which were germinated in the greenhouse and placed into a field after 10 days. The researchers aimed to gain insights into the bacterial, fungal and prokaryotic microbiome of the plant and therefore performed Illumina amplicon sequencing of 16S rRNA, ITS2 and 18S rRNA regions. The analysis enabled the identification of a core microbiome and therefore the assembly of the SynCom. The community is based on epiphytic microbes of the *A. thaliana* phyllosphere microbiome. It contains fungal strains present in >95 % of plant samples and bacterial strains present in > 98 % plant samples. 13 bacteria and 3 fungi were chosen for the community and represent strains of typical plant microbiome genera like *Pseudomonas spp.*, *Bacillus spp.*, *Methylobacterium spp.*, *Rhodotorula spp.* or *Sphingomonas spp.* In addition to being core microbiome members of *A. thaliana*, some SynCom strains were identified as hub organisms over different seasons based on their

connectivity and centrality in the phyllosphere community [89]. All SynCom strains can be cultured on agar plates in the lab and grow stable on *A. thaliana* plants in a laboratory setup. Therefore, the SynCom is a suitable and representative model system for investigating interactions and dynamics driving the community and the phyllosphere microbiome.

AIM OF THE STUDY

In the present study, the SynCom is used as a stable model system to investigate microbial interactions with the potential to drive community dynamics. Since the presence of biosynthetic gene clusters to produce secondary metabolites is high in the epiphytic *A. thaliana* microbiome [84], an involvement of these compounds in community dynamics was hypothesized. Therefore, the study focused 1) on the characterization of secondary metabolites produced by SynCom members, 2) on the detection of microbe-microbe interactions and 3) on the identification of important key microorganisms with the potential to be used as biocontrol agents. It was aimed to obtain further insights into mechanisms shaping and stabilizing the SynCom on *A. thaliana*.

The first part of the work (manuscript 1) investigated microbe-microbe interactions under different conditions with the goal to identify relationships between SynCom members, which can explain the SynCom's composition. Therefore, co-abundance networks of natural epiphytic *A. thaliana* microbiomes were compared to *in vitro* pairwise interactions of SynCom members. By following up inhibiting pairwise interactions of *Pseudomonas koreensis* based on pseudobactin from *in vitro* to *in planta* experiments, the potential of antimicrobials to shape the SynCom was investigated. Furthermore, the question if producers of antimicrobials are dominant strains in the SynCom was addressed. The findings showed that co-abundance networks display more positive correlations of SynCom members compared to *in vitro* pairwise interactions. Furthermore, the antimicrobial siderophore pseudobactin was not responsible for the dominance of its producer *P. koreensis* in the community. The low abundance of other strong pairwise inhibitors like *Bacillus altitudinis* suggested that antimicrobials might play minor roles in SynCom dynamics.

The second part of the work (manuscript 2) aimed to identify more microbial metabolites with a potential involvement in community dynamics. Therefore, a non-targeted metabolomics approach should not only reveal which known microbial metabolites the SynCom members are able to produce, but also identify compounds present in the community. By comparing whole SynCom co-cultures with single strain cultures, it was hypothesized that compounds present in higher concentrations in co-cultures have more potential to play a major role in the community. Several metabolites with possible functions for the whole community were identified following the metabolomic approach. Among them, the vitamin biotin was

upregulated in the community. Biotin was found to promote the growth of *Bacillus altitudinis*, leading to the hypothesis that cross-feeding might be a mechanism driving community dynamics. Additionally, a cytokinin was produced only in co-cultures, suggesting that the SynCom interferes with the plant metabolism.

INFORMATION ON THE MANUSCRIPTS

MANUSCRIPT 1: STRONG PAIRWISE INTERACTIONS DO NOT DRIVE INTERACTIONS IN A PLANT LEAF ASSOCIATED MICROBIAL COMMUNITY

Content

The study explores microbial interactions of a synthetic microbial community (SynCom) from *Arabidopsis thaliana* leaves to understand factors shaping community composition and stability. It found discrepancies between *in vitro* interactions and those inferred *in planta*, suggesting that secondary metabolites like antimicrobials are not key drivers in a community context. Despite identifying the siderophore pseudobactin as an effective antimicrobial *in vitro*, no impact *in planta* was observed. The research suggests that synergistic mechanisms drive community dynamics, rather than competition.

Status

Published in *ISME communications*, accepted 04. October 2024, DOI:10.1093/ismeco/ycae117

MANUSCRIPT 2: IDENTIFYING POTENTIAL COMMUNITY-DRIVING METABOLITES IN A MICROBIAL PLANT LEAF ASSOCIATED COMMUNITY

Content

This study focuses on identifying key metabolites involved in microbial interactions within a synthetic community (SynCom) derived from *Arabidopsis thaliana* leaf microbiomes. Using non-targeted metabolomics, the researchers compared metabolite profiles of individual SynCom members to those of the entire community. They identified key metabolites, such as biotin and N-acyl lysine produced by *Massilia aurea*, which are upregulated in the community and may influence microbial dynamics. Biotin was found to promote the growth of *B. altitudinis* through cross-feeding. The study shows the effectiveness of non-targeted metabolomics approaches for identifying key metabolites and highlights the potential role of these in shaping microbial communities.

Status

Not submitted yet.

MANUSCRIPT 1

Title: Strong pairwise interactions do not drive interactions in a plant leaf associated microbial community

Authors: Franziska Höhn, Dr. Vasvi Chaudhry, Dr. Caner Bagci, Maryam Mahmoudi, Elke Klenk, Lara Berg, Dr. Paolo Stincone, Dr. Chambers C. Hughes, Dr. Daniel Petras, Prof. Heike Brötz-Oosterhelt, Prof. Eric Kemen, Prof. Nadine Ziemert

DECLARATIONS ON THE CONTRIBUTION OF CO-AUTHORS TO THE MANUSCRIPT

Author	Author position	Scientific ideas %	Data generation %	Analysis & interpretation %	Paper writing %
Franziska Höhn	First author	40	60	50	60
Dr. Dr. Vasvi Chaudhry	Co-author	10	-	-	-
Dr. Caner Bagci	Co-author	-	10	5	5
Maryam Mahmoudi	Co-author	-	10	5	5
Elke Klenk	Co-author	-	5	-	-
Lara Berg	Co-author	-	5	-	-
Dr. Paolo Stincone	Co-author	-	-	5	-
Dr. Chambers C. Hughes	Co-author	-	10	5	5
Dr. Daniel Petras	Co-author	-	-	5	0
Prof. Heike Brötz-Oosterhelt	Co-author	10	-	5	5
Prof. Eric Kemen	Corresponding author	15	-	10	10
Prof. Nadine Ziemert	Corresponding author	25	-	10	10
Titel of paper	Strong pairwise interactions do not drive interactions in a plant leaf associated microbial community				
Status in publication process	Accepted 04.10.2024				

TITLE: STRONG PAIRWISE INTERACTIONS DO NOT DRIVE INTERACTIONS IN A PLANT LEAF ASSOCIATED MICROBIAL COMMUNITY

RUNNING TITLE: INTERACTIONS IN LEAF MICROBIAL COMMUNITY

Franziska Höhn^{1,3}, Dr. Vasvi Chaudhry², Dr. Caner Bagci¹, Maryam Mahmoudi², Elke Klenk², Lara Berg^{1,3}, Dr. Paolo Stincone^{2,3}, Dr. Chambers C. Hughes^{3,4,6}, Dr. Daniel Petras^{3,5}, Prof. Heike Brötz-Oesterhelt^{3,4,6}, Prof. Eric Kemen^{2,3*}, Prof. Nadine Ziemert^{1,3,4*}

Franziska Höhn	
Dr. Caner Bagci	
Dr. Vasvi Chaudhry	
Dr. Paolo Stincone	
Maryam Mahmoudi	
Lara Berg	
Elke Klenk	
Dr. Chambers Hughes	
Dr. Daniel Petras	
Dr. Heike Brötz-Oesterhelt	
Dr. Eric Kemen	
Dr. Nadine Ziemert	

¹Translational Genome Mining for Natural Products, Interfaculty Institute of Microbiology and Infection Medicine (IMIT) and Institute for Bioinformatics and Medical Informatics (IBMI), University of Tübingen, Tübingen, Germany

²Center for Plant Molecular Biology (ZMBP), Interfaculty Institute of Microbiology and Infection Medicine (IMIT), University of Tübingen, Tübingen, Germany

³ Cluster of Excellence Controlling Microbes to Fight Infections (CMFI), University of Tübingen, Tübingen, Germany

⁴German Centre for Infection Research (DZIF), Partner Site Tübingen, Tübingen, Germany

⁵Department of Biochemistry, University of California Riverside, Riverside, USA

⁶Department of Microbial Bioactive Compounds, Interfaculty Institute of Microbiology and Infection Medicine (IMIT), University of Tübingen, Tübingen, Germany

Corresponding author:

Dr. Nadine Ziemert

Department of Translational Genome Mining for Natural Products

Interfaculty Institute of Microbiology and Infection Medicine

University of Tübingen

ABSTRACT

Microbial communities that promote plant growth show promise in reducing the impacts of climate change on plant health and productivity. Understanding microbe-microbe interactions in a community context is paramount for designing effective microbial consortia that enhance plant resilience. In this study, we investigated the dynamics of a synthetic microbial community (SynCom) assembled from *Arabidopsis thaliana* leaves to elucidate factors shaping community composition and stability. We found notable disparities between *in vitro* pairwise interactions and those inferred from correlation networks *in planta*. Our findings suggested that secondary metabolites, particularly antimicrobials, might mediate interactions *in vitro*, but are no key drivers of microbial interactions in a community context. Through co-cultivation experiments, we identified the siderophore pseudobactin as a potent antimicrobial agent against several SynCom members, but its impact on community composition *in planta* was negligible. Notably, dominant SynCom members, such as *Pseudomonas koreensis*, *Flavobacterium pectinovorum*, and *Sporobolomyces roseus*, exhibited only positive correlations, suggesting synergism based on for example exopolysaccharides and biotransformation might drive community dynamics rather than competition. Two correlations between SynCom members in the co-abundance network corresponded with their pairwise *in vitro* interactions, highlighting the potential for further research, and demonstrating the usefulness of correlation networks in identifying key microbe-microbe interactions. Our findings highlight the importance of considering microbiome-wide interaction studies and synthetic communities in understanding and manipulating plant microbiomes.

Key words: synthetic communities, plant leaf microbiomes, pyoverdines, pseudobactin, microbe-microbe interactions, correlation networks, *Arabidopsis thaliana*, secondary metabolites

INTRODUCTION

The microbiome is essential for plant survival: not only does the microbiome promote plant growth, but it also increases stress tolerance to drought, salinity and iron limitation, as well as resistance to pathogens [1-4]. Strategies fighting against climate change to promote plant growth and stress tolerance are becoming more urgent. Engineering the plant microbiome using nature-derived synthetic communities, biocontrol organisms and probiotics can be a

prudent way to promote plant growth under the challenging conditions of climate change [2, 3, 5, 6]. As a proof of concept, Schmitz *et al.*, used a synthetic community assembled from the rhizosphere of the desert plant *Indigofera* and were able to increase the salt tolerance of tomato plants [5].

For sustainable and long-term use of synthetic communities as biocontrol agents, understanding the mechanisms that shape and stabilize such communities on plants is crucial [7-9]. In this respect, not only microbe-host interactions but also overlooked microbe-microbe interactions play a role in community dynamics. Correlation networks based on co-abundance and co-occurrence of microbiome members of plants are a promising source for the detection of microbe-microbe dependencies in a community context [10-12]. Correlation network analyses of whole *Arabidopsis thaliana* microbiomes have already shown that microbe-microbe interactions are affected by environmental impacts and the plant phenotype [13-15]. Nevertheless, these factors explain only a part of the dynamics that drive microbiomes. *In vitro* pairwise interactions studies and *in situ* genome mining have revealed the enormous potential of microbiome members to produce secondary metabolites [16-19]. The identification of many genes dedicated to non-ribosomal peptides (NRPs), polyketides (PKs), ribosomally synthesized and post-translationally modified peptides (RiPPs), and toxins in plant microbiomes indicates a rich repertoire of potential antimicrobial agents [17, 20, 21]. Therefore, these metabolites are assumed to play a major role in plant microbiomes, but little is known about how direct pairwise interactions of microbial members are reflected in complex microbiome interactions.

The objective of this study was to elucidate microbe-microbe interactions among core microbiome members of the *A. thaliana* leaf microbiome. Here we refer microbe-microbe interactions to interactions observed between bacterial and fungal microbiome members. As a model system, we used a synthetic community from *A. thaliana* leaves based on high occurrences across multiple plant samples [13]. We investigated correlations within the community and with other members of the *A. thaliana* epiphytic microbiome based on co-abundance. We then explored correlations of these microbiome members through *in vitro* pairwise interaction studies and observed significant differences between *in vitro* relations and *in planta* correlation networks. The high number of inhibitions in pairwise interactions suggests that pairwise interactions might be driven by the production of antimicrobial secondary metabolites. This initial observation led us to question why interactions based on antimicrobial compounds are not displayed in correlation networks. By using the siderophore pseudobactin from *Pseudomonas koreensis* as an example, we showed that this strong antimicrobial agent is potent in pairwise interactions but has no effect on the SynCom composition. Strong pairwise inhibitors like *P. koreensis* and *Sporobolomyces roseus* showed more than 70 % positive correlations *in planta* indicating that competition based on antimicrobials might play a subordinate role in the *A. thaliana* leaf microbiome. Our findings help to understand the

dynamics within plant-associated microbiomes and highlight microbiome-wide correlation networks and synthetic communities as promising tools for the pre-selection of relevant microbe-microbe interactions in plant microbiome engineering efforts.

MATERIALS AND METHODS

MICROBIAL STRAINS AND SYNCOM ASSEMBLY

Microbial strains for the construction of an epiphytic synthetic leaf-associated community from *Arabidopsis thaliana* were isolated through a three year garden experiment (2014-2017) by Almario *et al.* In the garden experiment, plants were germinated for 10 days in the greenhouse before transferring into a field. Strain selection was based on high occurrence of operational taxonomic units (OTUs) across all plant samples from different seasons (occurrence in $\geq 95\%$ of samples for fungi and $\geq 98\%$ of samples for bacteria, cut off ≥ 10 reads per sample) as obtained by 16S rRNA / ITS2 MiSeq Illumina amplicon sequencing [13]. Taxonomical classification of the synthetic community (SynCom) members, comprising 13 bacteria and 3 fungi (Table 1), was performed through 16S rRNA and ITS2 analysis using BlastN.

Table 1: SynCom members characterized by 16S rRNA and ITS2 similarity (BlastN)

Closest Type species match	Short name used in this study	Closest type strain match	% identity type species	Genome NCBI accession number
<i>Aeromicrobium fastidiosum</i>	<i>A. fastidiosum</i>	DSM 10552(T)	99.30	JAMKCA000000000
<i>Arthrobacter humicola</i>	<i>A. humicola</i>	KV-653(T)	100.00	JAFKON000000000
<i>Bacillus altitudinis</i>	<i>B. altitudinis</i>	41KF2b(T)	100.00	JAFKOO000000000
<i>Dioszegia hungarica</i>	<i>D. hungarica</i>	CBS 4214	100.00	JAMRJJ000000000
<i>Flavobacterium pectinovorum</i>	<i>F. pectinovorum</i>	DSM 6368(T)	98.61	JAFEVZ000000000
<i>Frigoribacterium faeni</i>	<i>F. faeni</i>	801(T)	99.82	JAIXNG000000000
<i>Massilia aurea</i>	<i>M. aurea</i>	AP13T	100.00	JBFMMP000000000
<i>Methylobacterium goesingense</i>	<i>M. goesingense</i>	iEII3(T)	99.43	JAFGZG000000000
<i>Microbacterium proteolyticum</i>	<i>M. proteolyticum</i>	RZ36(T)	99.29	JAFKOM000000000
<i>Nocardioides cavernae</i>	<i>N. cavernae</i>	YIM A1136(T)	99.23	JALQCQ000000000
<i>Paenibacillus amylolyticus</i>	<i>P. amylolyticus</i>	NBRC 15957(T)	99.49	JAMGVX000000000
<i>Pseudomonas koreensis</i>	<i>P. koreensis</i>	Ps 9-14(T)	100.00	JAFEVY000000000
<i>Rhizobium skieniewicense</i>	<i>R. skieniewicense</i>	Ch11(T)	99.64	JAFFPP000000000
<i>Rhodotorula kratochvilovae</i>	<i>R. kratochvilovae</i>	CBS 7436	99.82	JAFEUJ000000000
<i>Sphingomonas faeni</i>	<i>S. faeni</i>	MA-olki(T)	99.50	JALPNF000000000
<i>Sporobolomyces roseus</i>	<i>S. roseus</i>	CBS 486	99.29	JAFEUI000000000

CULTURE MEDIA AND CONDITIONS

Bacterial strains were pre-cultured on nutrient agar NA (BD, USA) or in nutrient broth NB (BD, USA) for 48 h. Fungi were pre-cultured on potato dextrose agar PDA (Carl Roth, Germany) potato dextrose broth PDB (Carl Roth, Germany) for 48 h. For cross-streaking experiments with *Pseudomonas koreensis* WT and the *P. koreensis* pseudobactin deficient mutant ($\Delta pvdI/J$), siderophore promotive F-base agar, which is used for the identification of fluorescent Pseudomonades, (Merck, Germany) was used. Growth measurements were performed in MM9 minimal medium [22]. and enriched MM9 medium, where MM9 was mixed 1:5 with NB, for bacteria and in PDB for fungi (Table S1 and S2). MM9/7 agar was used to culture the SynCom for 5 days for amplicon sequencing (Table S3). Therefore, MM9 medium was modified to a more defined agar, by exchanging casamino acids with a defined amino acid solution and the addition of agar-agar. This was done to mimic amino acids present on the leaf surface [23]. All cultures were incubated at 22 °C and liquid cultures were shaken at 120 rpm.

STERILE PLANTS AND PLANT SPRAYING

Seeds of *A. thaliana* Ws-0 (Wassilewskija) were sterilized over night with chlorine gas. Therefore, seeds were incubated in presence of 4 ml concentrated hydrochloric acid in 100 ml sodium hypo chloride and 35 mbar vacuum for 6-8 h. Sterile seeds were immediately sown on 0.5 x MS agar (1.5 mM CaCl₂, 0.63 mM KH₂PO₄, 9.4 mM KNO₃, 0.75 mM MgSO₄, 10.3 mM NH₄NO₃, 0.055 μM CoCl₂ x 6 H₂O, 0.05 μM CuSO₄ x 5 H₂O, 50.00 μM FeNaEDTA, 50.15 μM H₃BO₃, 2.5 μM KI, 50 μM MnSO₄ x H₂O, 0.52 μM Na₂MoO₄ x 2 H₂O, 15 μM ZnSO₄ x 7 H₂O, 8 g/L agar-agar). Plates were sealed with leukopor (BSN medical GmbH, Germany) and grown in a short day chamber (8 h light, 16 h dark, 21 °C, 50 % humidity) for 1 - 2 weeks. Seedlings were picked and placed in 12 well plates containing 0.5 MS agar. Plants were further incubated for 2 weeks in a short-day chamber.

For spraying, each SynCom strain was pre-cultured in 20 ml of liquid medium. Cultures were harvested after 48 h of incubation through centrifugation at 7.000 rpm for 5 minutes. Afterwards, cells were washed twice and resuspended in 10 ml of 10 mM MgCl₂. For each strain, the optical density at wavelength 600 nm (OD₆₀₀) was measured and the cultures were diluted to OD₆₀₀ = 0.2. Equal volumes of each strain dilution were combined to form the different SynCom groups used for amplicon sequencing. The mixtures, augmented with 0.02 % silwet

700 for finer droplet distribution, were sprayed onto sterile 3-week-old *A. thaliana* plants using an airbrush system with 2 mbar pressure applied through 2 brushes. Following inoculation plants were incubated in short-day chambers (8 hours light, 16 hours dark) at 22°C.

CORRELATION NETWORK ANALYSIS

To investigate the abundance and connectivity of SynCom members in the epiphytic leaf microbiome of wild *A. thaliana* plants, correlation networks were constructed. Since the study from which the SynCom was assembled [13] was based on a common garden experiment, we used a different dataset based on samples from wild *A. thaliana* plants to calculate correlation networks. The networks were based on OTU tables generated in the study of Mahmoudi *et al.* [24]. There, the data was collected from 351 wild *A. thaliana* plants sampled around Tübingen. Plants were collected for 5 years (2014-2019) in fall and spring, the DNA was isolated and 16S/ITS2 amplicon sequencing was performed. In brief, bacterial and eukaryotic (fungal and non-fungal) OTU tables were filtered to retain only those OTUs present in at least 5 samples with more than 10 reads. The OTU tables were used to calculate SparCC correlations [25] (with default parameters) in the FastSpar platform [26]. Permuted P-values for each correlation were derived from 1.000 bootstraps datasets. Only correlations with $P \leq 0.001$ were kept for further analysis. The preparation of OTU tables from the raw data followed the workflow of Mahmoudi *et al.* [24], afterwards correlations were calculated as shown in the workflow stored at zenodo repository (Strong pairwise interactions do not drive interactions in a plant leaf associated microbial community), [<https://zenodo.org/records/12795858>]. 16S and ITS2 regions of all SynCom members were aligned by BlastN to the most common 16S and ITS2 regions of OTUs after correlation. The closest BlastN match for each SynCom member was assigned as representative (Table 2). Cytoscape (version 3.10.0) [27] was used for visualization of interactions of epiphytic leaf microbiome members and SynCom microorganisms on genus level.

CROSS STREAKING EXPERIMENTS

Pairwise interactions of SynCom members were observed on NB and PDA. Previous experiments determine the media as best fit for an equally growth of all SynCom members. Solid pre-cultures were taken with cotton swabs, resuspended in 10 mM MgCl₂ and diluted to OD₆₀₀ 1,0. Using a fresh cotton swap, test strains were streaked out on NA/PDA agar plates. Once the test strain was dry, all SynCom members were streaked crosswise onto the test strain. Inhibiting interactions were visually observed after 48 h incubation by the production of inhibition zones. Therefore, cross streakings are qualitative observations of pairwise

interactions. Promoting interactions were observed by higher growth in contact zones (Fig. S1). Cross streaking experiments to test the effect of pseudobactin on all SynCom members were performed on F-base agar for 48 h using *P. koreensis* WT and the $\Delta pvdI/J$ mutant. Cross streaking experiments on NA/PDA were repeated three times. Cross streakings on F-base agar were repeated two times.

GENOME MINING

Genomes of SynCom members (references see Table 1) were analyzed by AntiSMASH 7 [28] for the presence of biosynthetic gene clusters of secondary metabolites. Similarities to known compounds were further investigated by MIBiG [29] comparison and BlastN/BlastP analysis.

PSEUDOBACTIN IDENTIFICATION AND PURIFICATION

P. koreensis cultivated in 1 L MM9 medium for 48 h at RT and 100 rpm shaking was used for HPLC-MS and NMR analysis. Cells were harvested by centrifugation at 8.000 rpm for 5 minutes and supernatant was collected. The supernatant was tested for the presence of pseudobactin under UV light (365 nm) and by HPLC-MS analysis. HPLC-MS measurements were performed on an Agilent 1260 Infinity (Agilent technology, USA) using a Kinetex 5 μ m 100 Å, 100 x 4.6 mm C18 column and a single-quadrupole G6125B MSD in positive ion mode. Analytical HPLC was performed by using the following parameters: 5 μ L injection; solvent A: H₂O (0.1 % TFA); B: acetonitrile (0.1 % TFA); gradient eluent: 10-100% B over 10 minutes, 100 % B for 2 minutes, and equilibration to initial conditions over 3 minutes; flow rate: 1.0 mL/min; UV detection: 254 nm; retention time: 1.2 min; pseudomolecular ion: m/z [M+H]⁺ = 989.4. For the purification of pseudobactin, the supernatant was loaded onto a C18 cartridge (Supelco, USA). The cartridge was washed with 100% water (0.1 % TFA), and pseudobactin was eluted with 10 % acetonitrile (0.1 % TFA). The fraction was dried using a rotary evaporator and lyocell vacuum evaporator. 20 mg of the dry sample was resuspended in methanol (1 mL), and preparative HPLC was performed by using the following parameters: solvent A: water (0.1 % TFA); solvent B: methanol (0.1 % TFA); isocratic eluent: 15 % B; flow rate: 10 mL/min; UV detection: 254 nm; retention time: 20.5 min. Fractions containing pseudobactin were collected, dried, and analyzed by NMR spectroscopy. ¹H NMR and 2D spectra were recorded at 700 MHz in D₂O (4.79 ppm). ¹³C NMR spectra were recorded at 175 MHz in D₂O (not referenced).

DELETION MUTANT CREATION

For the investigation of interaction between SynCom members and pseudobactin, a pseudobactin deletion mutant of *P. koreensis* was constructed. For the deletion, genes *pvdI* and *pvdJ* were chosen [30, 31]. The deletion of the genes was performed as described by Huang *et al* [32]. In short, the deleted gene region was cloned in the vector plasmid pEX18Gm by gibbs assembly. The vector containing the deleted region was transferred into *P. koreensis* by conjugation with *E. coli* S17- λ as donor. The genes were introduced into the *P. koreensis* genome through a single crossover and the plasmid backbone containing the wildtype copy of gene region was subsequently eliminated under selection pressure on antibiotic plates. The success for the deletion was confirmed by PCR of the deletion region, HPLC-MS analysis and UV measurement. All primers for the construction and verification of the deletion are shown in supplementary material (Table S4).

PSEUDOBACTIN INTERACTION STUDIES

Feeding experiments were performed by growing SynCom members in medium supplemented with *P. koreensis* WT and $\Delta pvdI/J$ mutant supernatant. Therefore, the supernatant of 1 L *P. koreensis* WT and mutant was collected by culturing the strains in MM9 medium. Cells were harvested at 8.000 rpm for 5 minutes and supernatant was sterilized by filtering (0.2 μ m pore size). The optimal growth media were developed as MM9 and enriched MM9 medium supplemented with the sterile supernatant of *P. koreensis* WT or $\Delta pvdI/J$ mutant. For a detailed recipe, see supplements (Table S1 and S2). Since MM9 is a minimal medium, some SynCom strains were not able to grow under these conditions. For these organisms, enriched MM9 medium was used with minimal additions of NB or PDA medium. For the growth curves, each SynCom strain was pre-cultured, washed and diluted to OD₆₀₀ = 0.2 with MM9 or enriched MM9 medium. 1 ml of each dilution was added into one well of a 24-well plate. Experiments were performed in triplicates. Plates were incubated at 22 °C and 100 rpm shaking, and OD₆₀₀ was measured after T₀ = 0 h; T₁ = 16 h; T₂ = 18 h; T₃ = 20 h; T₄ = 22 h; T₅ = 24 h; T₆ = 40 h; T₇ = 42 h with a TECAN 2000 (Tecan, Switzerland) device. For additional growth curves with *Arthrobacter humicola*, 48-well plates and 800 μ l total volume were used. Strain was diluted to OD₆₀₀=0.2 in the well. For complementing the inhibiting effect of pseudobactin, *A. humicola* was further investigated in WT + FeSO₄ MM9 medium. For complementing the $\Delta pvdI/J$ mutant, *A. humicola* was cultivated in *pvdI/J* + pure pseudobactin MM9 medium (Table S1 and S2). Growth curves for all SynCom members were prepared in two independent experiments.

Additionally, cross-streaking experiments of all SynCom members against *P. koreensis* WT and $\Delta pvdI/J$ were performed on F-base agar to investigate inhibitions caused by the production of pseudobactin. See materials and methods part -Cross-streaking experiment- for more details.

AMPLICON SEQUENCING

Sample preparation. For investigating the relative abundance of SynCom members *in vitro*, amplicon sequencing from the microorganisms grown on MM9/7 agar plates was performed. In detail, each SynCom member was pre-cultured in 20 ml liquid medium and harvested after 48 h incubation by centrifugation at 7.000 rpm for 5 minutes. Cells were washed twice using 10 ml of 10 mM MgCl₂ and resuspended in MgCl₂. OD₆₀₀ = 1 was adjusted, and strains were mixed in equal volumes. 1 ml mixture was streaked on MM9/7 agar plates and incubated for 5 days at 22 °C. After incubation, cells were scratched off the agar in bead filled tubes (MP fastDNA spin kit) and immediately frozen in liquid nitrogen. Samples were prepared in three independent experiments.

For investigating the relative composition of the SynCom *in planta*, amplicon sequencing from plants was performed. Therefore, SynCom WT, SynCom mutant and SynCom pseudobactin sprayed plants were picked in bead filled tubes (MP fastDNA spin kit) after 5 and 9 days of incubation. Tubes were immediately frozen in liquid nitrogen and plants were crushed at – 30 °C using a Precellyse device (Bertin, France) (2 x 20 s, 6.400 rpm). Samples were prepared in three independent experiments. In each experiment, each group was sampled in biological triplicates including two pooled technical replicates. In total 108 plants were sampled.

DNA isolation. DNA for amplicon sequencing was isolated using the MP fastDNA spin (MP biomedical, Germany) kit for soil according to manufacturer's instructions. DNA was eluted in 75 µl elution buffer. Concentration was measured by nanodrop.

Library preparation. The library preparation was done following the studies of Agler *et al.*, and Mayer *et al.*, [15, 33]. Shortly, DNA was used to amplify the 16S rRNA region of bacteria and the ITS2 region of fungi by PCR. A second PCR was used to introduce custom-designed, single indexed Illumina sequencing adapters to each sample. The primers used contained blocking regions to limit the amplification of plant chloroplast DNA as described in the study of Mayer *et al.*, All libraries were pooled in equimolar concentrations and sent to NCCT/University of Tübingen for MiSeq Illumina sequencing (300 cycles). Primers and Illumina adapters used in this study can be found in the article of Agler *et al.* [15]

Data analysis. Quality control and trimming of raw reads were performed using fastp (v0.23.4) [34] with default parameters. The demultiplexed raw reads were denoised using DADA2 [35] truncating left and right reads at the 250th and 200th positions, respectively, based on a manual inspection of quality scores. The taxonomic analysis of the amplicon sequence variants (ASV) was carried out using QIIME2 with sklearn classifier [36] against the SILVA database (v138, 99%) [37] for bacterial sequencing runs and the UNITE database (v0.9, 99%) [38] for fungal sequencing runs. The raw read counts for ASVs were exported from QIIME artefacts

and used in further analysis. Any taxa that have less than 1% cumulative mean relative abundance were grouped under the category "Other" in the figures. ASVs assigned to *Chloroplast sp.* and *Penicillium sp.* were excluded from the analysis. Significances between experimental conditions and taxa were tested by a Kruskal test, followed by pairwise Wilcoxin test. *P*-values were corrected using Bonferroni. Additionally, a t-test was performed to determine differences in organismic abundances (p -value $\leq 0.05\%$).

RESULTS

SynCom members are mainly positively correlated with the epiphytic microbiome

The SynCom was assembled in garden experiments from *Arabidopsis thaliana* leaves based on the occurrence of the taxonomic unit in plant samples. Bacteria present in > 98 % and fungi present in > 95 % of plant samples during different seasons were collected [13].

Since the SynCom was assembled from *A. thaliana* grown on an experimental field, we first aimed to analyze the abundance and connectivity of the SynCom members in naturally grown *A. thaliana* plants. Therefore, we correlated the co-abundance of OTUs with closest similarity to the SynCom members in a new dataset from wild *A. thaliana* samples. The data was generated in the study from Mahmoudi *et al.*[24]. The authors therefore sampled plants over 5 years at different spots around Tübingen, isolated DNA and performed 16S / ITS2 amplicon sequencing. The positive and negative correlations shown in the network were based on co-abundance in all field samples. OTUs showing no significant abundance dependencies ($p > 0.001$) are not shown in the network. Alignment of the most common sequence of each OTU to 16S rRNA and ITS2 sequences of SynCom members facilitated the identification of OTUs closest related SynCom members (Table 2). The generated network ($p \leq 0.001$) allowed the identification of positive (blue) and negative (red) correlations between SynCom members and the *A. thaliana* epiphytic microbiome (Fig. 1a).

Overall, SynCom organisms showed a total of 4.116 correlations with OTUs from the phyllosphere microbiome. Among these correlations, the majority (59.5%) was positive, while 40.5% were negative. Four SynCom members, namely *Bacillus altitudinis*, *Frigoribacterium faeni*, *Dioszegia hungarica*, and *Rhodotorula kratchovilovae*, remained uncorrelated within the network due to their infrequent occurrence and/or low read counts (Table S5). Among the represented SynCom strains, nine exhibited notably high positive correlations (> 60% OTUs positively correlated) within the microbiome. Noteworthy exceptions included *Arthrobacter humicola* (54.6 % OTUs positively correlated), which also displayed the highest total number of correlations (811 interactions), along with *Flavobacterium pectinovorum* (46.6 % OTUs positively correlated) and *Nocardioides cavernae* (44.1 % OTUs positively correlated). The highest positive correlation was recorded for *Sporobolomyces roseus* (82.8 %), closely followed by *Pseudomonas koreensis* (74.0 %) (Fig S3). Analysis of connections between SynCom members derived from the microbiome network revealed predominantly positive associations, comprising 20 correlations, with only two relationships exhibiting negative ratios (Fig. 1b). Particularly noteworthy were the highly positive correlations observed for *F. pectinovorum* and *Sphingomonas faeni*, both displaying positive linkages with six other SynCom members. Notably, *Paenibacillus amylolyticus* emerged as the sole OTU exhibiting

negative correlations with two other SynCom members (*F. pectinovorum* and *Rhizobium skierniewicense*). In summary, the SynCom members exhibited predominantly positive correlations within the microbiome, both with other microbiome constituents and among themselves.

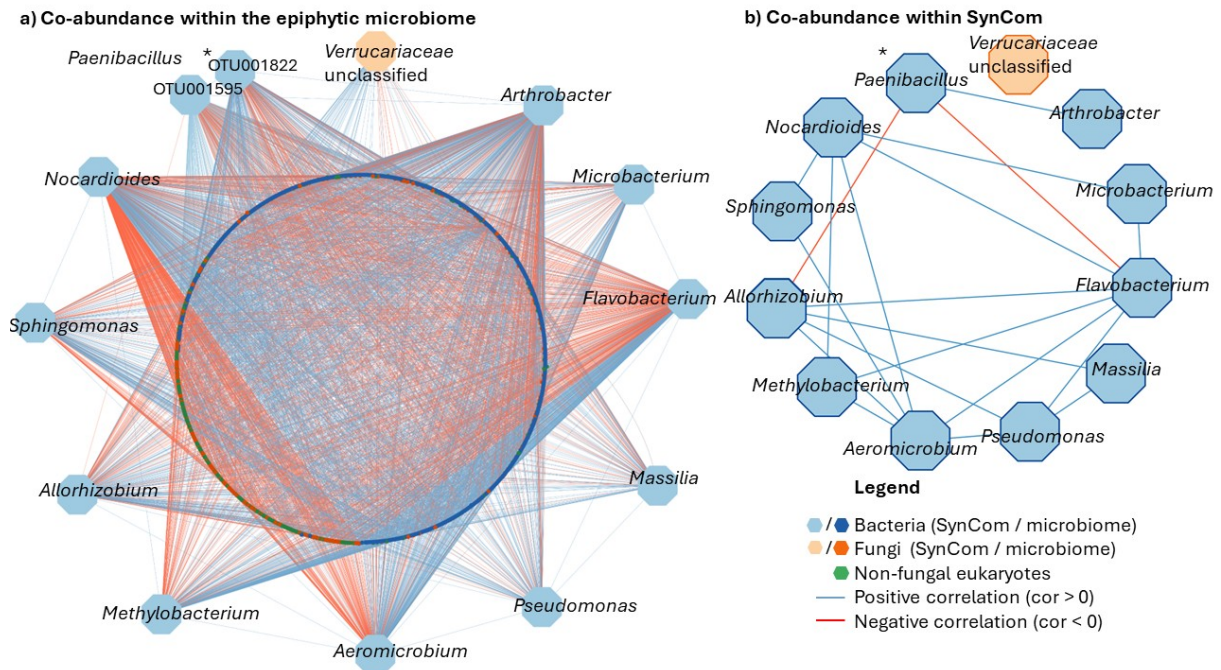


Figure 1: Correlation of SynCom members within the *Arabidopsis thaliana* epiphytic microbiome based on co-abundance. a) Each node represents an OTU calculated by 16S rRNA/ITS2 Illumina amplicon sequencing. OTUs were identified on genus level. Based on 16S rRNA/ITS2 similarity (BlastN) to SynCom members, closest related OTUs were presented. The network shows correlations with $p \leq 0.001$. Positive correlations (cor > 0) are indicated with blue edges, negative correlations (cor < 0) with red edges. * OTU001822 and OTU001595 showed the same BlastN similarity to *P. amylolyticus* and were both kept in the network. B) SynCom related OTUs and edges were extracted from network a. * OTU001822 showed less, but same correlations as OTU001595 and therefore was replaced.

Table 2: Correlation network OTU annotation by 16S rRNA/ITS2 BlastN against SynCom members. The most common 16S rRNA/ITS2 sequence of each OTU was blasted against 16S RNA/ITS2 regions of SynCom members to identify the closest related nodes in the correlation network for each SynCom members.

Node name (family or genus)	OTU number	Related SynCom strain	BlastN similarity of 16S rRNA/ITS2 in %
<i>Verrucariaceae</i>	OTU00184	<i>S. roseus</i>	100.00
<i>Arthrobacter</i>	OTU000363	<i>A. humicola</i>	99.50
<i>Microbacterium</i>	OTU000360	<i>M. proteolyticum</i>	100.00
<i>Flavobacterium</i>	OTU000009	<i>F. pectinovorum</i>	99.20
<i>Massilia</i>	OTU000172	<i>M. aurea</i>	98.90
<i>Pseudomonas</i>	OTU000144	<i>P. koreensis</i>	99.50

<i>Aeromicrobium</i>	OTU000030	<i>A. fastidiosum</i>	98.90
<i>Methylobacterium</i>	OTU000003	<i>M. goesingense</i>	98.90
<i>Allorhizobium</i>	OTU000014	<i>R. skierniewicense</i>	99.70
<i>Sphingomonas</i>	OTU000002	<i>S. faeni</i>	100.00
<i>Nocardioides</i>	OTU000071	<i>N. cavernae</i>	99.70
<i>Paenibacillus</i>	OTU001595	<i>P. amylolyticus</i>	100.00

Pairwise interactions do not explain relations from correlation networks

We further investigated whether relations shown in the correlation network (Fig.1b) could be followed up in pairwise interactions *in vitro*. Therefore, we compared the network data with pairwise interactions observed between SynCom members in cross-streaking experiments on agar plates. Each organism within the SynCom was subjected to cross-streaking against every other member, resulting in a total of 256 tested interactions (Fig 2).

While most strains exhibited neutral co-existence, six reproducible growth-promoting interactions were identified among SynCom members across two repetitive experiments. Notably, the yeast *D. hungarica* promoted the growth of four SynCom members (*Methylobacterium goesingense*, *F. pectinovorum*, *S. faeni*, and *R. skierniewicense*) on their optimal growth agar (PDA). Only one positive interaction was observed between the bacteria *F. pectinovorum* and *N. cavernae*, aligning with the positive correlation observed in the correlation network. The pairwise interaction network predominantly featured negative interactions (Fig. 2). A total of 37 inhibitory relationships were identified, exhibiting 59 % reproducibility across three independent experiments and 41 % occurring in two of the three repetitions. Among these, 21 interactions originated from bacteria, and 22 from fungi. Notably, *B. altitudinis* emerged as the most potent bacterial inhibitor within the SynCom, displaying inhibitory effects against 12 SynCom strains in pairwise assessment. However, despite its strong inhibitory activity, *B. altitudinis* was not represented in the correlation networks due to low OTU reads for the strain (Table S5).

Another prominent inhibitor in pairwise interactions was *P. koreensis*, which inhibited four other SynCom members (*M. goesingense*, *F. faeni*, *D. hungarica*, *S. roseus*) reproducibly. Interestingly, *P. koreensis* exhibited solely positive correlations with SynCom members within the correlation network.

The most susceptible strain was *M. goesingense*, which displayed sensitivity to five partners in the cross-streaking experiment. However, the strain showed a high number of positive relationships with the SynCom and other epiphytic microorganisms in the correlation network.

Among the fungi, *R. kratochvilovae* (11) and *S. roseus* (10) exhibited the highest number of inhibitory interactions. Interestingly, the inhibitory potential of both fungi was only evident when grown on PDA. *R. kratochvilovae* and *S. roseus* consistently restricted the growth of potent

bacterial inhibitors such as *B. altitudinis* and *P. koreensis* on this medium. Conversely, *B. altitudinis* and *P. koreensis* inhibited *S. roseus* on NA. These findings underscore the significant impact of optimal nutrient availability on the SynComs pairwise interactions. Collectively, contrary to the correlation network analysis, pairwise interactions unveiled a substantial repertoire of inhibitory interactions among SynCom members. This prompted us to investigate the reasons behind this discrepancy.

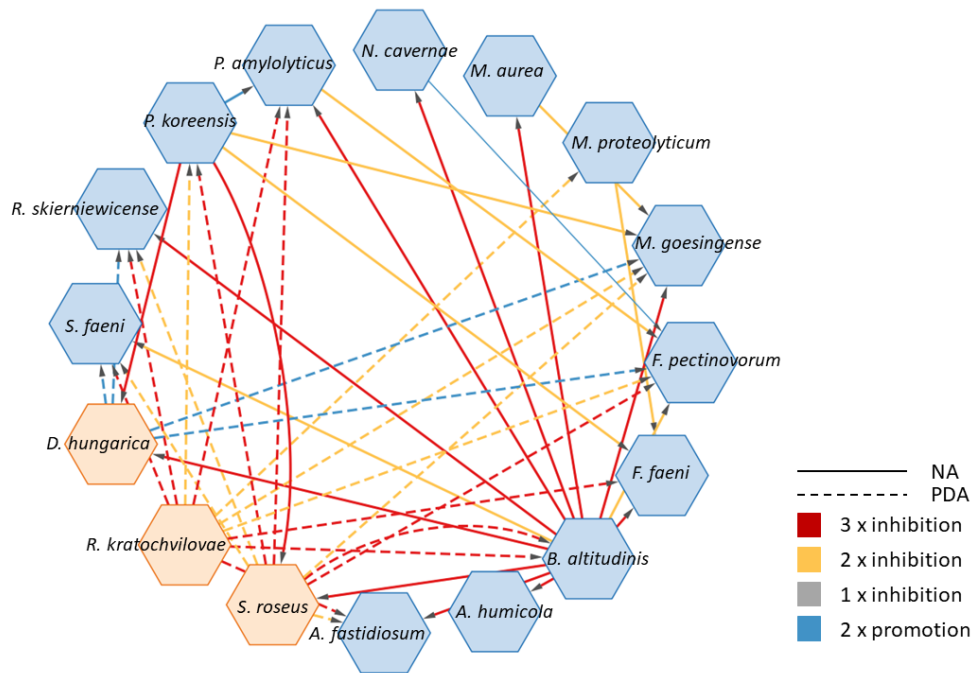


Figure 2: Pairwise interactions of SynCom members in vitro. Strains were grown on optimal growth medium for three days at 22 °C (NA for bacteria, PDA for fungi). Contact zones were visually assessed for growth-promoting or inhibiting interactions (examples see Fig. S1). SynCom bacteria are displayed as blue nodes, SynCom fungi as orange nodes.

The SynCom encodes a variety of secondary metabolite gene clusters

Antagonistic microbe-microbe interactions are a common phenomenon in pairwise interactions of members from the *A. thaliana* leaf microbiome [17, 39]. Most inhibitions are attributed to the vast repertoire of antimicrobial compounds synthesized by a diversity of biosynthetic enzyme classes [16, 17]. To investigate whether the observed inhibitory pairwise interactions are caused by antimicrobial compounds, we analyzed the potential of each SynCom member to produce secondary metabolites. Therefore, we utilized AntiSMASH, a tool for predicting biosynthetic gene clusters (BGCs). Figure 3 illustrates the abundance of BGCs among SynCom strains, totaling 103 gene clusters. *P. amylolyticus* encodes the highest number of BGCs (13), followed by *B. altitudinis* (12), *R. skierniewicense* (11), *P. koreensis* (10), and *M. goesingense* (10). Interestingly, these organisms, except for *M. goesingense*, exhibit significant potential for antimicrobial compound production, based on the presence of RiPP, PKS, NRPS, and hybrid gene clusters. Furthermore, examination of gene clusters from the inhibitor strains in pairwise interactions revealed similarities to BGCs encoding known antimicrobials. For instance, *B. altitudinis* possesses BGCs closely resembling those encoding antimicrobials such as bacilysin (100 % similarity), surfactin (85 % similarity), and bacillibactin (53 % similarity). *P. koreensis* exhibits genes associated with the production of the siderophore pseudobactin from the pyoverdine class, while a 100 % similarity to the BGC of polymyxin B was predicted for one NRPS gene cluster of *P. amylolyticus*. In contrast, strains showing higher sensitivity in pairwise interactions, such as *F. pectinovorum* and *F. faeni*, lack NRPS and PKS gene clusters, and are characterized by the presence of terpene and betalactone BGCs (Table S6). The two strong inhibitory fungi *R. kratochvilovae* and *S. roseus* carry a low number of BGCs (4) compared to their bacterial equivalents. Both strains contain two NRPS gene clusters with no similarity to known BGCs. Notably, *D. hungarica* carrying 3 NRPS BGCs shows no inhibition in pairwise interactions.

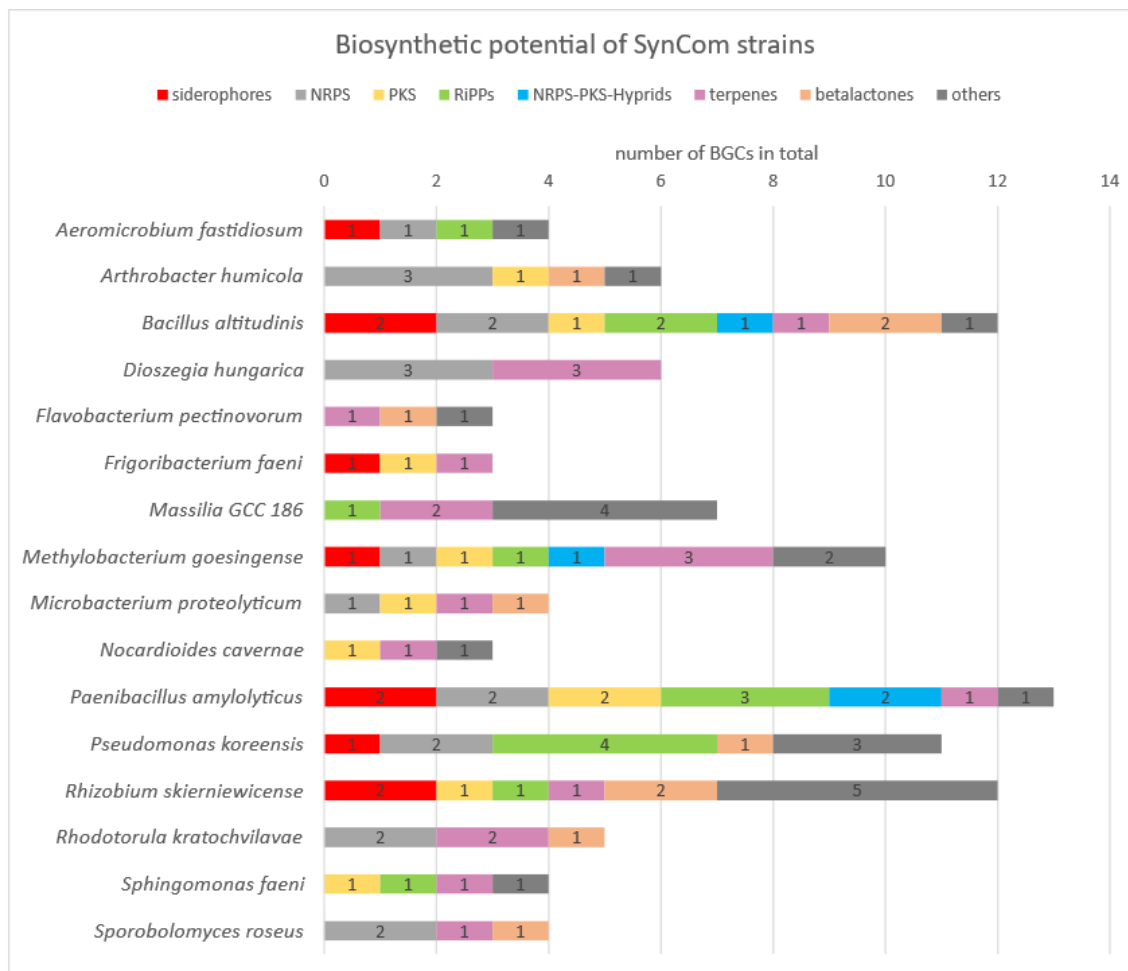


Figure 3: Potential of SynCom strains to produce secondary metabolites. The potential to produce secondary metabolites is based on the presence of biosynthetic gene clusters BGCs as revealed by AntiSMASH 7 analysis.

Pairwise inhibitors are not inherently dominant strains in the SynCom *in vitro*

As a next step, we wanted to investigate whether pairwise interactions play a role in shaping the SynCom *in vitro*. We posited that inhibitor strains might exhibit a colonization advantage within the community by producing antimicrobial compounds, leading to their dominant abundance. To investigate this, amplicon sequencing of the entire SynCom cultivated together on minimal agar was conducted (Fig. 4). Therefore, equal volumes of $OD_{600} = 1$ mixtures of each strain were mixed. For the experiment, MM9/7 minimal agar was chosen to mimic the limited nutrient bioavailability on plant leaf surfaces [40, 41]. Following a 5-day incubation period, *P. koreensis* emerged as the most prevalent bacterium within the SynCom, with an 89 % relative abundance. Notably, the relative abundance of *P. koreensis* increased fourfold over the incubation period (Fig. S5). Regarding fungi, *R. kratochvilovae* showed the highest relative abundance at 70 %. Interestingly, both *R. kratochvilovae* and *P. koreensis*, recognized as

potent inhibitor strains in pairwise interactions, displayed the highest abundance within the SynCom on the plate. In contrast, *B. altitudinis*, able to inhibit 14 SynCom strains in the preceding experiment, showed a ~ 19-fold reduction in abundance over the incubation period, resulting in a total relative abundance of < 0.5 % (Fig. S4). Strains susceptible to inhibition, such as *F. pectinovorum* and *R. skierniewicense*, were relatively abundant compared to the main bacterial inhibitor strain, *B. altitudinis*. Furthermore, besides *P. koreensis*, *F. pectinovorum* was the only bacterial strain with high abundance after the incubation period. Although the strong inhibitors *P. koreensis* and *R. kratochvilovae* were dominant colonizers, the low abundance of other strong inhibitor strains like *B. altitudinis* and *S. roseus* indicates that inhibitors do not inherently have a colonization advantage within the SynCom *in vitro*. Therefore, pairwise interactions are not necessarily reflected by the composition of the SynCom on agar plates.

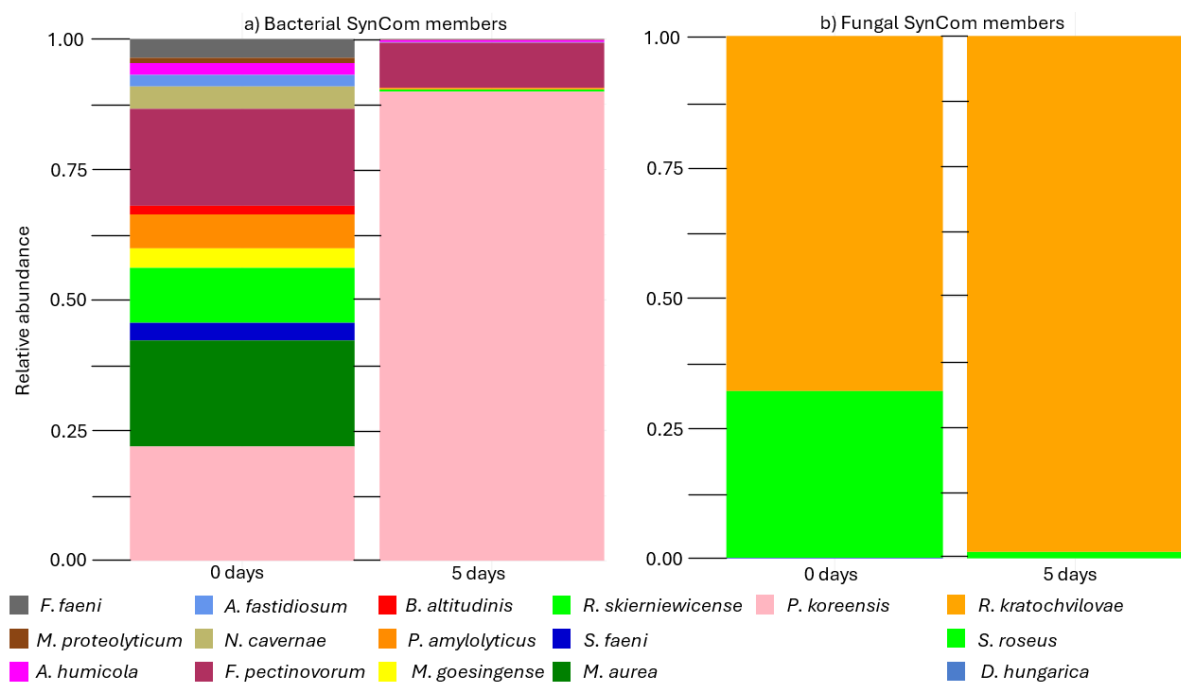


Figure 4: SynCom composition *in vitro* based on the relative abundance. The SynCom composition *in vitro* was calculated as relative abundance of each strain by 16S rRNA/ITS2 MiSeq Illumina amplicon sequencing from MM9/7 agar at inoculation after 0 days and after 5 days incubation at 22 °C. a) Histograms show the relative abundance of bacterial SynCom members calculated by amplicon sequencing using 16S rRNA specific primers. b) Histograms show the relative abundance of fungal SynCom members calculated by amplicon sequencing using ITS2 specific primers.

Pseudobactin drives inhibitory pairwise interactions of *Pseudomonas koreensis*

Next, we aimed to answer the question why strong pairwise interactions are not reflected in the correlation networks. Therefore, we aimed to identify the mechanism behind a specific

inhibitory pairwise interaction, track it through subsequent studies from pairwise interactions to co-cultures with the entire SynCom, and finally, examine it *in planta*.

Due to its high abundance in the SynCom on the plate, its ability to inhibit individual SynCom members and its opposing interactions in the correlation network, *P.s koreensis* was chosen for further investigations. Previous studies showed that a pyoverdine siderophore with antimicrobial activity contributes to shaping the root microbiome of *A. thaliana*, suggesting its importance in microbial communities [16]. Since a BGC encoding a pyoverdine was detected in the *P. koreensis* genome, we investigated its role in the leaf associated SynCom. The fluorescent compound was isolated, and its structure confirmed by NMR as pseudobactin, a member of the pyoverdine siderophore class (Fig S6-S13). The successful creation of a deletion mutant was verified by HPLC-MS (Fig. S14). Growing strains in the presence or absence of pseudobactin showed inhibitions of growth for eight SynCom members (Fig. 5c) (growth curves of SynCom strains: Fig. S15). *A. humicola*, was significantly inhibited by pseudobactin. The addition iron to *A. humicola* cultures abolished the inhibiting effect (Fig. 5a), leading to normal growth in pseudobactin-containing medium. The restoring of the inhibition by the addition of iron indicates that *P. koreensis* inhibits SynCom members indirectly by the chelation of iron. The addition of purified pseudobactin to the supernatant of the pseudobactin mutant strain, reestablished the inhibiting effect (Fig. 5b).

The inhibitory effects of *P. koreensis* on four SynCom members can therefore be explained by the production of pseudobactin. Notably, three strains, namely *R. kratochvilovae*, *B. altitudinis*, and *A. humicola*, which were not initially inhibited in pairwise interactions, demonstrated susceptibility when exposed to the siderophore in growth curves. The five SynCom strains (*N. cavernae*, *M. goesingense*, *D. hungarica*, *Massilia aurea* and *R. skierniewicense*) exhibited instability in growth when cultivated in minimal medium. Consequently, it was not possible to ascertain their growth rate in the presence of pseudobactin, precluding the formulation of definitive statements regarding their response to this antimicrobial agent. To investigate the effect of pseudobactin under condition, where these strains were able to grow, cross streaking experiments on siderophore production agar (f-base agar) were performed (Fig 5c). Therefore, all SynCom members were streaked against *P. koreensis* WT and the pseudobactin mutant. Although, *M. goesingense*, *N. cavernae* and *D. hungarica* were sensitive against both, WT and mutant *P. koreensis*, they showed larger zones of inhibition in contact with the wildtype, indicating some sensitivity to pseudobactin but also other compounds produced by *P. koreensis*. *M. aurea* and *R. skierniewicense* were resistant against pseudobactin on f-base agar. Interestingly, the second most abundant bacterium, *F. pectinovorum*, confirmed its resistance to *P. koreensis* WT observed in pairwise interactions in the growth curves but showed susceptibility to pseudobactin on F-base agar. Five SynCom members (Fig 5c, red) were susceptible to pseudobactin in growth curves, but not on f-base agar. In summary,

pseudobactin is a compound of *P. koreensis* showing antimicrobial activity in pairwise interaction studies on siderophore promotive agar (F-base) and in minimal medium.

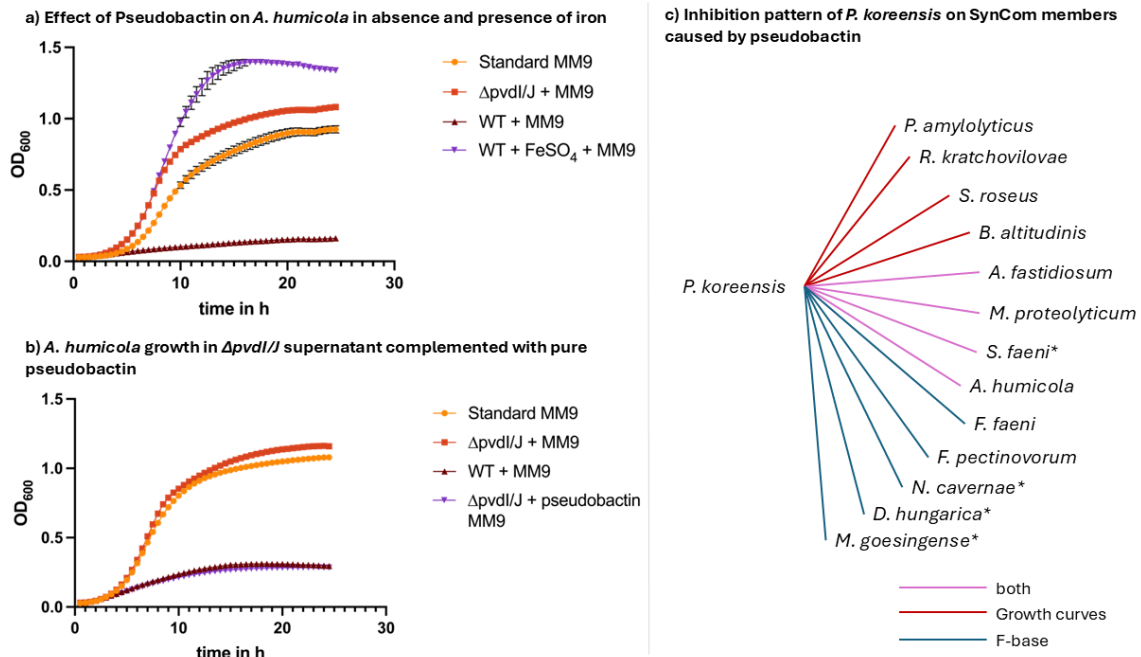


Figure 5: *In vitro* interaction of Pseudobactin with single SynCom members Growth curves of *A. humicola* were measured automatically in a TECAN 2000 device as OD₆₀₀ in 1 h intervals at 22 °C and 200 rpm shaking a) Growth curve of *A. humicola* in MM9 medium enriched with sterile supernatant of *P. koreensis* WT and *P. koreensis* $\Delta pvdI/J$ mutant. The growth in presence of pseudobactin complemented with FeSo₄ is shown in purple. Growth curves were prepared in triplicates and reproduced once. b) Repetition of growth curve of *A. humicola* with complementation of $\Delta pvdI/J$ mutant supernatant with pure pseudobactin (purple). c) Summary of inhibitions of pseudobactin on SynCom members in growth curves and cross streaking experiment on F-base agar. Cross-streakings on F-base agar were prepared in two independent experiments. * Strains showing inhibition zones in contact with both, WT and mutant *P. koreensis* but significantly bigger inhibition zones in contact with WT.

Pseudobactin interactions show no effect in a community context *in planta*

Since the pseudobactin-based inhibitory interactions of *P. koreensis* are not reflected in correlation networks, we further wanted to investigate which role pseudobactin plays within the SynCom *in planta*. Given the known influence of pyoverdines on microbiome composition, we assessed the contribution of pseudobactin by applying three different SynCom preparations to sterile *A. thaliana* plants through plant spraying: the wild type SynCom containing *P. koreensis* (SynCom WT), the SynCom with the *P. koreensis* pseudobactin mutant (SynCom mutant), and the SynCom mutant supplemented with pure pseudobactin (SynCom pseudobactin). Using amplicon sequencing, we determined SynCom member abundance on plants. After a 5-day and a 9-day incubation period, *P. koreensis* and *F. pectinovorum* emerged as the dominant bacteria, while *R. kratochvilovae* prevailed as the dominant yeast across all three experimental

groups. Notably, there were no significant differences in SynCom overall relative abundance between all three groups (SynCom WT, SynCom mutant, SynCom pseudobactin). To assess whether the presence or absence of pseudobactin had an impact on individual SynCom members, the relative abundance of each strain was separately analyzed, revealing no significant alterations among the different groups (Fig. S16 and Fig. S17). The results display that even though it shows strong inhibiting activity on SynCom strains in pairwise interactions, pseudobactin does not affect the SynCom composition or relative abundance of any member *in planta*.

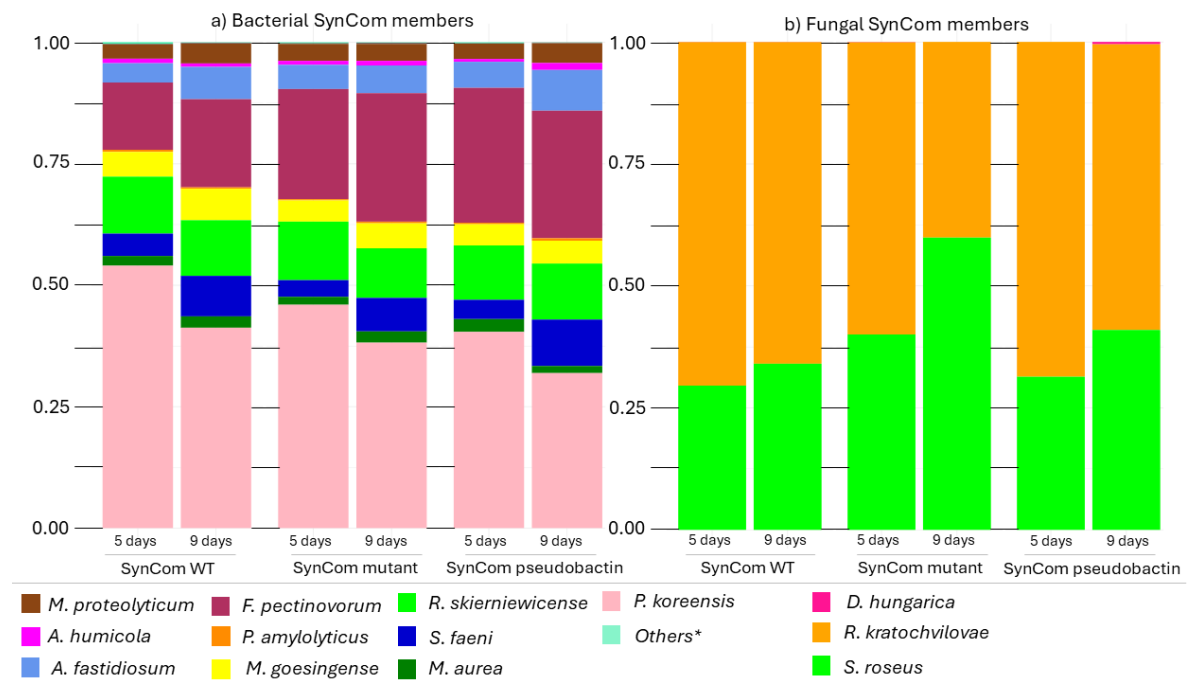


Figure 6: The effect of pseudobactin on the SynCom composition *in planta*. The composition of the SynCom is based on the relative abundance of each member calculated from 16S rRNA/ITS2 MiSeq Illumina amplicon data. Three-week-old plants were sprayed with 0.2 OD₆₀₀ SynCom mixture and incubated at 22 °C in a short light chamber. The sampling was done at two time points (5 days and 9 days after spraying). a) Histograms show the relative abundance of bacterial SynCom members calculated by amplicon sequencing using 16S rRNA specific primers. b) Histograms show the relative abundance of fungal SynCom members (fungi) calculated by amplicon sequencing using ITS2 specific primers. * Others include remaining SynCom members with rel. abundances < 1 % (*B. altitudinis*, *F. faeni* and *N. cavernae*)

DISCUSSION

In our study we aimed to investigate microbe-microbe interactions of a synthetic plant leaf community within the epiphytic microbiome compared to pairwise interaction studies. Our findings revealed notable disparities between pairwise interactions observed *in vitro* and those

inferred from correlation networks *in planta*. Whereas the correlations in the microbiome were mainly positive, pairwise interactions showed a huge number of inhibitory interactions between SynCom members. The huge repertoire of genes to produce secondary metabolites indicated that pairwise interactions are driven by antimicrobial compounds. Accordingly, we identified pseudobactin from *Pseudomonas koreensis* as a potent antimicrobial agent against several SynCom members in pairwise interaction experiments. However, pseudobactin had no effect on the SynCom composition *in planta*, mirroring the correlation networks, where *P. koreensis* showed no negative correlation to any SynCom member.

Pairwise interactions do not affect co-abundance of SynCom members in the epiphytic microbiome.

Pairwise interaction studies via cross streaking experiments are a common method for the identification of secondary metabolites, especially antimicrobial compounds. AntiSMASH analysis revealed the high potential of *P. koreensis*, *Bacillus altitudinis* and *Paenibacillus amylolyticus* to produce secondary metabolites, and it was already shown that secondary metabolites produced by plant microbiome members drive strong pairwise interactions [16]. Therefore, it is most likely that the observed inhibitions in the cross-streaking experiments are based on antimicrobials. Why the interactions within our SynCom are not reflected in the correlation networks remains unclear. Even the addition of pure pseudobactin did not alter the SynCom significantly, suggesting that the inhibitory effect of pseudobactin is limited to pairwise interactions and plays a subsidiary role in a microbiome context. Although Getzke *et. al.* could show an effect of pyoverdine on the composition of the root microbiome [16], pyoverdines might play a minor role in shaping plant leaf associated communities as compared to root microbiomes. Indeed, while in the rhizosphere iron is limiting and production of siderophores may confer a growth advantage [41, 42] the phyllosphere has higher iron concentrations, decreasing the need for siderophore production [43]. Another possibility might be, that pseudobactin was depleted by other SynCom members as this was shown to be the case for lipopeptides produced by *Pseudomonas* spp [44, 45].

We hypothesized that strong inhibitors would have a colonization advantage in communities. Therefore, we anticipated an increase in the relative abundance of the inhibitory strain and a decrease in that of the sensitive strains over the incubation period. However, for *B. altitudinis*, we observed the opposite effect. Although the genome of this strain encodes a high potential to produce secondary metabolites — possibly a reservoir activated only in the presence of certain competitors or pathogens [46, 47] — the strong inhibitor *B. altitudinis* might be constrained by the community. Long-term co-evolution of plant microbiomes has allowed the adjustment of an optimal balance in microbial composition and microbe-microbe interactions [41, 48, 49]. Thus, it is not surprising that a potent member of the synthetic community (SynCom) is unable to dominate others, despite its substantial antimicrobial potential. This restraint, for example through suppressed production of antimicrobial compounds, can be

further investigated using transcriptomic approaches. Since *B. altitudinis* shows a low relative abundance in the SynCom, the colonization density could have not been sufficient to activate the production of antimicrobials. Tyc *et al.*, demonstrated that the antimicrobial activity of certain soil microbiome members is significantly suppressed in co-cultures with commensals compared to monocultures, attributing this to interference with the quorum sensing apparatus or nutrient limitations [50].

Nevertheless, the question remains what *P.s koreensis*, *Flavobacterium pectinovorum* and *Sporobolomyces roseus* have in common to assert their dominant abundance in the SynCom. It is known that both, *S. roseus* and *P. koreensis*, produce exopolysaccharides (EPS), which help them survive harsh environmental conditions [51]. It is furthermore known that EPS are important components of biofilms and that microbiome members can benefit from biofilm producers in their community [52, 53]. *S. roseus* is additionally capable of breaking down leaf surface waxes improving the surface adhesion of organisms on plants [54]. Highlighting their supportive roles, *S. roseus* and *P. koreensis* showed the highest number of positive correlations with the epiphytic microbiome. Their positive linkage strengthens recent findings that adaption by using extracellular metabolites might be a driving force within microbial communities rather than competition by producing antimicrobials [55]. Within the SynCom, *P. koreensis* was again one of the strains counting high number of positive relations but was exceeded by *F. pectinovorum* and *Sphingomonas faeni*. Interestingly, *F. pectinovorum* was also a dominant bacterium in the SynCom *in vitro* and *in planta*, despite being highly sensitive in pairwise interactions. *Flavobacterium* spp. are common members of plant microbiomes and known for their great ability to degrade extracellular macromolecules like starch. Furthermore *Flavobacterium* spp. indirectly promote plant growth, suggesting that they support the microbiome by biotransformation [10, 56, 57]. The high abundance and positive linkage of *F. pectinovorum* in the SynCom strengthens the hypothesis that synergism plays a huge role in shaping microbial communities.

Correlation networks for the pre-selection of relevant microbe-microbe interactions

Two correlations of SynCom members in the correlation network mirrored the findings in pairwise interactions. *Nocardioides cavernae* and *F. pectinovorum* showed a growth promoting effect in cross-streaking experiments and were positively correlated in the epiphytic microbiome. Moreover, *P. amylolyticus* inhibited *F. pectinovorum* *in vitro* and the strains were negatively correlated in the microbiome. Whether the pairwise interactions for these strains are truly reflected in correlation networks needs to be further investigated. The mechanistic basis behind the positive connections of *N. cavernae* and *F. pectinovorum* in the plant microbiome is not yet understood. For *P. amylolyticus* strains it was already shown that they are able to produce polymyxin antibiotics [58, 59]. Interestingly, the *P. amylolyticus* strain from the SynCom carries a gene cluster with 100 % similarity to polymyxin B. The production of the

compound might explain the antimicrobial activity in pairwise interactions since it is potent against gram negative bacteria like *F. pectinovorum* [60]. Whether the inhibitory interaction is so dominant to be observed within the epiphytic microbiome in correlation networks, remains unknown but it is a promising start for future investigations. Furthermore, it shows that correlation networks are promising methods for preselecting microbe-microbe interactions involved in microbiome shaping. Several publications successfully used bottom-up methods such as pairwise interaction analysis for further investigations in microbial communities and microbiomes [16, 17, 61]. As shown by Sun *et al.*, pairwise interaction studies were successfully combined with genome scale metabolic modelling to explain positive and negative correlations in a synthetic biofilm community [62].

In correlation networks, OTUs for four SynCom members, including *B. altitudinis*, were absent due to the read count threshold applied in the study. We hypothesize that these strains may have been outcompeted in their niches by closely related species, as previously observed for the gut microbiome [63]. The identification of the SynCom members as part of the core microbiome in the original study, from which the SynCom was assembled [13], and the low abundance of *B. altitudinis* and others in the correlation network raw data [24], underscore the spatiotemporal dependency of microbiome compositions. Therefore, it is essential to recognize that correlation networks reflect not only microorganismic interactions but also environmental influences. Mahmoudi *et al.* demonstrated that up to 25% of correlations in the *A. thaliana* leaf microbiome can be attributed to environmental factors. However, the majority of correlations were not explainable by environmental factors investigated by the authors suggesting underlying microbe-host and microbe-microbe interactions [24].

Our findings indicate that when investigating microbiome interactions on a pairwise basis, there is a high likelihood that these interactions prove to be less significant than expected. As soon as three and more interaction partners exist together in a model system, the complexity of the interaction network increases drastically, limiting the meaningfulness of pairwise interaction approaches [64]. Therefore, beyond-pairwise interaction methods especially computational approaches are getting more and more into the focus of research [65, 66]. Our results demonstrate the limitations of pairwise interaction approaches and suggest the use of microbiome-wide studies like correlation networks for the investigation of dynamics shaping and stabilizing microbial communities. Furthermore, the use of synthetic communities can give insights into the importance of a compound or strain in a microbiome context and therefore is a promising method for investigating microbiome dynamics.

DATA AVAILABILITY

1. The raw datasets generated from amplicon sequencing for the relative abundance of SynCom members *in vitro* and *in planta* are available in the Zenodo repository (Strong pairwise interactions do not drive interactions in a plant leaf associated microbial community), [<https://zenodo.org/records/12795858>] DOI: 10.5281/zenodo.12795858
2. The datasets for the visualization of the correlation networks are available in the Zenodo repository (Strong pairwise interactions do not drive interactions in a plant leaf associated microbial community), [<https://zenodo.org/records/12795858>], DOI: 10.5281/zenodo.12795858
3. The OTU data and workflows used for correlation network calculation are available in the Zenodo repository (Strong pairwise interactions do not drive interactions in a plant leaf associated microbial community), [<https://zenodo.org/records/12795858>], DOI: 10.5281/zenodo.12795858
4. All raw data for correlation networks based on co-abundance analysed during this study are included in the published article of Mahmoudi *et al.*, and its supplementary information files.

REFERENCES

1. Bhat MA, Mishra AK, Jan S, Bhat MA, Kamal MA, Rahman S *et al.* Plant growth promoting rhizobacteria in plant health: A perspective study of the underground interaction. *Plants*. 2023;**12**:629
2. Durán P, Thiergart T, Garrido-Oter R, Agler M, Kemen E, Schulze-Lefert P *et al.* Microbial interkingdom interactions in roots promote arabidopsis survival. *Cell*. 2018;**175**:973-83.e14 <https://doi.org/https://doi.org/10.1016/j.cell.2018.10.020>
3. Gupta A, Mishra R, Rai S, Bano A, Pathak N, Fujita M *et al.* Mechanistic insights of plant growth promoting bacteria mediated drought and salt stress tolerance in plants for sustainable agriculture. *International Journal of Molecular Sciences*. 2022;**23**:3741
4. Armada E, Probanza A, Roldán A, Azcón R. Native plant growth promoting bacteria bacillus thuringiensis and mixed or individual mycorrhizal species improved drought tolerance and oxidative metabolism in lavandula dentata plants. *Journal of Plant Physiology*. 2016;**192**:1-12 <https://doi.org/https://doi.org/10.1016/j.jplph.2015.11.007>
5. Schmitz L, Yan Z, Schneijderberg M, de Roij M, Pijnenburg R, Zheng Q *et al.* Synthetic bacterial community derived from a desert rhizosphere confers salt stress resilience to tomato in the presence of a soil microbiome. *The ISME Journal*. 2022;**16**:1907-20 <https://doi.org/10.1038/s41396-022-01238-3>
6. Fiodor A, Singh S, Pranaw K. The contrivance of plant growth promoting microbes to mitigate climate change impact in agriculture. *Microorganisms*. 2021;**9**:1841
7. Santos LF, Olivares FL. Plant microbiome structure and benefits for sustainable agriculture. *Current Plant Biology*. 2021;**26**:100198 <https://doi.org/https://doi.org/10.1016/j.cpb.2021.100198>
8. Leveau JHJ. A brief from the leaf: Latest research to inform our understanding of the phyllosphere microbiome. *Current Opinion in Microbiology*. 2019;**49**:41-49 <https://doi.org/https://doi.org/10.1016/j.mib.2019.10.002>
9. Ahmad Ansari F, Ahmad I, Pichtel J. Synergistic effects of biofilm-producing pgpr strains on wheat plant colonization, growth and soil resilience under drought stress. *Saudi Journal of Biological Sciences*. 2023;**30**:103664 <https://doi.org/https://doi.org/10.1016/j.sjbs.2023.103664>
10. Sun W, Xiao E, Pu Z, Krumins V, Dong Y, Li B *et al.* Paddy soil microbial communities driven by environment- and microbe-microbe interactions: A case study of elevation-resolved microbial communities in a rice terrace. *Science of The Total Environment*. 2018;**612**:884-93 <https://doi.org/https://doi.org/10.1016/j.scitotenv.2017.08.275>
11. He X, Zhang Q, Li B, Jin Y, Jiang L, Wu R. Network mapping of root-microbe interactions in arabidopsis thaliana. *npj Biofilms and Microbiomes*. 2021;**7**:72 <https://doi.org/10.1038/s41522-021-00241-4>
12. Regalado J, Lundberg DS, Deusch O, Kersten S, Karasov T, Poersch K *et al.* Combining whole-genome shotgun sequencing and rna gene amplicon analyses to improve detection of microbe-microbe interaction networks in plant leaves. *The ISME Journal*. 2020;**14**:2116-30 <https://doi.org/10.1038/s41396-020-0665-8>
13. Almario J, Mahmoudi M, Kroll S, Agler M, Placzek A, Mari A *et al.* The leaf microbiome of arabidopsis displays reproducible dynamics and patterns throughout the growing season. *mBio*. 2022;**13**:e02825-21 <https://doi.org/doi:10.1128/mbio.02825-21>
14. van der Heijden MGA, Hartmann M. Networking in the plant microbiome. *PLOS Biology*. 2016;**14**:e1002378 <https://doi.org/10.1371/journal.pbio.1002378>

15. Agler MT, Ruhe J, Kroll S, Morhenn C, Kim S-T, Weigel D *et al.* Microbial hub taxa link host and abiotic factors to plant microbiome variation. *PLOS Biology*. 2016;**14**:e1002352 <https://doi.org/10.1371/journal.pbio.1002352>
16. Getzke F, Hassani MA, Crüsemann M, Malisic M, Zhang P, Ishigaki Y *et al.* Cofunctioning of bacterial exometabolites drives root microbiota establishment. *Proceedings of the National Academy of Sciences*. 2023;**120**:e2221508120 <https://doi.org/doi:10.1073/pnas.2221508120>
17. Helfrich EJM, Vogel CM, Ueoka R, Schäfer M, Ryffel F, Müller DB *et al.* Bipartite interactions, antibiotic production and biosynthetic potential of the arabidopsis leaf microbiome. *Nature Microbiology*. 2018;**3**:909-19 <https://doi.org/10.1038/s41564-018-0200-0>
18. Bach E, Passaglia LMP, Jiao J, Gross H. Burkholderia in the genomic era: From taxonomy to the discovery of new antimicrobial secondary metabolites. *Critical Reviews in Microbiology*. 2022;**48**:121-60 <https://doi.org/10.1080/1040841X.2021.1946009>
19. Lin T, Lu C, Shen Y. Secondary metabolites of aspergillus sp. F1, a commensal fungal strain of trewia nudiflora. *Natural Product Research*. 2009;**23**:77-85 <https://doi.org/10.1080/14786410701852826>
20. Aghdam SA, Brown AMV. Deep learning approaches for natural product discovery from plant endophytic microbiomes. *Environmental Microbiome*. 2021;**16**:6 <https://doi.org/10.1186/s40793-021-00375-0>
21. Dror B, Wang Z, Brady SF, Jurkevitch E, Cytryn E. Elucidating the diversity and potential function of nonribosomal peptide and polyketide biosynthetic gene clusters in the root microbiome. *mSystems*. 2020;**5**:10.1128/msystems.00866-20 <https://doi.org/doi:10.1128/msystems.00866-20>
22. Murugappan RM, Aravinth A, Karthikeyan M. Chemical and structural characterization of hydroxamate siderophore produced by marine vibrio harveyi. *Journal of Industrial Microbiology and Biotechnology*. 2011;**38**:265-73 <https://doi.org/10.1007/s10295-010-0769-7>
23. Weibull J, Ronquist F, Brishammar S. Free amino acid composition of leaf exudates and phloem sap 1: A comparative study in oats and barley. *Plant Physiology*. 1990;**92**:222-26 <https://doi.org/10.1104/pp.92.1.222>
24. Mahmoudi M, Almario J, Lutap K, Nieselt K, Kemen E. Microbial communities living inside plant leaves or on the leaf surface are differently shaped by environmental cues. *ISME Communications*. 2024;**4** <https://doi.org/10.1093/ismeco/ycae103>
25. Friedman J, Alm EJ. Inferring correlation networks from genomic survey data. *PLOS Computational Biology*. 2012;**8**:e1002687 <https://doi.org/10.1371/journal.pcbi.1002687>
26. Watts SC, Ritchie SC, Inouye M, Holt KE. Fastspar: Rapid and scalable correlation estimation for compositional data. *Bioinformatics*. 2018;**35**:1064-66 <https://doi.org/10.1093/bioinformatics/bty734>
27. Shannon P, Markiel A, Ozier O, Baliga NS, Wang JT, Ramage D *et al.* Cytoscape: A software environment for integrated models of biomolecular interaction networks. *Genome Res*. 2003;**13**:2498-504 <https://doi.org/10.1101/gr.1239303>
28. Blin K, Shaw S, Augustijn HE, Reitz ZL, Biermann F, Alanjary M *et al.* Antismash 7.0: New and improved predictions for detection, regulation, chemical structures and visualisation. *Nucleic Acids Research*. 2023;**51**:W46-W50 <https://doi.org/10.1093/nar/gkad344>
29. Terlouw BR, Blin K, Navarro-Muñoz JC, Avalon NE, Chevrette MG, Egbert S *et al.* Mibig 3.0: A community-driven effort to annotate experimentally validated biosynthetic gene clusters. *Nucleic Acids Research*. 2022;**51**:D603-D10 <https://doi.org/10.1093/nar/gkac1049>
30. Visca P, Imperi F, Lamont IL. Pyoverdine siderophores: From biogenesis to biosignificance. *Trends in Microbiology*. 2007;**15**:22-30 <https://doi.org/https://doi.org/10.1016/j.tim.2006.11.004>

31. Taguchi F, Suzuki T, Inagaki Y, Toyoda K, Shiraishi T, Ichinose Y. The siderophore pyoverdine of *Pseudomonas syringae* pv. Tabaci 6605 is an intrinsic virulence factor in host tobacco infection. *Journal of Bacteriology*. 2010;**192**:117-26 <https://doi.org/10.1128/jb.00689-09>
32. Huang W, Wilks A. A rapid seamless method for gene knockout in *Pseudomonas aeruginosa*. *BMC Microbiol*. 2017;**17**:199 <https://doi.org/10.1186/s12866-017-1112-5>
33. Mayer T, Mari A, Almario J, Murillo-Roos M, Syed M, Abdullah H, Dombrowski N *et al*. Obtaining deeper insights into microbiome diversity using a simple method to block host and nontargets in amplicon sequencing. *Molecular Ecology Resources*. 2021;**21**:1952-65 <https://doi.org/https://doi.org/10.1111/1755-0998.13408>
34. Chen S. Ultrafast one-pass fastq data preprocessing, quality control, and deduplication using fastp. *iMeta*. 2023;**2**:e107 <https://doi.org/https://doi.org/10.1002/imt2.107>
35. Callahan BJ, McMurdie PJ, Rosen MJ, Han AW, Johnson AJA, Holmes SP. Dada2: High-resolution sample inference from illumina amplicon data. *Nature Methods*. 2016;**13**:581-83 <https://doi.org/10.1038/nmeth.3869>
36. Bolyen E, Rideout JR, Dillon MR, Bokulich NA, Abnet CC, Al-Ghalith GA *et al*. Reproducible, interactive, scalable and extensible microbiome data science using qiime 2. *Nature Biotechnology*. 2019;**37**:852-57 <https://doi.org/10.1038/s41587-019-0209-9>
37. Quast C, Pruesse E, Yilmaz P, Gerken J, Schweer T, Yarza P *et al*. The SILVA ribosomal RNA gene database project: Improved data processing and web-based tools. *Nucleic Acids Research*. 2012;**41**:D590-D96 <https://doi.org/10.1093/nar/gks1219>
38. Nilsson RH, Larsson K-H, Taylor AF S, Bengtsson-Palme J, Jeppesen TS, Schigel D *et al*. The UNITE database for molecular identification of fungi: Handling dark taxa and parallel taxonomic classifications. *Nucleic Acids Research*. 2018;**47**:D259-D64 <https://doi.org/10.1093/nar/gky1022>
39. Li K, Cheng K, Wang H, Zhang Q, Yang Y, Jin Y *et al*. Disentangling leaf-microbiome interactions in *Arabidopsis thaliana* by network mapping. *Frontiers in Plant Science*. 2022;**13** <https://doi.org/10.3389/fpls.2022.996121>
40. Mercier J, Lindow SE. Role of leaf surface sugars in colonization of plants by bacterial epiphytes. *Applied and Environmental Microbiology*. 2000;**66**:369-74 <https://doi.org/doi:10.1128/AEM.66.1.369-374.2000>
41. Chaudhry V, Runge P, Sengupta P, Doehlemann G, Parker JE, Kemen E. Shaping the leaf microbiota: Plant-microbe-microbe interactions. *Journal of Experimental Botany*. 2020;**72**:36-56 <https://doi.org/10.1093/jxb/eraa417>
42. Loper JE, Henkels MD. Availability of iron to *Pseudomonas fluorescens* in rhizosphere and bulk soil evaluated with an ice nucleation reporter gene. *Applied and Environmental Microbiology*. 1997;**63**:99-105 <https://doi.org/10.1128/aem.63.1.99-105.1997>
43. Joyner DC, Lindow SE. Heterogeneity of iron bioavailability on plants assessed with a whole-cell GFP-based bacterial biosensor. *Microbiology (Reading)*. 2000;**146 (Pt 10)**:2435-45 <https://doi.org/10.1099/00221287-146-10-2435>
44. Rigolet A, Argüelles Arias A, Anckaert A, Quinton L, Rigali S, Tellatin D *et al*. Lipopeptides as rhizosphere public goods for microbial cooperation. *Microbiology Spectrum*. 2023;**12**:e03106-23 <https://doi.org/10.1128/spectrum.03106-23>
45. Hansen ML, Dénes Z, Jarmusch SA, Wibowo M, Lozano-Andrade CN, Kovács ÁT *et al*. Resistance towards and biotransformation of a *Pseudomonas*-produced secondary metabolite during community invasion. *The ISME Journal*. 2024;**18** <https://doi.org/10.1093/ismejo/wrae105>
46. Andrić S, Rigolet A, Argüelles Arias A, Steels S, Hoff G, Balleux G *et al*. Plant-associated *Bacillus* mobilizes its secondary metabolites upon perception of the siderophore pyochelin

- produced by a pseudomonas competitor. *The ISME Journal*. 2023;**17**:263-75
<https://doi.org/10.1038/s41396-022-01337-1>
47. Lyng M, Jørgensen JPB, Schostag MD, Jarmusch SA, Aguilar DKC, Lozano-Andrade CN *et al*. Competition for iron shapes metabolic antagonism between bacillus subtilis and pseudomonas marginalis. *The ISME Journal*. 2024;**18** <https://doi.org/10.1093/ismejo/wrad001>
 48. Thrall PH, Hochberg ME, Burdon JJ, Bever JD. Coevolution of symbiotic mutualists and parasites in a community context. *Trends in Ecology & Evolution*. 2007;**22**:120-26
<https://doi.org/https://doi.org/10.1016/j.tree.2006.11.007>
 49. Hassani MA, Durán P, Hacquard S. Microbial interactions within the plant holobiont. *Microbiome*. 2018;**6**:58 <https://doi.org/10.1186/s40168-018-0445-0>
 50. Tyc O, van den Berg M, Gerards S, van Veen JA, Raaijmakers JM, de Boer W *et al*. Impact of interspecific interactions on antimicrobial activity among soil bacteria. *Front Microbiol*. 2014;**5**:567 <https://doi.org/10.3389/fmicb.2014.00567>
 51. Kot AM, Kieliszek M, Piwowarek K, Błażej S, Mussagy CU. Sporobolomyces and sporidiobolus – non-conventional yeasts for use in industries. *Fungal Biology Reviews*. 2021;**37**:41-58 <https://doi.org/https://doi.org/10.1016/j.fbr.2021.06.001>
 52. Ren D, Madsen JS, Sørensen SJ, Burmølle M. High prevalence of biofilm synergy among bacterial soil isolates in cocultures indicates bacterial interspecific cooperation. *The ISME Journal*. 2014;**9**:81-89 <https://doi.org/10.1038/ismej.2014.96>
 53. Ansari FA, Ahmad I. Fluorescent pseudomonas -fap2 and bacillus licheniformis interact positively in biofilm mode enhancing plant growth and photosynthetic attributes. *Scientific Reports*. 2019;**9**:4547 <https://doi.org/10.1038/s41598-019-40864-4>
 54. Hunter PJ, Pink DAC, Bending GD. Cultivar-level genotype differences influence diversity and composition of lettuce (lactuca sp.) phyllosphere fungal communities. *Fungal Ecology*. 2015;**17**:183-86 <https://doi.org/https://doi.org/10.1016/j.funeco.2015.05.007>
 55. Molina-Santiago C, Vela-Corcía D, Petras D, Díaz-Martínez L, Pérez-Lorente AI, Sopena-Torres S *et al*. Chemical interplay and complementary adaptative strategies toggle bacterial antagonism and co-existence. *Cell Reports*. 2021;**36**:109449
<https://doi.org/https://doi.org/10.1016/j.celrep.2021.109449>
 56. Kolton M, Erlacher A, Berg G, Cytryn E The flavobacterium genus in the plant holobiont: Ecological, physiological, and applicative insights. In: Castro-Sowinski S (ed.). *Microbial models: From environmental to industrial sustainability*, Singapore: Springer Singapore. 189-207. Retrieved from https://doi.org/10.1007/978-981-10-2555-6_9
 57. Yang J-K, Zhang J-J, Yu H-Y, Cheng J-W, Miao L-H. Community composition and cellulase activity of cellulolytic bacteria from forest soils planted with broad-leaved deciduous and evergreen trees. *Applied Microbiology and Biotechnology*. 2014;**98**:1449-58
<https://doi.org/10.1007/s00253-013-5130-4>
 58. DeCrescenzo Henriksen E, Phillips DR, Peterson JBD. Polymyxin e production by p. Amylolyticus. *Letters in Applied Microbiology*. 2007;**45**:491-96 <https://doi.org/10.1111/j.1472-765X.2007.02210.x>
 59. Naghmouchi K, Hammami R, Fliss I, Teather R, Baah J, Drider D. Colistin a and colistin b among inhibitory substances of paenibacillus polymyxa jb05-01-1. *Archives of Microbiology*. 2012;**194**:363-70 <https://doi.org/10.1007/s00203-011-0764-z>
 60. Mohapatra SS, Dwibedy SK, Padhy I. Polymyxins, the last-resort antibiotics: Mode of action, resistance emergence, and potential solutions. *J Biosci*. 2021;**46**
<https://doi.org/10.1007/s12038-021-00209-8>
 61. Chevrette MG, Thomas CS, Hurley A, Rosario-Meléndez N, Sankaran K, Tu Y *et al*. Microbiome composition modulates secondary metabolism in a multispecies bacterial

- community. *Proceedings of the National Academy of Sciences*. 2022;**119**:e2212930119
<https://doi.org/doi:10.1073/pnas.2212930119>
62. Sun X, Xie J, Zheng D, Xia R, Wang W, Xun W *et al*. Metabolic interactions affect the biomass of synthetic bacterial biofilm communities. *mSystems*. 2023;**8**:e01045-23
<https://doi.org/10.1128/msystems.01045-23>
63. Lam TJ, Stambouliau M, Han W, Ye Y. Model-based and phylogenetically adjusted quantification of metabolic interaction between microbial species. *PLOS Computational Biology*. 2020;**16**:e1007951 <https://doi.org/10.1371/journal.pcbi.1007951>
64. Ludington WB. Higher-order microbiome interactions and how to find them. *Trends in Microbiology*. 2022;**30**:618-21 <https://doi.org/10.1016/j.tim.2022.03.011>
65. Battiston F, Cencetti G, Iacopini I, Latora V, Lucas M, Patania A *et al*. Networks beyond pairwise interactions: Structure and dynamics. *Physics Reports*. 2020;**874**:1-92
<https://doi.org/https://doi.org/10.1016/j.physrep.2020.05.004>
66. Ishizawa H, Tashiro Y, Inoue D, Ike M, Futamata H. Learning beyond-pairwise interactions enables the bottom-up prediction of microbial community structure. *Proceedings of the National Academy of Sciences*. 2024;**121**:e2312396121
<https://doi.org/doi:10.1073/pnas.2312396121>

ACKNOWLEDGEMENTS

NZ, EK, HBO, CH, FH, VC, DP acknowledge funding of the study by the Cluster of Excellence EXC 2124: Controlling Microbes to Fight Infection (CMFI, project ID 390838134). NZ and CB acknowledge funding by the German Federal Ministry for Education and Research (BMBF, Grant MicroMATRIX161L0284C). Furthermore, NZ is grateful for the funding by the German Center for Infection Research (DZIF, Grant TTU09.716). EK, VC, MM and EKI Have been funded by the European Research Council (ERC) under the DeCoCt research program (grant agreement: ERC-2018-COG 820124). PS thanks the European Union's Horizon Europe research and innovation programm for support through a Marie Skłodowska-Curie fellowship n.101108450-MeStaLeM. All authors thank Dr. Libera Lo Presti for helpful comments on the manuscript. Prof. Christoph Mayer for providing the pEXGm18 vector system and Prof. Ewa Musiol-Kroll for *E.coli* S17- λ . We furthermore thank the NGS competence center Tübingen (NCCT) of the University Tübingen for the Illumina MiSeq amplicon sequencing.

AUTHOR CONTRIBUTION

FH, VC, HBO, EK, NZ designed the research; FH conducted the experiments and analyzed the data; CB analyzed data obtained by Illumina amplicon sequencing; MM participated in the analyzation of the data for correlation networks; CH, PS, DP conducted HPLC-MS analyses

and structure elucidation. LB created the $\Delta pvdI/J$ mutant; EKI participated in designing and preparing the library for amplicon sequencing. FH, HBO, EK, NZ wrote the paper.

COMPETING INTERESTS

The authors declare no competing interests.

SUPPLEMENTAL INFORMATION MANUSCRIPT 1

Strong Pairwise Interactions do not Drive Interactions in a Plant Leaf Associated Microbial Community

Franziska Höhn^{1,3}, Dr. Vasvi Chaudhry², Dr. Caner Bagci¹, Maryam Mahmoudi², Elke Klenk²,
Lara Berg^{1,3}, Dr. Paolo Stincone^{2,3}, Dr. Chambers C. Hughes^{3,4,6}, Dr. Daniel Petras^{3,5}, Prof.
Heike Brötz-Oesterhelt^{3,4,6}, Prof. Eric Kemen^{2,3*}, Prof. Nadine Ziemert^{1,3,4*}

¹Translational Genome Mining for Natural Products, Interfaculty Institute of Microbiology and Infection Medicine (IMIT) and Institute for Bioinformatics and Medical Informatics (IBMI), University of Tübingen, Tübingen, Germany

²Center for Plant Molecular Biology (ZMBP), Interfaculty Institute of Microbiology and Infection Medicine (IMIT), University of Tübingen, Tübingen, Germany

³ Cluster of Excellence Controlling Microbes to Fight Infections (CMFI), University of Tübingen, Tübingen, Germany

⁴German Centre for Infection Research (DZIF), Partner Site Tübingen, Tübingen, Germany

⁵Department of Biochemistry, University of California Riverside, Riverside, USA

⁶Department of Microbial Bioactive Compounds, Interfaculty Institute of Microbiology and Infection Medicine (IMIT), University of Tübingen, Tübingen, Germany

List of figures

Figure S1: Pictures of cross-streaking experiments as examples.	51
Figure S2: Growth curves of <i>P. koreensis</i> WT and pseudobactin mutant in MM9 medium ..	53
Figure S3: Total number of OTUs connected to SynCom members by edges in correlation networks based on co-abundance.	54
Figure S4: Relative abundance of <i>B. altitudinis</i> after 0 days and 5 days incubation.	58
Figure S5: Time-fold increase or decrease of relative abundance of SynCom members over incubation time	59
Figure S6: Structure of pseudobactin A TFA salt (1) with ¹ H and ¹³ C chemical shift assignments in D ₂ O at 700 MHz	60
Figure S7: ¹ H NMR (D ₂ O, 700 MHz) of pseudobactin A TFA salt (1).....	61
Figure S8: ¹³ C NMR (D ₂ O, 175 MHz) of pseudobactin A TFA salt (1)	62
Figure S9: COSY NMR (D ₂ O, 700 MHz) of pseudobactin A TFA salt (1)	63
Figure S10: TOCSY NMR (D ₂ O, 700 MHz) of pseudobactin A TFA salt (1)	64
Figure S11: Figure S5 HSQC NMR (D ₂ O, 700 MHz) of pseudobactin A TFA salt (1).....	65
Figure S12:HMBC NMR (D ₂ O, 700 MHz) of pseudobactin A TFA salt (1).....	66
Figure S13: HR-MS spectrum of pseudobactin A TFA salt (1)	67
Figure S14: Pseudobactin production and activity in <i>P. koreensis</i> WT and Δ pvdI/J mutant.	70
Figure S15: Growth curves of SynCom members in presence or absence of pseudobactin.	71
Figure S16: T-test of each SynCom member for the experiment (Fig.6) after 5 days of incubation:.....	72
Figure S17: T-test of each SynCom member for the experiment (Fig.6) after 9 days of incubation:.....	72

Table Index:

Table S1: MM9 medium used in growth curves for investigating the effect of pseudobactin on SynCom members.....	48
Table S2: Enriched MM9 medium used in growth curves for investigating the effect of pseudobactin on SynCom members.....	48
Table S3: MM9/7 defined minimal agar for 16S rRNA/ITS2 amplicon sequencing of SynCom strains in vitro.. ..	49
Table S4: List of Primers used for the creation of the pseudobactin deletion mutant Δ pvdI/J.	52
Table S5: OTUs representing SynCom members which were removed from correlation network.....	53
Table S6: AntiSMASH biosynthetic gene cluster prediction of SynCom strains and similarity to known BGCs.	55

Table S3: MM9 medium used in growth curves for investigating the effect of pseudobactin on SynCom members. *P. koreensis* WT and pseudobactin mutant were grown in MM9 to obtain WT and $\Delta pvdI/J$ supernatant. The medium was highly iron-limited and used for growth curves of *A. humicola* and *S. faeni*.

Medium additive	Standard MM9	WT + MM9	$\Delta pvdI/J$ + MM9	WT + FeSO ₄	$\Delta pvdI/J$ + Pseudobactin + MM9
MM9 medium	100 ml	90 ml	90 ml	90 ml	90 ml
WT supernatant	-	10 ml	-	10 ml	
$\Delta pvdI/J$ supernatant	-		10 ml	-	10 ml
FeSO ₄ (1.5 mg/ml)	-			100 μ l	
Pure Pseudobactin (100 μ g/ml)	-				100 μ l

Table S4: Enriched MM9 medium used in growth curves for investigating the effect of pseudobactin on SynCom members. *P. koreensis* WT and pseudobactin mutant were grown in MM9 to obtain WT and $\Delta pvdI/J$ supernatant. Strains not able to grow in iron-limited MM9 medium were grown in enriched MM9 containing low amounts of optimal growth medium NB (for bacteria) or PDB (for yeasts). Enriched MM9 medium was used for growth curves of *B. altitudinis*, *A. fastidiosum*, *P. amylolyticus*, *M. proteolyticum*, *S. roseus*, *R. kratchovilovae*.

Medium additive	Standard enriched	WT + MM9	$\Delta pvdI/J$ + MM9	WT + FeSO ₄	$\Delta pvdI/J$ + pseudobactin + MM9
MM9 medium	80 ml	70 ml	70 ml	70 ml	70 ml
NB/PDA	20 ml	20 ml	20 ml	20 ml	20 ml
WT supernatant	-	10 ml	-	10 ml	
$\Delta pvdI/J$ supernatant	-		10 ml	-	10 ml
FeSO ₄ (1.5 mg/ml)	-			100 μ l	
Pure pseudobactin (100 μ g/ml)	-				100 μ l

Table S5: MM9/7 defined minimal agar for 16S rRNA/ITS2 amplicon sequencing of SynCom strains in vitro. MM9 medium was modified as shown in the table to obtain a defined minimal agar suitable for amplicon sequencing and inspired by the plant leaf surface.

Solution	Chemical	Volume
Pre autoclave solution in 950 ml	KH ₂ PO ₄	0.30 g
	NaCl	0.50 g
	NH ₄ Cl	1.00 g
	Agar	15.00 g
Autoclave at 121 °C, 20 min		
Post autoclave solution (filter sterilize 0.2 µm and add to pre autoclave solution)	Glucose 20 %	10.00 ml
	MgSO ₄ 1 M	1.00 ml
	CaCl ₂ 100 mM	1.00 ml
	amino acid solution	30.00 ml
	Trace element solution	10.00 ml
Amino acid solution preparation filter sterilized (0.2µm)		
Solution I (in 100 ml dH ₂ O)	Phe	0.99 g
	Lys	1.10 g
	Arg	2.50 g
Solution II (in 100 ml dH ₂ O)	Gly	0.20 g
	Val	0.70 g
	Ala	0.84 g
	Trp	0.41 g,
Solution III (in 100 ml dH ₂ O)	Thr	0.71g
	Ser	8.40 g
	Pro	4.60 g
	Asn	0.96 g
Solution IV (in 90 ml dH ₂ O + 10 ml HCl (36 %))	Asp (free acid)	1.04 g
	Gln	14.60 g
Solution V (dissolve K.Glu in 80 ml dH ₂ O, add rest and fill up to 100 ml with dH ₂ O)	K.Glu	18.70 g
	Tyr	0.36 g
	NaOH	4.00 g

Solution VI (in 100 ml dH ₂ O)	Ile	0.79 g
	Leu	0.77 g
Trace element solution preparation (filter sterilized 0.2 µm)		
EDTA-solution (in 800 ml dH ₂ O, pH 7.5)	EDTA	5.00 g
Final solution (fill up to 1 L with dH ₂ O)	FeCl ₃ - 6 H ₂ O	0.83 g
	ZnCl ₂	84.00 mg
	CuCl ₂ - 2H ₂ O	13.00 mg
	CoCl ₂ - 2H ₂ O	10.00 mg
	H ₃ BO ₃	10.00 mg
	MnCl ₂ - 4H ₂ O	1.60 mg

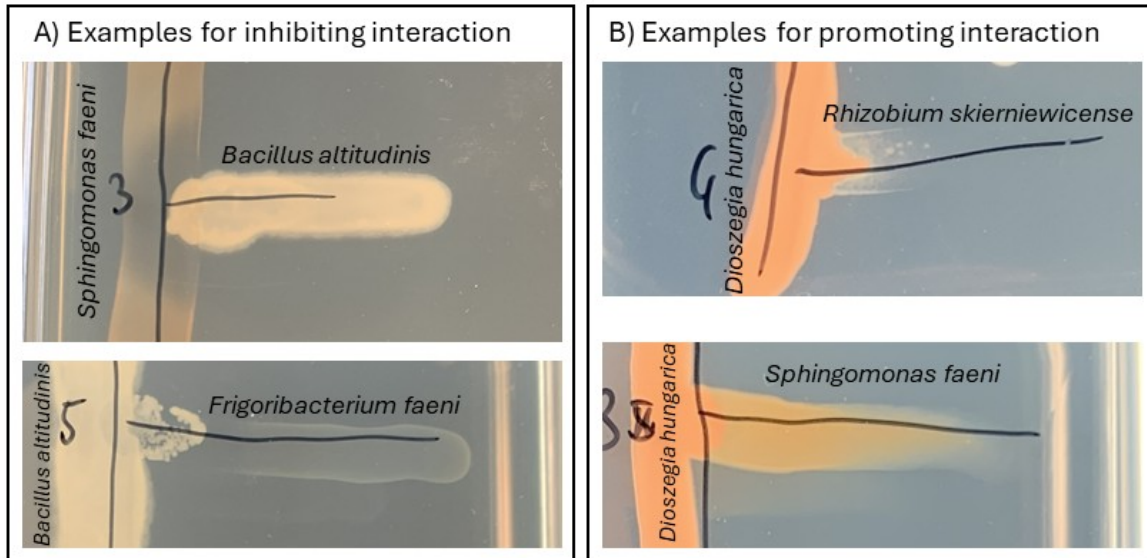


Figure S7: Pictures of cross-streaking experiments as examples. A) Inhibiting interactions between SynCom members were visually observed by the presence of inhibition zones. The here shown cross-streakings were performed on NA. B) Promotive interactions were visually observed by better growth in the contact zone. The here shown cross-streakings were performed on PDA.

Table S6: List of Primers used for the creation of the pseudobactin deletion mutant $\Delta pvdI/J$. The deletion was performed as described by Huang *et al.* * Primers can additionally be used for the verification of a successful deletion.

Primer	Sequence 5' -> 3'	purpose
pEX18seq_fw	GGATGTGCTGCAAGGCGATTAAG	Forward primer for verification of single cross-over upstream of pvdI .
pEX18seq_rv	GGCTCGTATGTTGTGTGGAATTGTG	Reverse primer for verification of single cross-over downstream of pvdJ .
pvd_upstream_f	GATCCCCGGGTACCGAGCTCGATG AATGCCGCAGACGCACAGAAAC	Forward primer for the amplification of the left part of the deleted gene region for integration into vector. Region is upstream from pvdI . *
pvd_upstream_rv	CAGCATCGCCAATGCCGCTGGCCGT TCGCTGTCCGGCAGCATC	Reverse primer for the amplification of the left part of the deleted gene region for integration into vector. Region is upstream from pvdI .
pvd_downstream_f	GATGCTCGCCGACAGCGAACGGCCA GCGGCATTGGCGATGCTGCC	Forward primer for the amplification of the right part of the deleted gene region for integration into vector. Region is downstream from pvdJ .
pvd_downstream_rv	GAAACAGCTATGACCATGATTACGCG AGGGATAGACGTTTGAGGGCCTCCAGTG	Reverse primer for the amplification of the right part of the deleted gene region for integration into vector. Region is downstream from pvdJ .
pvdI+pvdJ_before	CGTTCGAAGGGCCGCGCAAAGTC	Forward primer for the verification of deletion success.
pvdI+pvdJ_after	GCGATGCTGCGTTCCAGTGCCG	Reverse primer for the verification of deletion success.
behind_up_rw	GAACAGGCTTTGCACGCTGGTAAAC	Reverse primer for verification of single cross-over upstream of pvdI . *
before_down_f	GAACGCTTGCTGCACATGCTC	Forward primer for verification of single cross-over downstream of pvdJ .

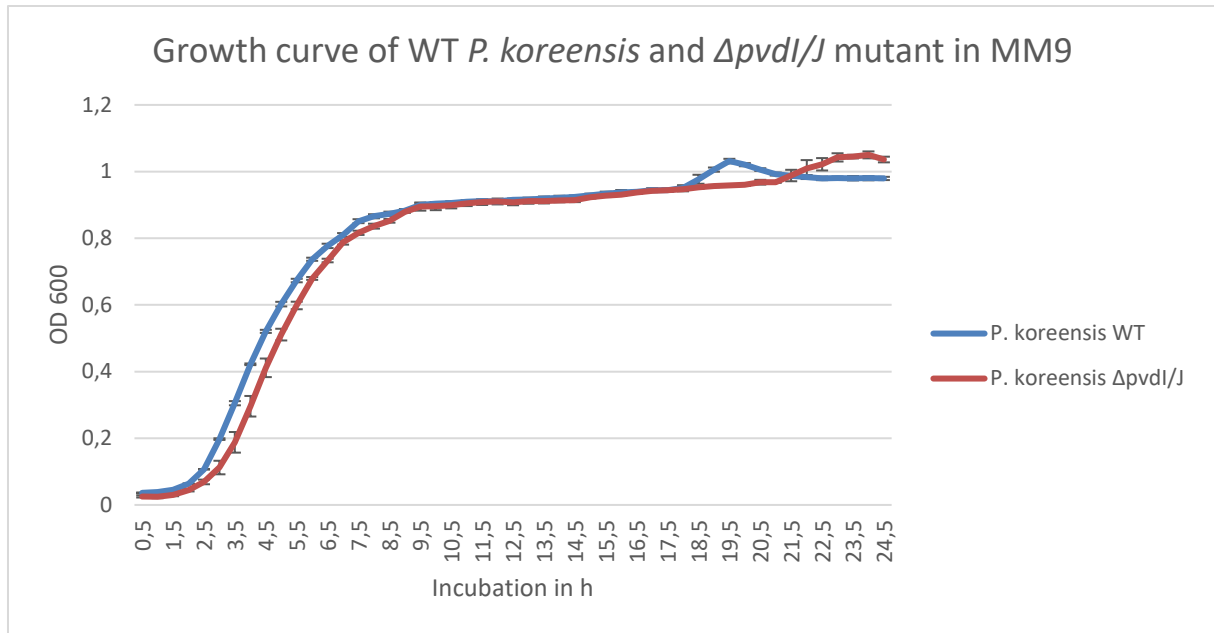


Figure S8: Growth curves of *P. koreensis* WT and pseudobactin mutant in MM9 medium Similar growth for *P. koreensis* WT and $\Delta pvdI/J$ mutant was observed in MM9 medium. This was important, since the supernatant was used in pseudobactin interaction studies.

Table S7: OTUs representing SynCom members which were removed from correlation network. The OTUs showed highest BlastN similarity to the 16S rRNA/ITS2 sequence of the named SynCom member. OTUs showing < 10 reads per sample and/or occurrence in < 5 sample

OTU	related SynCom strain	BlastN similarity	samples with OTU occurrence	samples with > 10 reads
Otu002983	<i>B. altitudinis</i>	98.70%	9	3
Otu004835	<i>F. faeni</i>	100.00%	35	0
Otu02956	<i>D. hungarica</i>	100.00%	29	0
Otu00955	<i>R. kratchovilovae</i>	100.00%	3	2

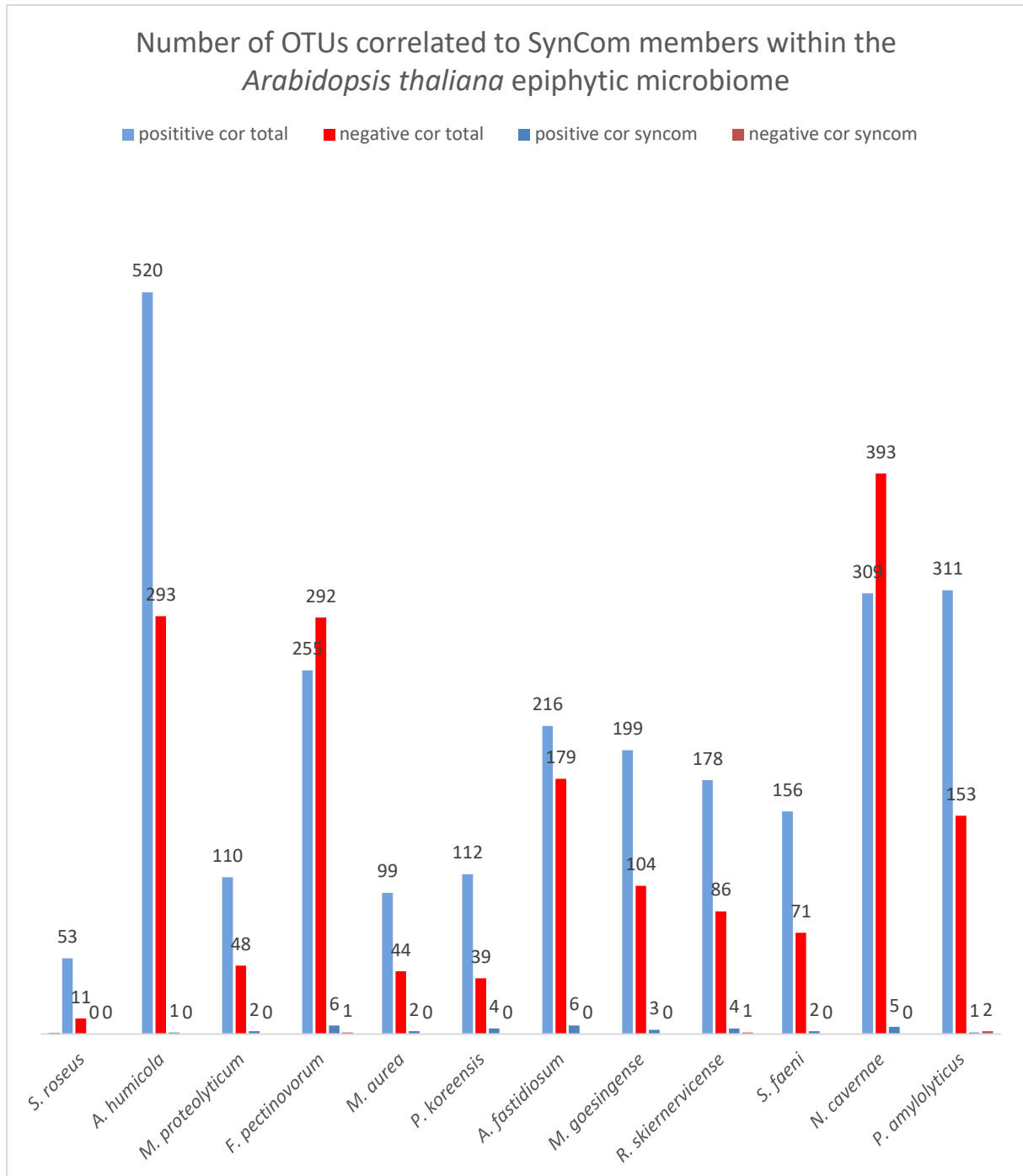


Figure S9: Total number of OTUs connected to SynCom members by edges in correlation networks based on co-abundance. Total positive correlations ($cor > 0$) (light blue) and negative correlations ($cor < 0$) (red) of SynCom members to the epiphytic microbiome of *A. thaliana*. Positive (dark blue) and negative (orange) correlations of SynCom members to each other extracted of the whole correlation network. For *P. amylolyticus* edge numbers of OTU001595 were used.

Table S8: AntiSMASH biosynthetic gene cluster prediction of SynCom strains and similarity to known BGCs. AntiSMASH 7.0 was used for the identification of BGCs of SynCom members and their similarity to known clusters. *Two split NRPS BGCs of *P. koreensis*

Strain	Cluster prediction	Most similar known cluster	similarity
<i>A. fastidiosum</i>	redox-cofactor		
	NI-siderophore	desferrioxamine E	75 %
	RiPP-like		
	NAPAA	e-Poly-L-Lysine	100 %
<i>A. humicola</i>	NRPS-like	SLI- 2138	11 %
	type 3 PKS	pentalenolactone	15 %
	betalactone	microansamycin	7 %
	NAPAA	stenothricin	31 %
	NAPAA		
	RRE-containing		
<i>B. altitudinis</i>	betalactone	-	-
	RiPP-like		
	type 3 PKS		
	NRPS	lichenysin	85 %
	NRP-metallophore	bacillibactin	80 %
	RiPP-like		
	type 1 PKS / NRPS	zwittermycin A	18 %
	betalactone	fengycine	53 %
	terpene		
	NRPS-like	locillomycin	21 %
	NI-siderophore	schizokinen	60 %
	RRE-containing		
<i>F. pectinovorum</i>	arylpolyene/resorcinol	flexirubin	91 %
	terpene	carotenoid	28 %
	betalactone		
<i>F. faeni</i>	type 3 PKS	funisamine	7 %
	NI-siderophore	FW0622	37 %
	terpene	carotenoid	50 %
<i>M. aurea</i>	terpene		
	RiPP-like	paulomycin	3 %
	arylpolyene	APE Vf	35 %
	hserlactone		
	hserlactone, RRe-		
	hydrogen-cyanide		
	terpene	carotenoid	100 %

<i>M. goesingense</i>	terpene	carotenoid	100 %
	RiPP-like		
	redox-cofactor		
	type 1 PKS	oryzanaphthopyran A	6 %
	NRP-metallophore	taiwachelin	22 %
	hserlactone		
	terpene		
	terpene		
	type 1 PKS/ NRPS		
	NAPAA		
<i>M. proteolyticum</i>	betalactone	microansamycin	7 %
	terpene	carotenoid	21 %
	NAPAA	e-Poly-L-Lysin	100 %
	type 3 PKS		
<i>N. cavernae</i>	terpene	carotenoid	14 %
	Betalactone / NRPS-like	formicamycins A-M	4 %
	type 3 PKS	alkylresorcinol	100 %
<i>P. amylolyticus</i>	type 3 PKS		
	type 3 PKS	corynecin II	13 %
	NRPS-like		
	lassopeptide	paeninodin	60 %
	proteusin		
	NI-siderophore		
	trans-AT PKS / NRPS	pellasoren	33 %
	trans-AT PKS / NRPS	paenilipoheptin	23 %
	terpene	carotenoid	33 %
	Opine-like-metallophore	bacillopaline	100 %
	lanthipeptide-class-ii	Gramicidin S	15 %
	lanthipeptide-class-iv		
	NRPS	polymyxin	100 %
<i>P. koreensis</i>	NAGGN		
	NRPS	Pf-5 pyoverdine*	21 %
	arylpolyene	APE Vf	40 %
	NRPS-like	fragin	37 %
	RiPP-like		
	NRP-metallophore	Pf-5 pyoverdine*	10 %
	RiPP-like		
	RiPP-like		
	betalactone	fengycin	13 %
	hydrogen-cyanide	hydrogen cyanide	100 %

	redox-cofactor	lankacidin C	13 %
	RiPP-like		
<i>R. skierniewicense</i>	terpene		
	arylpolyene	persiamycin A	5 %
	lanthipeptide-class V		
	NI-siderophore	desferrioxamine E	50 %
	betalactone	xantholipin	4 %
	NI-siderophore	roseobactin	50 %
	thioamitides		
	betalactone		
	hserlactone		
	hydrogen-cyanide		
	hserlactone		
	type 1 PKS		
<i>S. faeni</i>	RiPP-like		
	terpene	carotenoid	50 %
	type 3 PKS		
	redox-cofactor	lankacidin C	13 %
<i>D. hungarica</i>	terpene		
	NRPS-like		
	NRPS-like		
	terpene		
	NRPS-like		
	terpene		
<i>R. kratchovilovae</i>	NRPS-like		
	NRPS		
	terpene		
	betalactone		
	terpene		
<i>S. roseus</i>	NRPS-like		
	terpene		
	betalactone		
	NRPS		

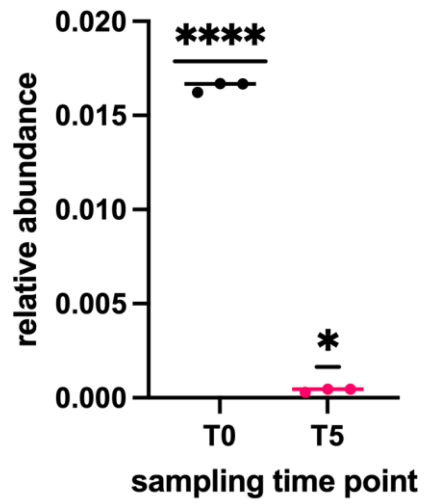


Figure S10: Relative abundance of *B. altitudinis* after 0 days and 5 days incubation. The decrease of relative abundance of *B. altitudinis*, when grown in the SynCom on MM9/7 agar at inoculation and after 5 days of incubation at 22 °C.

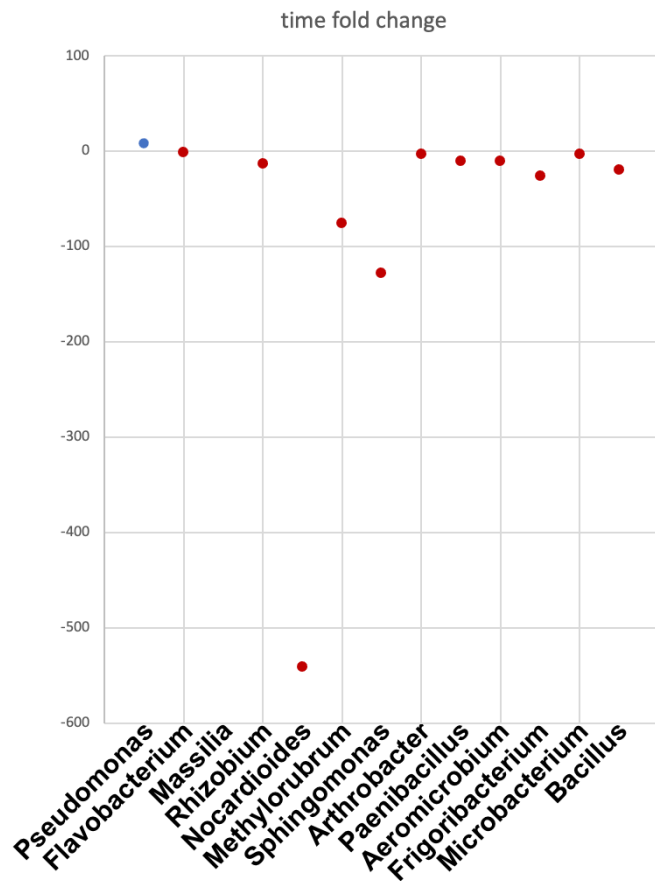


Figure S11: Time-fold increase or decrease of relative abundance of SynCom members over incubation time The calculation of the increase (blue) or decrease (red) was based on the relative abundance after 0 and 5 days of incubation in a whole SynCom co-culture (0.2 OD600 of each strain). The SynCom was cultured on MM9/7 agar at 22 °C and relative abundance was investigated by 16S rRNA/ITS2 MiSeq illumina amplicon sequencing.

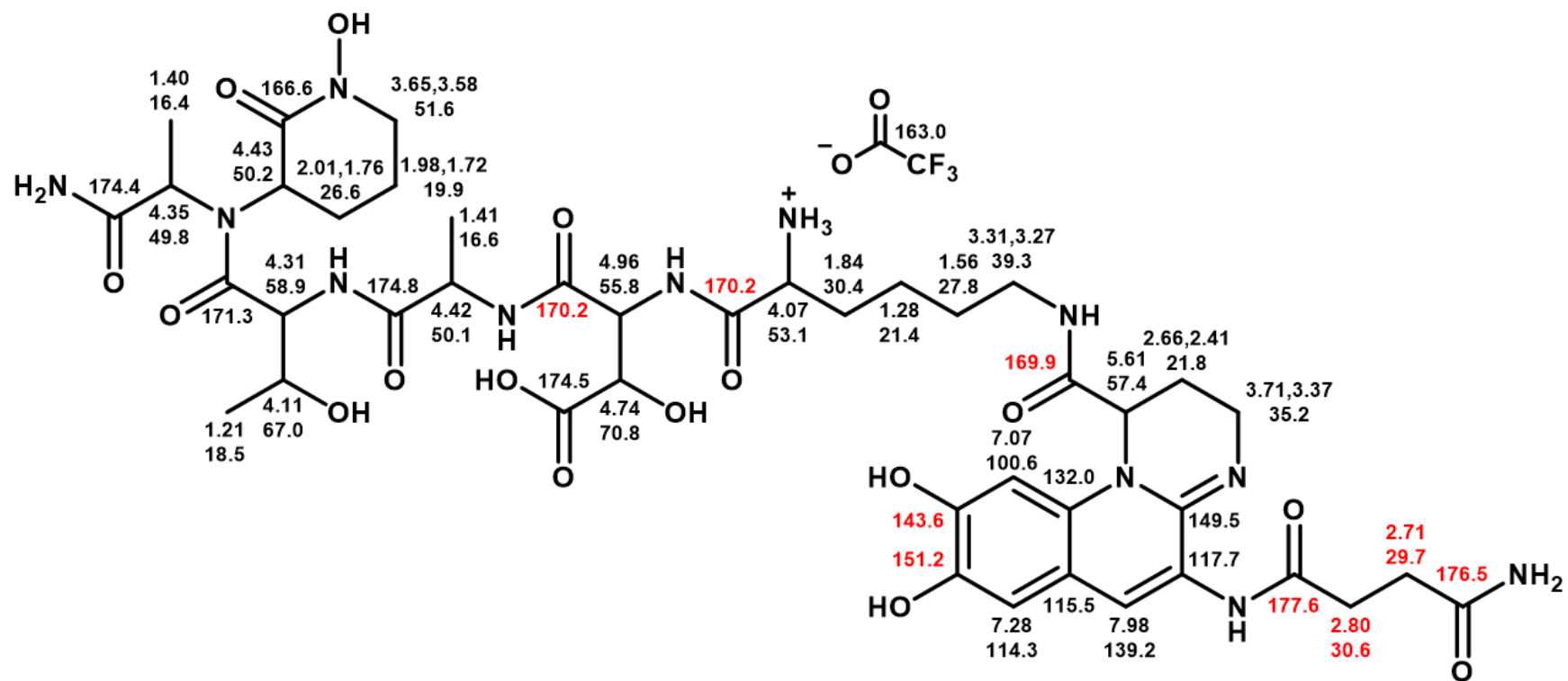


Figure S12: Structure of pseudobactin A TFA salt (1) with ^1H and ^{13}C chemical shift assignments in D_2O at 700 MHz NB: 1) ^1H NMR chemical shifts are in good agreement with Teintze, and M.; Leong*, J. 2) Some uncertainty is associated with the assignments in red.

Z:/AVIII700/data/NA/nmr/10-21052021-CH/10/fid

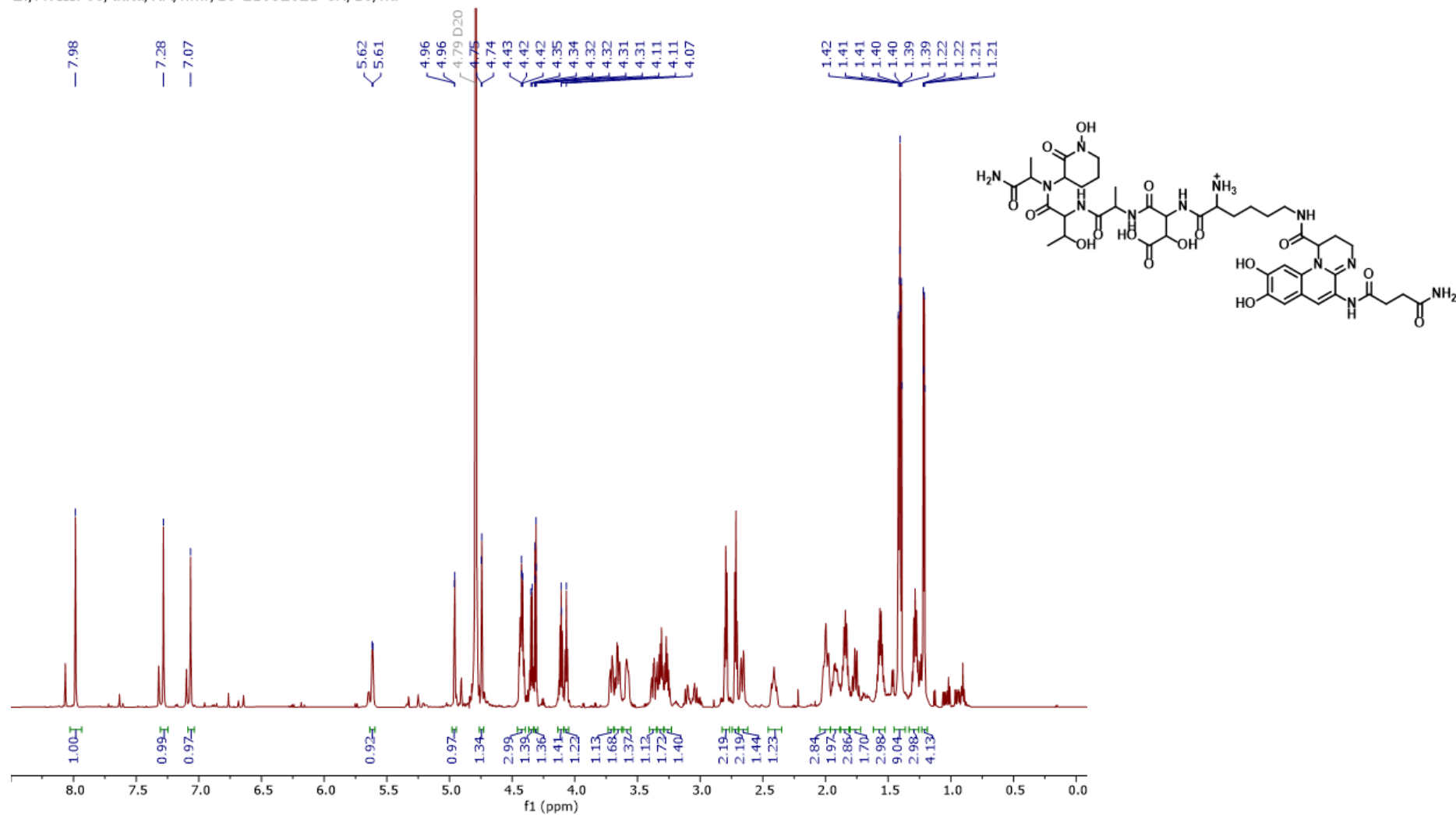


Figure S13: ¹H NMR (D₂O, 700 MHz) of pseudobactin A TFA salt (1)

Z:/AVIII700/data/NA/nmr/10-21052021-CH/15/pdata/1/1r

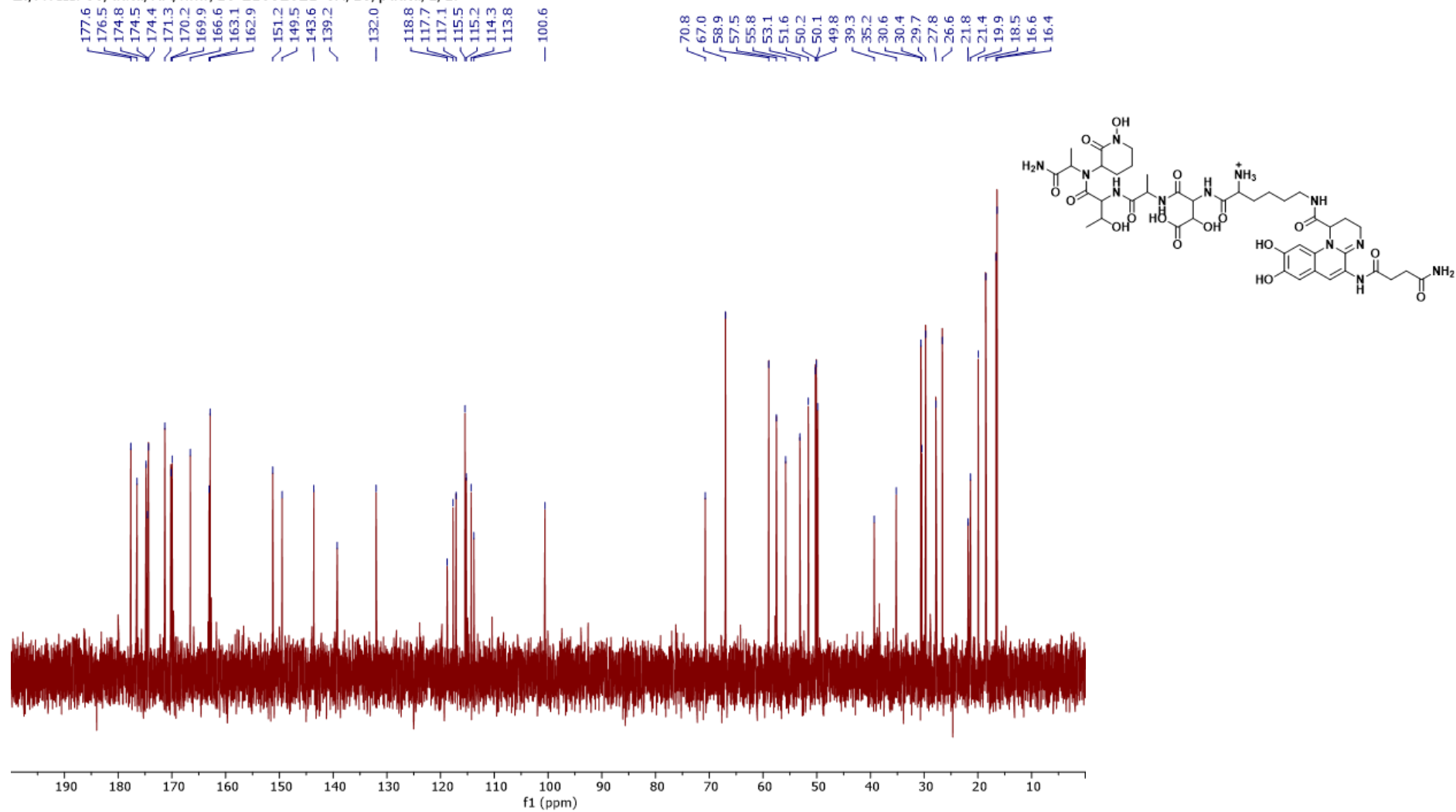


Figure S14: ^{13}C NMR (D₂O, 175 MHz) of pseudobactin A TFA salt (1)

Z:/AVIII700/data/NA/nmr/10-21052021-CH/11/pdata/1/2rr

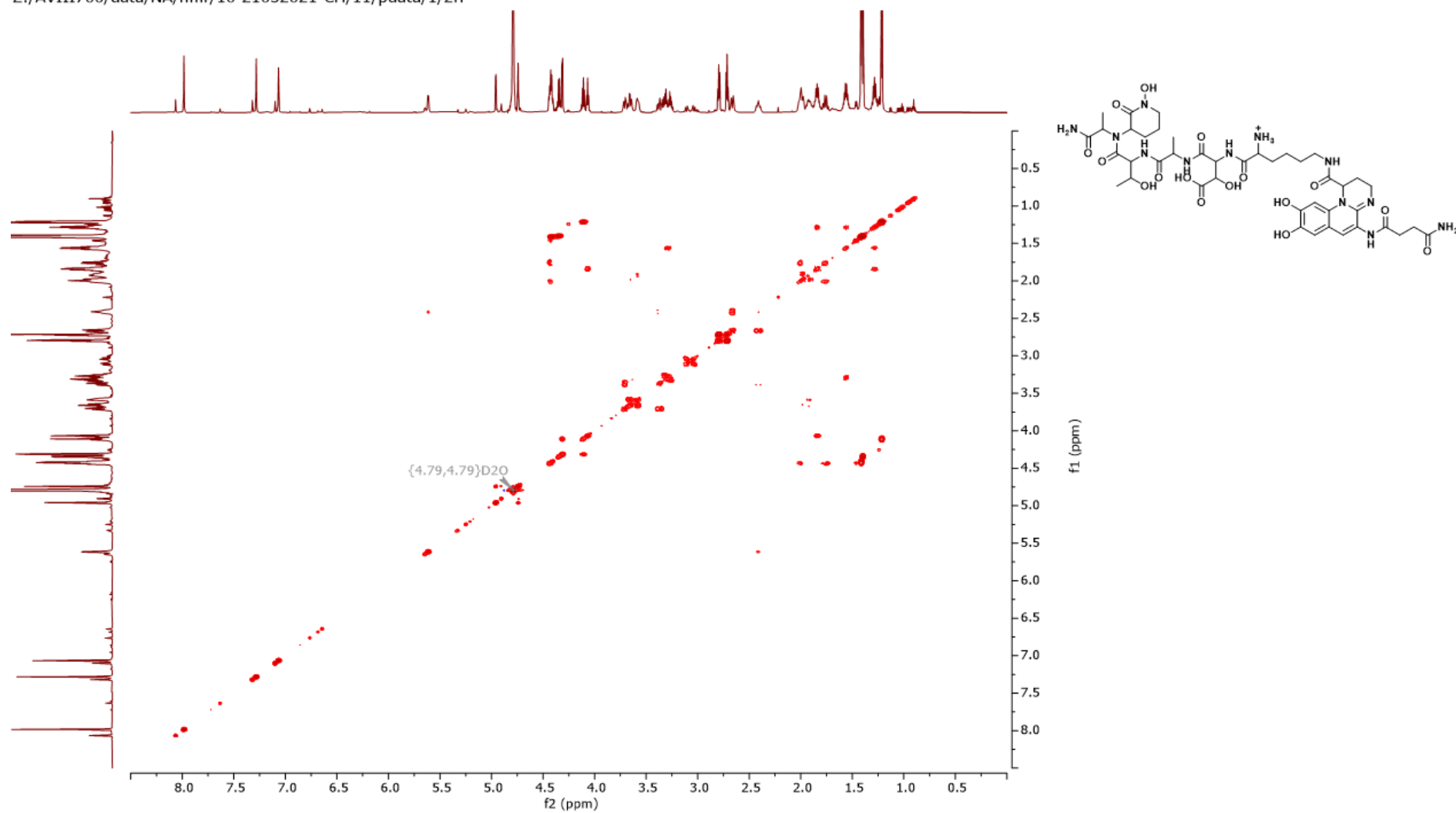


Figure S15: COSY NMR (D₂O, 700 MHz) of pseudobactin A TFA salt (1)

Z:/AVIII700/data/NA/nmr/10-21052021-CH/12/pdata/1/2rr

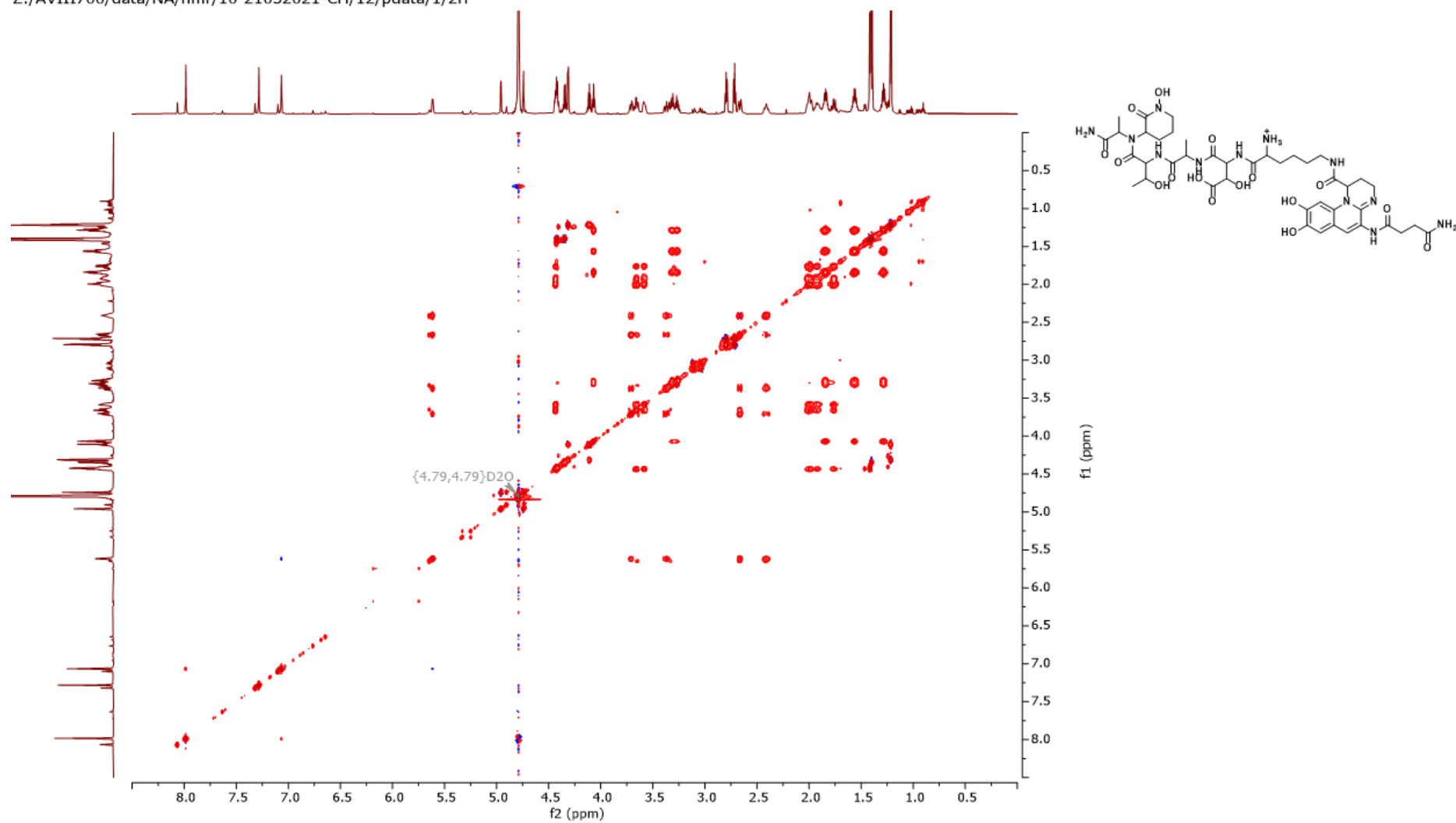


Figure S16: TOCSY NMR (D2O, 700 MHz) of pseudobactin A TFA salt (1)

Z:/AVIII700/data/NA/nmr/10-21052021-CH/13/pdata/1/2rr

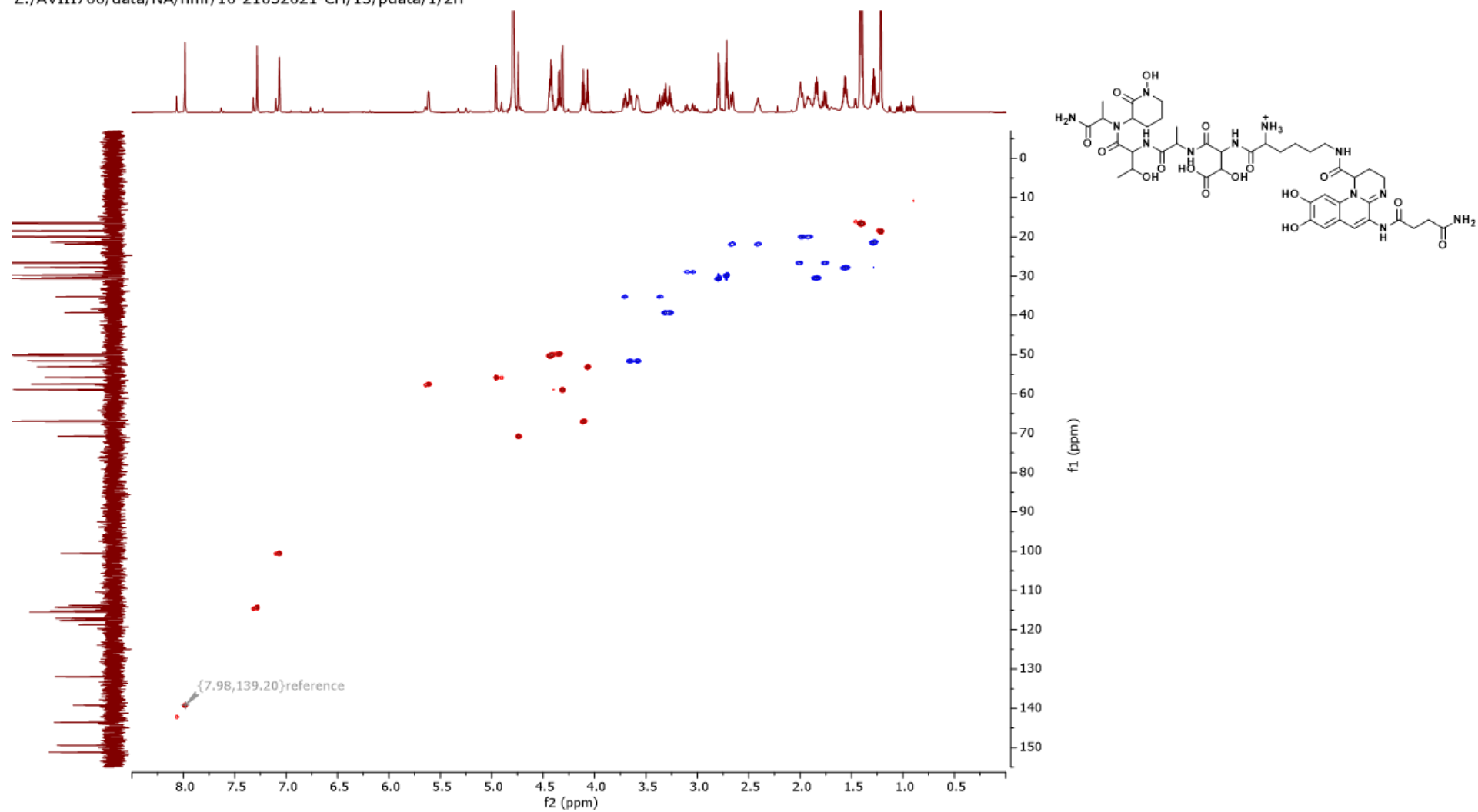


Figure S17: HSQC NMR (D₂O, 700 MHz) of pseudobactin A TFA salt (1)

Z:/AVIII700/data/NA/nmr/10-21052021-CH/14/pdata/1/2rr

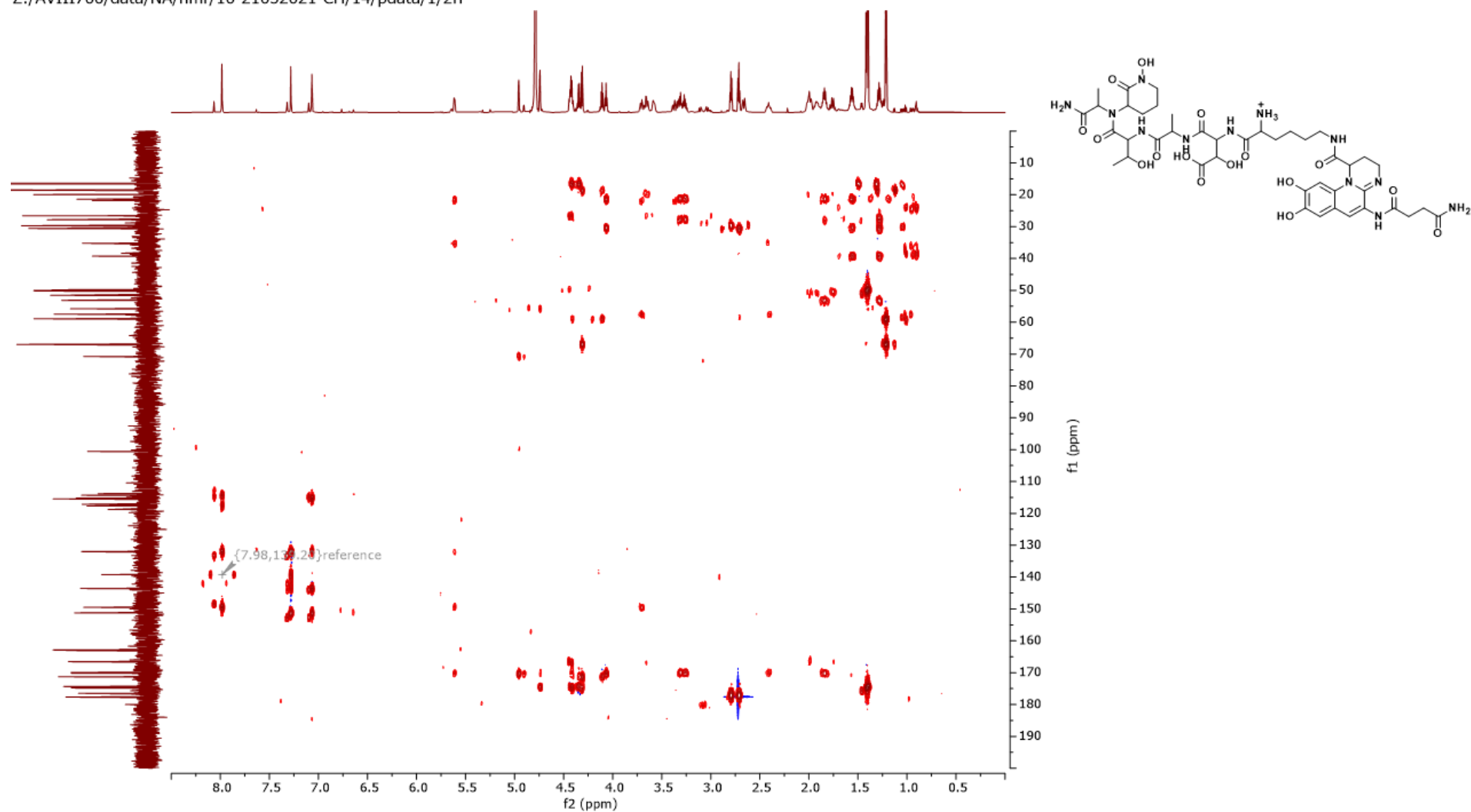
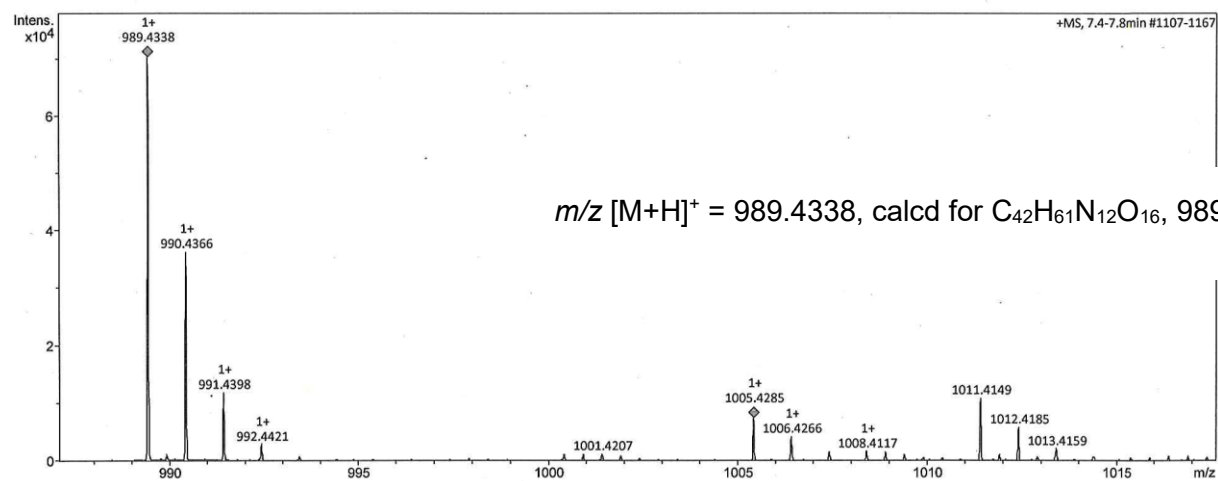


Figure S18:HMBC NMR (D₂O, 700 MHz) of pseudobactin A TFA salt (1)

Display Report

Analysis Info		Acquisition Date			
Analysis Name	D:\Data\oil\Hughes_CHPKWT_GB5_01_45560.d	11/27/2020 3:51:22 AM			
Method	automsms_50-1800_pos_spez.fraglist_xx_0.3.m	Operator	BDAL@DE		
Sample Name	Hughes_CHPKWT	Instrument	maXis	288882.21253	
Comment					
Acquisition Parameter					
Source Type	ESI	Ion Polarity	Positive	Set Nebulizer	2.0 Bar
Focus	Not active	Set Capillary	4500 V	Set Dry Heater	200 °C
Scan Begin	50 m/z	Set End Plate Offset	-500 V	Set Dry Gas	8.0 l/min
Scan End	1800 m/z	Set Charging Voltage	0 V	Set Divert Valve	Waste
		Set Corona	0 nA	Set APCI Heater	0 °C



Hughes_CHPKWT_GB5_01_45560.d
Bruker Compass DataAnalysis 4.2

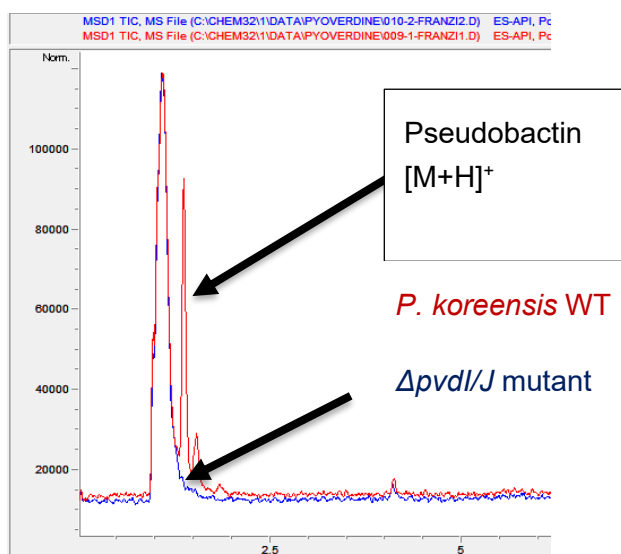
printed: 12/15/2020 1:19:15 PM

by: BDAL@DE

Page 1 of 1

Figure S19: HR-MS spectrum of pseudobactin A TFA salt (1)

a) HPLC-MS measurement of *P. koreensis* WT and mutant supernatant



b) Cross-streaking experiment of *P. koreensis* WT and mutant

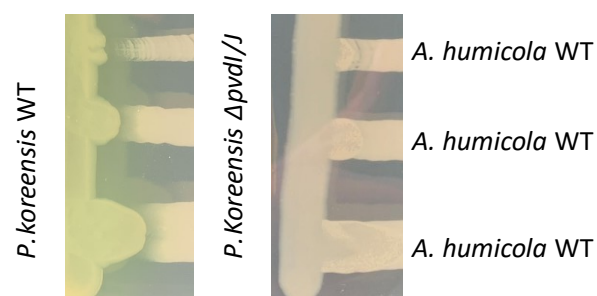


Figure S20: Pseudobactin production and activity in *P. koreensis* WT and $\Delta pvdI/J$ mutant. a) HPLC-MS of *P. koreensis* WT supernatant (red) and $\Delta pvdI/J$ supernatant (blue) was prepared as explained in material and methods section. A clear peak for the mass of pseudobactin is visible in WT supernatant and no peak can be seen in mutant supernatant. b) Cross-streaking experiments on f-base agar for the detection of pseudobactin's inhibitory interaction with *A. humicola*. Inhibition zones and fluorescence of pseudobactin can be seen on the left (*P. koreensis* WT). Loss of inhibitory activity and fluorescence is observed for the mutant (right).

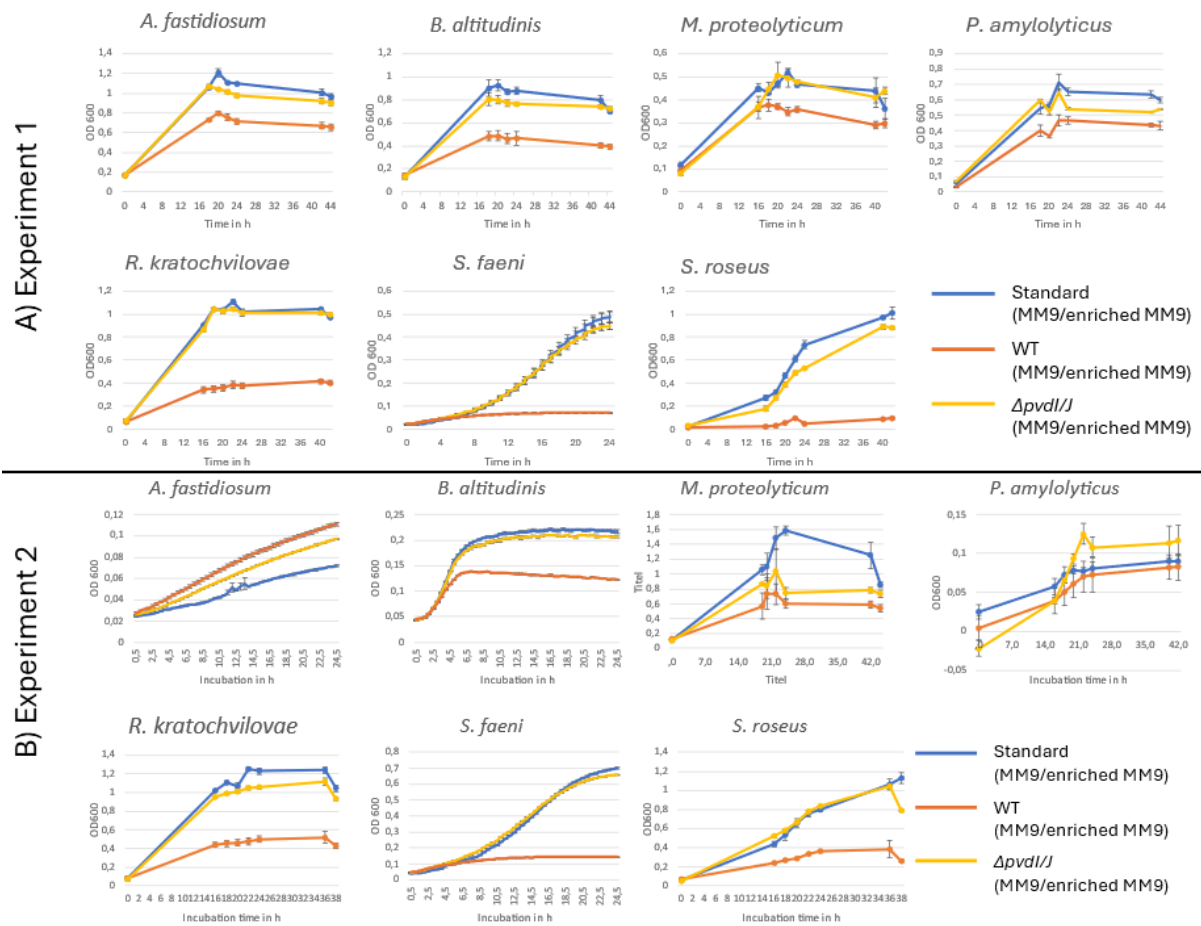


Figure S21: Growth curves of SynCom members in presence or absence of pseudobactin SynCom members were grown in MM9 or enriched MM9 in presence of sterile supernatant of *P. koreensis* WT (containing pseudobactin) and in presence of sterile supernatant of *P. koreensis* $\Delta pvdI/J$ mutant (no pseudobactin). Growth was observed by OD₆₀₀ measurement at RT and 180 rpm shaking in an TECAN 2000 device. Experiments were performed in triplicates. For information on media (MM9 or enriched MM9) used for each strain see table. S1 and S2. *A. humicola* growth curve is not shown here, since it is shown in the article.

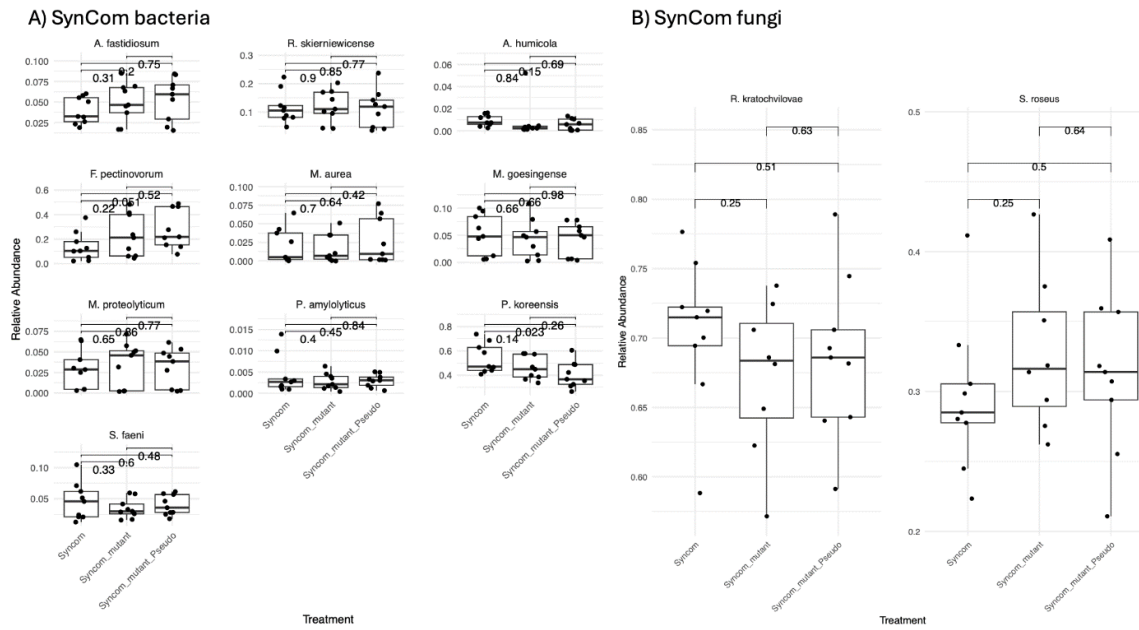


Figure S22: T-test of each SynCom member for the experiment (Fig.6) after 5 days of incubation: T-test was performed to see significant changes of the relative abundance of SynCom members grown on *A. thaliana* with SynCom WT, SynCom mutant and SynCom pseudobactin. *No data for *D. hungarica*, *N. cavernae* and *B. altitudinis* because the relative abundance was too low for the organisms.

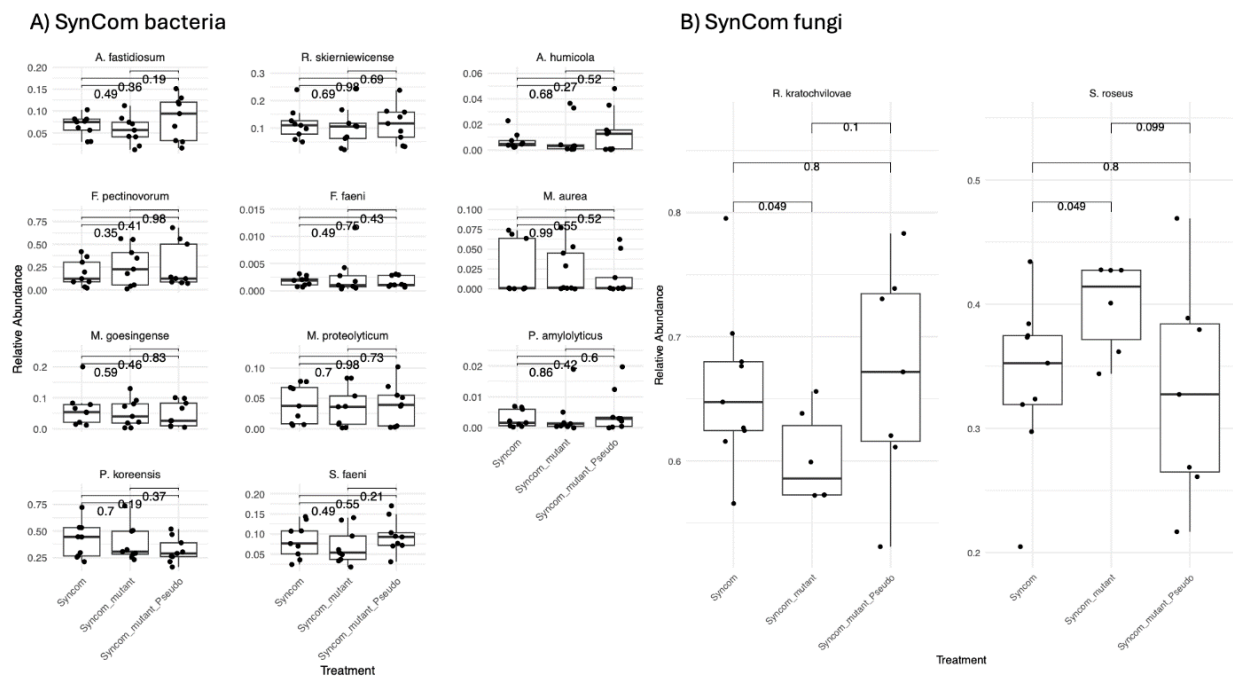


Figure 23: T-test of each SynCom member for the experiment (Fig.6) after 9 days of incubation: T-test was performed to see significant changes of the relative abundance of SynCom members grown on *A. thaliana* with SynCom WT, SynCom mutant and SynCom pseudobactin. *No data for *D. hungarica*, *N. cavernae* and *B. altitudinis* because the relative abundance was too low for the organisms.

References

*Huang et al., Huang W, Wilks A. A rapid seamless method for gene knockout in *Pseudomonas aeruginosa*. *BMC Microbiol.* 2017;17:199 <https://doi.org/10.1186/s12866-017-1112-5>

*Teintze, M.; Leong, J. Structure of pseudobactin A, a second siderophore from plant growth promoting *Pseudomonas B10*. *Biochemistry* 1981, 20, 6457–6462. DOI:10.1021/bi00525a026.

MANUSCRIPT 2

Title: Identifying Potential Community-Driving Metabolites in a microbial Plant Leaf associated community

Authors: Franziska Höhn, Dr. Paolo Stincone, Dr. Chambers C. Hughes, Dr. Daniel Petras, Prof. Heike Brötz-Oesterhelt, Prof. Eric Kemen, Prof. Nadine Ziemert

DECLARATIONS ON THE CONTRIBUTION OF CO-AUTHORS TO THE MANUSCRIPT

Author	Author position	Scientific ideas %	Data generation %	Analysis & interpretation %	Paper writing %
Franziska Höhn	First author	50	60	50	90
Dr. Paolo Stincone	Co- author	10	20	15	10
Dr. Chambers C. Hughes	Co- author	-	10	5	-
Dr. Daniel Petras	Co- author	15	10	15	-
Prof. Heike Brötz-Oesterhelt	Contributing author	-	-	5	-
Prof. Eric Kemen	Contributing author	10	-	5	-
Prof. Nadine Ziemert	Contributing author	15	-	5	-
Title of paper	Identifying Potential Community-Driving Metabolites in a microbial Plant Leaf associated community				
Status in publication process	Not submitted				

IDENTIFYING POTENTIAL COMMUNITY-DRIVING METABOLITES IN A MICROBIAL PLANT LEAF ASSOCIATED COMMUNITY

Franziska Höhn^{1,3}, Dr. Paolo Stincone^{2,3}, Dr. Chambers C. Hughes^{3,4,6}, Dr. Daniel Petras^{3,5}, Prof. Heike Brötz-Oesterhelt^{3,4,6}, Prof. Eric Kemen^{2,3*}, Prof. Nadine Ziemert^{1,3,4*}

Franziska Höhn	
Dr. Paolo Stincone	
Dr. Chambers Hughes	
Dr. Daniel Petras	
Prof. Heike Brötz-Oesterhelt	
Prof. Eric Kemen	
Prof. Nadine Ziemert	

¹Translational Genome Mining for Natural Products, Interfaculty Institute of Microbiology and Infection Medicine (IMIT) and Institute for Bioinformatics and Medical Informatics (IBMI), University of Tübingen, Tübingen, Germany

²Center for Plant Molecular Biology (ZMBP), Interfaculty Institute of Microbiology and Infection Medicine (IMIT), University of Tübingen, Tübingen, Germany

³ Cluster of Excellence Controlling Microbes to Fight Infections (CMFI), University of Tübingen, Tübingen, Germany

⁴German Centre for Infection Research (DZIF), Partner Site Tübingen, Tübingen, Germany

⁵Department of Biochemistry, University of California Riverside, Riverside, USA

⁶Department of Microbial Bioactive Compounds, Interfaculty Institute of Microbiology and Infection Medicine (IMIT), University of Tübingen, Tübingen, Germany

ABSTRACT

Ensuring plant growth and health is critical for global food security, especially amidst rising challenges such as climate change and increasing crop demands. The natural plant microbiome, comprising microorganisms essential for plant survival and stress tolerance, has emerged as a target for enhancing agricultural productivity. This study investigates microbial metabolite production within synthetic communities (SynComs) assembled from *Arabidopsis thaliana* leaf microbiomes. Using a non-targeted metabolomics approach, we compared the metabolomes of individual SynCom members to whole SynCom co-cultures. We hypothesized that metabolites present in higher concentrations in the community compared to single strain cultures are more likely to be regulated by microbial interactions, and to play a role in community dynamics. Our analysis identified several SynCom members as producers of strain-specific specialized metabolites present in the community, with some being significantly upregulated. Among them, biotin and N-acyl lysine produced by *Massilia aurea* were detected. Biotin supplementation of auxotrophic *B. altitudinis* cultures revealed the growth promoting effect of the vitamin on the strain, highlighting biotin cross-feeding as a potential mechanism of microbe-microbe interactions in the SynCom. Furthermore, the cytokinin trans-zeatin was notably triggered within the SynCom. Our results shed new light on microbial interactions in the phyllosphere-associated SynCom and identified metabolites that may drive synergistic dynamics in microbial communities.

INTRODUCTION

Plants are the primary nutrient source for humans and animals globally. Ensuring their growth and health is crucial for securing our food supply. However, agriculture is increasingly facing significant crop losses due to drought and diseases, a trend increasing due to climate change [1, 2]. Simultaneously, higher food yields are necessary to feed the growing population [3]. This urgent need for sustainable and long-term plant treatments to improve growth, health, and harvests has shifted the focus to the natural plant microbiome. Microorganisms that colonize plants are essential for their survival and are closely linked to plant health, disease resistance, and stress tolerance, making the microbiome a promising target for engineering [4, 5].

Research has made progress in promoting plant health by introducing microbial metabolites as fertilizers, employing single beneficial strains as biocontrol agents, or incorporating whole synthetic communities into natural microbiomes [5-7]. Nevertheless, the microbiome is a complex ecosystem, and the stability and integration of such treatments into natural microbiomes remain challenging [5, 8]. To optimize biocontrol agents and probiotic communities for sustainable treatment, it is vital to understand the interactions that drive and

stabilize the plant holobiont. Investigating microbe-microbe interactions and microbial metabolites that drive these interactions is particularly challenging due to the complexity and variability of microbiomes.

Synthetic communities (SynComs) have emerged as a valuable model system for detecting and investigating potent biocontrol agents, metabolites, and probiotic communities [9-12]. SynComs, which are subsets of the natural microbiome, allow for manipulation and observation under controlled conditions [13]. In this study, we used a SynCom to detect microbial metabolites that potentially play roles in microbe-microbe interactions within the plant microbiome. The SynCom was assembled from *A. thaliana* leaves in a garden experiment performed by Almario *et al.*, based on their occurrence in >95 % of plant samples for fungi and >98 % for bacteria [8]. Our hypothesis was based on findings that the production of microbial metabolites, such as antibiotics [14-16], proteins [17], and siderophores [18] is often triggered by microbe-microbe interactions during co-cultivations. Given nature's efficiency and resource conservation, we hypothesized that metabolites upregulated or triggered in co-cultures are produced because they are urgently needed under these conditions and thus play significant roles in the community. Such metabolites could be potential biocontrol agents or stabilizers for probiotic communities. To identify them, we employed a non-targeted metabolomics approach to compare the metabolomes of individual SynCom members and whole SynCom co-cultures. This method has been successfully used to depict metabolic shifts in ocean water [19] and microbial co-cultures [20]. We investigated metabolic shifts within the co-cultures with the aim to identify key organisms based on their metabolic overlap with the community, and significant upregulated or triggered metabolites in whole SynCom samples.

MATERIALS AND METHODS

SYNCOM STRAINS AND CULTURE CONDITIONS

The SynCom was assembled from microorganisms of the *Arabidopsis thaliana* leaf microbiome based on occurrence [8, 21]. 13 bacteria and 3 fungi (Table 1) were cultivated in pre-cultures from stocks on their optimal rich medium. For bacterial pre-cultures, nutrient agar (NA) (BD, USA) was used. Fungi were pre-cultured on potato-dextrose agar (PDA) (Carl Roth, DE). For UHPLC-MS/MS measurements, pre-cultures were taken from solid cultures on NA/PDA and cultured in nutrient broth for bacteria (NB, (BD,USA)) and in potato-dextrose broth (PDB (Carl Roth, Germany)) for fungi. Solid and liquid cultures were incubated for 2-3 days at 22 °C and 120 rpm shaking. Samples directly used for UHPLC-MS/MS were taken from liquid pre-cultures and incubated on MM9/7 minimal agar [21] for 5 days at 22 °C. MM9/7-Asp medium was used for biotin cross-feeding experiments. Therefore, MM9/7 [21] was modified by omitting agar-agar and aspartic acid.

Table 9: SynCom strains and their availability SynCom members were identified by BlastN analysis of their 16S rRNA and ITS2 region. Their genomes are available on NCBI.

Closest Type species match	Short name used in this study	Closest type strain match	% identity type species	Genome NCBI accession number
<i>Aeromicrobium fastidiosum</i>	<i>A. fastidiosum</i>	DSM 10552(T)	99.30	JAMKCA000000000
<i>Arthrobacter humicola</i>	<i>A. humicola</i>	KV-653(T)	100.00	JAFKON000000000
<i>Bacillus altitudinis</i>	<i>B. altitudinis</i>	41KF2b(T)	100.00	JAFKOO000000000
<i>Dioszegia hungarica</i>	<i>D. hungarica</i>	CBS 4214	100.00	JAMRJJ000000000
<i>Flavobacterium pectinovorum</i>	<i>F. pectinovorum</i>	DSM 6368(T)	98.61	JAFEVZ000000000
<i>Frigoribacterium faeni</i>	<i>F. faeni</i>	801(T)	99.82	JAIXNG000000000
<i>Massilia aurea</i>	<i>M. aurea</i>	AP13T	100.00	JBFMMP000000000
<i>Methylobacterium goesingense</i>	<i>M. goesingense</i>	iEII3(T)	99.43	JAFGZG000000000

<i>Microbacterium proteolyticum</i>	<i>M. proteolyticum</i>	RZ36(T)	99.29	JAFKOM000000000
<i>Nocardioides cavernae</i>	<i>N. cavernae</i>	YIM A1136(T)	99.23	JALQCQ000000000
<i>Paenibacillus amylolyticus</i>	<i>P. amylolyticus</i>	NBRC 15957(T)	99.49	JAMGVX000000000
<i>Pseudomonas koreensis</i>	<i>P. koreensis</i>	Ps 9-14(T)	100.00	JAFEVY000000000
<i>Rhizobium skirniwicense</i>	<i>R. skirniwicense</i>	Ch11(T)	99.64	JAFFPP000000000
<i>Rhodotorula kratochvilovae</i>	<i>R. kratochvilovae</i>	CBS 7436	99.82	JAFEUJ000000000
<i>Sphingomonas faeni</i>	<i>S. faeni</i>	MA-olki(T)	99.50	JALPNF000000000
<i>Sporobolomyces roseus</i>	<i>S. roseus</i>	CBS 486	99.29	JAFEUI000000000

SAMPLE PREPARATION FOR NON-TARGETED METABOLOMICS

SynCom strains were precultured in 20 ml liquid NB/PDB. *N. cavernae* was taken directly from stock due to low growth in NB. Strains were harvested by centrifugation at 8.000 rpm for 5 min and washed twice by using MgCl₂ (10 mM). Each strain was further diluted to an optical density at 600 nm (OD₆₀₀) of 1. For the whole SynCom sample, 1 ml of each strain dilution was mixed. One ml of each diluted SynCom member and the whole SynCom mixture were centrifuged at 7.000 rpm for 2 min and 600 µl supernatant was discarded. Cells were resuspended in the remaining supernatant and plated each on one MM9/7 agar plate. For each group, three biological replicates were prepared.

After incubation, cells were harvested by scratching them off the agar using a cell scraper, collected in 1.5 ml tubes and immediately frozen at – 80 °C for storage.

For the preparation of extracts, 1 ml 80 % MeOH (HPLC-grade) was added to the frozen biomass in each tube. Cells were mixed and extracted for 2,5 h at 22 °C in an over-head shaker. As controls, MM9/7 agar was extracted. After the extraction time, tubes were centrifuged at 15.000 rpm for 5 min at RT. The supernatants were collected in pre- weight 1.5 ml tubes and dried completely in a Speedvac (Thermo fisher, USA) at 45 °C. The tubes were weighted for dry mass detection and each extract was dissolved in 50 % MeOH (HPLC-grade) to a concentration of 5 mg dry mass/ml. Right before UHPLC-MS/MS measurement, extracts were centrifuged at 15.000 rpm for 15 min and transferred into HPLC-vials.

UHPLC-MS/MS MEASUREMENTS FOR NON-TARGETED METABOLOMICS

UHPLC-MS-MS measurements were performed by liquid chromatography-tandem mass spectrometry using a Vanquish UHPLC-system coupled with a Q Extractive HF mass spectrometer (thermos fisher, USA). The measurements were performed according to the method of Stincone et al [22]. Briefly, UHPLC-measurements were performed on a C18 column (Kinetex, 50 × 2.1 mm, 1.7 μm particle size, 100 Å pore size, Phenomenex, Torrance, USA). As solvent A) of the mobile phase, H₂O (LC/MS grade, Fisher Scientific) + 0.1% Formic Acid (FA) was used. Solvent B) was acetonitrile (LC/MS grade, Fisher Scientific) + 0.1% FA. Samples were separated using a linear gradient of 10 min at a flow rate of 500 μl/min. The gradient consisted of 5 % to 50 % solvent B) from 0-8 min and 50 % to 99 % solvent B) from 8-10 min. 99 % solvent B) were hold for 3 min as a washing step and the column was re-equilibrated at 5 % solvent B) for 3 more min. Mass spectrometry was performed in positive mode using a Heated Electrospray Ionization (HESI). The parameters for ionization were set as follows: 50 l/min sheath gas flow rate, 12 l/min auxiliary gas flow rate, 1 l/min sweep gas flow rate, 3.50 kV spray voltage, 250 °C inlet capillary temp., 50 V S-lens RF level and 400 °C auxiliary gas heater temp. The scan range was 120-1.800 m/z at a default resolution of 45.000, 1 micro-scan and AGC = 1E6. The ion injection was set to 100 ms.

The data-dependent acquisition (DDA) mode with TopN was set to (5) with a MS/MS spectra resolution of 15,000, an AGC target of 5E5, and a max. injection time of 50 ms. Additional parameters were: 1 m/z width, a stepwise increased normalized collision energy of 25-25-45 %, a dynamic exclusion set to 5 s and an apex trigger within 2-15 s [22].

DATA PROCESSING FOR NON-TARGETED METABOLOMICS

Raw data gained from UHPLC-MS/MS measurements were processed and analyzed following the pipeline of Petras *et al* [19]. In short, raw data files were converted to .mzML files by proteowizard. MS1 and MS2 feature extraction and filtering was performed by MZmine3.9.0 [23, 24]. Therefore, the following major settings were used. Mass detection was performed at 3.0E5 noise level for MS1 and 1.0E4 noise level for MS2 data. ADAP chromatograms were built with minimum 5 consensus scans and a minimum intensity of 2.0E5, with a mass tolerance of 0.002 m/z or 10 ppm. Local minimum feature resolver was set up to 85 % chromatographic threshold and a peak duration range of 0.01-2.00 (min/mobility). Isotope filtering was performed with 0.0015 m/z or 5 ppm mass and 0.01 min retention time tolerance. Isotopic peaks finder was set up to a mass tolerance of 0.0006 m/z or 10 ppm and a maximum charge of isotope m/z at 2. Features were aligned in join aligner at 0.002 m/z or 10 ppm mass and 0.15 retention time tolerance. The weight for m/z was 3. ¹³C isotope pattern were validated in the feature list row filter step. Gaps within the feature list were filled in the peak finder step at 20 % intensity tolerance, 0.001 m/z or 5 ppm mass tolerance and 0.05 min retention time tolerance. Duplicated peaks were filtered at 3 ppm mass and 0.1 min retention

time tolerance. The batchmode for MZmine 3 used in this study can be obtained in data storage <https://doi.org/10.57754/FDAT.72xh4-dxf33> (runs/external_supplements_manuscript).

The obtained feature table and the consensus MS/MS spectra were further used for GNPS2 feature based molecular networking with analog search and SIRIUS structure annotation.

DATA ANALYSIS FOLLOWING A NON-TARGETED METABOLOMICS PIPELINE

Feature based molecular networking was performed using GNPS2. Therefore, the MZmine3 generated feature table, the MS/MS spectra file and the metadata was uploaded to the GNPS2 website. Standard networking parameters were used as provided by the website. Analog search was activated to search library hits within a larger precursor mass tolerance (100 Da) and therefore take mass shifted peaks into account [25].

Molecular formulas and compound classes were predicted by SIRIUS (5.8.6). Therefore, the spectrum file from MZmine3 created for an export to SIRIUS was used. Molecular formulas were identified at 10 ppm accuracy under standard tool settings. ZODIAC was activated at standard parameters for the improvement of SIRIUS formula ranking. CSI fingerprint prediction was done for M+H adducts using the Bio database. Canopus compound class prediction was activated for feature classification. Compounds (881 features) with masses > 850 Da were excluded from the SIRIUS analysis due to computational power [26-29].

The GNPS2 generated network was visualized in cytoscape (10.0.0) including the SIRIUS molecular formulas and compound class predictions. The GNPS2 output and the created network can be found in the data storage <https://doi.org/10.57754/FDAT.72xh4-dxf33> (runs/external_supplements_manuscript).

STATISTICAL ANALYSIS FOR METABOLITE QUANTIFICATION

Statistical analysis of the network was performed by using the fbmn-statsguide.gnps2.org [30]. Therefore, the network data was directly loaded into the webapp from GNPS2 by using the Job ID. Blanks were filtered out according to the metadata annotation with cutoff 0.3. Imputation was performed and the data was normalized with “total ion current or sample-centric” normalization. Principal coordinate analysis (PCoA) of all strains was performed using the canberra distance matrix. Significantly upregulated metabolites in SynCom samples were identified by performing an one-way ANOVA-analysis. The ANOVA-significance table for p -values ≤ 0.05 was merged with the processed quantification table of fbmn-statsguide.gnps2.org to filter for significant metabolites with highest feature intensities in SynCom samples. Highest significantly upregulated (present in SynCom and single strain samples) and highest significantly triggered (present only in SynCom samples) metabolites with GNPS2 annotation were further analysed in Cytoscape for their clustering to other

metabolites and in the GNPS2 Dashboard webapp for the comparison of their fragmentation pattern to the library annotation.

To analyse the distribution of compound classes within significantly triggered metabolites ($m/z < 850$ Da), they were matched to SIRIUS NPC#pathway predictions.

MEASUREMENT OF COMPOUND STANDARD FOR LEVEL 1 ANNOTATION

The standards of biotin (iba lifesciences, Germany), trans-zeatin (Thermos Fisher Scientific, USA), trans-zeatin riboside (Sigma-Aldrich, USA) and 6N-(isopentenyl)adenosine (Cayman Chemicals, USA) were commercially available. Stock solutions of trans-zeatin, trans-zeatin riboside and isopentenyl-adenosine were prepared in ethanol at concentration 1 mg/ml. A biotin stock was prepared in 50 % MeOH at concentration 1 mg/ml. The stock solutions were diluted to 100 μ g/ml with 50 % MeOH and measured with UHPLC-MS/MS. Therefore, the same method as described for non-targeted metabolomics was used.

GENOME MINING FOR BIOTIN BIOSYNTHESIS GENES

The biosynthesis of biotin in microorganisms is encoded by the genes *bioF*, *bioA*, *bioD* and *bioB* [31]. Microorganisms which carry all four biosynthesis genes are potentially able to produce biotin and therefore are estimated to be biotin prototrophs. Microorganisms lacking some or all genes are estimated to be biotin auxotrophs. To investigate, which SynCom members carry genes for biotin biosynthesis we annotated the SynCom genomes using prokka 1.11 with default setting and searched for the annotation of the biotin biosynthesis genes. The prokka annotated genomes can be found in the data storage <https://doi.org/10.57754/FDAT.72xh4-dxf33> (runs/external_supplements_manuscript).

GROWTH CURVES WITH BIOTIN CROSS-FEEDING

The effect of biotin on the growth of auxotrophic SynCom members was tested by performing growth curve assays. The auxotrophic organisms *B. altitudinis*, *D. hungarica*, *A. humicola* and *A. faeni* were pre-cultured on NA/PDA. After 3 days of incubation at 22 °C, the organisms were inoculated into liquid pre-cultures in MM9/7 medium. After 2 days of incubation, cells were harvested by centrifugation at 8000 rpm for 2 min. Cells were washed twice in 1 ml MgCl₂ (10 mM) and resuspended in MM9/7-Asp. MM9/7-Asp was the medium used for biotin cross-feeding experiments, since it contained minimal nutrient concentrations and lacked aspartic acid, which is known to take over some roles of biotin in a cell [32]. The OD₆₀₀ was measured, and the cells were diluted with MM9/7-Asp to OD₆₀₀ = 0.2. 1 ml of each cell dilution was added into a well of a 24-well plate. For each strain growth curves in MM9/7-Asp and MM9/7-Asp +

biotin were measured in triplicates. For biotin supplementation, we first tested different concentrations of biotin (10 μ M, 1 μ M and 100 nM) in the first experiment and chose 1 μ M biotin supplementation in the second experiment. Biotin from stock (100 μ M) was added to the wells. Plates were incubated at 22 °C for around 24-28 h and 120 rpm shaking. OD₆₀₀ was measured with a spectrophotometer (SpectroStar Nano, BMG Labtech, DE) at the timepoints shown in the figures (Fig. 8 and Fig. S1) For *B. altitudinis*, two independent experiments were performed.

RESULTS AND DISCUSSION

Metabolomic analysis represents a promising approach for detecting metabolites produced by microorganisms under various conditions [33, 34]. Non-targeted metabolomics facilitates the comprehensive measurement of a strain's entire metabolic profile without concentrating on specific metabolites [35, 36]. This technique can be employed to investigate metabolic shifts under altered conditions, providing insights into a strain's metabolic adaptation to environmental changes [37, 38]. In our study, we utilized non-targeted metabolomics to compare the metabolic profiles of individual SynCom members with those of co-cultures comprising the entire community. This approach aimed to elucidate the production of secondary metabolites by specific strains, which potentially play a role in community dynamics of the plant leaf-associated SynCom. By comparing individual SynCom members to whole SynCom co-cultures, we identified metabolites that are present at higher concentrations in the co-cultures (SynCom samples). Given that the production of specific metabolites in nature is often triggered only when required [39-41], we hypothesized that these SynCom-specific metabolites are integral to microbe-microbe interactions.

N-ACYL AMINO ACIDS ARE THE MOST ABUNDANT GROUP DETECTED IN SINGLE AND SYNCOM CULTURES

To investigate metabolites, present in individual SynCom strains and whole SynCom co-cultures grown on MM9/7 agar, we employed non-targeted metabolomics. Raw UHPLC-MS/MS data were filtered and processed using MZmine3 [23], followed by further analysis with GNPS2 [42]. Feature-based molecular networking via GNPS2 enabled the creation of a network based on MS1 and MS2 similarities, detecting known metabolites through comparison with the GNPS2 database. Each node in the network represents a metabolite detected in the sample.

Our study began with the analysis of secondary metabolites produced by individual SynCom members and SynCom co-cultures by examining GNPS2 annotations to likely known compounds within the network. The network comprised 9.265 metabolites (features) (blanks excluded), of which 3.644 were annotated by GNPS2 (annotated features in table ES1 (ES = external supplements)). Among these, several metabolites showed GNPS2 library hits for known secondary metabolites, such as siderophores like rhodotorulic acid, and biosurfactants like surfactin A-D. Rhodotorulic acid and surfactins were detected in both single cultures and SynCom samples. The identification of siderophores in the SynCom co-cultures was anticipated, given that several SynCom members possess gene clusters for siderophore production, as discovered in our previous study [21]. The production of siderophores can confer a competitive advantage to the producer in environments with a high concentration of potential competitors, as demonstrated in the rhizosphere microbiome [43]. The presence of surfactins in SynCom samples is likely attributable to *B. altitudinis*, as we previously identified

a biosynthetic gene cluster for surfactin production in this strain [21]. Our data uncovered the presence of rhodotorulic acid and surfactins in the community, therefore highlighting these compounds for further investigations on their role within the SynCom.

From the 3.644 GNPS2 annotated metabolites, 2.828 annotated metabolites were detected in one or more single strain samples, and 752 were present in both single strains and SynCom samples. Notably, 64 annotated metabolites were specific to SynCom samples, indicating their exclusive presence in co-cultures. The annotated metabolites table (table ES1) serves as a reference database for putative secondary metabolites produced by SynCom members, facilitating further investigations of microbe-microbe interactions.

Even though GNPS2 annotations require verification through comparison of fragmentation patterns for level 2 annotations and measurement of standards for level 1 annotations [19], non-targeted metabolomics proves to be an effective method for detecting and prioritizing metabolites with known functions potentially driving microbial interactions. Thus, metabolomics is a crucial component of a multi-omics approach necessary for understanding the complex structure of microbiomes [44-46].

One of the largest compound groups found in SynCom and in single strain samples were annotated by GNPS2 as N-acyl amino acids. In total 236 putative N-acyl amino acids could be detected. 172 compounds were detected only in one or more single strain samples, whereas 64 were found in both, SynCom and single strains samples. No N-acyl amino acid was annotated in SynCom samples only. The high abundance of N-acyl amino acids was striking since no other compound group counted so many specific annotations from GNPS2. N-acyl amino acids are known to be produced by various environmental microorganisms and are an abundant group of metabolites [47-50]. The family of N-acyl amino acids covers a huge diversity of compounds, but all share the common structure of an amine linked to a fatty acid via an amide bond [50]. In our study we focused on N-acyl amino acids annotated by GNPS2 as single amino acids connected to unmodified saturated or unsaturated fatty acids. All 16 SynCom members carried metabolites annotated as N-acyl amino acids in their metabolome. Whereas 119 N-acyl amino acids were produced by more than one SynCom member, *B. altitudinis* (36) and *F. pectinovorum* (20) produced the most unique N-acyl amino acids (table ES2). In *Bacillus* spp. N-acyl amino acids like N-acyl homoserine lactone are known as signaling molecules for quorum sensing mechanisms [51]. Besides their role as signaling molecules, some N-acyl amino acids from *Streptomyces* spp. have antimicrobial activities [52]. It was furthermore shown that the function of an N-acyl amino acid varies with their chain length and therefore can be very different [47, 50]. Knowledge about the functions of the vast majority of N-acyl amino acids has however remained limited. The variety of N-acyl amino acids and their unknown function, make them an interesting compound group in the context of microbe-microbe interaction dynamics.

THE RELATIVE ABUNDANCE OF COMPOUND CLASSES REMAINS STABLE OVER SINGLE AND CO-CULTURES

As a next step, we aimed to compare the metabolome of individual bacterial strains to that of the synthetic community (SynCom). Given that a minority of metabolites within the GNPS2 network (network file in external supplements) were annotated, we employed the SIRIUS tool to predict the compound class of each metabolite (table ES3). SIRIUS uses the fragmentation patterns of metabolites to make predictions on the compound class and structure of a metabolite. This approach allowed us to investigate changes in the relative compound composition of all single strain samples compared to the SynCom samples, as depicted in figure 1. Due to computational limitations, SIRIUS was performed on metabolites with masses < 850 Da.

For both groups, the largest predicted compound class was amino acids and peptides, comprising 31.1% of single strain metabolites and 35.1% of SynCom metabolites, with 490 metabolites shared between the single and SynCom samples. Notably, 16.9% of SynCom metabolites could not be classified, whereas 32.4% of single strain metabolites lacked annotation. A possible reason for missing predictions is the mass limit (<850 Da) used in the present study. Therefore, metabolites with higher masses were not analyzed by SIRIUS, which remains a limitation of our study. Future investigations are necessary to uncover the compound classes of the unknown metabolite group detected here.

The SIRIUS analysis revealed that single strains exhibit a high coverage of metabolites also present in the SynCom, with only 10.9% of SynCom metabolites being specific to the community and therefore absent in single cultures. This can be attributed to differences in sample sizes. While single strain data was derived from 48 samples (three replicate per strain), each covering more than 8,000 features in the raw data, SynCom data was based on only three samples, each with more than 8,000 features. Furthermore, UHPLC-MS/MS measurements detect all present metabolites, including both strain-specific secondary metabolites and compounds from primary metabolism [53]. Given that microorganisms share a substantial number of common structures, such as components of bacterial cell walls, it is unsurprising that no significant differences in the compound class composition of single strains and SynCom were detected [54]. Nevertheless, at a compound class level, it is difficult to observe metabolomic changes since the annotation is broad. To dive deeper into metabolomic differences between single strain cultures and SynCom co-cultures, we applied statistical analyses on the metabolomic dataset.

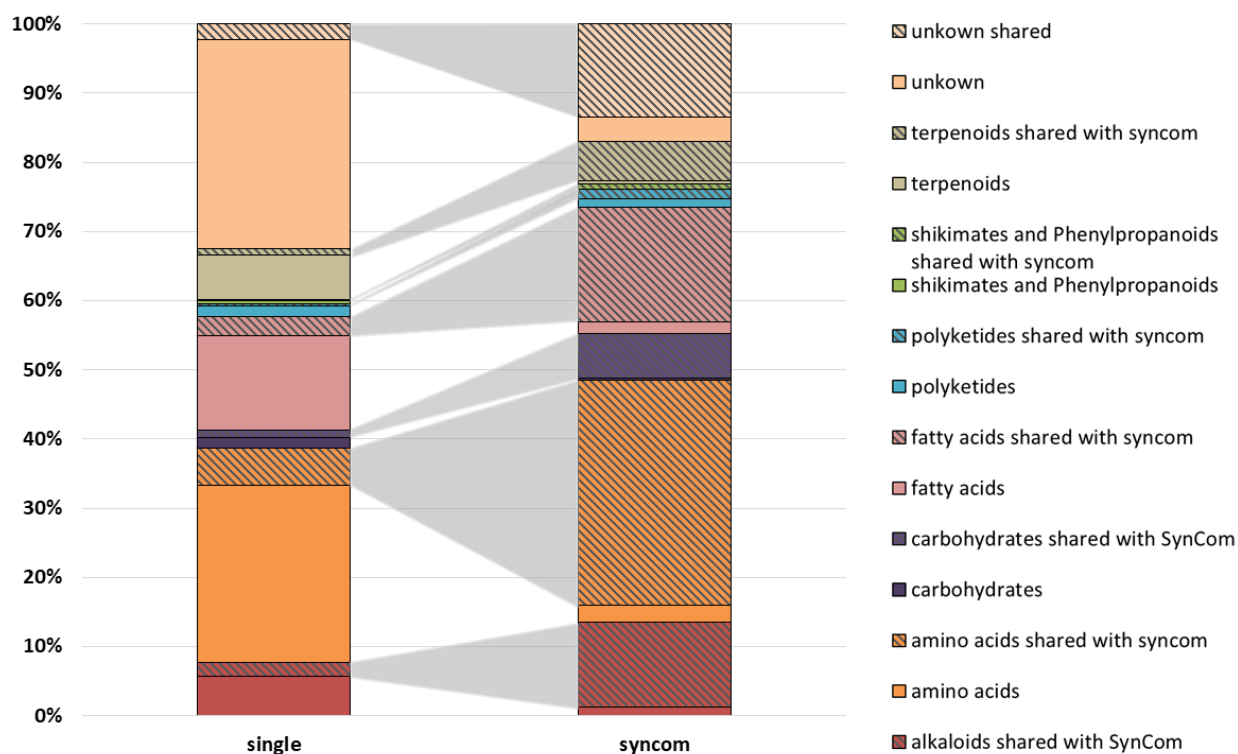


Figure 24: Relative compound composition in all single SynCom strains compared to whole SynCom samples based on SIRIUS class predictions. The SIRIUS analysis was based on 1506 features with masses < 850 Da.

THE SYNCOM METABOLOME CLUSTERS WITH MOST SINGLE STRAIN METABOLOMES

Statistical analysis of the GNPS2 feature based molecular network was performed with fbmn-stats.guide.gnps2.org. The majority of compounds detected in SynCom samples were shared with the overall single strain metabolome (figure 1). To further investigate whether the shared compounds of the SynCom metabolome are equally distributed among all SynCom strains or if the SynCom metabolome shows a higher similarity to the metabolome of certain strains, we examined the node distribution of the GNPS2 network. Each metabolite was sorted according to the sample in which it occurred (figure 2). This approach allowed us to display the metabolome of each SynCom strain, indicating which metabolites were specific for this single strain (blue), which were specific for the strain and found in SynCom samples (green), which were produced by the strain and additionally present in single samples of other SynCom members (red) and which were present in multiple single and in SynCom samples (violet).

Our non-targeted-metabolomics analysis revealed that *S. faeni*, *M. aurea*, and *B. altitudinis* had the most extensive metabolomes. These strains also harbored a significant number of strain-specific metabolites (blue) not present in SynCom samples. The extensive metabolome of *B. altitudinis* reflects the well-documented metabolic capabilities of bacilli, which are known

to produce a wide variety of secondary metabolites including antimicrobials, siderophores, and carotenoids [55, 56]. *Bacillus spp.* are also recognized for their variety of extracellular signaling molecules, like surfactins [57, 58]. Several surfactins from *B. altitudinis* were found in both single strain and SynCom samples underlining the strain's extensive metabolic capability and its substantial metabolome.

Strain-specific metabolites present in SynCom samples were predominantly produced by *P. koreensis* and *B. altitudinis* (green). Interestingly, these strains were identified as strong pairwise inhibitors in our previous study and demonstrated a high potential for antimicrobial production based on the presence of biosynthetic gene clusters [21]. Additionally, pseudomonads and bacilli are known biofilm producers, an ability that is particularly advantageous in communities inhabiting harsh environments, such as the plant leaf surface [59-62]. Both biofilm formation and antimicrobial production require the secretion of various metabolites, which might explain the dominance of strain-specific metabolites from these strains within the SynCom. The nature of strain-specific metabolites from *P. koreensis* and *B. altitudinis* needs to be further investigated to draw conclusion on their functions.

Strains with the lowest number of strain-specific metabolites in both single strain cultures and SynCom co-cultures were *F. faeni*, *A. fastidiosum*, *D. hungarica*, and *M. proteolyticum*. Some of these strains were found to be sensitive in pairwise interactions with *B. altitudinis* and *P. koreensis*. Except for *M. proteolyticum*, these strains also carried a low number of biosynthetic gene clusters for secondary metabolite production, which could account for their smaller metabolomes and fewer strain-specific metabolites in SynCom samples [21].

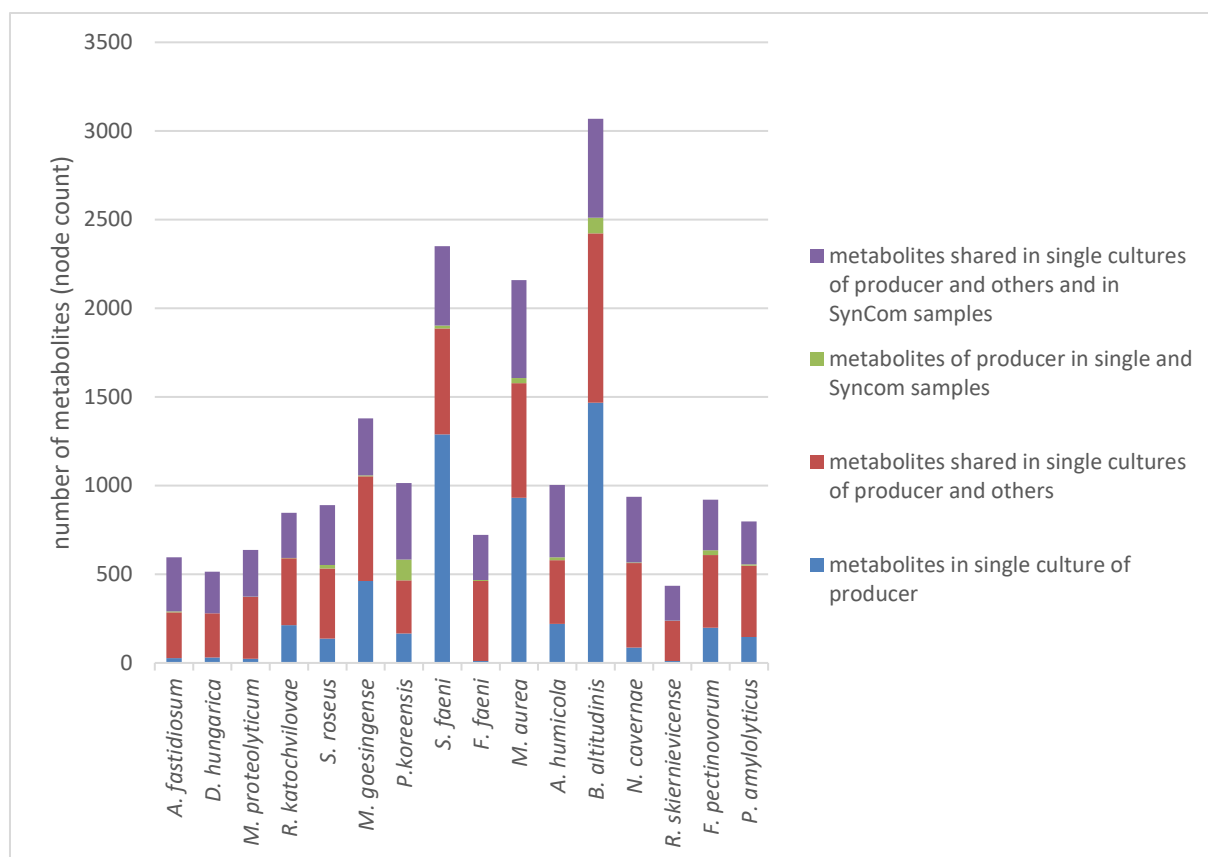


Figure 25: Node distribution analysis to detect the number of metabolites in the metabolome of each SynCom member. Number was based on node counts that were detected in cultures of a strain. Metabolites were sorted in four categories to determine the overlap in single strain samples and SynCom samples. Metabolites produced by one SynCom member were estimated to be strain specific and were observed in either only the single strain culture (blue) or in the single strain culture and the SynCom (green). Metabolites that are produced by multiple SynCom members were detected either in multiple single strain samples (red) or in multiple single strain cultures and SynCom samples (violet).

The node distribution analysis provides only qualitative information about the presence of metabolites in different samples, indicating merely whether a metabolite is present or absent. To detect significant differences between the metabolomes of single strain and co-culture samples, a quantitative approach is necessary, considering the feature intensities and therefore the concentration of each metabolite. We further analyzed the GNPS2 data using the statistical analysis tool fbmn-statsguide.gnps2.org.

We performed a principal coordinate analysis (PCoA) to compare the metabolomes of each strain and the SynCom. This analysis allowed us to investigate the similarities between the metabolomes (figure 3). Interestingly, most SynCom members and the SynCom samples themselves clustered together (figure 4), while three SynCom members exhibited high distances from the cluster (figure 3). The most distant metabolome was that of *S. faeni*, followed by *M. aurea* and *B. altitudinis*. While *S. faeni* and *M. aurea* displayed highly similar

metabolomes across all three replicates, *B. altitudinis* showed heterogeneous results, with one sample clustering with the SynCom.

The distance of SynCom samples from *B. altitudinis* samples was surprising, given that SynCom samples contain a high number of *B. altitudinis*-derived compounds. However, the high distance of all three strains can be explained by the results observed in the node distribution analysis. These strains had the highest number of strain-specific metabolites, which were absent in SynCom samples (figure 2, blue). Therefore, their metabolomes appear as the most distinct from the SynCom metabolome. Strains with metabolomes most similar to the SynCom samples included *D. hungarica*, *A. fastidiosum*, *R. skierniewicense*, and *M. proteolyticum*. These strains had the lowest numbers of strain-specific metabolites in the node distribution analysis but showed the highest number of shared metabolites. Although the node distribution analysis and the PCoA are not directly comparable, as PCoA considers feature intensities, they yield similar results. The SynCom metabolome appears to be composed predominantly of metabolites shared among many strains, rather than metabolites from a few specific strains. Taking into account that non-targeted metabolomics approaches capture not only secondary metabolites produced by microorganisms but furthermore metabolites from primary metabolism [63], a huge metabolic overlap is not surprising. Therefore, strains with low metabolic capacity are clustering together, whereas strains with high metabolic capacity are distinct. It would be interesting to investigate further, why so much strain-specific compounds from *B. altitudinis*, *S. faeni* and *M. aurea* are not present in the community. One explanation could be that these strains showed a low relative abundance in the community *in vitro* under the same culture conditions as used in the present study [21]. Therefore, their strain-specific metabolites were not detected in the SynCom metabolome. Another possibility is that some strain-specific metabolites are highly expressed in single-strain cultures, but their production might be downregulated in the community as shown for soil microbiome members [64]. Unfortunately, our data did not allow for a comprehensive investigation of significantly downregulated metabolites. This limitation arises because a low concentration of a metabolite in SynCom samples could simply reflect the low abundance of the producing strain within the community, rather than a true downregulation of metabolite production. Therefore, any observed lower feature intensity could be misleading. In further investigations, a normalization of the metabolite intensities to the relative abundance of a strain in the community could give insights into downregulations. Additionally, transcriptomic analysis can be performed to cover also metabolites that fell below the detection level in the metabolomics approach.

PRINCIPAL COORDINATE ANALYSIS

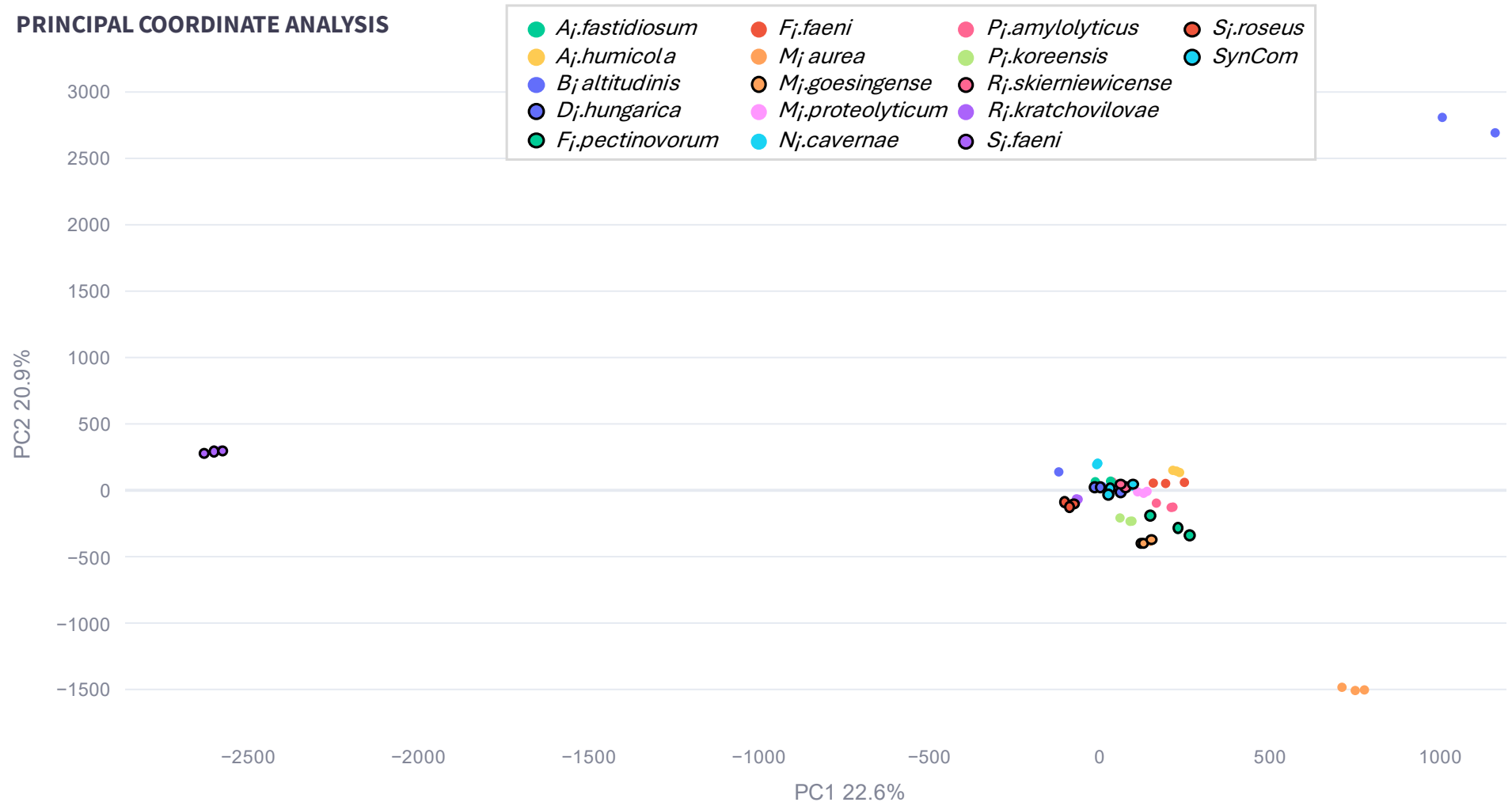


Figure 26: Principal coordinate analysis of the metabolomes of single strain samples and SynCom co-cultures

PRINCIPAL COORDINATE ANALYSIS

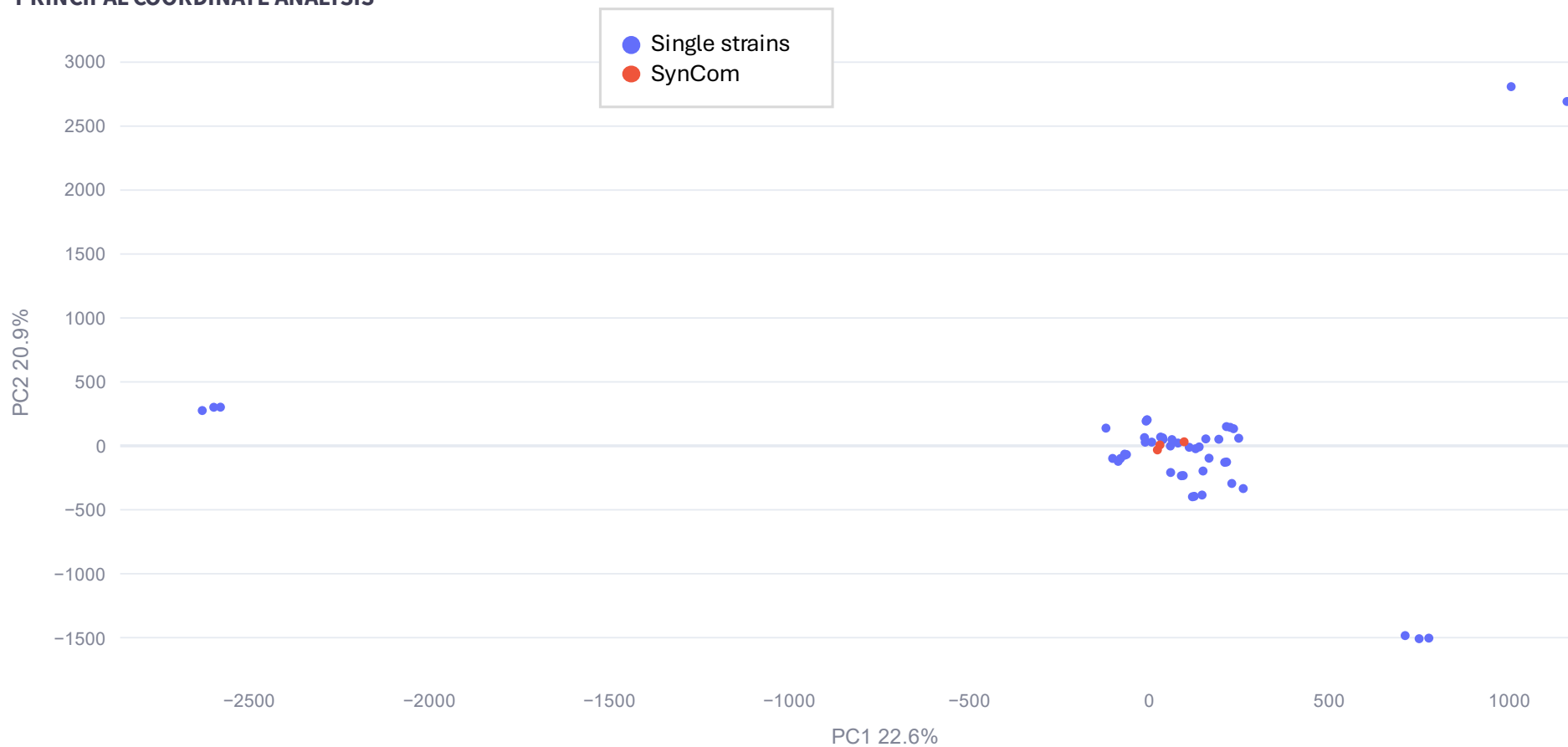


Figure 27: Principal coordinate analysis of metabolomes of single strain samples and SynCom co-cultures with focus on SynCom samples (red)

N-ACYL LYSINE AND BIOTIN ARE THE MOST SIGNIFICANT UPREGULATED ANNOTATED METABOLITES IN THE SYNCOM

We next hypothesized that metabolites present in higher concentrations in SynCom samples might be involved in microbe-microbe interactions due to their high abundance in the community and low abundance in single cultures. To identify such metabolites, we matched the quantification table from fbmn-statsguide.gnps2.org (which included feature intensities, table ES4) with the ANOVA-significance table (p -value < 0.05, which included significance information, table ES5). This allowed us to filter our data for significant metabolites that showed the highest feature intensities in SynCom samples (table ES6).

We categorized the results into two groups: upregulated metabolites and triggered metabolites. Metabolites detected in both single strain samples and SynCom samples, but with significantly higher feature intensities in SynCom samples, were classified as upregulated metabolites. These were considered to have increased production levels within the community setting. Consequently, we focused on metabolites produced by only one SynCom member to identify which strains produce upregulated compounds. The second group, triggered metabolites, consisted of significant metabolites detected only in SynCom samples and not in single strain samples. These were presumed to be produced within the community as a result of co-cultivation, indicating that their production was specifically triggered by the presence of other microbial strains in the SynCom.

In total, we identified 133 significant metabolites exhibiting the highest feature intensities in SynCom samples, of which 41 metabolites have been annotated by the GNPS2 library. Among these, 13 significant metabolites were present in single samples and therefore upregulated in SynCom samples. 28 annotated metabolites were only present in the SynCom and therefore triggered in the community (figure 5 and table ES6). *P. koreensis* was the producer of the most upregulated metabolites (9), followed by *B. altitudinis* (5) and *M. aurea* (5) (figure 5). Notably, *P. koreensis*, *B. altitudinis*, and *M. aurea* also exhibited a high number of strain-specific metabolites in the SynCom samples (figure 2), with some of these being among the most significantly upregulated compounds. In our previous study, we observed that *P. koreensis* was the most abundant SynCom member after 5 days of incubation [21]. This high abundance likely explains the substantial number of strain-specific and significantly upregulated metabolites produced by *P. koreensis*. In contrast, *B. altitudinis*, despite being one of the least abundant strains in the SynCom as shown in the previous study [21], still exhibited a large number of strain-specific and upregulated metabolites present in the community. This suggests that a strain's dominance in the community might influence the abundance of its products but is not a strict requirement for producing significantly upregulated metabolites.

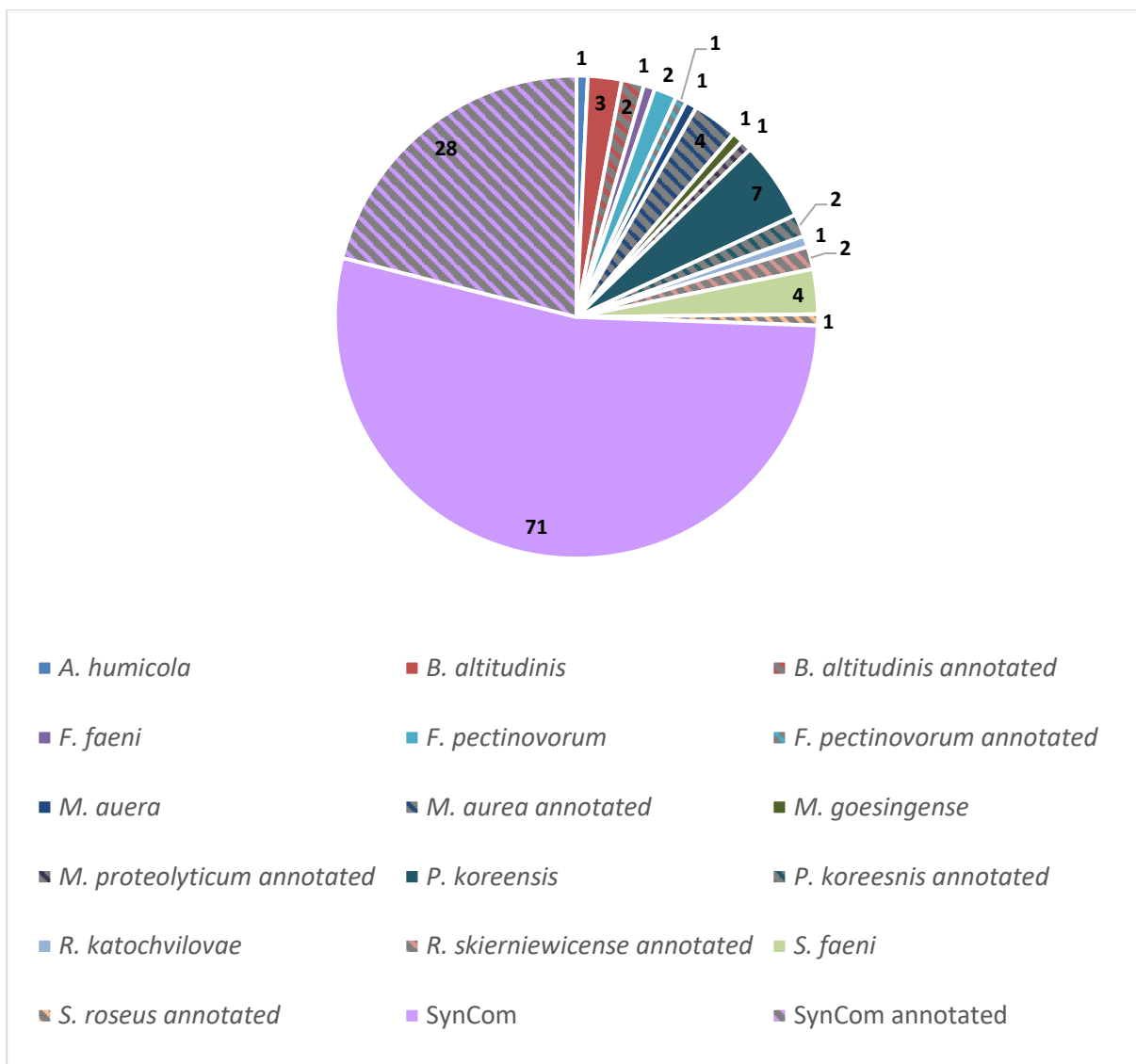


Figure 28: Number of significant metabolites present in the community assigned to their producer. The significance of a metabolite was determined by one-way ANOVA analysis using fbrn-statsguide.gnps2.org based on significant differences in feature intensities between a strain monoculture and the SynCom co-culture. The metabolites shown in the figure were significant, when feature intensities were significantly higher ($p < 0.005$) in the co-culture, than in monocultures. For metabolites in the groups SynCom and SynCom annotated, no assignment to producers was possible, since these compounds were not detected in monocultures. Additionally indicated is, whether a metabolite was annotated in the GNPS2 feature based molecular network.

To identify secondary metabolites with potential effects on community dynamics, we focused on significantly upregulated metabolites annotated by GNPS2. We investigated which of the 13 annotated and upregulated metabolites showed the highest significance based on the lowest p -value. Additionally, we assessed the accuracy of the GNPS2 annotations by comparing the fragmentation patterns of our compounds to those in the GNPS2 library (figure S1 and S2).

We found that feature 4437 (373.1988 *m/z*; rt: 0.78 min), annotated as N-acyl lysine C4:0 (figure 6A), was the most significantly upregulated and annotated compound, followed by feature 7883 (245.0956 *m/z*; rt: 1.78 min), annotated as biotin (figure 7A). Interestingly, both metabolites were detected in SynCom co-cultures and single strain cultures of *M. aurea*, suggesting the strain might be the producer.

Whereas the precursor mass of feature 7883 exactly matched the mass of the library hit for biotin (figure 7B), the mass of feature 4437 differed from N-acyl lysine C4:0 by 156.04 Da (figure 6B). Since the fragmentation pattern showed fragments corresponding to lysine, the mass difference was likely due to variations in the fatty acid chain length (Figure S1). Within the GNPS2 network, our N-acyl lysine clustered with metabolites annotated as other N-acyl lysines with different chain lengths produced by various SynCom members. Although N-acyl lysines are abundant in both SynCom and single cultures, differences in chain length can significantly affect the function of N-acyl amino acids [47, 48]. Therefore, investigating our N-acyl lysine in microbial interactions, such as in agar diffusion tests, can provide more insights into its role in the SynCom. It has already been shown that N-acyl lysines can be chemically synthesized using the carboxylic acid anhydride method. Moreover, N-lauryl lysine has been characterized as a potent surfactant [65], further suggesting that the identified significant metabolite might be a key driver of SynCom interactions and warrants further investigation.

Feature 7883, annotated as biotin, clustered in the GNPS2 network with a metabolite annotated as dethiobiotin (figure S3), which was only produced in single strain cultures of *M. aurea*, *B. altitudinis*, and *D. hungarica*. Literature research revealed that dethiobiotin is the precursor molecule of biotin and synthesized by the genes *bioF*, *bioA*, and *bioD*. The precursor is further processed by biotin synthase (*bioB*) to the product biotin [66-68]. Studies have shown that in marine microbial ecosystems, the biotin cycle is a crucial cross-feeding platform [31]. Since the vitamin acts as a co-factor for numerous enzymes involved in carboxylation reactions in the primary metabolism of microorganisms, for example in fatty acid synthesis, it is essential for organismic growth [66].

Investigating the marine biotin cycle, Wienhausen *et al.* demonstrated that the ecosystem contains microorganisms capable of performing different steps of biotin biosynthesis. Complete auxotrophs lack all four genes for biotin synthesis from pimeloyl-CoA and thus rely on external biotin uptake. Some organisms exhibit obligate auxotrophy, missing the first three genes (*bioF*, *bioA*, *bioD*) but possessing biotin synthase (*bioB*) to synthesize biotin from externally received dethiobiotin. Lastly, biotin prototrophs, which possess all four genes for biotin biosynthesis, can supply the vitamin to their surrounding [31]. Biotin can then be taken up by microorganisms with the bioMNY transporter system [69]. We screened all SynCom strains for the presence of biotin biosynthesis and biotin uptake genes and found five SynCom members to be biotin auxotrophic due to the lack of all four biosynthesis genes and four SynCom members as obligate auxotrophs lacking some of the genes (table S1). Interestingly *F. pectinovorum*, *M. goesingense*, *P. koreensis*, and *S. faeni* possess all four genes for biotin

production but did not show dethiobiotin or biotin in their metabolomes (network file). *M. aurea* in contrast carries all genes necessary for biotin production and could be the primary supplier of biotin within the SynCom, as the metabolite is solely present in its monoculture. Although, *M. aurea* produces biotin in single cultures, it cannot be excluded that biotin present in SynCom co-cultures is additionally produced by other prototrophic SynCom members. When screening for genes involved in biotin uptake (*bioM*, *bioN*, *bioY*) we found, that biotin auxotrophs and obligate auxotrophs carry at least genes for the transporter *bioY*, which was identified to singly act as a high capacity transporter [69]. Interestingly, transporter genes were completely absent in all biotin prototrophs, suggesting the system is not needed since they are able to produce the vitamin on their own (table S1). The precursor dethiobiotin is produced by *M. aurea*, *B. altitudinis* and *D. hungarica* but is completely absent in the SynCom, suggesting its total conversion to biotin in the community. Dropout experiments or the introduction of biotin synthase-deficient *M. aurea* mutants can help verify biotin production by the strain within the SynCom.

For *B. altitudinis* dethiobiotin was detected in the metabolome of the strain although genome annotation by prokka revealed only the presence of biotin synthase *bioB* and lacked the genes for dethiobiotin production. Whereas for *D. hungarica* and *M. aurea* all three replicates showed dethiobiotin production, for *B. altitudinis* only one sample contained this precursor. To determine whether this sample corresponds to the outlier observed in the PCoA (figure 3) for *B. altitudinis*, we conducted a further comparison, which revealed that the sample in question was not the outlier. Nonetheless, the possibility of contamination leading to the detection of dethiobiotin in this single sample cannot be ruled out. To confirm whether *B. altitudinis* is capable of producing dethiobiotin, it is recommended to repeat the UHPLC-MS/MS measurement. Given the solely presence of the *bioB* gene, it is plausible that *B. altitudinis* can utilize dethiobiotin for the biosynthesis of biotin but is not able to produce dethiobiotin. This is consistent with findings by Wienhausen *et al.*, who reported that over 26% of auxotrophic bacilli possess only the *bioB* gene [31]. Although some *Bacillus* species are known to produce biotin independently [70], the absence of biotin in *B. altitudinis* monocultures suggests that this strain is likely an obligate auxotroph, relying on dethiobiotin for biotin production. Supporting this hypothesis, *B. altitudinis* also carries the *bioY* gene, encoding the biotin transporter responsible for the uptake of both biotin and its precursor, dethiobiotin [71].

Both identified upregulated metabolites can be produced by the SynCom member *M. aurea*. Almario *et al.* characterized *M. aurea* not only as a core bacterium of the *A. thaliana* leaf microbiome but also as a hub organism with high connectivity in the microbiome during December and February. Given the stability of *M. aurea*'s abundance and its peak connectivity during months with overall low microbiome connectivity, the authors hypothesized that this strain might play a role in microbiome stabilization [8]. As a potential biotin supplier within the SynCom, *M. aurea* could stabilize the community through its cross-feeding abilities.

Further research is needed to determine whether N-acyl lysine is another metabolite involved in microbe-microbe cross-feeding or if it serves a different purpose in the community. Nonetheless, *M. aurea* was identified as an important SynCom members supplying significant metabolites to the community. *Massilia* spp. have been shown to positively affect the flowering time and biomass of maize by influencing nutrient supply. Researchers have suggested that their impact on the nitrogen cycle could explain its plant-promotive ability [72, 73]. Little is known about the exchange of biotin between plants and their microbiome. Since the biotin cycle plays a crucial role in plants [74], it is worth investigating whether biotin produced by *Massilia* spp. contributes to its plant-promotive effects. Overall, *Massilia* spp. appear capable of influencing the nutrient supply of both microorganisms and plants, thereby positively affecting their growth. These attributes make *Massilia* spp. promising candidates for further investigation as biocontrol agents.

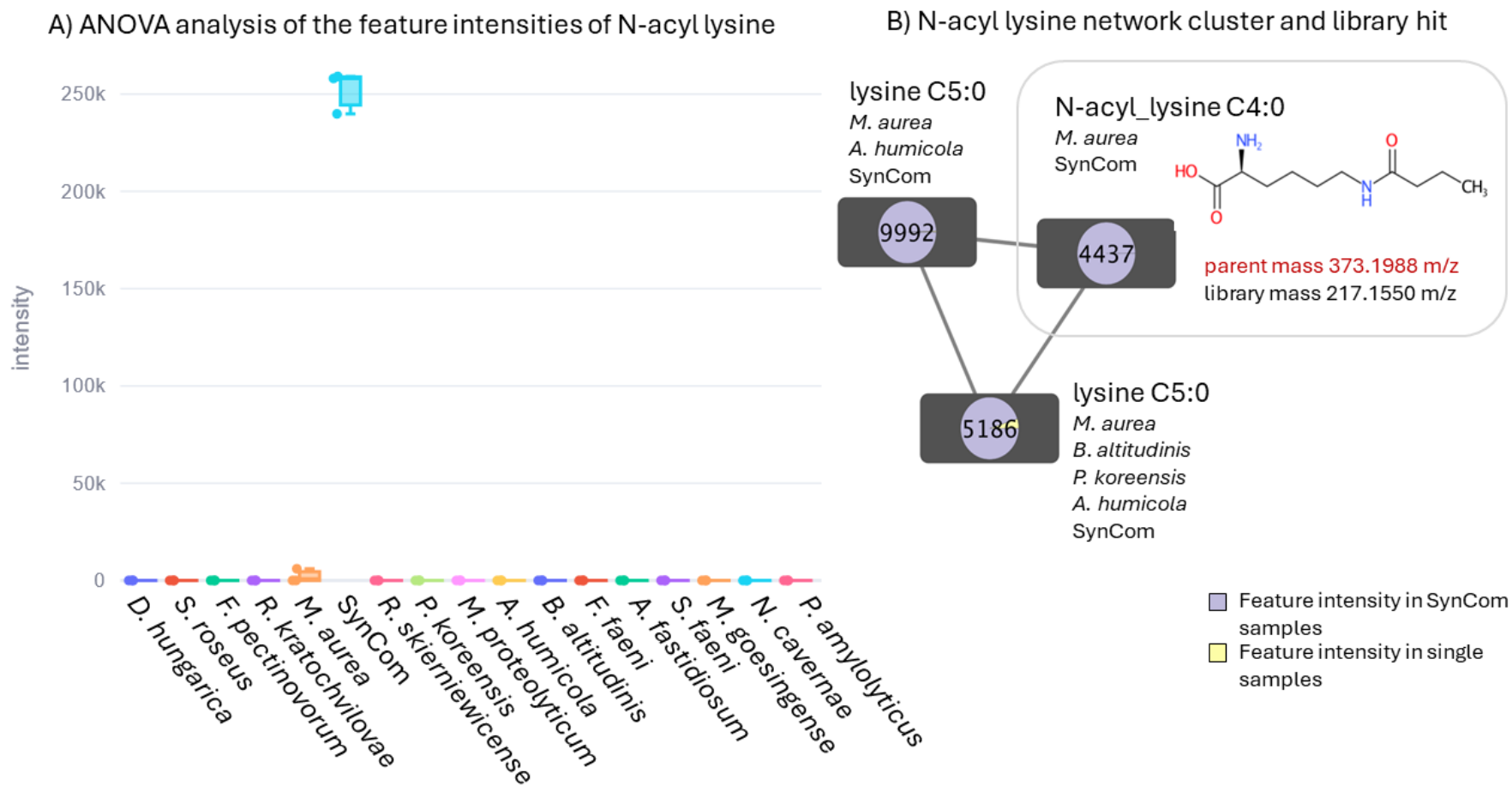


Figure 29: N-acyl lysine as an upregulated metabolite in the SynCom A) Feature intensities of N-acyl lysine in single strain cultures and SynCom co-cultures (blue). In single strain cultures, N-acyl lysine was solely present in cultures of *M. aurea* (orange). B) The N-acyl lysine C4:0 containing cluster from GNPS2 feature based molecular networking. The node coloring reflects the feature intensities of the metabolite in single and SynCom co-cultures. The structure of N-acyl lysine was based on the GNPS2 library hit.

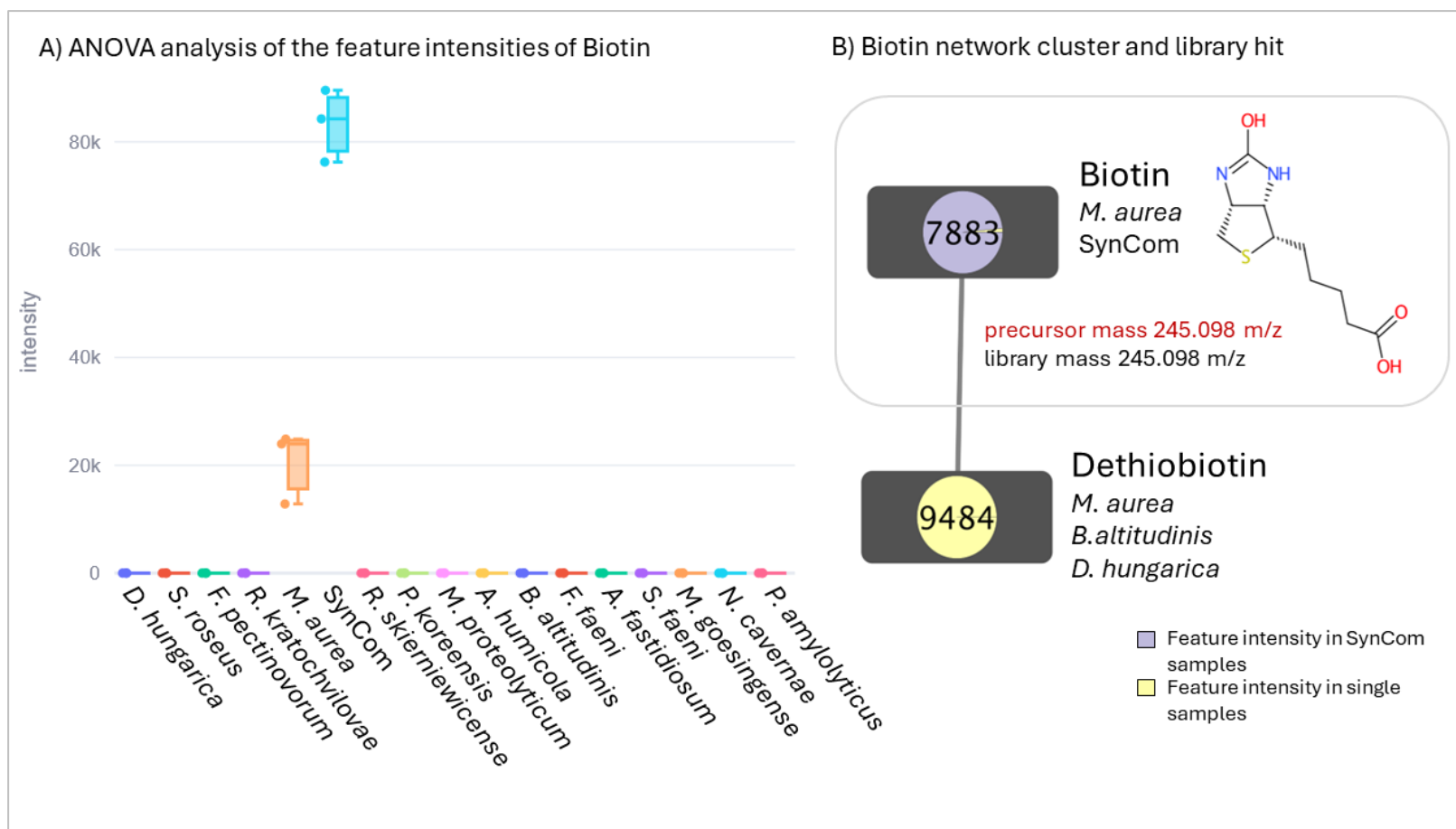


Figure 30: Biotin as an upregulated metabolite in the SynCom A) Feature intensities of biotin in single strain cultures and SynCom co-cultures (blue). In single strain cultures, biotin was solely present in cultures of *M. aurea* (orange). B) The biotin containing cluster from GNPS2 feature-based molecular networking. The node coloring reflects the feature intensities of the metabolite in single and SynCom co-cultures. The structure of biotin was based on the GNPS2 library hit.

EVIDENCE FOR BIOTIN CROSS-FEEDING IN THE SYNCOM

To verify the production of biotin, we aimed at level 1 annotation of metabolite 7883. Therefore, a biotin standard (245.0952 m/z ; rt: 1.66 min) was bought and tested in UHPLC-MS/MS. The comparison of fragmentation pattern and retention time confirmed that feature 7883 is biotin (figure S4). As a next step, we investigated whether biotin has an influence on the growth of SynCom members. In literature, we found that aspartic acid can take over some activities of biotin in the cell [75]. To avoid this, we created MM9/7 medium without aspartic acid (MM9/7-Asp), which we complemented with biotin for growth curve analysis. We selected *B. altitudinis* for growth curve observation, since the strain was identified as obligate auxotroph. Therefore, we focused on determining the growth curve of *B. altitudinis* in two independent experiments. In both experiments, *B. altitudinis* grew to a significantly higher OD₆₀₀ in presence of biotin (figure 8 and S5). In the first experiment, we determined that 100 nM of biotin were already enough to promote the growth of the strain in MM9/7-Asp. This concentration was in a range consistent with previous cross-feeding studies, where 410 nM biotin were used [76]. Our results suggest that supplementation of biotin can promote auxotrophic SynCom members and therefore, the biotin cycle might play an important role in the community. However, it would be interesting to quantify how much biotin is available in the community to estimate to which extent auxotrophic SynCom members can profit from cross-feeding by prototrophs. Furthermore, it would be interesting to investigate if all auxotrophic SynCom members are promoted by biotin supplementation. Given that *B. altitudinis* is likely an obligate auxotroph capable of synthesizing biotin from dethiobiotin, it would be valuable to investigate whether the strain can utilize externally supplemented dethiobiotin for biotin production. Should this be confirmed, it would also be intriguing to explore whether *M. aurea* not only supplies biotin but, in conjunction with *D. hungarica*, also contributes dethiobiotin to the microbial community.

Taken together, we identified biotin as an upregulated metabolite in the community, which is probably produced by *M. aurea*. We further showed that the biotin auxotrophic SynCom member *B. altitudinis* was promoted in its growth in MM9/7-Asp medium by the supplementation of biotin. The findings suggest that biotin cross-feeding might be one mechanism driving community dynamics *in vitro*. If this mechanism is also true *in planta* can be further investigated by addressing the question, whether biotin is bioavailable on plant leaves or if auxotrophic microorganisms are dependent on the biotin production by prototrophs. Further analyses can include biotin cross-feeding *in planta*, the creation of a biotin deficient mutant and drop out experiments of strains. These will give further insights into the effect of the vitamin on the community composition.

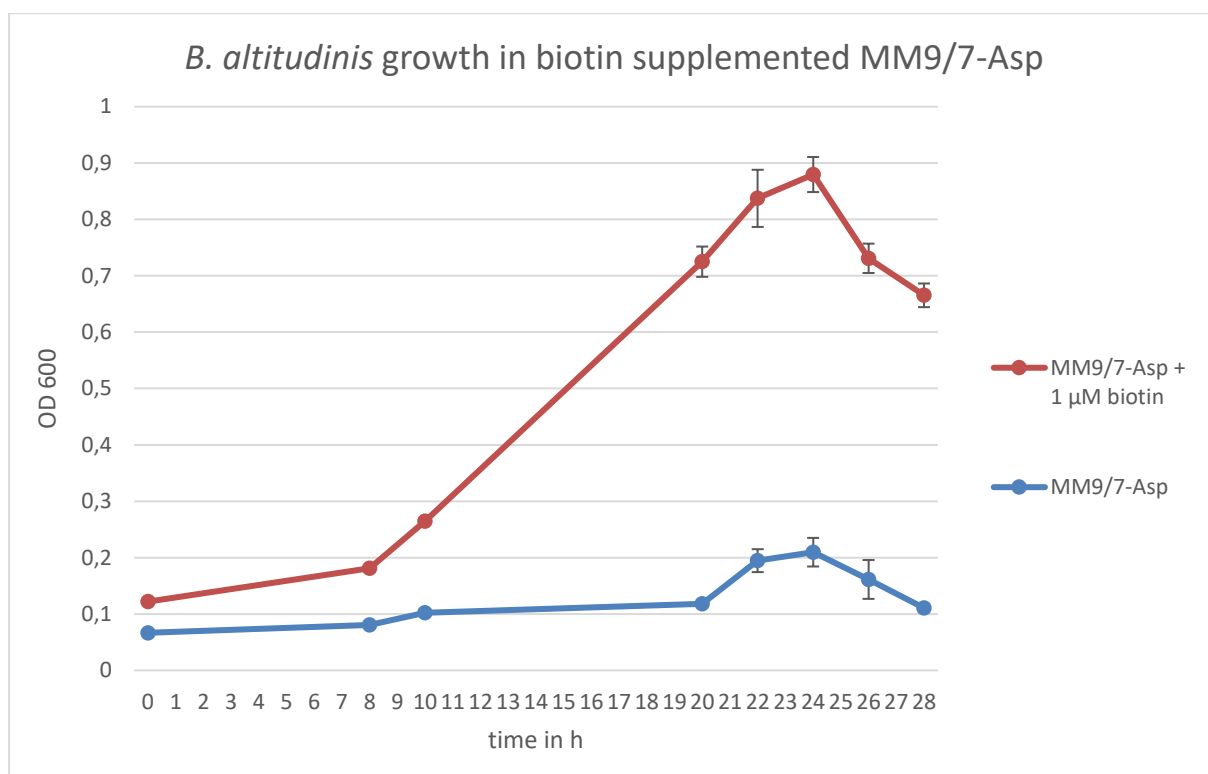


Figure 31: Biotin supplementation assay with *Bacillus altitudinis* in MM9/7-Asp medium Due to its obligate biotin auxotrophy, *B. altitudinis* was chosen for supplementation experiments. The strain was grown in presence (red) and absence (blue) of biotin in aspartic acid depleted minimal medium. Growth curves as OD₆₀₀ were observed with a spectrophotometer at 22°C and 120 rpm shaking.

THE PRODUCTION OF A TRANS-ZEATIN RIBOSIDE DERIVATIVE IS TRIGGERED IN THE SYNCOM

Based on the one-way ANOVA analysis by fbmn-statsguide.gnps2.org, the production of 99 metabolites was significantly triggered in SynCom samples. Most of these compounds (71) could not be annotated by GNPS2 (figure 5). To determine whether specific compound classes were triggered in co-cultures of the whole community, SIRIUS annotations were matched to the 99 significantly triggered metabolites (figure 9). More than 30% of these compounds were not assigned to specific compound classes by SIRIUS including metabolites with masses > 850 Da. However, some of these unknown compounds were annotated by GNPS2, primarily as amino acid chains (table ES6).

The classes of amino acids and peptides were the largest group triggered within the SynCom. Interestingly, polyketides were the second most abundant annotated group. Many antimicrobials, such as erythromycin [77], belong to the class of polyketides. Since antimicrobial production is often triggered in the presence of competitors, the high occurrence of polyketides among the significantly triggered compounds in the SynCom could indicate ongoing competition within the community. However, polyketides are also known as cross-

kingdom signalling molecules, like arginoketides produced by *Streptomyces* spp., which have been identified to induce other organisms to produce natural products [78], form biofilms [79], undergo symbiosis [80] or change their morphology [81]. The various activities of polyketides make them potential drivers of microbe-microbe interactions in microbial communities. Therefore, their high abundance in SynCom samples may also indicate microbe-microbe communication.

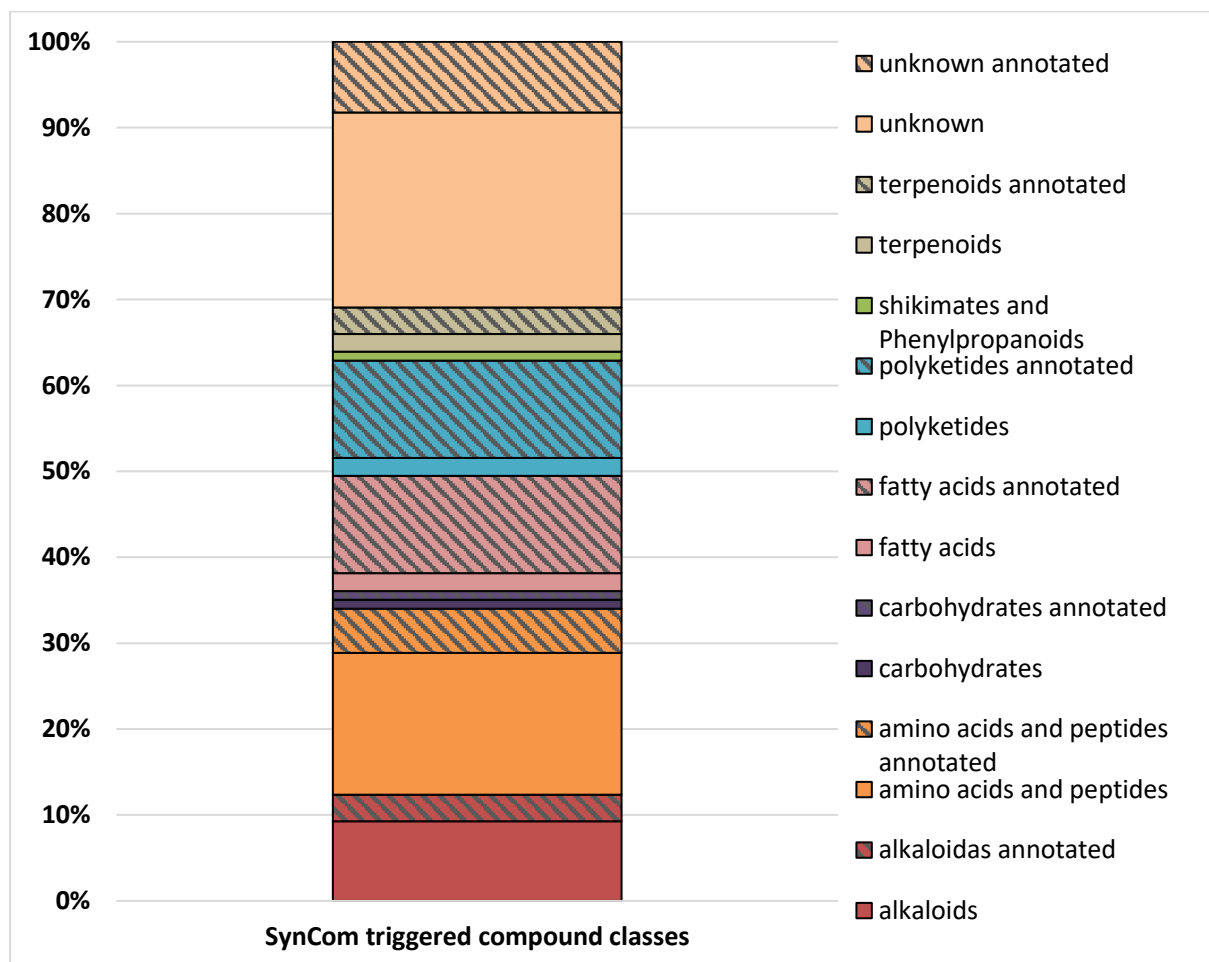


Figure 32: Relative distribution of compound classes within significantly triggered metabolites in SynCom samples. Compound class prediction was based on SIRIUS for metabolites < 850 Da. The figure is based on the 99 significantly triggered metabolites detected in one-way ANOVA analysis ($p < 0.05$).

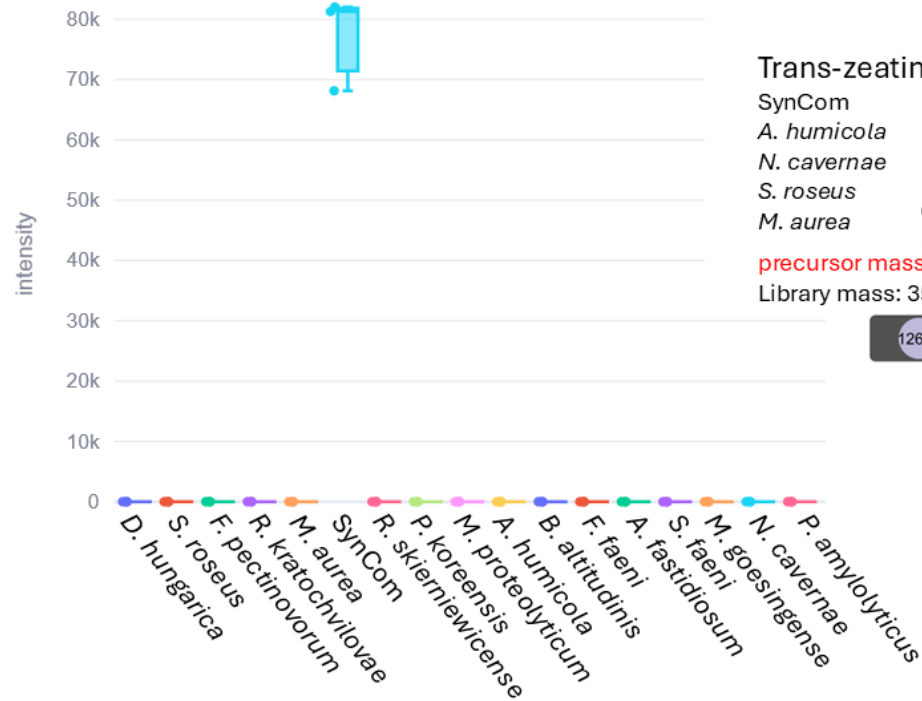
We next aimed to identify the most significantly triggered and annotated metabolite in SynCom samples, which was absent in monocultures. Following the approach used for detecting the most significantly upregulated and annotated metabolites, we screened for the lowest p-value and compared fragmentation patterns in GNPS2. We identified feature 6671 (336.1668 m/z ; rt: 1.41 min) as the most significantly triggered annotated metabolite, with a library hit for 9-(beta-d-ribofuranosyl)zeatin (figure 10A). This compound is known as trans-zeatin riboside in literature, a cytokinin phytohormone [82]. However, the precursor mass of feature 6671 differed

from 9-(beta-d-ribofuranosyl)zeatin by 16 Da (Figure 10B). By comparing the fragmentation pattern using GNPS2 metabolomics USI the peak of the precursor mass 336.1668 m/z was not detected (figure S6) but the highest peak was 220.1193 m/z . If a mass of 220.1193 m/z is assumed for feature 6671, it would fit the mass of the cytokinin trans-zeatin [83]. Lastly, a cytokinin with the mass of 336.1668 m/z is known in literature to be isopentenyl-adenosine [84] concluding three possible identities for feature 6671. To characterize the triggered compound further, standards of all three possible cytokinins (CKs) were bought and measured with UHPLC-MS/MS. We repeated FBMN including the standards and found no mass with a fitting fragmentation pattern to feature 6671 in the isopentenyladenosine standard. The standards of trans-zeatin and trans-zeatin riboside showed matching fragmentation pattern to the metabolite (figure S7 and S8). But feature 6671 showed fragments in the lower mass spectrum, which were absent in both standards. However, for trans-zeatin riboside, the mass peak of 352.1613 m/z was missing in our sample (figure S7). Therefore, the best fit to our metabolite was found to be the trans-zeatin standard (220.1193 m/z ; rt: 1.14 min) (figure S8). Nevertheless, it would be important to further confirm the identity of feature 6671 by NMR.

Trans-zeatin (tZ) is a well-known phytohormones from the cytokinin family, produced by plants and microorganisms that directly interfere with plant regulatory mechanisms [85-87]. cytokinins take over several roles in the plant physiology ranging from an involvement in shoot and root growth, over shoot branching and germination to signaling for the bioavailability of nitrogen or the presence of pathogens [88]. Microorganisms like *Methylobacterium spp.* or *Bacillus spp.* are documented to produce trans-zeatin [89, 90]. Whereas it remains unclear if *Methylobacterium spp.* use trans-zeatin for plant stimulation, it has been shown that *Bacillus spp.* use tZ to force the plant to release amino acids from the root into the surrounding soil [89].

Feature 6671 clusters in a larger network of masses, which would fit to derivatives of trans-zeatin. For instance, feature 6546 (352.1618 m/z ; rt: 1.37 min) fits the mass of trans-zeatin riboside. Interestingly, it was found that tZ shows higher bioactivity than its riboside and that trans-zeatin ribose is often cleaved to trans-zeatin at a certain location in the plant. This indicated that trans-zeatin riboside is a transport form and precursor of tZ [91, 92]. Whereas trans-zeatin riboside was present in SynCom but also single strain samples, it seems like the more active tZ is solely present in the community. We hypothesize that the community triggers the conversion of trans-zeatin riboside into tZ. If this indicates that the community is preparing for a more effective plant stimulation can be addressed in future research. Therefore, it would be interesting to identify the producer of tZ in the community by drop out experiments of single strains and investigate, whether the plant stimulation is changing e.g. by measuring the plant hormone concentrations. It remains intriguing that plant CKs are produced by microorganisms in the absence of the plant itself, suggesting they might also play a role in the community. While less is known about the possible roles of tZ-type CKs in microbe-microbe interactions, this would be an interesting topic for further research.

A) ANOVA analysis of the feature intensities of 9-(beta-d-ribofuranosyl)zeatin



B) 9-(beta-d-ribofuranosyl)zeatin network cluster and library hit

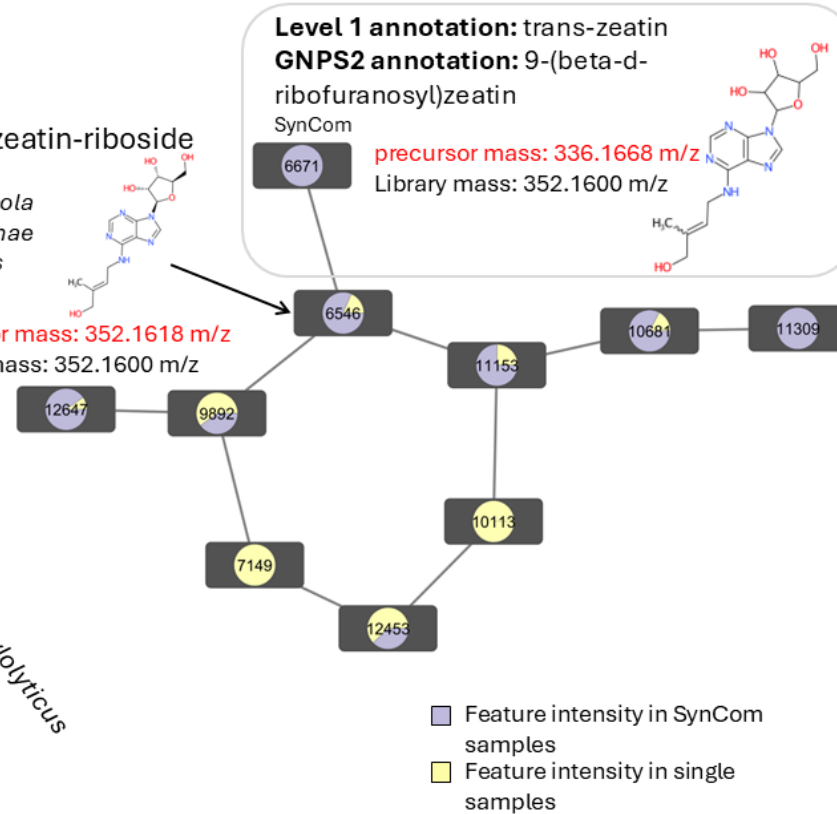


Figure 33: Trans-zeatin as a triggered metabolite in the SynCom A) Feature intensities of trans-zeatin in single strain cultures and SynCom co-cultures (blue). B) The trans-zeatin containing cluster from GNPS2 feature based molecular networking. The node coloring reflects the feature intensities of the metabolite in single and SynCom co-cultures. The molecular structure shown for node 6671 was based on the GNPS2 library hit.

CONCLUSION

Overall, our study identified several metabolites and SynCom strains as interesting candidates for further research (figure 11). *P. koreensis*, *B. altitudinis* and *M. aurea* were detected as producers of most strain-specific metabolites present in SynCom samples, highlighting their potential role as key drivers of microbial interactions. It might be interesting to investigate how the community reacts in absence of one of these members. Furthermore, these organisms are promising candidates as biocontrol agents or probiotic stabilizers. In the feature based molecular network, several metabolites with functions potentially influencing the community were detected in SynCom samples. Compounds like surfactins and rhodotorulic acid might play a role in community dynamics due to their known functions in literature. Therefore, the metabolites are interesting candidates for further research in a plant microbiome context. We further identified biotin and a N-acyl lysin as upregulated metabolites in the SynCom suggesting a potential effect on microbe-microbe dynamics. Since biotin is an essential cofactor in carboxylation reactions, it is likely that a cross-feeding cycle of biotin is a major stabilizer of the SynCom. This hypothesis was strengthened by the supplementation experiment on *B. altitudinis*, which grew significantly better in presence of biotin. The role of our N-acyl lysine in the community needs further investigation. Lastly, we identified the cytokinin trans-zeatin as significantly triggered in the community, suggesting an effect of co-cultivation on the production of plant interactive metabolites. Our study contributes to the understanding of microbe-microbe interactions involved in dynamics of beneficial plant SynComs and the identification of key metabolites produced in such communities.

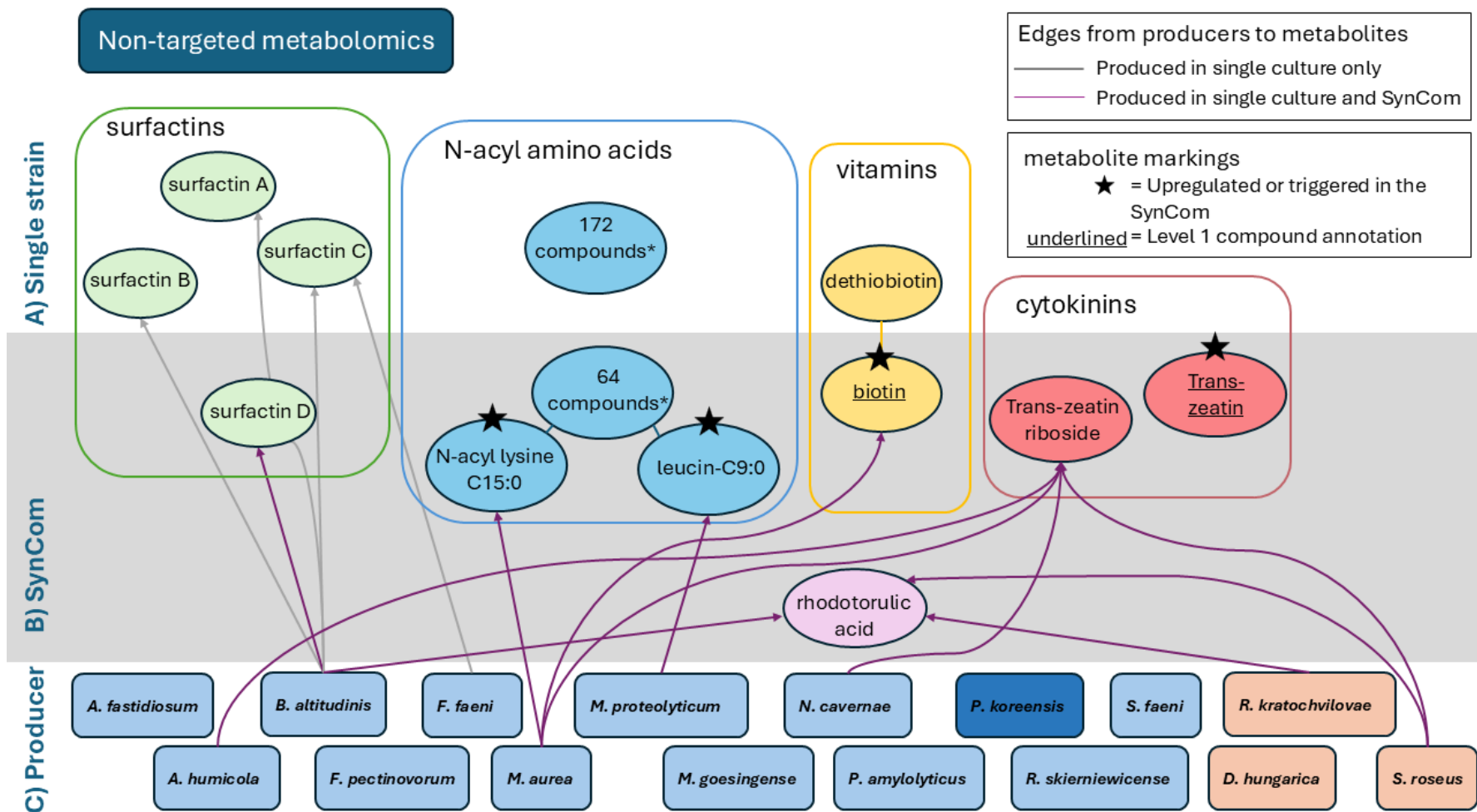


Figure 34: Graphical conclusion of metabolites detected in the non-targeted metabolomics approach of SynCom and single strain samples. Metabolites are annotated by GNPS2 or verified by the measurement of standards (level 1 annotation, underlined). A) Metabolites of a compound family that were solely produced in single strain samples. B) Metabolites that were detected in single strain samples and/or SynCom samples. C) Producers of the metabolites were linked to them with arrows.

DATA AVAILABILITY

1. Raw UHPLC-MS/MS data as well as corresponding metadata and a detailed workflow can be found in the data storage: <https://doi.org/10.57754/FDAT.72xh4-dxf33> (folder: assays)
2. All raw results from GNPS2, MZmine3, SIRIUS and fbmn-statsguide.gnps2.org can be found in the data storage: <https://doi.org/10.57754/FDAT.72xh4-dxf33> (folder: runs/feature_based_molecular_networking_single_and_syncom)
3. Tables and figures marked with ES (external supplements) can be found in the data storage: <https://doi.org/10.57754/FDAT.72xh4-dxf33> (folder: runs/external_supplements_manuscript)

REFERENCES

1. Pareek A, Dhankher OP, Foyer CH. Mitigating the impact of climate change on plant productivity and ecosystem sustainability. *Journal of Experimental Botany*. 2020;**71**:451-56 <https://doi.org/10.1093/jxb/erz518>
2. Secretariat I, Gullino M, Albajes R *et al*. *Scientific review of the impact of climate change on plant pests*: FAO on behalf of the IPPC Secretariat, 2021.
3. Evans LT. *Feeding the ten billion: Plants and population growth*: Cambridge University Press, 1998.
4. Chaudhry V, Runge P, Sengupta P *et al*. Shaping the leaf microbiota: Plant–microbe–microbe interactions. *Journal of Experimental Botany*. 2020;**72**:36-56 <https://doi.org/10.1093/jxb/eraa417>
5. Orozco-Mosqueda MdC, Rocha-Granados MdC, Glick BR *et al*. Microbiome engineering to improve biocontrol and plant growth-promoting mechanisms. *Microbiological Research*. 2018;**208**:25-31 <https://doi.org/https://doi.org/10.1016/j.micres.2018.01.005>
6. Arif I, Batool M, Schenk PM. Plant microbiome engineering: Expected benefits for improved crop growth and resilience. *Trends in Biotechnology*. 2020;**38**:1385-96 <https://doi.org/https://doi.org/10.1016/j.tibtech.2020.04.015>
7. Hu J, Wei Z, Friman V-P *et al*. Probiotic diversity enhances rhizosphere microbiome function and plant disease suppression. *mBio*. 2016;**7**:10.1128/mbio.01790-16 <https://doi.org/doi:10.1128/mbio.01790-16>
8. Almario J, Mahmoudi M, Kroll S *et al*. The leaf microbiome of arabidopsis displays reproducible dynamics and patterns throughout the growing season. *mBio*. 2022;**13**:e0282521 <https://doi.org/10.1128/mbio.02825-21>
9. Herren CM, McMahon KD. Keystone taxa predict compositional change in microbial communities. *Environmental Microbiology*. 2018;**20**:2207-17 <https://doi.org/https://doi.org/10.1111/1462-2920.14257>
10. Qiao Y, Wang Z, Sun H *et al*. Synthetic community derived from grafted watermelon rhizosphere provides protection for ungrafted watermelon against fusarium oxysporum via microbial synergistic effects. *Microbiome*. 2024;**12**:101 <https://doi.org/10.1186/s40168-024-01814-z>

11. Wang Z, Hu X, Solanki MK *et al.* A synthetic microbial community of plant core microbiome can be a potential biocontrol tool. *Journal of Agricultural and Food Chemistry*. 2023;**71**:5030-41 <https://doi.org/10.1021/acs.jafc.2c08017>
12. Emmenegger B, Massoni J, Pestalozzi CM *et al.* Identifying microbiota community patterns important for plant protection using synthetic communities and machine learning. *Nature Communications*. 2023;**14**:7983 <https://doi.org/10.1038/s41467-023-43793-z>
13. Vorholt JA, Vogel C, Carlström CI *et al.* Establishing causality: Opportunities of synthetic communities for plant microbiome research. *Cell Host & Microbe*. 2017;**22**:142-55 <https://doi.org/https://doi.org/10.1016/j.chom.2017.07.004>
14. Marmann A, Aly AH, Lin W *et al.* Co-cultivation—a powerful emerging tool for enhancing the chemical diversity of microorganisms. *Marine Drugs*. 2014;**12**:1043-65
15. Lucke M, Correa MG, Levy A. The role of secretion systems, effectors, and secondary metabolites of beneficial rhizobacteria in interactions with plants and microbes. *Frontiers in Plant Science*. 2020;**11** <https://doi.org/10.3389/fpls.2020.589416>
16. Netzker T, Flak M, Krespach MKC *et al.* Microbial interactions trigger the production of antibiotics. *Current Opinion in Microbiology*. 2018;**45**:117-23 <https://doi.org/https://doi.org/10.1016/j.mib.2018.04.002>
17. Hu X, Vandamme P, Boon N. Co-cultivation enhanced microbial protein production based on autotrophic nitrogen-fixing hydrogen-oxidizing bacteria. *Chemical Engineering Journal*. 2022;**429**:132535 <https://doi.org/https://doi.org/10.1016/j.cej.2021.132535>
18. Vinale F, Nicoletti R, Borrelli F *et al.* Co-culture of plant beneficial microbes as source of bioactive metabolites. *Scientific Reports*. 2017;**7**:14330 <https://doi.org/10.1038/s41598-017-14569-5>
19. Petras D, Minich JJ, Cancelada LB *et al.* Non-targeted tandem mass spectrometry enables the visualization of organic matter chemotype shifts in coastal seawater. *Chemosphere*. 2021;**271**:129450 <https://doi.org/https://doi.org/10.1016/j.chemosphere.2020.129450>
20. Hao J, Wang Z, Zhao Y *et al.* Inhibition of potato fusarium wilt by bacillus subtilis zwz-19 and trichoderma asperellum pt-29: A comparative analysis of non-targeted metabolomics. *Plants*. 2024;**13**:925
21. Höhn F, Chaudhry V, Bagci C *et al.* Strong pairwise interactions do not drive interactions in a plant leaf associated microbial community. *bioRxiv*. 2024:2024.05.22.595276 <https://doi.org/10.1101/2024.05.22.595276>
22. Stincone P, Pakkir Shah AK, Schmid R *et al.* Evaluation of data-dependent ms/ms acquisition parameters for non-targeted metabolomics and molecular networking of environmental samples: Focus on the q exactive platform. *Analytical Chemistry*. 2023;**95**:12673-82 <https://doi.org/10.1021/acs.analchem.3c01202>
23. Heuckeroth S, Damiani T, Smirnov A *et al.* Reproducible mass spectrometry data processing and compound annotation in mzmine 3. *Nature Protocols*. 2024 <https://doi.org/10.1038/s41596-024-00996-y>
24. Schmid R, Heuckeroth S, Korf A *et al.* Integrative analysis of multimodal mass spectrometry data in mzmine 3. *Nature Biotechnology*. 2023;**41**:447-49 <https://doi.org/10.1038/s41587-023-01690-2>
25. Mongia M, Yasaka TM, Liu Y *et al.* Fast mass spectrometry search and clustering of untargeted metabolomics data. *Nature Biotechnology*. 2024 <https://doi.org/10.1038/s41587-023-01985-4>
26. Dührkop K, Fleischauer M, Ludwig M *et al.* Sirius 4: A rapid tool for turning tandem mass spectra into metabolite structure information. *Nature Methods*. 2019;**16**:299-302 <https://doi.org/10.1038/s41592-019-0344-8>
27. Dührkop K, Nothias L-F, Fleischauer M *et al.* Systematic classification of unknown metabolites using high-resolution fragmentation mass spectra. *Nature Biotechnology*. 2021;**39**:462-71 <https://doi.org/10.1038/s41587-020-0740-8>

28. Hoffmann MA, Nothias L-F, Ludwig M *et al.* Assigning confidence to structural annotations from mass spectra with cosmic. *bioRxiv*. 2021:2021.03.18.435634
<https://doi.org/10.1101/2021.03.18.435634>
29. Ludwig M, Nothias L-F, Dührkop K *et al.* Database-independent molecular formula annotation using gibbs sampling through zodiac. *Nature Machine Intelligence*. 2020;**2**:629-41
<https://doi.org/10.1038/s42256-020-00234-6>
30. Shah AKP, Walter A, Ottosson F *et al.* The hitchhiker's guide to statistical analysis of feature-based molecular networks from non-targeted metabolomics data. 2023
31. Wienhausen G, Bruns S, Sultana S *et al.* The overlooked role of a biotin precursor for marine bacteria - desthiobiotin as an escape route for biotin auxotrophy. *The ISME Journal*. 2022;**16**:2599-609 <https://doi.org/10.1038/s41396-022-01304-w>
32. Lardy HA, Peanasky R. Metabolic functions of biotin. *Physiological Reviews*. 1953;**33**:560-65
33. Pahalagedara ASNW, Flint S, Palmer J *et al.* Non-targeted metabolomic profiling identifies metabolites with potential antimicrobial activity from an anaerobic bacterium closely related to terrisporobacter species. *Metabolites*. 2023;**13**:252
34. Mishra S, Priyanka, Sharma S. Metabolomic insights into endophyte-derived bioactive compounds. *Frontiers in Microbiology*. 2022;**13** <https://doi.org/10.3389/fmicb.2022.835931>
35. Li B, Liu K, Kwok L-Y *et al.* Development of a non-target metabolomics-based screening method for elucidating metabolic and probiotic potential of bifidobacteria. *Innovative Food Science & Emerging Technologies*. 2022;**77**:102971
<https://doi.org/https://doi.org/10.1016/j.ifset.2022.102971>
36. Fernandez-Cantos MV, Babu AF, Hanhineva K *et al.* Identification of metabolites produced by six gut commensal bacteroidales strains using non-targeted lc-ms/ms metabolite profiling. *Microbiological Research*. 2024;**283**:127700
<https://doi.org/https://doi.org/10.1016/j.micres.2024.127700>
37. Zampieri M, Zimmermann M, Claassen M *et al.* Nontargeted metabolomics reveals the multilevel response to antibiotic perturbations. *Cell Rep*. 2017;**19**:1214-28
<https://doi.org/10.1016/j.celrep.2017.04.002>
38. Wang H, de Carvalho LPS. Metabolomic profiling reveals bacterial metabolic adaptation strategies and new metabolites. *Current Opinion in Chemical Biology*. 2023;**74**:102287
<https://doi.org/https://doi.org/10.1016/j.cbpa.2023.102287>
39. Mao D, Okada BK, Wu Y *et al.* Recent advances in activating silent biosynthetic gene clusters in bacteria. *Current Opinion in Microbiology*. 2018;**45**:156-63
<https://doi.org/https://doi.org/10.1016/j.mib.2018.05.001>
40. Niehus R, Picot A, Oliveira NM *et al.* The evolution of siderophore production as a competitive trait. *Evolution*. 2017;**71**:1443-55 <https://doi.org/10.1111/evo.13230>
41. Liang J, Bai Y, Men Y *et al.* Microbe–microbe interactions trigger mn(ii)-oxidizing gene expression. *The ISME Journal*. 2016;**11**:67-77 <https://doi.org/10.1038/ismej.2016.106>
42. Nothias LF, Petras D, Schmid R *et al.* Feature-based molecular networking in the gnps analysis environment. *Nat Methods*. 2020;**17**:905-08 <https://doi.org/10.1038/s41592-020-0933-6>
43. Gu S, Wei Z, Shao Z *et al.* Competition for iron drives phytopathogen control by natural rhizosphere microbiomes. *Nature Microbiology*. 2020;**5**:1002-10
<https://doi.org/10.1038/s41564-020-0719-8>
44. Hultman J, Waldrop MP, Mackelprang R *et al.* Multi-omics of permafrost, active layer and thermokarst bog soil microbiomes. *Nature*. 2015;**521**:208-12
<https://doi.org/10.1038/nature14238>
45. Ferrocino I, Rantsiou K, McClure R *et al.* The need for an integrated multi-omics approach in microbiome science in the food system. *Comprehensive Reviews in Food Science and Food Safety*. 2023;**22**:1082-103 <https://doi.org/https://doi.org/10.1111/1541-4337.13103>

46. Mishra AK, Sudalaimuthasari N, Hazzouri KM *et al.* Tapping into plant–microbiome interactions through the lens of multi-omics techniques. *Cells*. 2022;**11**:3254
47. Arul Prakash S, Kamlekar RK. Function and therapeutic potential of n-acyl amino acids. *Chemistry and Physics of Lipids*. 2021;**239**:105114
<https://doi.org/https://doi.org/10.1016/j.chemphyslip.2021.105114>
48. Bruns H, Ziesche L, Taniwal NK *et al.* N-acylated amino acid methyl esters from marine roseobacter group bacteria. *Beilstein Journal of Organic Chemistry*. 2018;**14**:2964-73
<https://doi.org/10.3762/bjoc.14.276>
49. Kashima N, Yamanaka S, Mitsugi K *et al.* Inhibition of bacteriophages of amino acid producing bacteria by n-acylamino acids. *Agricultural and Biological Chemistry*. 1976;**40**:41-47
<https://doi.org/10.1080/00021369.1976.10862009>
50. Bhandari S, Bisht KS, Merkler DJ. The biosynthesis and metabolism of the n-acylated aromatic amino acids: N-acylphenylalanine, n-acyltyrosine, n-acyltryptophan, and n-acylhistidine. *Frontiers in Molecular Biosciences*. 2022;**8**
<https://doi.org/10.3389/fmolb.2021.801749>
51. Dong Y-H, Gusti AR, Zhang Q *et al.* Identification of quorum-quenching *n*-acyl homoserine lactonases from *Bacillus* species. *Applied and Environmental Microbiology*. 2002;**68**:1754-59 <https://doi.org/doi:10.1128/AEM.68.4.1754-1759.2002>
52. Solecka J, Rajnisz A, Postek M *et al.* N-acetyl-3,4-dihydroxy-L-phenylalanine, a second identified bioactive metabolite produced by streptomyces sp. 8812. *The Journal of Antibiotics*. 2012;**65**:219-21 <https://doi.org/10.1038/ja.2012.2>
53. Hartl J, Kiefer P, Kaczmarczyk A *et al.* Untargeted metabolomics links glutathione to bacterial cell cycle progression. *Nature Metabolism*. 2020;**2**:153-66 <https://doi.org/10.1038/s42255-019-0166-0>
54. Mielko KA, Jabłoński SJ, Łukaszewicz M *et al.* Comparison of bacteria disintegration methods and their influence on data analysis in metabolomics. *Scientific Reports*. 2021;**11**:20859
<https://doi.org/10.1038/s41598-021-99873-x>
55. Sansinenea E, Ortiz A. Secondary metabolites of soil bacillus spp. *Biotechnology Letters*. 2011;**33**:1523-38 <https://doi.org/10.1007/s10529-011-0617-5>
56. Mondol MAM, Shin HJ, Islam MT. Diversity of secondary metabolites from marine bacillus species: Chemistry and biological activity. *Marine Drugs*. 2013;**11**:2846-72
57. Chen B, Wen J, Zhao X *et al.* Surfactin: A quorum-sensing signal molecule to relieve ccr in bacillus amyloliquefaciens. *Frontiers in Microbiology*. 2020;**11**
<https://doi.org/10.3389/fmicb.2020.00631>
58. Shank EA, Kolter R. Extracellular signaling and multicellularity in bacillus subtilis. *Current Opinion in Microbiology*. 2011;**14**:741-47
<https://doi.org/https://doi.org/10.1016/j.mib.2011.09.016>
59. Arnaouteli S, Bamford NC, Stanley-Wall NR *et al.* Bacillus subtilis biofilm formation and social interactions. *Nature Reviews Microbiology*. 2021;**19**:600-14 <https://doi.org/10.1038/s41579-021-00540-9>
60. Sadiq FA, Flint S, Sakandar HA *et al.* Molecular regulation of adhesion and biofilm formation in high and low biofilm producers of bacillus licheniformis using rna-seq. *Biofouling*. 2019;**35**:143-58 <https://doi.org/10.1080/08927014.2019.1575960>
61. Mann EE, Wozniak DJ. Pseudomonas biofilm matrix composition and niche biology. *FEMS Microbiology Reviews*. 2012;**36**:893-916 <https://doi.org/10.1111/j.1574-6976.2011.00322.x>
62. Ueda A, Saneoka H. Characterization of the ability to form biofilms by plant-associated pseudomonas species. *Current Microbiology*. 2015;**70**:506-13 <https://doi.org/10.1007/s00284-014-0749-7>

63. Zanella D, Liden T, York J *et al.* Exploiting targeted and untargeted approaches for the analysis of bacterial metabolites under altered growth conditions. *Analytical and Bioanalytical Chemistry*. 2021;**413**:5321-32 <https://doi.org/10.1007/s00216-021-03505-2>
64. Tyc O, van den Berg M, Gerards S *et al.* Impact of interspecific interactions on antimicrobial activity among soil bacteria. *Frontiers in Microbiology*. 2014;**5** <https://doi.org/10.3389/fmicb.2014.00567>
65. Mhaskar SY, Prasad RBN, Lakshminarayana G. Synthesis of n-acyl amino acids and correlation of structure with surfactant properties of their sodium salts. *Journal of the American Oil Chemists' Society*. 1990;**67**:1015-19 <https://doi.org/10.1007/BF02541868>
66. Satiaputra J, Shearwin KE, Booker GW *et al.* Mechanisms of biotin-regulated gene expression in microbes. *Synthetic and Systems Biotechnology*. 2016;**1**:17-24 <https://doi.org/https://doi.org/10.1016/j.synbio.2016.01.005>
67. Sirithanakorn C, Cronan JE. Biotin, a universal and essential cofactor: Synthesis, ligation and regulation. *FEMS Microbiology Reviews*. 2021;**45** <https://doi.org/10.1093/femsre/fuab003>
68. Streit WR, Entcheva P. Biotin in microbes, the genes involved in its biosynthesis, its biochemical role and perspectives for biotechnological production. *Applied Microbiology and Biotechnology*. 2003;**61**:21-31 <https://doi.org/10.1007/s00253-002-1186-2>
69. Hebbeln P, Rodionov DA, Alfandega A *et al.* Biotin uptake in prokaryotes by solute transporters with an optional atp-binding cassette-containing module. *Proceedings of the National Academy of Sciences*. 2007;**104**:2909-14 <https://doi.org/doi:10.1073/pnas.0609905104>
70. Bower S, Perkins JB, Yocum RR *et al.* Cloning, sequencing, and characterization of the bacillus subtilis biotin biosynthetic operon. *Journal of Bacteriology*. 1996;**178**:4122-30 <https://doi.org/doi:10.1128/jb.178.14.4122-4130.1996>
71. Ikeda T, Ogawa T, Aono T. Dethiobiotin uptake and utilization by bacteria possessing bioyb operon. *Research in Microbiology*. 2023;**174**:104131 <https://doi.org/https://doi.org/10.1016/j.resmic.2023.104131>
72. Wang D, He X, Baer M *et al.* Lateral root enriched massilia associated with plant flowering in maize. 2023 <https://doi.org/10.21203/rs.3.rs-3369311/v1>
73. He X, Wang D, Jiang Y *et al.* Heritable microbiome variation is correlated with source environment in locally adapted maize varieties. *Nature Plants*. 2024;**10**:598-617 <https://doi.org/10.1038/s41477-024-01654-7>
74. Alban C, Job D, Douce R. Biotin metabolism in plants. *Annual Review of Plant Biology*. 2000;**51**:17-47 <https://doi.org/https://doi.org/10.1146/annurev.arplant.51.1.17>
75. Jungo C, Urfer J, Zocchi A *et al.* Optimisation of culture conditions with respect to biotin requirement for the production of recombinant avidin in pichia pastoris. *Journal of Biotechnology*. 2007;**127**:703-15 <https://doi.org/https://doi.org/10.1016/j.jbiotec.2006.08.001>
76. Ryback B, Bortfeld-Miller M, Vorholt JA. Metabolic adaptation to vitamin auxotrophy by leaf-associated bacteria. *The ISME Journal*. 2022;**16**:2712-24 <https://doi.org/10.1038/s41396-022-01303-x>
77. Keatinge-Clay A. Crystal structure of the erythromycin polyketide synthase dehydratase. *Journal of Molecular Biology*. 2008;**384**:941-53 <https://doi.org/https://doi.org/10.1016/j.jmb.2008.09.084>
78. Paguirigan JA, Liu R, Im SM *et al.* Evaluation of antimicrobial properties of lichen substances against plant pathogens. *Plant Pathol J*. 2022;**38**:25-32 <https://doi.org/10.5423/ppj.Oa.12.2021.0176>
79. Stubbendieck RM, Straight PD. Linearmycins activate a two-component signaling system involved in bacterial competition and biofilm morphology. *Journal of Bacteriology*. 2017;**199**:10.1128/jb.00186-17 <https://doi.org/doi:10.1128/jb.00186-17>

80. Krespach MKC, Stroe MC, Flak M *et al.* Bacterial marginolactones trigger formation of algal gloeocapsoids, protective aggregates on the verge of multicellularity. *Proceedings of the National Academy of Sciences*. 2021;**118**:e2100892118
<https://doi.org/doi:10.1073/pnas.2100892118>
81. Baráthová H, Betina V, Nemeč P. Morphological changes induced in fungi by antibiotics. *Folia Microbiologica*. 1969;**14**:475-83 <https://doi.org/10.1007/BF02872794>
82. Kuroha T, Kato H, Asami T *et al.* A trans-zeatin riboside in root xylem sap negatively regulates adventitious root formation on cucumber hypocotyls. *Journal of Experimental Botany*. 2002;**53**:2193-200 <https://doi.org/10.1093/jxb/erf077>
83. Kasahara H, Takei K, Ueda N *et al.* Distinct isoprenoid origins of cis- and trans-zeatin biosyntheses in Arabidopsis. *Journal of Biological Chemistry*. 2004;**279**:14049-54
84. Novák O, Hauserová E, Amakorová P *et al.* Cytokinin profiling in plant tissues using ultra-performance liquid chromatography–electrospray tandem mass spectrometry. *Phytochemistry*. 2008;**69**:2214-24
<https://doi.org/https://doi.org/10.1016/j.phytochem.2008.04.022>
85. Sokolova MG, Akimova GP, Vaishlya OB. Effect of phytohormones synthesized by rhizosphere bacteria on plants. *Applied Biochemistry and Microbiology*. 2011;**47**:274-78
<https://doi.org/10.1134/S0003683811030148>
86. Takei K, Yamaya T, Sakakibara H. Arabidopsis cyp735a1 and cyp735a2 encode cytokinin hydroxylases that catalyze the biosynthesis of trans-zeatin*. *Journal of Biological Chemistry*. 2004;**279**:41866-72 <https://doi.org/https://doi.org/10.1074/jbc.M406337200>
87. Frébortová J, Frébort I. Biochemical and structural aspects of cytokinin biosynthesis and degradation in bacteria. *Microorganisms*. 2021;**9**:1314
88. Gajdošová S, Spíchal L, Kamínek M *et al.* Distribution, biological activities, metabolism, and the conceivable function of cis-zeatin-type cytokinins in plants. *Journal of Experimental Botany*. 2011;**62**:2827-40 <https://doi.org/10.1093/jxb/erq457>
89. Kudoyarova GR, Melentiev AI, Martynenko EV *et al.* Cytokinin producing bacteria stimulate amino acid deposition by wheat roots. *Plant Physiology and Biochemistry*. 2014;**83**:285-91
<https://doi.org/https://doi.org/10.1016/j.plaphy.2014.08.015>
90. Koenig Robbin L, Morris Roy O, Polacco Joe C. Trna is the source of low-level trans-zeatin production in methylobacterium spp. *Journal of Bacteriology*. 2002;**184**:1832-42
<https://doi.org/10.1128/jb.184.7.1832-1842.2002>
91. Osugi A, Kojima M, Takebayashi Y *et al.* Systemic transport of trans-zeatin and its precursor have differing roles in Arabidopsis shoots. *Nat Plants*. 2017;**3**:17112
<https://doi.org/10.1038/nplants.2017.112>
92. Jameson PE. Zeatin: The 60th anniversary of its identification. *Plant Physiology*. 2023;**192**:34-55 <https://doi.org/10.1093/plphys/kiad094>

ACKNOWLEDGEMENTS

NZ, EK, HBO, CH, FH, DP acknowledge funding of the study by the Cluster of Excellence EXC 2124: Controlling Microbes to Fight Infection (CMFI, project ID 390838134). NZ acknowledge funding by the German Federal Ministry for Education and Research (BMBF, Grant MicroMATRIX161L0284C). Furthermore, NZ is grateful for the funding by the German Center for Infection Research (DZIF, Grant TTU09.716). EK have been funded by the European Research Council (ERC) under the DeCoCt research program (grant agreement: ERC-2018-COG 820124). PS thanks the European Union's Horizon Europe research and innovation program for support through a Marie Skłodowska-Curie fellowship n.101108450-MeStaLeM. All authors thank Dr. Libera Lo Presti for helpful comments on the manuscript.

SUPPLEMENTAL INFORMATION MANUSCRIPT 2

Identifying Potential Community-Driving Metabolites in a microbial Plant Leaf associated community

Franziska Höhn^{1,3}, Dr. Paolo Stincone^{2,3}, Dr. Chambers C. Hughes^{3,4,6}, Dr. Daniel Petras^{3,5}, Prof. Heike Brötz-Oesterhelt^{3,4,6}, Prof. Eric Kemen^{2,3*}, Prof. Nadine Ziemert^{1,3,4*}

¹Translational Genome Mining for Natural Products, Interfaculty Institute of Microbiology and Infection Medicine (IMIT) and Institute for Bioinformatics and Medical Informatics (IBMI), University of Tübingen, Tübingen, Germany

²Center for Plant Molecular Biology (ZMBP), Interfaculty Institute of Microbiology and Infection Medicine (IMIT), University of Tübingen, Tübingen, Germany

³ Cluster of Excellence Controlling Microbes to Fight Infections (CMFI), University of Tübingen, Tübingen, Germany

⁴German Centre for Infection Research (DZIF), Partner Site Tübingen, Tübingen, Germany

⁵Department of Biochemistry, University of California Riverside, Riverside, USA

⁶Department of Microbial Bioactive Compounds, Interfaculty Institute of Microbiology and Infection Medicine (IMIT), University of Tübingen, Tübingen, Germany

Figure Index:

Figure S1: Biotin supplementation experiment with <i>B. altitudinis</i> grown in MM9/7- Asp.....	110
Figure S2: Fragmentation pattern of feature 4437 compared to the GNPS2 library hit for lysine C4:0	111
Figure S3: Fragmentation pattern comparison of feature 7883 and the GNPS2 library hit for biotin..	112
Figure S4: Fragmentation pattern comparison of feature 9484 to the GNPS2 library hit for dethiobiotin	113
Figure S5: Fragmentation pattern of feature 7883 compared to the biotin standard.....	114
Figure S6: Fragmentation pattern of feature 6671 compared to the GNPS2 library hit9-(beta-d- ribofuranosyl)zeatin.....	116
Figure S7: Fragmentation pattern of metabolite 6671 compared to trans-zeatin riboside standard....	117
Figure S8: Fragmentation pattern of metabolite 6671 compared to trans-zeatin standard	118

Table Index

Table S1: Presence of biotin biosynthesis genes in Syncom members.....	115
--	-----

External supplement tables can be found in Github storage

runs/external supplements manuscript: <https://doi.org/10.57754/FDAT.72xh4-dxf33>

Table ES1: GNPS2 annotated compounds and their producers
Table ES2: annotated N-acyl amino acids
Table ES3: compound class predictions by SIRIUS
Table ES4: quantification table after fbmn processing
Table ES5: ANOVA significance table
Table ES6: final table of significant metabolites in SynCom

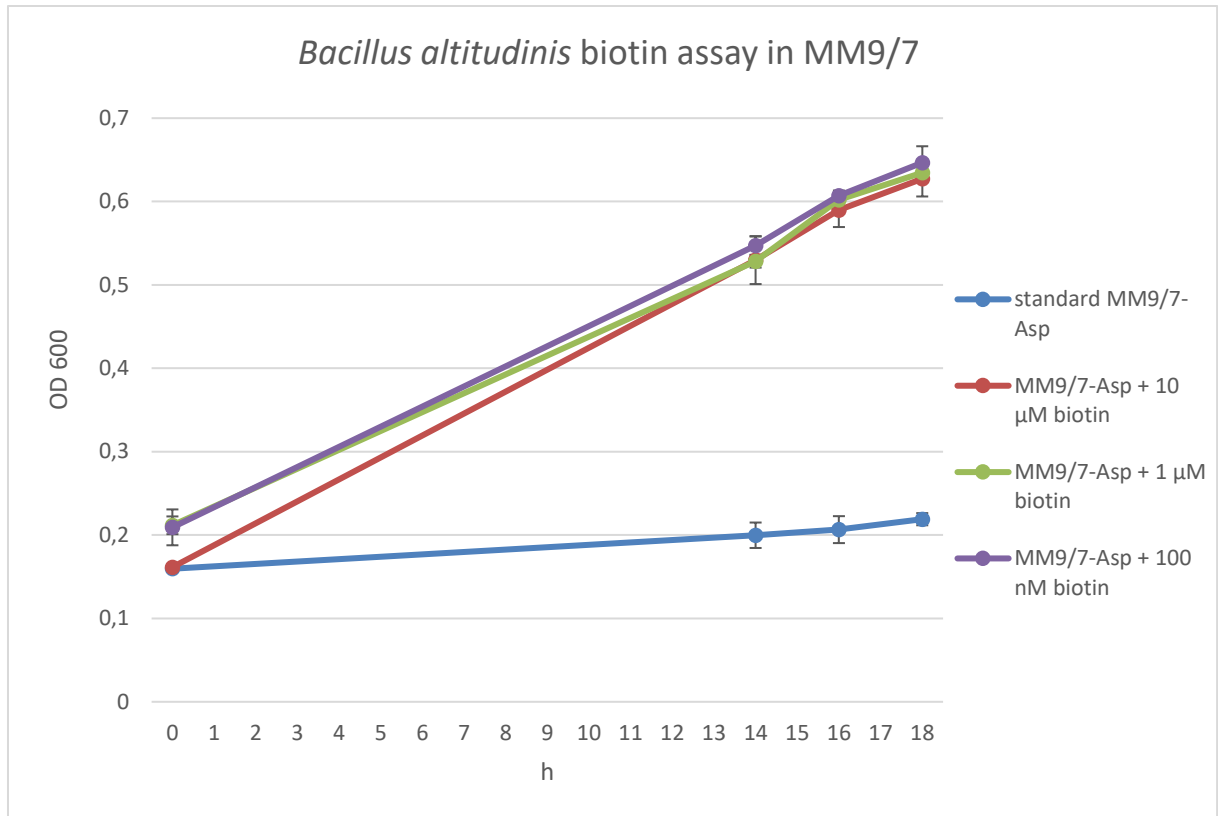


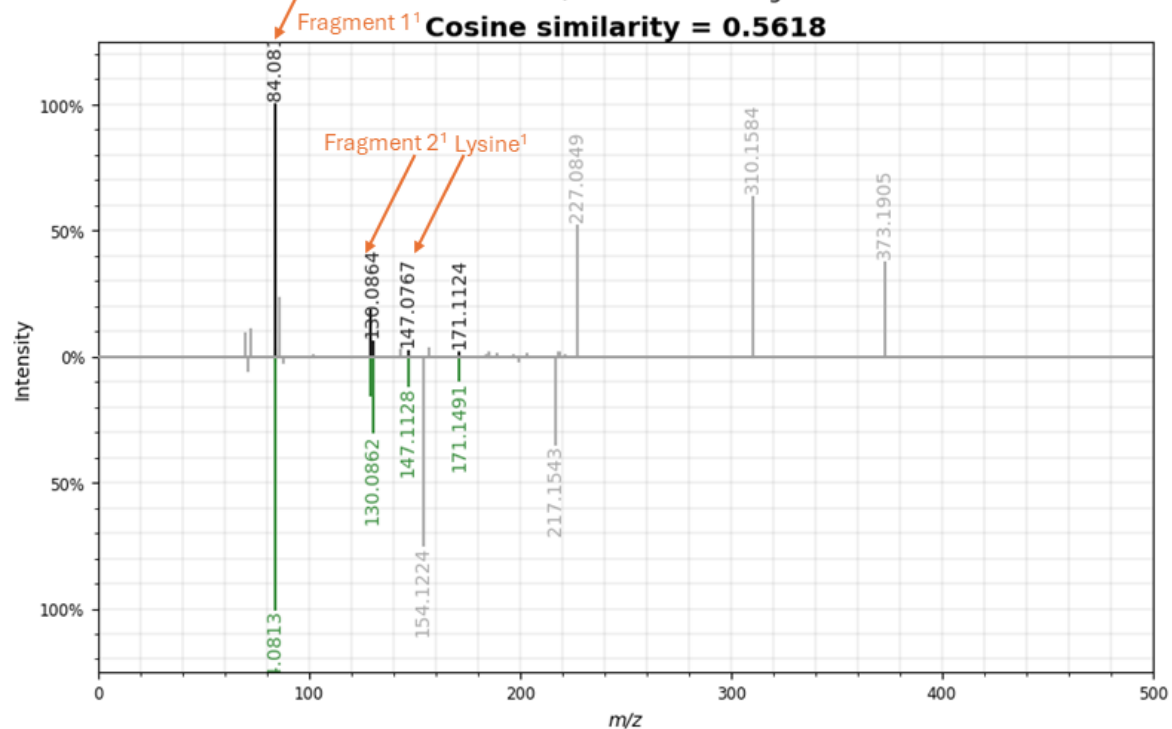
Figure S1: Biotin supplementation experiment with *B. altitudinis* grown in MM9/7- Asp Growth curves were measured in triplicates in 24-well plates at 22 °C and 120 rpm shaking. Biotin was added in different concentrations do determine the concentration with the highest effect on *B. altitudinis* growth. *B. altitudinis* was used since it is biotin auxotrophic.

Top: mzspect:GNPS2:TASK-2ea06a0b4a1c42e0ba6d80b3b52f0f70-nf_output/clustering/spectra_reformatted.mgf:scan:4437

Precursor m/z: 373.1899 Charge: 0

Bottom: mzspect:GNPS:GNPS-LIBRARY:accession:CCMSLIB00012471765

Precursor m/z: 217.1550 Charge: 1



1) National Center for Biotechnology Information (2024). PubChem Compound Summary for CID 5962, Lysine. Retrieved July 18, 2024 from <https://pubchem.ncbi.nlm.nih.gov/compound/Lysine>.

Figure S2: Fragmentation pattern of feature 4437 compared to the GNPS2 library hit for lysine C4:0 Metabolite 4437 was detected in feature based molecular networking by GNPS2. It was annotated as lysine C4:0 from GNPS2. The metabolite was significantly upregulated in SynCom samples compared to *Massilia aurea* single cultures. The fragments for lysine (orange) were annotated based on information available on PubChem ¹.

Top: mzspec:GNPS2:TASK-2ea06a0b4a1c42e0ba6d80b3b52f0f70-nf_output/clustering/spectra_reformatted.mgf:scan:7883

Precursor m/z: 245.0956 Charge: 0

Bottom: mzspec:GNPS:GNPS-LIBRARY:accession:CCMSLIB00006678721

Precursor m/z: 245.0950 Charge: 1

Cosine similarity = 0.9934

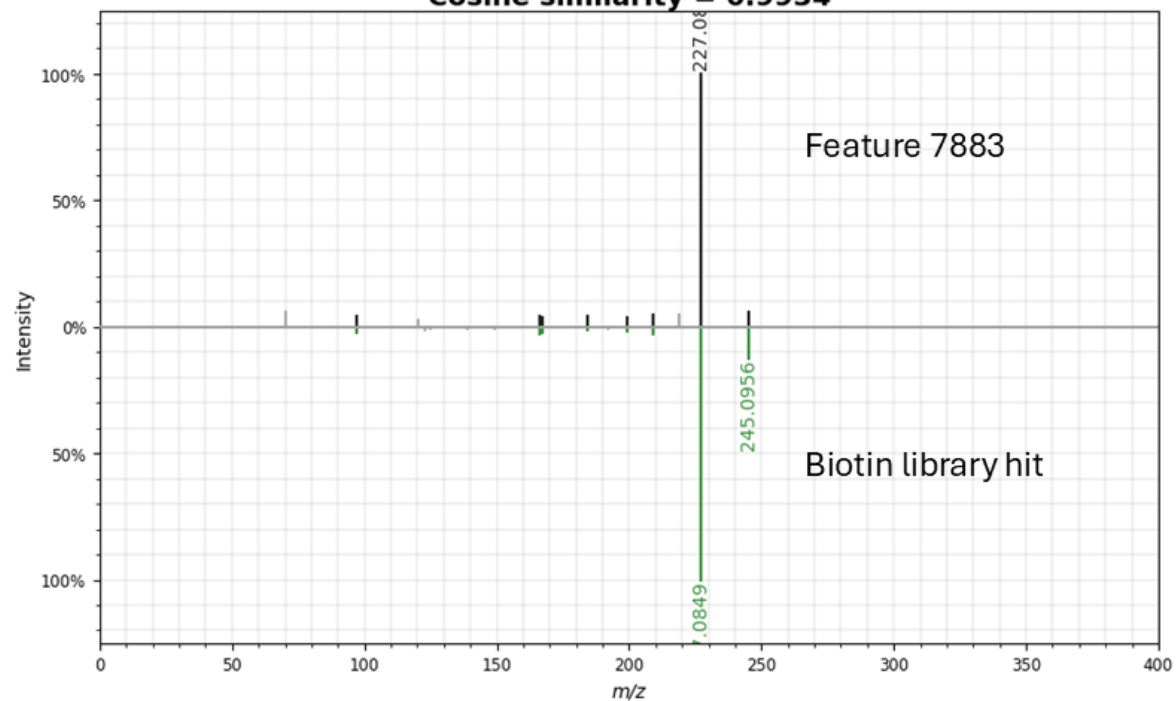


Figure S3: Fragmentation pattern comparison of feature 7883 and the GNPS2 library hit for biotin. Metabolite 7883 was detected in feature-based molecular networking by GNPS2. It was annotated as biotin from GNPS2. The metabolite was significantly upregulated in SynCom samples compared to *Massilia aurea* single cultures.

Top: mzspec:GNPS2:TASK-2ea06a0b4a1c42e0ba6d80b3b52f0f70-nf_output/clustering/spectra_reformatted.mgf:scan:9484

Precursor m/z: 215.1393 Charge: 0

Bottom: mzspec:GNPS:GNPS-LIBRARY:accession:CCMSLIB00005436151

Precursor m/z: 215.1390 Charge: 1

Cosine similarity = 0.9946

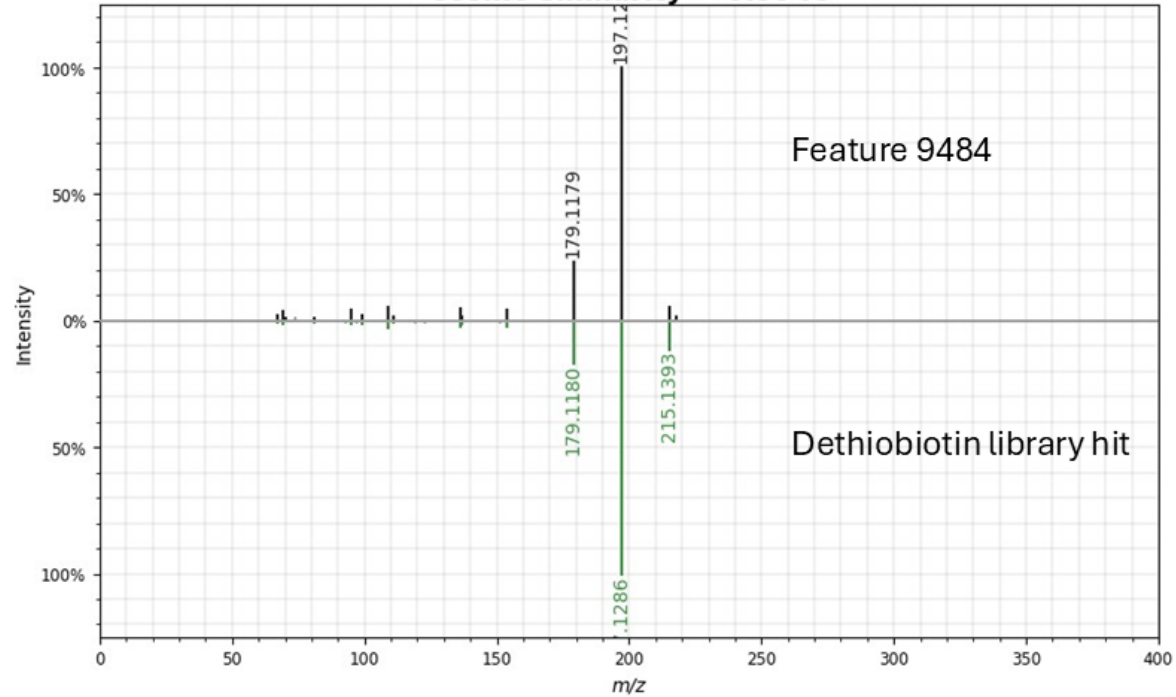


Figure S4: Fragmentation pattern comparison of feature 9484 to the GNPS2 library hit for dethiobiotin. Metabolite 9484 was detected in feature-based molecular networking by GNPS2. It was annotated as dethiobiotin from GNPS2. The metabolite was present in *Massilia aurea*, *Dioszegia hungarica* and one *Bacillus altitudinis* single culture(s).

Top: mzspec:GNPS2:TASK-ebfab2aaae648439c92de5c79d0590a-nf_output/clustering/spectra_reformatted.mgf:scan:1884
 Precursor m/z: 245.0952 Charge: 0

Bottom: mzspec:GNPS2:TASK-2ea06a0b4a1c42e0ba6d80b3b52f0f70-nf_output/clustering/spectra_reformatted.mgf:scan:7883
 Precursor m/z: 245.0956 Charge: 0

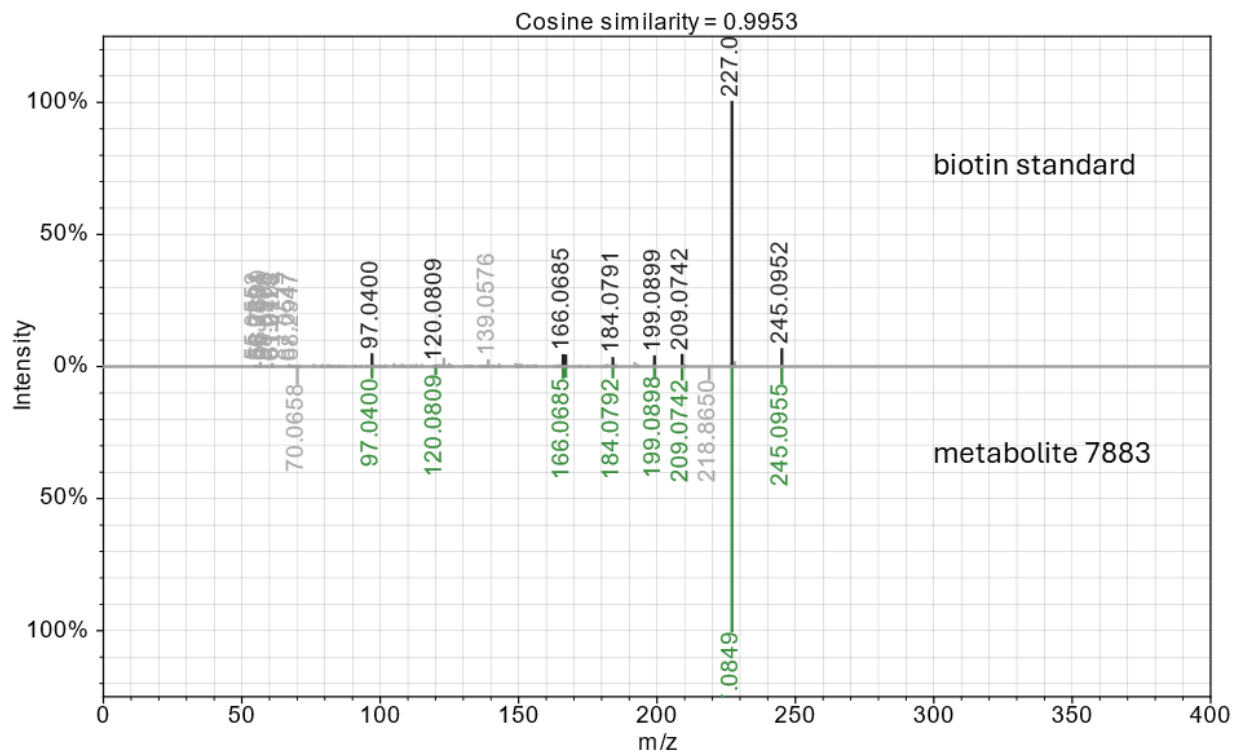


Figure S5: Fragmentation pattern of feature 7883 compared to the biotin standard. Metabolite 7883 was detected in feature based molecular networking by GNPS2. In the network, it was annotated as biotin by GNPS2 and present in SynCom and *Massilia aurea* samples. The biotin standard (iba lifesciences, Germany) was measured under the same conditions as SynCom and *M. aurea* samples and feature based molecular networking was done to enable fragmentation pattern comparison with GNPS2 metabolomics USI.

Table S1: Presence of biotin biosynthesis genes in Syncom members Genome mining was performed by annotating the genomes of all SynCom members with prokka 1.11. Complete biotin auxotrophs lack all four biosynthesis genes (*bioF*, *bioA*, *bioD* and *bioB*) (white), obligate auxotrophs harbour some genes (light orange) and biotin prototrophs carry all biosynthesis genes (dark orange). The genes *bioM*, *bioN* and *bioY* are included in biotin transport.

organism	<i>bioF</i>	<i>bioA</i>	<i>bioD</i>	<i>bioB</i>	<i>bioM</i>	<i>bioN</i>	<i>bioY</i>
<i>A. fastidiosum</i>	no	no	no	no	YES	YES	YES
<i>A. humicola</i>	no	no	no	YES	YES	no	YES
<i>F. pectinovorum</i>	YES	YES	YES	YES	no	no	no
<i>B. altitudinis</i>	no	no	no	YES	no	no	YES
<i>F. faeni</i>	no	no	no	no	no	no	YES
<i>M. aurea</i>	YES	YES	YES	YES	no	no	no
<i>M. goesingense</i>	YES	YES	YES	YES	no	no	no
<i>M. proteolyticum</i>	no	no	no	no	YES	no	YES
<i>N. cavernae</i>	no	no	no	no	YES	YES	YES
<i>P. amylolyticus</i>	no	no	no	YES	no	no	YES
<i>D. hungarica</i>	YES	YES	no	YES	no	no	no
<i>P. koreensis</i>	YES	YES	YES	YES	no	no	no
<i>R. skierniewicense</i>	no	no	no	no	YES	YES	YES
<i>S. faeni</i>	YES	YES	YES	YES	no	no	no

Top: mzspec:GNPS2:TASK-2ea06a0b4a1c42e0ba6d80b3b52f0f70-nf_output/clustering/spectra_reformatted.mgf:scan:6671

Precursor m/z: 336.1668 Charge: 0

Bottom: mzspec:GNPS:GNPS-LIBRARY:accession:CCMSLIB00006398301

Precursor m/z: 352.1600 Charge: 1

Cosine similarity = 0.8958

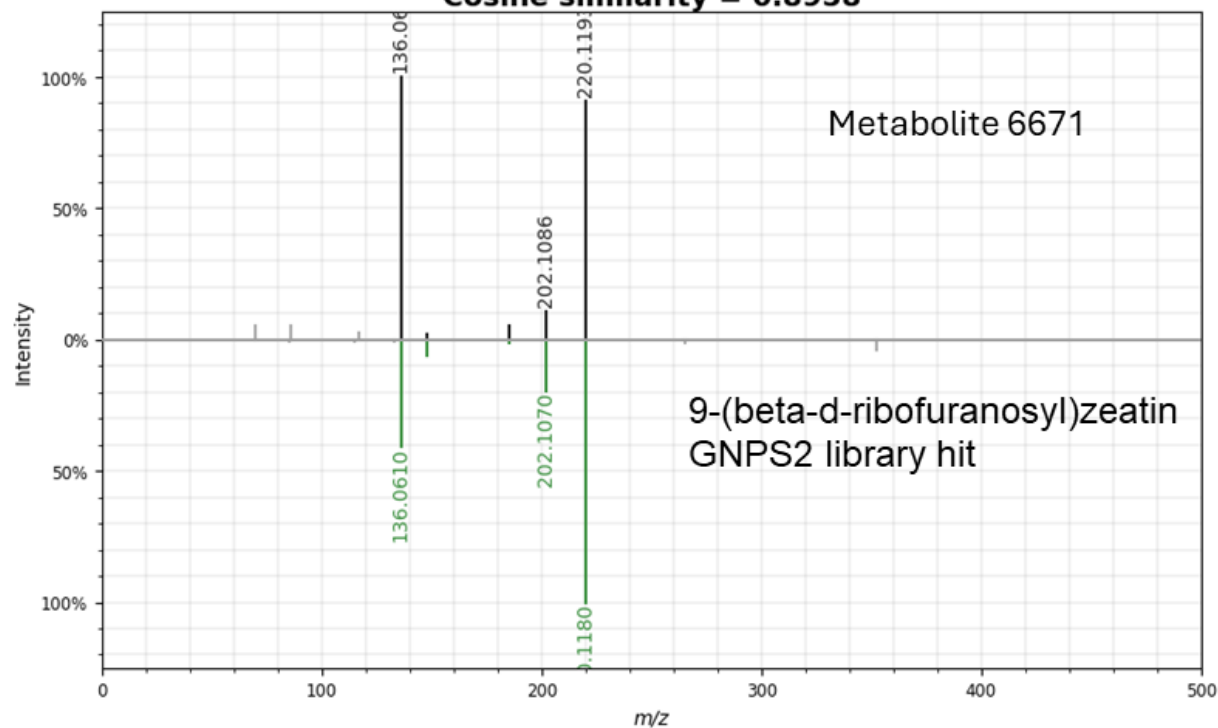


Figure S6: Fragmentation pattern of feature 6671 compared to the GNPS2 library hit 9-(beta-d-ribofuranosyl)zeatin. Metabolite 6671 was detected in feature based metabolic networking by GNPS2 and present in SynCom samples. By GNPS2 it was annotated as 9-(beta-d-ribofuranosyl)zeatin (bottom).

Top: mzspect:GNPS2:TASK-2ea06a0b4a1c42e0ba6d80b3b52f0f70-nf_output/clustering/spectra_reformatted.mgf:scan:6671

Precursor m/z : 336.1668 Charge: 0

Bottom: mzspect:GNPS2:TASK-8de0e0d9ee5645e39f4849a0d3b2a1ad-nf_output/clustering/spectra_reformatted.mgf:scan:1314

Precursor m/z : 352.1613 Charge: 0

Cosine similarity = 0.9406

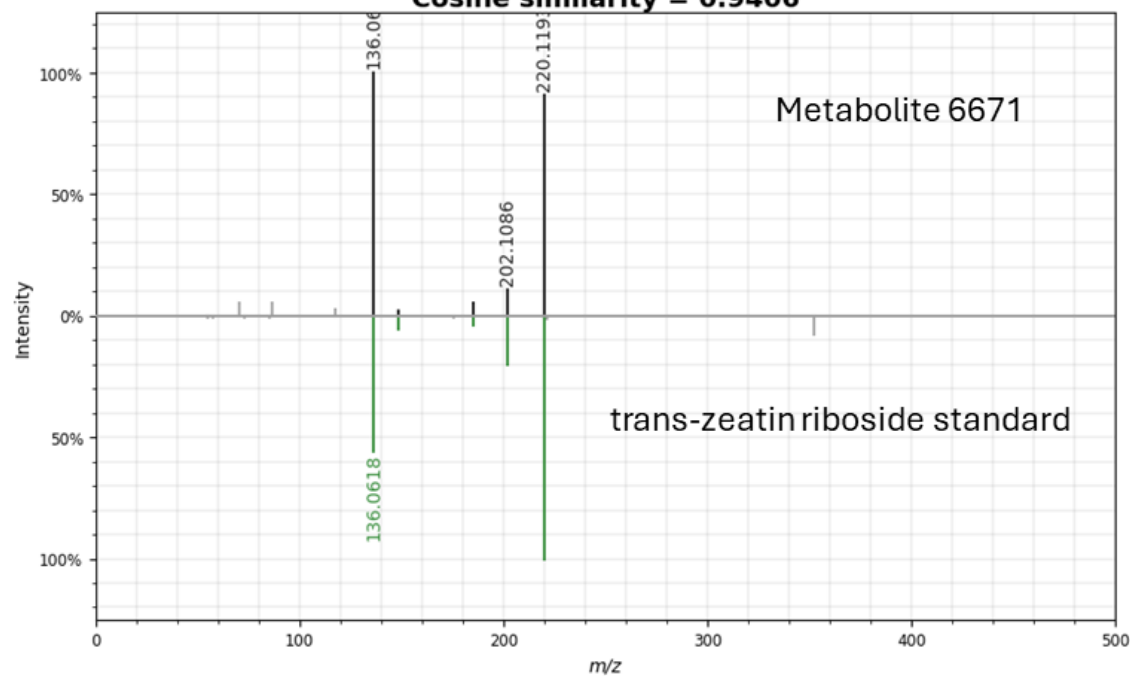


Figure S7: Fragmentation pattern of metabolite 6671 compared to trans-zeatin riboside standard Metabolite 6671 was detected in feature based metabolic networking by GNPS2 and present in SynCom samples. By GNPS2 it was annotated as 9-(beta-d-ribofuranosyl)zeatin. For further level 1 annotation, trans-zeatin riboside (Sigma-Aldrich, USA) was bought and measured under the same conditions. Feature based molecular networking was done with the standard to enable fragmentation pattern comparison with GNPS2 metabolomics USI.

Top: mzspec:GNPS2:TASK-2ea06a0b4a1c42e0ba6d80b3b52f0f70-nf_output/clustering/spectra_reformatted.mgf:scan:6671

Precursor m/z: 336.1668 Charge: 0

Bottom: mzspec:GNPS2:TASK-8de0e0d9ee5645e39f4849a0d3b2a1ad-nf_output/clustering/spectra_reformatted.mgf:scan:1255

Precursor m/z: 220.1192 Charge: 0

Cosine similarity = 0.9132

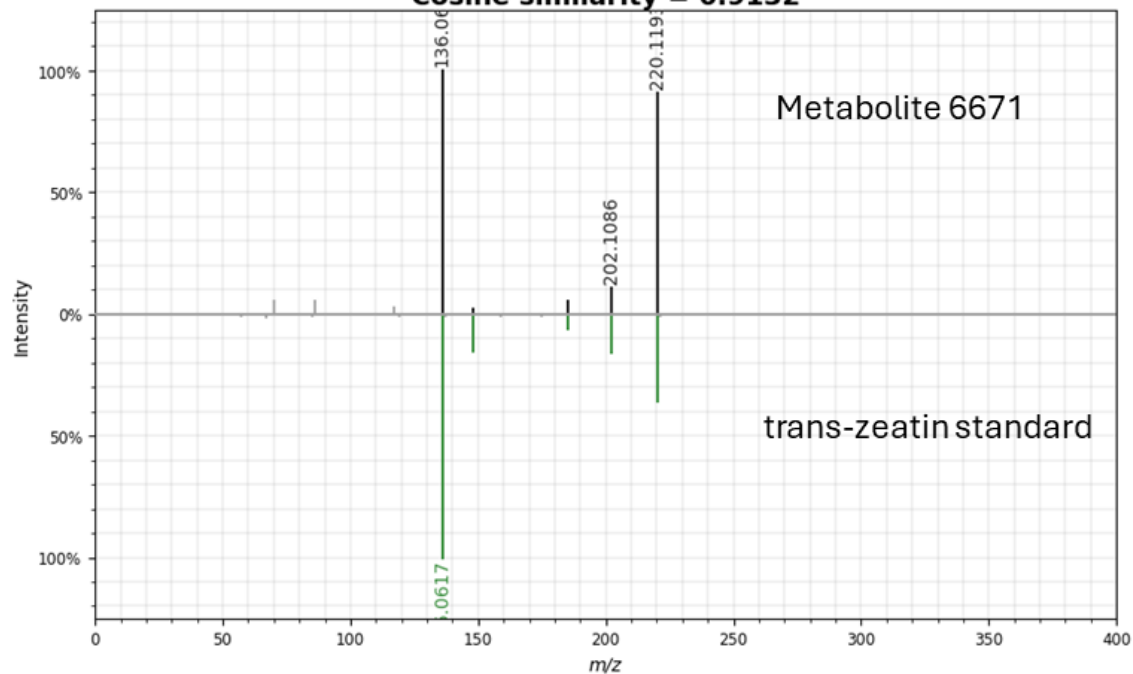


Figure S8: Fragmentation pattern of metabolite 6671 compared to trans-zeatin standard Metabolite 6671 was detected in feature based metabolic networking by GNPS2 and present in SynCom samples. By GNPS2 it was annotated as 9-(beta-d-ribofuranosyl)zeatin. For further level 1 annotation, trans-zeatin was bought (Thermo Fisher Scientific, USA) and measured under the same conditions. Feature based molecular networking was done with the standard to enable fragmentation pattern comparison with GNPS2 metabolomics USI.

THESIS - DISCUSSION

In this PhD project, a synthetic community (SynCom) was assembled from *Arabidopsis thaliana* leaves. The members were selected based on co-occurrence and connectivity within the plant microbiome during garden experiments [89]. The primary objectives of the PhD project were to identify microbe-microbe interactions and investigate the role of secondary metabolites in these processes.

The first manuscript (manuscript 1) details the findings related to microbe-microbe interactions at different levels. Microbial interactions *in planta*, based on co-abundance correlation networks, were compared with pairwise interactions of SynCom members *in vitro*. Significant discrepancies between the interaction patterns were observed. In the *in planta* correlation network, positive interactions predominated, whereas pairwise *in vitro* interactions were primarily negative. Due to the biosynthetic potential of the SynCom members, it was assumed that pairwise interactions might be driven by antimicrobial secondary metabolites. To test the hypothesis, the siderophore pseudobactin was identified as an antimicrobial agent produced by *Pseudomonas koreensis*, which exhibited inhibitory activity against several SynCom members. Investigating the effect of pseudobactin on individual SynCom members and the whole SynCom revealed that, despite driving pairwise inhibitions, pseudobactin had no effect on the community composition *in planta*. Furthermore, the study indicated that strong pairwise inhibitors like *Bacillus altitudinis* are not inherently dominant species within the community. The findings of the study suggested that antimicrobial activity might play a subordinate role in a community context.

Since the first manuscript provided evidence that antimicrobials might play a subordinate role in the SynCom, non-targeted metabolomics was employed to detect which metabolites are upregulated or triggered in a community context (manuscript 2). This approach aimed not only to detect key metabolites in the SynCom, but also to verify or refute the hypothesis of manuscript 1 regarding the presence or absence of chemical warfare within the SynCom. The underlying assumption of the non-targeted metabolomics approach was that community-driving compounds might only be present when needed, leading to the upregulation or activation of important metabolites in the community compared to single-strain cultures. By comparing the metabolomes of single SynCom members with co-cultures of the entire SynCom *in vitro*, *P. koreensis*, *Massilia aurea*, and *B. altitudinis* were identified as organisms producing the most strain-specific metabolites in whole SynCom co-cultures. Significantly upregulated metabolites in the community included biotin and N-acyl lysine, both produced by *M. aurea*. Additionally, the phytohormone trans-zeatin from the functional class of cytokinins was significantly triggered in the community. Biotin supplementation experiments demonstrated that *B. altitudinis* experienced growth promotion in the presence of biotin. These

results suggest that cross-feeding by biotin prototrophs like *M. aurea* might be a driving force behind SynCom dynamics *in vitro*.

The present work contributed to the identification of hub organisms and key metabolites in the SynCom *in vitro*. It enabled predictions about microbe-microbe interactions with the potential to drive community dynamics and discovered several mechanisms, interesting for further research. The findings of manuscript 1 and 2 are addressed in detail in the discussion of each manuscript. The following discussion aims to draw connections between both studies and addresses their impact on contemporary research.

THE DISCOVERY OF HUB ORGANISMS AND KEY METABOLITES IN THE SYNCOM

In the present study, various methods were employed to identify organisms and metabolites within the SynCom that potentially play roles in shaping and stabilizing the community. These methods facilitated the analysis of relevant metabolites at different detection levels. Pairwise *in vitro* interactions provided initial insights into microorganisms capable of producing metabolites involved in microbe-microbe dynamics. Genome mining further elucidated the potential of each SynCom member to produce metabolites that could impact the entire community. Lastly, non-targeted metabolomics enabled the identification of metabolites present in single SynCom samples and/or the whole community. Across all detection levels, metabolites and producers related to significant functions were identified (Fig. D1). The following section discusses the observations that led to the characterization of certain compounds as key metabolites and specific SynCom members as hub organisms. Additionally, the hypothetical roles and the potential for further investigations of these metabolites and organisms are explored.

Massilia aurea

Due to its ability to produce the two most significantly upregulated and annotated metabolites in SynCom co-cultures, *M. aurea* was identified as an important hub bacterium in the community. Several factors highlight this strain as a potential driver of SynCom dynamics. Previous studies have identified *Massilia* spp. as core and hub organisms in *A. thaliana* microbiomes due to their widespread occurrence [113, 114] and high connectivity within the microbiome throughout the plant's growth period [89]. In the non-targeted metabolomics approach, several strain-specific and upregulated metabolites produced by *M. aurea* were detected in the SynCom. This finding was particularly surprising given the strain's low abundance in the community on MM9/7 agar as shown in manuscript 1 [115]. The high relative concentration of two upregulated metabolites, despite the low abundance of their producer, underscores their importance in the community. One significantly upregulated metabolite was biotin, known to act as a cross-feeding compound in marine bacterial communities [116]. The

identity of biotin was further verified through genome mining and UHPLC-MS/MS measurement of a biotin standard. Interestingly, biotin supplementation of *B. altitudinis* grown in minimal medium led to the growth promotion of this SynCom strain, suggesting that biotin cross-feeding might be a common interaction within the community. Underlining this hypothesis, genes encoding biotin uptake systems were detected in biotin auxotrophic and obligate auxotrophic SynCom members but were absent in all SynCom prototrophs. Within the *A. thaliana* epiphytic microbiome, *M. aurea* was highly positively correlated to other microbiome members. Among these, two positive correlations were observed to two SynCom members. One positive correlation was with *Rhizobium skierniewicense*, identified as biotin auxotroph due to the absence of the known biosynthesis genes [115]. Therefore, biotin-cross feeding could be an explanation for the positive correlation to the strain. In conformity with these results, Ryback *et al.* demonstrated that biotin produced within a community from the *A. thaliana* leaf microbiome can be utilized by auxotrophic microbiome members. They found that auxotrophic *Rhizobium sp.* and *Arthrobacter sp.* benefit from biotin produced by prototrophic members in co-cultures [117]. Notably, *Arthrobacter humicola* and *R. skierniewicense*, which are present in the SynCom, were identified as biotin auxotrophs, suggesting that cross-feeding might also promote their growth. If *A. humicola* and *R. skierniewicense* benefit from external biotin can be further investigated through supplemented growth curve analyses. Additionally, co-cultivations with *M. aurea* WT and biotin deficient mutants can verify a cross-feeding relation between these strains. Although *P. koreensis* possesses all the necessary genes for biotin production, no production by the strain was detected in the non-targeted metabolomics approach. This raises questions about the mechanism underlying the positive correlation observed. Further investigation is required, possibly by introducing biotin-deficient mutants into the SynCom and repeating supplementation experiments with *P. koreensis* to determine whether biotin cross-feeding explains the positive correlation. The identification of biotin as a significantly upregulated metabolite, along with the findings from Ryback *et al.* [117], suggests that biotin cross-feeding is indeed occurring within the SynCom.

Besides biotin, *M. aurea* was able to produce the precursor dethiobiotin (level 2 annotation) in single cultures. Interestingly, this compound was absent in the SynCom, suggesting complete transformation to biotin. *M. aurea* was not the only microbe capable of producing dethiobiotin; it was also found in single strain samples of *B. altitudinis* and *D. hungarica*. Additionally, genome mining revealed that, besides *M. aurea* and *P. koreensis*, *Flavobacterium pectinovorum*, *Methylobacterium goeasingense*, and *Sphingomonas faeni* were biotin prototrophs. Nonetheless, *M. aurea* appears to be the main producer of biotin on MM9/7 agar, though it cannot be conclusively stated that biotin in the SynCom sample is exclusively produced by this strain. Drop-out experiments could reveal whether other SynCom members can assume the role of biotin suppliers in the absence of *M. aurea*. The role of *M. aurea* as a biotin supplier supports the hypothesis that *Massilia* spp. are hub organisms in the microbiome due to their synergistic effects on neighboring microbes.

In a study by Ofek *et al.*, [118] it was found that *Massilia* spp. are highly sensitive to competitors but remain abundant and widely distributed among plant microbiomes. The authors explained this paradox by observing that *Massilia* spp. exploit a colonization window, particularly during the early growth phase of cucumber roots. They detected that the abundance of *Massilia* spp. decreased over time while the abundance of competitors increased. [118]. In the present project, *M. aurea* was found to be highly susceptible to *B. altitudinis* (manuscript 1). Despite this susceptibility, *M. aurea* was present in higher abundance on the plant. Notably, no decrease in *M. aurea* abundance was detected after 9 days of incubation, and no increase in *B. altitudinis* abundance was observed [115]. This finding suggests that the persistence of *M. aurea* in the current study is not due to the exploitation of a colonization window. Instead, it supports the hypothesis that *M. aurea*'s synergistic properties may confer an advantage in plant colonization.

In addition to the positive effects on the SynCom indicated in the present study, *Massilia* spp. are known to promote host plants by enhancing root development, increasing plant biomass, and aiding adaptation to nitrogen stress [119]. Furthermore, *Massilia* spp. have recently been identified as potent inhibitors of specific plant pathogens, such as *Ralstonia sp.*[120, 121]. The mechanisms underlying these beneficial abilities of *Massilia* spp. often remain unknown. In this project, N-acyl lysine was identified as a second upregulated metabolite within the SynCom. As discussed in detail in manuscript 2, N-acyl amino acids can serve various functions, including roles as signaling molecules, antimicrobials, and membrane components [122]. Therefore, it would be valuable to investigate whether N-acyl lysine contributes to some of the observed abilities of *M. aurea* and its relatives. This could be done by synthesizing the metabolite and examining its effects on community composition and plant health. Taken together, the findings on *M. aurea* highlight the strain as a key microorganism in the SynCom, which produces significant metabolites likely involved in community dynamics. The present project supports previous findings about *Massilia* spp. as hub organisms and their significance in the plant microbiome [113, 118, 119] and gives first ideas about the underlying mechanisms.

Bacillus altitudinis

B. altitudinis was the producer of most characterized metabolites in this study (see Fig. D1). It exhibited antimicrobial activity against a broad range of SynCom members in pairwise interactions [115]. As discussed in manuscript 1, *B. altitudinis* was a strong pairwise inhibitor but showed low abundance in the SynCom both *in vitro* and *in planta*, suggesting that its competitive abilities do not confer a colonization advantage in a community context. The strain carried several gene clusters potentially encoding antimicrobials, which might explain its strong inhibitory activity. In the non-targeted metabolomics approach, surfactins were detected in *B. altitudinis* monocultures. Additionally, a gene cluster with 85 % identity to lichenysin was found. Due to the similarity of the lichenysin and the surfactin gene cluster [123] it can be estimated to be responsible for the production of surfactins. Deletion mutants could help clarify if the lichenysin gene cluster is responsible for the production of surfactins and if they are

responsible for the bioactivity of the strain in pairwise interactions. Studies have already demonstrated that surfactins produced by *Bacillus* spp. are potent antimicrobial agents against various microorganisms [124-126], such as the plant pathogen *Fusarium moniliforme* [127]. However, surfactins are not solely known for their antimicrobial activity; they also play roles in biofilm formation, root colonization [128, 129], microbe-plant signaling and triggering the plant's immune system [130, 131]. Therefore, surfactins are important players in the plant microbiome, but their specific roles within the SynCom remain unknown. Further investigations are needed to determine whether surfactins function primarily as weapons against competitors, promote colonization, aid in cell-host communication, or perform all these functions simultaneously. Interestingly, in the non-targeted metabolomics approach of *B. altitudinis* monocultures, surfactins A-D were detected, whereas in SynCom co-cultures surfactin D was present. This raises the question of whether surfactin D is favored in the community, which could be investigated through supplementation experiments with different surfactins. It is also possible that the absence of surfactins A-C in the community is due to the low abundance of *B. altitudinis* in SynCom samples, resulting in the detection of surfactin D but not A-C. The production of surfactins D and C in this study was not solely attributed to *B. altitudinis*; these compounds were also detected in cultures of *Frigoribacterium faeni*. However, no gene cluster to produce lipopeptides was found in *F. faeni*, and there is no literature reporting surfactin production by *Frigoribacterium* spp. Given that the metabolites were detected in one of three *F. faeni* replicates, it is likely an artifact of the UHPLC-MS/MS measurement.

B. altitudinis was not only notable for its strong inhibitory properties in pairwise interactions but also for its production of several strain-specific metabolites, as detected by the non-targeted metabolomics approach, despite its low abundance *in vitro* and *in planta*. Of particular interest, *B. altitudinis* produced many significantly upregulated metabolites, suggesting that the strain has the ability to influence the SynCom even at low cell numbers. These findings align with previous studies where Bacillota were present in low or fluctuating abundance but were identified as hub organisms with high connectivity in the *A. thaliana* leaf microbiome [89, 132]. Interestingly, in the correlation networks analyzed in manuscript 1, the operational taxonomic unit (OTU) most similar to *B. altitudinis* was excluded due to its low occurrence across the overall samples. There is evidence that closely related microorganisms may compete more intensely for colonization dominance compared to more distantly related organisms [133-135]. Consequently, *B. altitudinis* may have been outcompeted in the epiphytic microbiome captured in manuscript 1. Nevertheless, it was a hub organism in the study from which the SynCom was assembled [89], and the present study showed the potential of the strain for SynCom dynamics due to the production of many strain-specific metabolites present in the community. However, its specific contribution to SynCom dynamics remains to be further elucidated. *Bacillus* spp. are known for various roles in the microbiome. For instance, *Bacillus velezensis* protects the holobiont against pathogens by secreting antimicrobials [136] a function also attributed to *B. licheniformis*, *B. pumilus*, and *B. subtilis* [137-139]. Other studies have shown that *Bacillus* spp. promote plant growth, crop yields, and overall plant health, making them suitable biocontrol agents beyond mere disease control [140-142]. To further elucidate the role of

B. altitudinis in the SynCom, it would be valuable to identify strain-specific and upregulated metabolites produced by the strain within the community. Transcriptomics could link these detected metabolites to biosynthetic gene clusters, while drop-out experiments could reveal *B. altitudinis*' impact on community composition. Additionally, infection experiments could assess the strain's potential as a disease control agent. Taken together, the project identified *B. altitudinis* as strong pairwise inhibitor and as producers of the known antimicrobial class of surfactins. *B. altitudinis* was highlighted as key microorganism due to its ability to produce several strain-specific and upregulated metabolites in a community context, despite its low abundance.

Pseudomonas koreensis

In manuscript 1, *P. koreensis* was identified as a strong pairwise inhibitor and the dominant bacterial member of the SynCom, both *in vitro* and *in planta*. This led to the hypothesis that *P. koreensis* exerts a significant influence on community dynamics. Given that the strain produced pseudobactin in liquid monocultures and that this metabolite exhibited strong inhibitory activity against several SynCom members, it was initially proposed that pseudobactin might play a role in shaping community composition. Interestingly, pseudobactin was not detected in the non-targeted metabolomics approach, and it appeared to have no effect on the community *in planta*. Since pseudobactin is listed in the GNPS2 library, it can be ruled out that its absence in the metabolomes of *P. koreensis* and the SynCom is due to a missing annotation. This suggests that pseudobactin is indeed absent in the non-targeted metabolomics data, potentially because it is not produced under the experimental conditions or due to limitations of the metabolomics workflow. Transcriptomic analysis of the gene cluster responsible for pseudobactin production could provide insights into its expression on MM9/7 agar and within the community. Additionally, MALDI imaging could reveal the presence of pseudobactin on plant leaves and offer insights into its natural role within the plant microbiome. Despite these considerations, the addition of pure pseudobactin did not affect the community composition on the plant, indicating that the compound likely plays a subordinate role in community dynamics [115]. It was especially surprising, since it was already shown that pyoverdines have an effect on the shape of the rhizosphere microbiome of *A. thaliana* [60]. The results of the present project demonstrate that pseudobactin as a representative of the pyoverdine class does not contribute to the composition of the phyllosphere-associated SynCom.

P. koreensis remained the most dominant bacterium and produced the majority of strain-specific and upregulated metabolites detected in the SynCom through non-targeted metabolomics. Since the project focused on the characterization of the most significant metabolites annotated by GNPS2, the strain-specific metabolites of *P. koreensis* remain to be of interest for further identification. A more detailed investigation into the metabolic capabilities of *P. koreensis* could provide valuable insights into the strain's role within the SynCom. Aside from pseudobactin, one other compound potentially produced by *P. koreensis* could be

annotated based on genomic data. This compound was identified as hydrogen cyanide (HCN), a known antifungal agent that enables its producers to function as effective biocontrol agents [143, 144]. Further research is needed to determine if a mass corresponding to HCN is present in the metabolomic data and whether this metabolite plays a role in SynCom dynamics.

As discussed in manuscript 1, other attributes of the strain may contribute to its dominance in the community beyond antimicrobial production. *Pseudomonas* spp. are widely recognized for their roles in plant growth promotion [145, 146], biofilm formation [147, 148] and pathogen inhibition [15, 149]. The comparison of masses of known biofilm components like exopolysaccharides [148] with masses detected in the non-targeted metabolomics approach can give further insights into the role of *P. koreensis* in the SynCom. The high presence of the strain and its metabolites in the community indicate its importance as a hub microorganism, making it an intriguing candidate for further analysis.

Other significant metabolites in the SynCom

Biotin and N-acyl lysine were not the only compounds highly upregulated in the SynCom. Another N-acyl amino acid, identified as leucine C9:0 by GNPS2, was also upregulated. This compound was detected in single-strain samples of *Microbacterium proteolyticum*, suggesting this strain as its producer. As with N-acyl lysine, the diverse roles of N-acyl amino acids preclude any definitive hypothesis about the specific effects of leucine C9:0 on the SynCom. *M. proteolyticum* did not exhibit notable correlations within the SynCom nor did it display significant pairwise interactions that might provide clues about the function of N-acyl leucine C9:0. Nevertheless, N-acyl amino acids were found to be highly abundant both in single-strain samples (172) and in the community (64) (Fig. D1). The non-targeted metabolomics approach revealed that every SynCom member was capable of producing at least one N-acyl amino acid with *B. altitudinis* and *F. pectinovorum* being able to produce most strain specific N-acyl amino acids. The potential roles of these compounds are discussed in more detail in manuscript 2. This project identified the class of N-acyl amino acids as highly abundant, suggesting their significance in microbial communities and highlighting them as promising candidates for further research.

Interestingly, a cluster of cytokinins was detected in the non-targeted metabolomics approach. One of the metabolites within the cluster was identified as significantly triggered, meaning the activation of its production in the community co-cultures. The metabolite was annotated by GNPS2 as 9-(beta-d-ribofuranosyl)zeatin, however, the mass differed from the library hit. Comparative analysis with purchased cytokinin standards indicated that the fragmentation pattern was most consistent with trans-zeatin. However, further analysis, such as NMR spectroscopy, is suggested to confirm the compound's identity. The trigger of a cytokinin within the community is intriguing, given their role as phytohormones that interact with plant metabolism and hormone balance [150-152]. Notably, less is known about the involvement of cytokinins in microbe-microbe interactions and it would be interesting to investigate these

compounds in supplementation experiments with the SynCom members. The trigger of trans-zeatin in the community raises more questions to address in further research. Which organisms are responsible for its production? And does this production suggest a plant-promotive effect of the SynCom? Addressing these will require a series of follow-up experiments, including single strain dropouts, plant growth promotion assays, hormone level tests, and the creation of deletion mutants. However, the detection of trans-zeatin as significantly triggered metabolite in the community indicates a plant influencing effect of the SynCom and confirms the non-targeted metabolomics approach as potent method for the detection of plant relevant metabolites.

Metabolites present in the SynCom metabolome and metagenome

Lastly, a metabolite annotated as rhodotorulic acid was identified in both single and SynCom samples within the feature-based molecular network. Rhodotorulic acid is a siderophore produced by various organisms such as *Rhodotorula* spp. [153] and *Sporobolomyces* spp. [154]. In this project, rhodotorulic acid was detected in single-strain samples of *Rhodotorula kratochvilovae*, *Sporobolomyces roseus*, and one sample of *B. altitudinis*. While there is limited information on the production of rhodotorulic acid by *B. altitudinis*, it is notable that this strain also produced additional derivatives of rhodotorulic acid, which clustered together in the feature-based molecular network, therefore suggesting the production of a siderophore by the strain, which might be structurally related. Rhodotorulic acid has been demonstrated to inhibit plant pathogenic fungi such as *Penicillium expansum* and *Botrytis cinerea* [155]. Interestingly, both *R. kratochvilovae* and *S. roseus* exhibited high antimicrobial activity in pairwise interactions on PDA against bacterial SynCom members. Whether the production of rhodotorulic acid underlies the observed antibacterial mechanism remains to be investigated in future research. This could be explored through agar diffusion tests or growth curve analyses.

At the genome mining level, additional metabolites are predicted to be produced by SynCom members. These predictions were made using AntiSMASH 7, to highlight gene clusters with > 90% similarity to known antimicrobials such as polymyxin, poly-L-lysine, bacillopaline, and hydrogen cyanide (Fig. D1). A possible role of these compounds on community dynamics remains hypothetical, as they were neither annotated in non-targeted metabolomics nor tested in interaction studies. Nonetheless, their antimicrobial functions suggest they could play a role in the community. Despite the feature-based molecular networking analysis, no masses were annotated by GNPS2 that matched any of these AntiSMASH predictions. This could indicate on the one hand that they are produced but not detected in the non-targeted metabolomics approach, or on the other hand that they might not be produced under the conditions used. The limitations of detecting metabolites in non-targeted metabolomics are discussed in detail in the section "Limitations of the project". Nevertheless, masses of the predicted antimicrobial compounds can be searched in the non-targeted metabolomics data reveal their production.

Additionally, transcriptomic approaches can be used to determine if these antimicrobial biosynthetic gene clusters are expressed *in vitro* and *in planta*.

Some products of the predicted biosynthesis gene clusters might account for interactions observed in the pairwise interaction study described in manuscript 1. For instance, *Paenibacillus amylolyticus* inhibited *F. pectinovorum* in pairwise interaction studies. In addition, the two strains were negatively correlated in the correlation network [115]. It would be intriguing to investigate if these interactions are mediated by the biosynthetic gene cluster with 100% similarity to polymyxin. If confirmed, this would be the first pairwise interaction linked to a correlation in this project. *Paenibacillus* spp. are known to produce polymyxins and are hypothesized to offer plant protection against pathogens [156, 157]. Several studies have identified *Paenibacillus* spp. as potential biocontrol agents due to their ability to produce antimicrobial lipopeptides [158, 159]. The role of these compounds in microbiome dynamics and microbe-microbe interactions among microbiome commensals is less studied. Future research should investigate whether polymyxin is present in the community by measuring polymyxin standards and comparing the data to masses found in the non-targeted metabolomics approach. The presence or absence of polymyxin could indicate whether it impacts the SynCom or acts as a silent reservoir activated during pathogen invasion. Similar investigations should be conducted for poly-L-lysine, bacillopaline, and hydrogen cyanide. The identification of their biosynthetic gene clusters in this project is an excellent starting point for investigating the role of these secondary metabolites in shaping and stabilizing plant microbiomes further.

In summary, this project identified several secondary metabolites, along with primary metabolism compounds like biotin, which were shown to interact with SynCom members. The identification of these compounds at different detection levels suggests varying degrees of involvement in community dynamics (Fig. D1). Notably, biotin was significantly upregulated in the SynCom and promoted the growth of *B. altitudinis*, suggesting a cross-feeding role. *M. aurea*, the producer of biotin, was highlighted as a hub organism due to its ability to produce the most significantly upregulated metabolites, despite its low relative abundance in the community. Other strains, such as *B. altitudinis* and *P. koreensis*, were also identified as potential hub organisms. *B. altitudinis* was noted for its high inhibitory activity in pairwise interactions and its production of a significant number of strain-specific metabolites within the community, despite its low relative abundance. Surfactins, specifically surfactin D, were identified as secondary metabolites produced by *B. altitudinis* and were also present in the SynCom. *P. koreensis* was distinguished by its dominance in the SynCom both *in vitro* and *in planta*, as well as its production of a large number of strain-specific metabolites. Additionally, several metabolites were identified as promising candidates for further research into their roles within the SynCom and plant leaf microbiome. The class of N-acyl amino acids was found to be the most abundant group of metabolites in both monocultures and SynCom co-cultures, raising questions about their functions in community dynamics. Among these, two N-acyl amino acids were significantly upregulated or triggered in the SynCom, underscoring their

potential role in co-cultures. Gene clusters with high similarity to known antimicrobial compounds, such as polymyxin, bacillopaline, poly-L-lysine, and hydrogen cyanide, were also detected at the genetic level. Their reported antimicrobial functions highlight them as key targets for further research on the role of antimicrobials in the community. Overall, the results of this study identified hub microorganisms and key metabolites in the SynCom, provided initial insights into the potential mechanisms underlying community dynamics, and present promising starting points for future investigations.

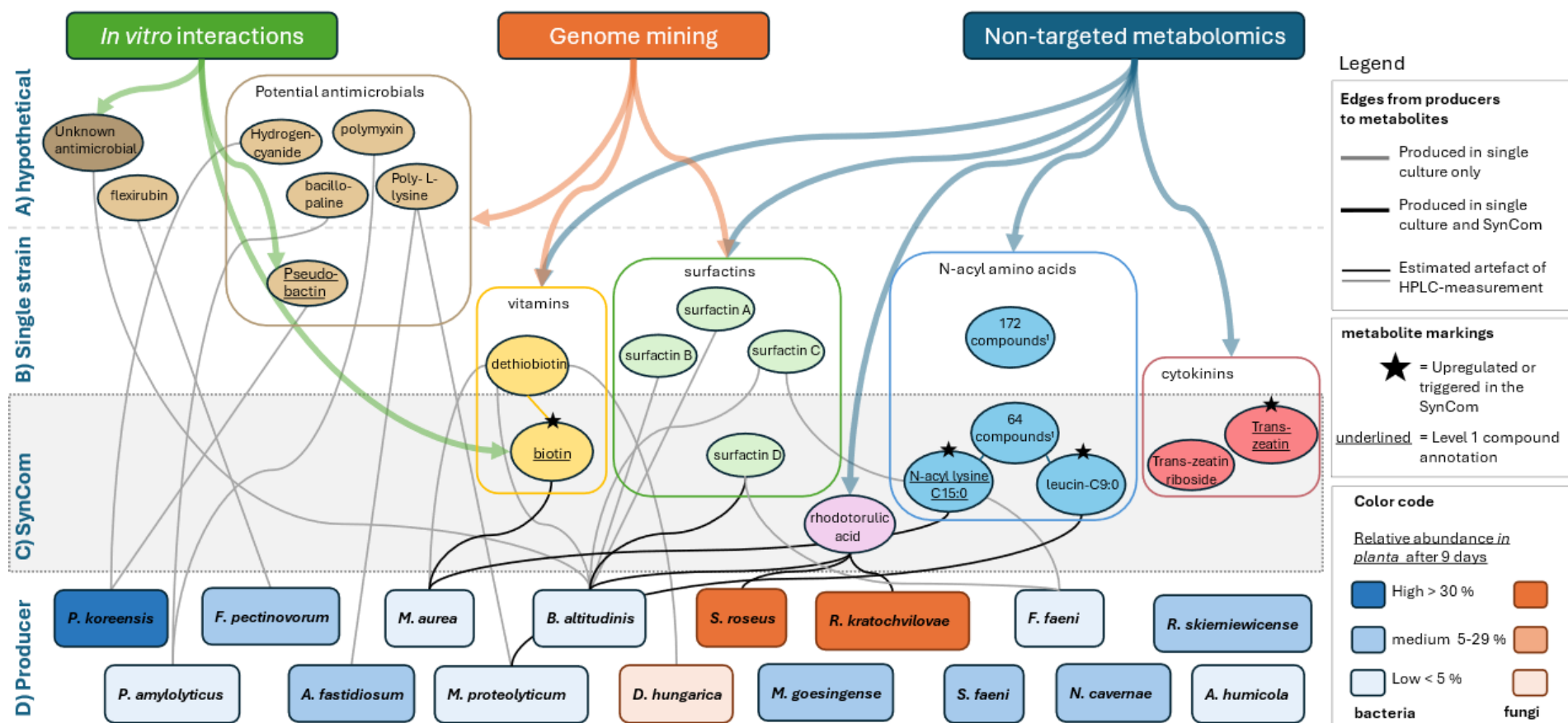


Figure D1: Graphical conclusion: Overview about the identified metabolites with community shaping potential on different detection levels and their producers. A) Metabolites with a hypothetical involvement in microbe-microbe interactions due to their functions described in literature. They were mainly detected in genome mining or assumed to underlie *in vitro* interactions and neither their production nor their identity was confirmed. B) Metabolites confirmed to be produced in single strain samples, but not in the SynCom co-culture. They were mostly identified by non-targeted metabolomics and partially confirmed by genome mining. C) Metabolites detected in single strain cultures **and/or** in the SynCom. Due to their presence in the community, they were estimated to have a high potential involvement in microbial interactions. D) SynCom members assigned to the detected or predicted metabolites. The color code indicates their relative abundance *in planta*.

ANTIMICROBIAL METABOLITES MIGHT PLAY A SUBORDINATE ROLE IN THE SYNCOM

Both manuscripts of this PhD thesis focused on identifying secondary metabolites involved in community dynamics. In the first manuscript, a significant influence of antimicrobials in community dynamics was hypothesized due to the SynCom's potential for producing known antimicrobial compounds and the predominance of inhibitory interactions in pairwise studies. However, many findings from the present studies support the possibility that antimicrobials might play a subordinate role in the SynCom. For example, the addition of purified pseudobactin to the SynCom on plants had no effect on SynCom composition, even though pseudobactin exhibited inhibitory activity against SynCom members in pairwise interactions. This suggests that even if pseudobactin is produced in the SynCom, its antimicrobial activity did not affect the relative abundance of SynCom members. Similarly, *Bacillus altitudinis* was a strong inhibitor in pairwise interactions but did not dominate the community rather it was among the least abundant microbes in the SynCom on agar plates and plants. In the non-targeted metabolomics approach, no masses corresponding to known antimicrobials were annotated, except for surfactin A-D. Instead, significantly upregulated and triggered metabolites with GNPS2 annotations like biotin and trans-zeatin are known to be involved in cross-feeding and plant stimulation.

Despite evidence of synergistic interactions within the SynCom, questions remain about why so many biosynthetic gene clusters (BGCs) encoding known antimicrobials are present among the members. For instance, Getzke *et al.* showed that two antimicrobial agents from *Pseudomonas* spp. influence the rhizosphere microbiome of *Arabidopsis thaliana* [60]. Therefore, antimicrobials might influence certain microbiomes more than others or that the production of antimicrobial is dependent on time and space. It might be that antimicrobials play a role in certain situations. For example, they could be produced in the community but act very locally. On plant leaves, microorganisms form interspecies micro-colonies where they live in close proximity [160-162]. Therefore, low concentrations of antimicrobials might suffice for competing with nearby neighbors. MALDI imaging could be a promising future approach to track the localization of antimicrobials on plant leaf surfaces. This technique has already been used to detect metabolites like saccharides and amino acids in higher concentrations [163] and antimicrobials in detectable concentrations on plant compartments and agar plates [84, 164]. However, higher resolution is needed to capture metabolites at low concentrations. Another possibility is that the detected BGCs are not expressed in the community and serve as a reservoir activated when needed. Studies have shown that high competition environments promote the production of antimicrobial agents [165, 166]. SynCom members like, *Pseudomonas koreensis*, *B. altitudinis* and *Paenibacillus amylolyticus* are known soil and rhizosphere dwellers, where more competition is estimated due to a higher microbial density [167-169]. The high biosynthetic potential of these strains might be an adaptation to such high-

competition niches. Since the plant leaf is a less colonized part of the plant compared to the rhizosphere or rhizoplane [5, 6, 31], competition e.g. for nutrients, might not be high enough to trigger antimicrobials production. However, this reservoir could be activated to combat pathogens invading the leaf microbiome. For example, the leaf microbiome of citrus leaves infected with a fungal pathogen shifted towards a more protective microbiome, increasing antifungal traits and the abundance of antifungal members [170]. Lastly, it might have been evolutionary advantageous to promote each other more than compete with each other [171]. Therefore, synergism might play a bigger role in healthy microbial communities than competition. Over 50 % of microbe-microbe correlations in the epiphytic microbiome were positive, with even more positive correlations observed in the SynCom. However, it is not fully understood to what extent correlation networks are based on direct microbe-microbe interactions. Mahmoudi *et al.* found that up to 25 % of correlations in co-abundance-based networks could be explained by environmental impacts [43] leaving > 70 % potentially influenced by other factors such as host genetic variations [172] and interspecies microbial interactions [173]. It is conceivable that synergistic microbe-microbe interactions explain the high number of positive correlations in the microbiome and the SynCom.

In manuscript 1, it was discussed that some abundant strains like *P. koreensis*, *Flavobacterium pectinovorum*, and *Sporobolomyces roseus* produce compounds for biofilm formation, cross-feeding, or surface colonization [174-176]. Metabolomic analysis in manuscript 2 further supports this hypothesis, as significant metabolites were involved in cross-feeding and plant alteration rather than antimicrobials. However, it was not further investigated whether biofilm components like exopolysaccharides are present in the non-targeted metabolomics approach. As discussed in manuscript 2, biotin was shown to be a common good in the marine ecosystem produced by prototrophs and consumed by auxotrophic organisms [116]. Even beyond vitamins, cross-feeding is a common mechanism in microbiome assembly [117, 177]. While less was known about cross-feeding pathways in the past, recent research has begun to identify underlying mechanisms, including the sharing of carbon sources, amino acids, co-factors, and trace elements as public goods [178]. Often public goods provided by community members are essential for the receiver to colonize or unfold their full metabolic potential [179] [180]. Therefore, knowledge about such strategies might be a key for effective microbiome engineering and the assembly of stable synthetic communities.

In conclusion, the present project provided first evidence that synergistic effects, such as cross-feeding, might be a key mechanism driving SynCom interactions. There was less evidence for the production and influence of antimicrobials within the community, suggesting that antimicrobial activity is a subordinate or locally limited mechanism. Consequently, it is hypothesized that synergism, rather than competition, primarily drives SynCom interactions. Further research is needed to verify this hypothesis. Nevertheless, several promising traits for future investigation were identified in this work. The following section will discuss the study's limitations and outline research directions that could address these.

LIMITATIONS AND PERSPECTIVES OF THE PROJECT

Despite several groundbreaking findings, such as the lack of effect of pseudobactin on the SynCom, the triggering of cytokinins, hinds for biotin cross-feeding, and the low abundance of strong pairwise inhibitors in the community, the results obtained in this PhD project might represent only a parts of the mechanisms driving SynCom interactions. The specific conditions used at the different detection levels (*in vitro* interactions and non-targeted metabolomics) likely limited the scope of the study, suggesting that much remains to be discovered. The condition-dependency of microbial metabolite production was evident in the pairwise interaction study on NA and PDA agar. These pairwise interactions, dominated by inhibitory interactions, may only reflect scenarios in rich media. It would be interesting to investigate whether pairwise interactions on a plant leaf-mimicking agar align more closely with the correlation network. The literature presents varying observations regarding the medium dependency of such experiments. Helfrich *et al.* used six different media for pairwise interaction studies of *Arabidopsis thaliana* leaf commensals, including leaf-mimicking agar, but found inhibiting interactions to be rather consistent [84]. Other studies have shown the nutrient dependency of antimicrobials production, suggesting that nutrient availability must be considered when drawing conclusions from specific conditions [94, 181].

The use of pseudobactin as an example antimicrobial compound demonstrated that inhibiting pairwise interactions did not affect community composition *in planta*. Along with the low abundance of strong pairwise inhibitors, these findings led to the hypothesis that antimicrobials may play a subordinate role in a community context. However, basing this hypothesis on one tested antimicrobial compound is limiting, and it would be interesting to repeat the experiment with other inhibiting compounds possibly underlying pairwise interactions e.g. surfactins and polymyxin. Further evidence supporting the hypothesis of a subordinate role of antimicrobials in the SynCom was found in the non-targeted metabolomics approach, where no metabolites related to antimicrobial activity were annotated by GNPS2, except for surfactin A-D. Yet, this study was limited to one culture condition, reflecting the SynCom metabolome only in this specific setup. For non-targeted metabolomics, a leaf-mimicking minimal medium was created, containing a carbon source and amino acids known to be present on plant leaf surfaces [58, 59]. It is possible that these conditions affected the production of antimicrobials. For instance, *Streptomyces* spp. are repressed in antibiotic production in the presence of glucose as a carbon source [182]. Since nutrient agar and potato dextrose agar used for pairwise interactions did not contain glucose, but MM9/7 agar used to determine metabolomics and the SynCom composition did, this could explain why antimicrobials might not have been produced on this agar. Additionally, the production of many antimicrobials is regulated by quorum sensing mechanisms [183] allowing producers to conserve nutrients and produce antimicrobials only in the presence of competitors or when their population is strong enough to engage in competition [184]. The use of minimal medium could have altered the growth rate of some SynCom members, which could have led to lower cell numbers and therefore

interfered also with their quorum sensing mechanism. Nevertheless, if the leaf mimicking MM9/7 agar better reflected real conditions on the plant leaf surface needs to be further addressed for instance by performing non-targeted metabolomics directly from the plant leaf. Such experiments are challenging, as microorganisms on the plant are present in lower densities, potentially causing microbial products to fall below detection levels [185]. This limitation could have already influenced the outcomes of the *in vitro* non-targeted metabolomics experiments conducted in this study. Nevertheless, the approach revealed the production of metabolites known for their cross-feeding ability and for plant stimulation, which verifies the suitability of the workflow for identifying metabolites with interaction-driving potential.

Gene clusters with high similarity to known antimicrobials such as bacillibactin, bacilysin, surfactin A, and polymyxin B were identified through genome mining, but except for surfactin A-D, these compounds were not detected among the GNPS2 library-annotated metabolites. It remains to be further investigated whether these compounds are not produced by the organisms or if the metabolomics pipeline used in this study was limited in their annotation or detection. Resolving this question is crucial, as it significantly influences the hypothesis regarding the subordinate role of antimicrobials in the community. Several factors could explain why these compounds were not detected in the non-targeted metabolomics workflow. One possibility is that the compounds were not effectively captured by the sample preparation method used in this study. Although methanol is commonly and efficiently used as a solvent in targeted and non-targeted metabolomics experiments [186, 187] it is possible that it failed to extract some antimicrobials. Previous studies have demonstrated that the use of different sampling techniques, homogenization methods, and solvents can significantly influence the outcomes of metabolomic approaches [187, 188]. Another reason could be that the compounds were present in the metabolomic GNPS2 network but were not annotated by the tool due to the absence of corresponding references in the GNPS2 library. Further research can be done to determine whether promising masses and fragmentation patterns for known antimicrobials can be detected in the generated metabolomics data. Lastly, the detection limit of the approach might have contributed to the absence of these compounds in the experiment. If the antimicrobials were produced in low concentrations, their feature intensities might have fallen below the detection threshold.

Taken together, the observed interactions and detected compounds in this project are related to the specific conditions used. To overcome this limitation, it would be valuable to investigate the observed mechanisms *in planta*. Transcriptomics from plant leaves could help determine whether the identified biosynthetic gene clusters (BGCs) with high similarity to known antimicrobials are expressed in the plant-associated community. Additionally, targeted analysis of masses and known compounds identified in this project on the plant leaf using MALDI imaging would not only confirm their production but also reveal their localization, thereby answering whether antimicrobials play a role in locally restricted areas. Non-targeted metabolomics was already very effective in identifying biotin and trans-zeatin as significant

metabolites, which are known in literature to drive dynamics in microbe-microbe and microbe-host interactions [116, 152]. Repeating the experiment under various conditions, such as different culture media and solvents, could help reveal the full metabolic capabilities of SynCom members. Comparing these results to non-targeted metabolomics from an *in planta*-grown SynCom could identify metabolites important in a plant microbiome context.

THESIS- CONCLUSION

In the present project, a synthetic community (SynCom) from *Arabidopsis thaliana* leaves was created to explore microbe-microbe interactions and the role of secondary metabolites in community dynamics. The first manuscript revealed that *in planta* interactions differed from *in vitro* pairwise interactions: positive *in planta* but mostly negative *in vitro*. The antimicrobial agent pseudobactin from *Pseudomonas koreensis* was identified, but it did not affect community composition *in planta*, suggesting antimicrobials may have a minor role in the community. The second manuscript employed non-targeted metabolomics to explore chemical interactions. It found that certain metabolites, such as biotin and trans-zeatin, were significantly upregulated in the community context. Supplementation experiments with biotin showed that the metabolite promoted growth, indicating that cross-feeding could drive community dynamics. The study contributed to the identification of key players in the SynCom, including strains known for synergistic effects like *Massilia* spp., compounds known for cross-feeding in different environments, and metabolites shown to stimulate various plant species. Several traits were detected that are likely to influence community dynamics and interesting for future research. The results highlight the effectiveness of the methods used for investigating microbial interactions and identifying hub organisms and key metabolites in multispecies microbial communities. The utilized workflow has proven its suitability as a first step in determining community dynamics.

THESIS - BIBLIOGRAPHY

1. Grice EA, Segre JA. The skin microbiome. *Nature Reviews Microbiology*. 2011;**9**:244-53 <https://doi.org/10.1038/nrmicro2537>
2. Banerjee S, van der Heijden MGA. Soil microbiomes and one health. *Nature Reviews Microbiology*. 2023;**21**:6-20 <https://doi.org/10.1038/s41579-022-00779-w>
3. Mallott EK, Amato KR. Host specificity of the gut microbiome. *Nature Reviews Microbiology*. 2021;**19**:639-53 <https://doi.org/10.1038/s41579-021-00562-3>
4. Turner TR, James EK, Poole PS. The plant microbiome. *Genome Biology*. 2013;**14**:209 <https://doi.org/10.1186/gb-2013-14-6-209>
5. Vandenkoornhuysen P, Quaiser A, Duhamel M, Le Van A, Dufresne A. The importance of the microbiome of the plant holobiont. *New Phytologist*. 2015;**206**:1196-206 <https://doi.org/https://doi.org/10.1111/nph.13312>
6. Hassani MA, Durán P, Hacquard S. Microbial interactions within the plant holobiont. *Microbiome*. 2018;**6**:58 <https://doi.org/10.1186/s40168-018-0445-0>
7. Munir N, Hanif M, Abideen Z, Sohail M, El-Keblawy A, Radicetti E *et al.* Mechanisms and strategies of plant microbiome interactions to mitigate abiotic stresses. *Agronomy*. 2022;**12**:2069
8. Li J, Wang C, Liang W, Liu S. Rhizosphere microbiome: The emerging barrier in plant-pathogen interactions. *Frontiers in Microbiology*. 2021;**12** <https://doi.org/10.3389/fmicb.2021.772420>
9. Hu J, Wei Z, Friman V-P, Gu S-h, Wang X-f, Eisenhauer N *et al.* Probiotic diversity enhances rhizosphere microbiome function and plant disease suppression. *mBio*. 2016;**7**:10.1128/mbio.01790-16 <https://doi.org/doi:10.1128/mbio.01790-16>
10. Singh SK, Wu X, Shao C, Zhang H. Microbial enhancement of plant nutrient acquisition. *Stress Biology*. 2022;**2**:3 <https://doi.org/10.1007/s44154-021-00027-w>
11. Santoyo G. How plants recruit their microbiome? New insights into beneficial interactions. *Journal of Advanced Research*. 2022;**40**:45-58 <https://doi.org/https://doi.org/10.1016/j.jare.2021.11.020>
12. Thapa S, Prasanna R, Ranjan K, Velmourougane K, Ramakrishnan B. Nutrients and host attributes modulate the abundance and functional traits of phyllosphere microbiome in rice. *Microbiological Research*. 2017;**204**:55-64 <https://doi.org/https://doi.org/10.1016/j.micres.2017.07.007>
13. Raaijmakers JM, Mazzola M. Diversity and natural functions of antibiotics produced by beneficial and plant pathogenic bacteria. *Annual Review of Phytopathology*. 2012;**50**:403-24 <https://doi.org/https://doi.org/10.1146/annurev-phyto-081211-172908>
14. Touré Y, Ongena M, Jacques P, Guirou A, Thonart P. Role of lipopeptides produced by bacillus subtilis ga1 in the reduction of grey mould disease caused by botrytis cinerea on apple. *Journal of Applied Microbiology*. 2004;**96**:1151-60 <https://doi.org/10.1111/j.1365-2672.2004.02252.x>
15. Wang NR, Wiesmann CL, Melnyk RA, Hossain SS, Chi M-H, Martens K *et al.* Commensal pseudomonas fluorescens strains protect *arabidopsis* from closely

- related pseudomonas pathogens in a colonization-dependent manner. *mBio*. 2022;**13**:e02892-21 <https://doi.org/doi:10.1128/mbio.02892-21>
16. Teixeira PJPL, Colaianni NR, Fitzpatrick CR, Dangl JL. Beyond pathogens: Microbiota interactions with the plant immune system. *Current Opinion in Microbiology*. 2019;**49**:7-17 <https://doi.org/https://doi.org/10.1016/j.mib.2019.08.003>
 17. Gupta A, Hisano H, Hojo Y, Matsuura T, Ikeda Y, Mori IC *et al*. Global profiling of phytohormone dynamics during combined drought and pathogen stress in arabidopsis thaliana reveals aba and ja as major regulators. *Scientific Reports*. 2017;**7**:4017 <https://doi.org/10.1038/s41598-017-03907-2>
 18. Henry RC, Engström K, Olin S, Alexander P, Arneth A, Rounsevell MDA. Food supply and bioenergy production within the global cropland planetary boundary. *PLOS ONE*. 2018;**13**:e0194695 <https://doi.org/10.1371/journal.pone.0194695>
 19. Santos LF, Olivares FL. Plant microbiome structure and benefits for sustainable agriculture. *Current Plant Biology*. 2021;**26**:100198 <https://doi.org/https://doi.org/10.1016/j.cpb.2021.100198>
 20. Ray DK, Gerber JS, MacDonald GK, West PC. Climate variation explains a third of global crop yield variability. *Nature Communications*. 2015;**6**:5989 <https://doi.org/10.1038/ncomms6989>
 21. Ajjah N, Fiodor A, Pandey AK, Rana A, Pranaw K. Plant growth-promoting bacteria (pgpb) with biofilm-forming ability: A multifaceted agent for sustainable agriculture. *Diversity*. 2023;**15**:112
 22. Orozco-Mosqueda MdC, Rocha-Granados MdC, Glick BR, Santoyo G. Microbiome engineering to improve biocontrol and plant growth-promoting mechanisms. *Microbiological Research*. 2018;**208**:25-31 <https://doi.org/https://doi.org/10.1016/j.micres.2018.01.005>
 23. Arif I, Batool M, Schenk PM. Plant microbiome engineering: Expected benefits for improved crop growth and resilience. *Trends in Biotechnology*. 2020;**38**:1385-96 <https://doi.org/https://doi.org/10.1016/j.tibtech.2020.04.015>
 24. Chihaoui S-A, Trabelsi D, Jdey A, Mhadhbi H, Mhamdi R. Inoculation of phaseolus vulgaris with the nodule-endophyte agrobacterium sp. 10c2 affects richness and structure of rhizosphere bacterial communities and enhances nodulation and growth. *Archives of microbiology*. 2015;**197**:805-13
 25. Mitter B, Pfaffenbichler N, Flavell R, Compant S, Antonielli L, Petric A *et al*. A new approach to modify plant microbiomes and traits by introducing beneficial bacteria at flowering into progeny seeds. *Frontiers in Microbiology*. 2017;**8**:11
 26. Wu J, Wang Y, Lin X. Purple phototrophic bacterium enhances stevioside yield by stevia rebaudiana bertonii via foliar spray and rhizosphere irrigation. *PloS one*. 2013;**8**:e67644
 27. Schmitz L, Yan Z, Schneijderberg M, de Roij M, Pijnenburg R, Zheng Q *et al*. Synthetic bacterial community derived from a desert rhizosphere confers salt stress resilience to tomato in the presence of a soil microbiome. *The ISME Journal*. 2022;**16**:1907-20 <https://doi.org/10.1038/s41396-022-01238-3>
 28. Wang Z, Fu X, Kuramae EE. Insight into farming native microbiome by bioinoculant in soil-plant system. *Microbiological Research*. 2024;**285**:127776 <https://doi.org/https://doi.org/10.1016/j.micres.2024.127776>
 29. Kong HG, Song GC, Ryu C-M. Inheritance of seed and rhizosphere microbial communities through plant–soil feedback and soil memory. *Environmental*

- Microbiology Reports*. 2019;**11**:479-86 <https://doi.org/https://doi.org/10.1111/1758-2229.12760>
30. Trivedi P, Leach JE, Tringe SG, Sa T, Singh BK. Plant–microbiome interactions: From community assembly to plant health. *Nature Reviews Microbiology*. 2020;**18**:607-21 <https://doi.org/10.1038/s41579-020-0412-1>
 31. Chaudhry V, Runge P, Sengupta P, Doehlemann G, Parker JE, Kemen E. Shaping the leaf microbiota: Plant–microbe–microbe interactions. *Journal of Experimental Botany*. 2020;**72**:36-56 <https://doi.org/10.1093/jxb/eraa417>
 32. Laveau JHJ. A brief from the leaf: Latest research to inform our understanding of the phyllosphere microbiome. *Current Opinion in Microbiology*. 2019;**49**:41-49 <https://doi.org/https://doi.org/10.1016/j.mib.2019.10.002>
 33. Zhang J, Liu W, Bu J, Lin Y, Bai Y. Host genetics regulate the plant microbiome. *Current Opinion in Microbiology*. 2023;**72**:102268 <https://doi.org/https://doi.org/10.1016/j.mib.2023.102268>
 34. Thiergart T, Durán P, Ellis T, Vannier N, Garrido-Oter R, Kemen E *et al*. Root microbiota assembly and adaptive differentiation among european arabidopsis populations. *Nature Ecology & Evolution*. 2020;**4**:122-31 <https://doi.org/10.1038/s41559-019-1063-3>
 35. Qu Q, Zhang Z, Peijnenburg WJGM, Liu W, Lu T, Hu B *et al*. Rhizosphere microbiome assembly and its impact on plant growth. *Journal of Agricultural and Food Chemistry*. 2020;**68**:5024-38 <https://doi.org/10.1021/acs.jafc.0c00073>
 36. Zhou Q, Zhang X, He R, Wang S, Jiao C, Huang R *et al*. The composition and assembly of bacterial communities across the rhizosphere and phyllosphere compartments of phragmites australis. *Diversity*. 2019;**11**:98
 37. Gkarmiri K, Mahmood S, Ekblad A, Alström S, Högberg N, Finlay R. Identifying the active microbiome associated with roots and rhizosphere soil of oilseed rape. *Applied and Environmental Microbiology*. 2017;**83**:e01938-17 <https://doi.org/doi:10.1128/AEM.01938-17>
 38. Lundberg DS, Lebeis SL, Paredes SH, Yourstone S, Gehring J, Malfatti S *et al*. Defining the core arabidopsis thaliana root microbiome. *Nature*. 2012;**488**:86-90 <https://doi.org/10.1038/nature11237>
 39. Sun A, Jiao X-Y, Chen Q, Wu A-L, Zheng Y, Lin Y-X *et al*. Microbial communities in crop phyllosphere and root endosphere are more resistant than soil microbiota to fertilization. *Soil Biology and Biochemistry*. 2021;**153**:108113 <https://doi.org/https://doi.org/10.1016/j.soilbio.2020.108113>
 40. Maymó-Gatell X, Chien Y-t, Gossett JM, Zinder SH. Isolation of a bacterium that reductively dechlorinates tetrachloroethene to ethene. *Science*. 1997;**276**:1568-71 <https://doi.org/doi:10.1126/science.276.5318.1568>
 41. Fagervold SK, Watts JEM, May HD, Sowers KR. Sequential reductive dechlorination of *meta*-chlorinated polychlorinated biphenyl congeners in sediment microcosms by two different *chloroflexi* phylotypes. *Applied and Environmental Microbiology*. 2005;**71**:8085-90 <https://doi.org/doi:10.1128/AEM.71.12.8085-8090.2005>
 42. Fuerst JA, Sagulenko E. Beyond the bacterium: Planctomycetes challenge our concepts of microbial structure and function. *Nature Reviews Microbiology*. 2011;**9**:403-13 <https://doi.org/10.1038/nrmicro2578>

43. Mahmoudi M, Almario J, Lutap K, Nieselt K, Kemen E. Microbial communities living inside plant leaves or on the leaf surface are differently shaped by environmental cues. *bioRxiv*. 2024:2023.12.17.572047 <https://doi.org/10.1101/2023.12.17.572047>
44. Malacrinò A, Mosca S, Li Destri Nicosia MG, Agosteo GE, Schena L. Plant genotype shapes the bacterial microbiome of fruits, leaves, and soil in olive plants. *Plants*. 2022;**11**:613
45. VanWallendael A, Benucci GMN, da Costa PB, Fraser L, Sreedasyam A, Fritschi F *et al*. Host genotype controls ecological change in the leaf fungal microbiome. *PLOS Biology*. 2022;**20**:e3001681 <https://doi.org/10.1371/journal.pbio.3001681>
46. Yan K, Han W, Zhu Q, Li C, Dong Z, Wang Y. Leaf surface microtopography shaping the bacterial community in the phyllosphere: Evidence from 11 tree species. *Microbiological Research*. 2022;**254**:126897 <https://doi.org/https://doi.org/10.1016/j.micres.2021.126897>
47. Doan HK, Ngassam VN, Gilmore SF, Tecon R, Parikh AN, Leveau JHJ. Topography-driven shape, spread, and retention of leaf surface water impacts microbial dispersion and activity in the phyllosphere. *Phytobiomes Journal*. 2020;**4**:268-80 <https://doi.org/10.1094/pbiomes-01-20-0006-r>
48. Vorholt JA. Microbial life in the phyllosphere. *Nature Reviews Microbiology*. 2012;**10**:828-40 <https://doi.org/10.1038/nrmicro2910>
49. Kikukawa H, Okaya T, Maoka T, Miyazaki M, Murofushi K, Kato T *et al*. Carotenoid nostoxanthin production by sphingomonas sp. Sg73 isolated from deep sea sediment. *Marine Drugs*. 2021;**19**:274
50. Yoshida S, Hiradate S, Koitabashi M, Kamo T, Tsushima S. Phyllosphere methylobacterium bacteria contain uva-absorbing compounds. *Journal of Photochemistry and Photobiology B: Biology*. 2017;**167**:168-75 <https://doi.org/https://doi.org/10.1016/j.jphotobiol.2016.12.019>
51. Villarreal P, Carrasco M, Barahona S, Alcaíno J, Cifuentes V, Baeza M. Tolerance to ultraviolet radiation of psychrotolerant yeasts and analysis of their carotenoid, mycosporine, and ergosterol content. *Current Microbiology*. 2016;**72**:94-101 <https://doi.org/10.1007/s00284-015-0928-1>
52. Moliné M, Flores MR, Libkind D, Carmen Diéguez MdC, Farías ME, van Broock M. Photoprotection by carotenoid pigments in the yeast *rhodotorula mucilaginosa*: The role of torularhodin. *Photochemical & Photobiological Sciences*. 2010;**9**:1145-51 <https://doi.org/10.1039/c0pp00009d>
53. Fessia A, Barra P, Barros G, Nesci A. Could bacillus biofilms enhance the effectivity of biocontrol strategies in the phyllosphere? *Journal of Applied Microbiology*. 2022;**133**:2148-66 <https://doi.org/10.1111/jam.15596>
54. Elias S, Banin E. Multi-species biofilms: Living with friendly neighbors. *FEMS Microbiology Reviews*. 2012;**36**:990-1004 <https://doi.org/10.1111/j.1574-6976.2012.00325.x>
55. Koch K, Bhushan B, Barthlott W. Multifunctional surface structures of plants: An inspiration for biomimetics. *Progress in Materials Science*. 2009;**54**:137-78 <https://doi.org/https://doi.org/10.1016/j.pmatsci.2008.07.003>
56. Raaijmakers JM, De Bruijn I, Nybroe O, Ongena M. Natural functions of lipopeptides from bacillus and pseudomonas: More than surfactants and antibiotics. *FEMS Microbiology Reviews*. 2010;**34**:1037-62 <https://doi.org/10.1111/j.1574-6976.2010.00221.x>

57. El-Khordagui L, Badawey SE, Heikal LA Application of biosurfactants in the production of personal care products, and household detergents and industrial and institutional cleaners. *Green sustainable process for chemical and environmental engineering and science*, Elsevier. 49-96
58. Weibull J, Ronquist F, Brishammar S. Free amino acid composition of leaf exudates and phloem sap 1: A comparative study in oats and barley. *Plant Physiology*. 1990;**92**:222-26 <https://doi.org/10.1104/pp.92.1.222>
59. Leveau JHJ, Lindow SE. Appetite of an epiphyte: Quantitative monitoring of bacterial sugar consumption in the phyllosphere. *Proceedings of the National Academy of Sciences*. 2001;**98**:3446-53 <https://doi.org/doi:10.1073/pnas.061629598>
60. Getzke F, Hassani MA, Crüseemann M, Malisic M, Zhang P, Ishigaki Y *et al*. Cofunctioning of bacterial exometabolites drives root microbiota establishment. *Proceedings of the National Academy of Sciences*. 2023;**120**:e2221508120 <https://doi.org/doi:10.1073/pnas.2221508120>
61. Leinweber A, Fredrik Inglis R, Kümmerli R. Cheating fosters species co-existence in well-mixed bacterial communities. *The ISME Journal*. 2017;**11**:1179-88 <https://doi.org/10.1038/ismej.2016.195>
62. Butaitė E, Baumgartner M, Wyder S, Kümmerli R. Siderophore cheating and cheating resistance shape competition for iron in soil and freshwater pseudomonas communities. *Nature Communications*. 2017;**8**:414 <https://doi.org/10.1038/s41467-017-00509-4>
63. Vorholt JA, Vogel C, Carlström CI, Müller DB. Establishing causality: Opportunities of synthetic communities for plant microbiome research. *Cell Host & Microbe*. 2017;**22**:142-55 <https://doi.org/https://doi.org/10.1016/j.chom.2017.07.004>
64. Schulz BJ, Rabsch L, Junker C Chemical warfare in the plant microbiome leads to a balance of antagonisms and a healthy plant. In: Verma SK, White JJF (eds.). *Seed endophytes: Biology and biotechnology*, Cham: Springer International Publishing. 171-89. Retrieved from https://doi.org/10.1007/978-3-030-10504-4_9
65. Hansen BL, Pessotti RdC, Fischer MS, Collins A, El-Hifnawi L, Liu MD *et al*. Cooperation, competition, and specialized metabolism in a simplified root nodule microbiome. *mBio*. 2020;**11**:10.1128/mbio.01917-20 <https://doi.org/doi:10.1128/mbio.01917-20>
66. Clardy J, Fischbach MA, Walsh CT. New antibiotics from bacterial natural products. *Nature Biotechnology*. 2006;**24**:1541-50 <https://doi.org/10.1038/nbt1266>
67. Cragg GM, Pezzuto JM. Natural products as a vital source for the discovery of cancer chemotherapeutic and chemopreventive agents. *Medical Principles and Practice*. 2015;**25**:41-59 <https://doi.org/10.1159/000443404>
68. Duke, Dayan, Romagni, Rimando. Natural products as sources of herbicides: Current status and future trends. *Weed Research*. 2000;**40**:99-111 <https://doi.org/https://doi.org/10.1046/j.1365-3180.2000.00161.x>
69. Zaker M. Natural plant products as eco-friendly fungicides for plant diseases control-a review. 2016
70. Gutiérrez-del-Río I, López-Ibáñez S, Magadán-Corpas P, Fernández-Calleja L, Pérez-Valero Á, Tuñón-Granda M *et al*. Terpenoids and polyphenols as natural antioxidant agents in food preservation. *Antioxidants*. 2021;**10**:1264
71. Liu J-K. Natural products in cosmetics. *Natural Products and Bioprospecting*. 2022;**12**:40 <https://doi.org/10.1007/s13659-022-00363-y>

72. Netzker T, Fischer J, Weber J, Mattern DJ, König CC, Valiante V *et al.* Microbial communication leading to the activation of silent fungal secondary metabolite gene clusters. *Frontiers in Microbiology*. 2015;**6** <https://doi.org/10.3389/fmicb.2015.00299>
73. Strieker M, Tanović A, Marahiel MA. Nonribosomal peptide synthetases: Structures and dynamics. *Current Opinion in Structural Biology*. 2010;**20**:234-40 <https://doi.org/10.1016/j.sbi.2010.01.009>
74. Risdian C, Mozef T, Wink J. Biosynthesis of polyketides in streptomyces. *Microorganisms*. 2019;**7**:124
75. Hudson GA, Mitchell DA. Ripp antibiotics: Biosynthesis and engineering potential. *Current Opinion in Microbiology*. 2018;**45**:61-69 <https://doi.org/10.1016/j.mib.2018.02.010>
76. Avalos M, Garbeva P, Vader L, van Wezel GP, Dickschat JS, Ulanova D. Biosynthesis, evolution and ecology of microbial terpenoids. *Natural Product Reports*. 2022;**39**:249-72
77. Teh SS, Ee GCL, Mah SH, Ahmad Z. Structure–activity relationship study of secondary metabolites from *Mesua beccariana*, *Mesua ferrea* and *Mesua congestiflora* for anti-cholinesterase activity. *Medicinal Chemistry Research*. 2016;**25**:819-23 <https://doi.org/10.1007/s00044-016-1531-0>
78. Robinson SL, Christenson JK, Wackett LP. Biosynthesis and chemical diversity of β -lactone natural products. *Natural product reports*. 2019;**36**:458-75
79. Timofeeva AM, Galyamova MR, Sedykh SE. Bacterial siderophores: Classification, biosynthesis, perspectives of use in agriculture. *Plants*. 2022;**11**:3065
80. Blin K, Kim HU, Medema MH, Weber T. Recent development of antimash and other computational approaches to mine secondary metabolite biosynthetic gene clusters. *Briefings in Bioinformatics*. 2019;**20**:1103-13 <https://doi.org/10.1093/bib/bbx146>
81. Agrawal S, Acharya D, Adholeya A, Barrow CJ, Deshmukh SK. Nonribosomal peptides from marine microbes and their antimicrobial and anticancer potential. *Frontiers in Pharmacology*. 2017;**8** <https://doi.org/10.3389/fphar.2017.00828>
82. Robertsen HL, Musiol-Kroll EM. Actinomycete-derived polyketides as a source of antibiotics and lead structures for the development of new antimicrobial drugs. *Antibiotics*. 2019;**8**:157
83. Crits-Christoph A, Bhattacharya N, Olm MR, Song YS, Banfield JF. Transporter genes in biosynthetic gene clusters predict metabolite characteristics and siderophore activity. *Genome research*. 2021;**31**:239-50
84. Helfrich EJM, Vogel CM, Ueoka R, Schäfer M, Ryffel F, Müller DB *et al.* Bipartite interactions, antibiotic production and biosynthetic potential of the Arabidopsis leaf microbiome. *Nature Microbiology*. 2018;**3**:909-19 <https://doi.org/10.1038/s41564-018-0200-0>
85. Amit G, Bashan A. Top-down identification of keystone taxa in the microbiome. *Nature Communications*. 2023;**14**:3951 <https://doi.org/10.1038/s41467-023-39459-5>
86. van der Heijden MGA, Hartmann M. Networking in the plant microbiome. *PLOS Biology*. 2016;**14**:e1002378 <https://doi.org/10.1371/journal.pbio.1002378>
87. Lee KK, Kim H, Lee Y-H. Cross-kingdom co-occurrence networks in the plant microbiome: Importance and ecological interpretations. *Frontiers in Microbiology*. 2022;**13** <https://doi.org/10.3389/fmicb.2022.953300>

88. Ling N, Zhu C, Xue C, Chen H, Duan Y, Peng C *et al.* Insight into how organic amendments can shape the soil microbiome in long-term field experiments as revealed by network analysis. *Soil Biology and Biochemistry*. 2016;**99**:137-49 <https://doi.org/https://doi.org/10.1016/j.soilbio.2016.05.005>
89. Almario J, Mahmoudi M, Kroll S, Agler M, Placzek A, Mari A *et al.* The leaf microbiome of *Arabidopsis* displays reproducible dynamics and patterns throughout the growing season. *mBio*. 2022;**13**:e02825-21 <https://doi.org/doi:10.1128/mbio.02825-21>
90. Connor N, Barberán A, Clauzet A. Using null models to infer microbial co-occurrence networks. *PLOS ONE*. 2017;**12**:e0176751 <https://doi.org/10.1371/journal.pone.0176751>
91. Comeau D, Balthazar C, Novinscak A, Bouhamdani N, Joly DL, Filion M. Interactions between bacillus spp., pseudomonas spp. And cannabis sativa promote plant growth. *Frontiers in Microbiology*. 2021;**12** <https://doi.org/10.3389/fmicb.2021.715758>
92. Nishisaka CS, Ventura JP, Bais HP, Mendes R. Role of bacillus subtilis exopolymeric genes in modulating rhizosphere microbiome assembly. *Environmental Microbiome*. 2024;**19**:33 <https://doi.org/10.1186/s40793-024-00567-4>
93. Gu Q, Yang Y, Yuan Q, Shi G, Wu L, Lou Z *et al.* Bacillomycin d produced by bacillus amyloliquefaciens is involved in the antagonistic interaction with the plant-pathogenic fungus fusarium graminearum. *Applied and Environmental Microbiology*. 2017;**83**:e01075-17 <https://doi.org/doi:10.1128/AEM.01075-17>
94. Matuszewska M, Maciąg T, Rajewska M, Wierzbicka A, Jafra S. The carbon source-dependent pattern of antimicrobial activity and gene expression in pseudomonas donghuensis p482. *Scientific Reports*. 2021;**11**:10994 <https://doi.org/10.1038/s41598-021-90488-w>
95. Afridi MS, Ali S, Salam A, César Terra W, Hafeez A, Sumaira *et al.* Plant microbiome engineering: Hopes or hypes. *Biology*. 2022;**11**:1782
96. Jing J, Garbeva P, Raaijmakers JM, Medema MH. Strategies for tailoring functional microbial synthetic communities. *The ISME Journal*. 2024;**18** <https://doi.org/10.1093/ismejo/wrae049>
97. Mee MT, Collins JJ, Church GM, Wang HH. Syntrophic exchange in synthetic microbial communities. *Proceedings of the National Academy of Sciences*. 2014;**111**:E2149-E56
98. Chodkowski John L, Shade A. A synthetic community system for probing microbial interactions driven by exometabolites. *mSystems*. 2017;**2**:10.1128/msystems.00129-17 <https://doi.org/10.1128/msystems.00129-17>
99. Beck AE, Kleiner M, Garrell A-K. Elucidating plant-microbe-environment interactions through omics-enabled metabolic modelling using synthetic communities. *Frontiers in Plant Science*. 2022;**13** <https://doi.org/10.3389/fpls.2022.910377>
100. Liu H, Brettell LE, Qiu Z, Singh BK. Microbiome-mediated stress resistance in plants. *Trends in plant science*. 2020;**25**:733-43
101. de Souza RSC, Armanhi JSL, Damasceno NdB, Imperial J, Arruda P. Genome sequences of a plant beneficial synthetic bacterial community reveal genetic features for successful plant colonization. *Frontiers in Microbiology*. 2019;**10** <https://doi.org/10.3389/fmicb.2019.01779>

102. Bittleston LS. Connecting microbial community assembly and function. *Current Opinion in Microbiology*. 2024;**80**:102512
<https://doi.org/https://doi.org/10.1016/j.mib.2024.102512>
103. Wang Y, Liu H, Shen Z, Miao Y, Wang J, Jiang X *et al*. Richness and antagonistic effects co-affect plant growth promotion by synthetic microbial consortia. *Applied Soil Ecology*. 2022;**170**:104300
<https://doi.org/https://doi.org/10.1016/j.apsoil.2021.104300>
104. Astudillo-García C, Bell JJ, Webster NS, Glasl B, Jompa J, Montoya JM *et al*. Evaluating the core microbiota in complex communities: A systematic investigation. *Environmental Microbiology*. 2017;**19**:1450-62
<https://doi.org/https://doi.org/10.1111/1462-2920.13647>
105. Zhou X, Wang J, Liu F, Liang J, Zhao P, Tsui CKM *et al*. Cross-kingdom synthetic microbiota supports tomato suppression of fusarium wilt disease. *Nature Communications*. 2022;**13**:7890 <https://doi.org/10.1038/s41467-022-35452-6>
106. Wang Z, Hu X, Solanki MK, Pang F. A synthetic microbial community of plant core microbiome can be a potential biocontrol tool. *Journal of Agricultural and Food Chemistry*. 2023;**71**:5030-41 <https://doi.org/10.1021/acs.jafc.2c08017>
107. Wagg C, Schlaeppli K, Banerjee S, Kuramae EE, van der Heijden MGA. Fungal-bacterial diversity and microbiome complexity predict ecosystem functioning. *Nature Communications*. 2019;**10**:4841 <https://doi.org/10.1038/s41467-019-12798-y>
108. Toju H, Abe MS, Ishii C, Hori Y, Fujita H, Fukuda S. Scoring species for synthetic community design: Network analyses of functional core microbiomes. *Frontiers in Microbiology*. 2020;**11** <https://doi.org/10.3389/fmicb.2020.01361>
109. Moyne O, Al-Bassam M, Lieng C, Thiruppathy D, Norton GJ, Kumar M *et al*. Guild and niche determination enable targeted alteration of the microbiome. *bioRxiv*. 2023 <https://doi.org/10.1101/2023.05.11.540389>
110. Park H, Patel A, Hunt KA, Henson MA, Carlson RP. Artificial consortium demonstrates emergent properties of enhanced cellulosic-sugar degradation and biofuel synthesis. *npj Biofilms and Microbiomes*. 2020;**6**:59
<https://doi.org/10.1038/s41522-020-00170-8>
111. Jousset A, Becker J, Chatterjee S, Karlovsky P, Scheu S, Eisenhauer N. Biodiversity and species identity shape the antifungal activity of bacterial communities. *Ecology*. 2014;**95**:1184-90
112. Feng Z, Sun H, Qin Y, Zhou Y, Zhu H, Yao Q. A synthetic community of siderophore-producing bacteria increases soil selenium bioavailability and plant uptake through regulation of the soil microbiome. *Science of The Total Environment*. 2023;**871**:162076
113. Chun S-J, Cui Y, Yoo S-H, Lee JR. Organic connection of holobiont components and the essential roles of core microbes in the holobiont formation of feral brassica napus. *Frontiers in Microbiology*. 2022;**13** <https://doi.org/10.3389/fmicb.2022.920759>
114. Lewin S, Francioli D, Ulrich A, Kolb S. Crop host signatures reflected by co-association patterns of keystone bacteria in the rhizosphere microbiota. *Environmental Microbiome*. 2021;**16**:18 <https://doi.org/10.1186/s40793-021-00387-w>
115. Höhn F, Chaudhry V, Bagci C, Mahmoudi M, Klenk E, Berg L *et al*. Strong pairwise interactions do not drive interactions in a plant leaf associated microbial community. *bioRxiv*. 2024:2024.05.22.595276 <https://doi.org/10.1101/2024.05.22.595276>

116. Wienhausen G, Bruns S, Sultana S, Dlugosch L, Groon L-A, Wilkes H *et al.* The overlooked role of a biotin precursor for marine bacteria - desthiobiotin as an escape route for biotin auxotrophy. *The ISME Journal*. 2022;**16**:2599-609 <https://doi.org/10.1038/s41396-022-01304-w>
117. Ryback B, Bortfeld-Miller M, Vorholt JA. Metabolic adaptation to vitamin auxotrophy by leaf-associated bacteria. *The ISME Journal*. 2022;**16**:2712-24 <https://doi.org/10.1038/s41396-022-01303-x>
118. Ofek M, Hadar Y, Minz D. Ecology of root colonizing massilia (oxalobacteraceae). *PLOS ONE*. 2012;**7**:e40117 <https://doi.org/10.1371/journal.pone.0040117>
119. He X, Wang D, Jiang Y, Li M, Delgado-Baquerizo M, McLaughlin C *et al.* Heritable microbiome variation is correlated with source environment in locally adapted maize varieties. *Nature Plants*. 2024;**10**:598-617 <https://doi.org/10.1038/s41477-024-01654-7>
120. Li C, Cao P, Du C, Zhang X, Bing H, Li L *et al.* Massilia rhizosphaerae sp. Nov., a rice-associated rhizobacterium with antibacterial activity against ralstonia solanacearum. *International Journal of Systematic and Evolutionary Microbiology*. 2021;**71** <https://doi.org/https://doi.org/10.1099/ijsem.0.005009>
121. Frediansyah A, Straetener J, Brötz-Oesterhelt H, Gross H. Massiliamide, a cyclic tetrapeptide with potent tyrosinase inhibitory properties from the gram-negative bacterium massilia albidiflava dsm 17472t. *The Journal of Antibiotics*. 2021;**74**:269-72 <https://doi.org/10.1038/s41429-020-00394-y>
122. Yagi H, Corzo G, Nakahara T. N-acyl amino acid biosynthesis in marine bacterium, deleya marina. *Biochimica et Biophysica Acta (BBA) - General Subjects*. 1997;**1336**:28-32 [https://doi.org/https://doi.org/10.1016/S0304-4165\(97\)00009-3](https://doi.org/https://doi.org/10.1016/S0304-4165(97)00009-3)
123. Nguyen DD, Wu C-H, Moree WJ, Lamsa A, Medema MH, Zhao X *et al.* Ms/ms networking guided analysis of molecule and gene cluster families. *Proceedings of the National Academy of Sciences*. 2013;**110**:E2611-E20 <https://doi.org/doi:10.1073/pnas.1303471110>
124. Chen X, Lu Y, Shan M, Zhao H, Lu Z, Lu Y. A mini-review: Mechanism of antimicrobial action and application of surfactin. *World Journal of Microbiology and Biotechnology*. 2022;**38**:143 <https://doi.org/10.1007/s11274-022-03323-3>
125. Xu B-H, Ye Z-W, Zheng Q-W, Wei T, Lin J-F, Guo L-Q. Isolation and characterization of cyclic lipopeptides with broad-spectrum antimicrobial activity from bacillus siamensis jfl15. *3 Biotech*. 2018;**8**:444 <https://doi.org/10.1007/s13205-018-1443-4>
126. Meena KR, Sharma A, Kanwar SS. Antitumoral and antimicrobial activity of surfactin extracted from bacillus subtilis klp2015. *International Journal of Peptide Research and Therapeutics*. 2020;**26**:423-33 <https://doi.org/10.1007/s10989-019-09848-w>
127. Jiang J, Gao L, Bie X, Lu Z, Liu H, Zhang C *et al.* Identification of novel surfactin derivatives from nrps modification of bacillus subtilis and its antifungal activity against fusarium moniliforme. *BMC Microbiology*. 2016;**16**:31 <https://doi.org/10.1186/s12866-016-0645-3>
128. Aleti G, Lehner S, Bacher M, Compant S, Nikolic B, Plesko M *et al.* Surfactin variants mediate species-specific biofilm formation and root colonization in bacillus. *Environmental Microbiology*. 2016;**18**:2634-45 <https://doi.org/https://doi.org/10.1111/1462-2920.13405>
129. Zerriouh H, de Vicente A, Pérez-García A, Romero D. Surfactin triggers biofilm formation of bacillus subtilis in melon phylloplane and contributes to the biocontrol

- activity. *Environmental Microbiology*. 2014;**16**:2196-211
<https://doi.org/https://doi.org/10.1111/1462-2920.12271>
130. Debois D, Fernandez O, Franzil L, Jourdan E, de Brogniez A, Willems L *et al.* Plant polysaccharides initiate underground crosstalk with bacilli by inducing synthesis of the immunogenic lipopeptide surfactin. *Environmental Microbiology Reports*. 2015;**7**:570-82 <https://doi.org/https://doi.org/10.1111/1758-2229.12286>
 131. Hoff G, Arias AA, Boubsi F, Pršić J, Meyer T, Ibrahim HMM *et al.* Surfactin stimulated by pectin molecular patterns and root exudates acts as a key driver of the <i>bacillus</i>-plant mutualistic interaction. *mBio*. 2021;**12**:e01774-21
<https://doi.org/doi:10.1128/mBio.01774-21>
 132. Bergelson J, Mittelstrass J, Horton MW. Characterizing both bacteria and fungi improves understanding of the arabidopsis root microbiome. *Scientific Reports*. 2019;**9**:24 <https://doi.org/10.1038/s41598-018-37208-z>
 133. Schäfer M, Pacheco AR, Künzler R, Bortfeld-Miller M, Field CM, Vayena E *et al.* Metabolic interaction models recapitulate leaf microbiota ecology. *Science*. 2023;**381**:eadf5121 <https://doi.org/doi:10.1126/science.adf5121>
 134. Lam TJ, Stambouliau M, Han W, Ye Y. Model-based and phylogenetically adjusted quantification of metabolic interaction between microbial species. *PLOS Computational Biology*. 2020;**16**:e1007951
<https://doi.org/10.1371/journal.pcbi.1007951>
 135. Russel J, Røder HL, Madsen JS, Burmølle M, Sørensen SJ. Antagonism correlates with metabolic similarity in diverse bacteria. *Proceedings of the National Academy of Sciences*. 2017;**114**:10684-88 <https://doi.org/doi:10.1073/pnas.1706016114>
 136. Rabbee MF, Ali MS, Choi J, Hwang BS, Jeong SC, Baek K-h. *Bacillus velezensis*: A valuable member of bioactive molecules within plant microbiomes. *Molecules*. 2019;**24**:1046
 137. Fira D, Dimkić I, Berić T, Lozo J, Stanković S. Biological control of plant pathogens by bacillus species. *Journal of Biotechnology*. 2018;**285**:44-55
<https://doi.org/https://doi.org/10.1016/j.jbiotec.2018.07.044>
 138. Jeong M-H, Lee Y-S, Cho J-Y, Ahn Y-S, Moon J-H, Hyun H-N *et al.* Isolation and characterization of metabolites from bacillus licheniformis mh48 with antifungal activity against plant pathogens. *Microbial Pathogenesis*. 2017;**110**:645-53
<https://doi.org/https://doi.org/10.1016/j.micpath.2017.07.027>
 139. Shafi J, Tian H, Ji M. *Bacillus* species as versatile weapons for plant pathogens: A review. *Biotechnology & Biotechnological Equipment*. 2017;**31**:446-59
<https://doi.org/10.1080/13102818.2017.1286950>
 140. Olasupo IO, Wang J, Wei X, Sun M, Li Y, Yu X *et al.* Chili residue and bacillus laterosporus synergy impacts soil bacterial microbiome and agronomic performance of leaf mustard (brassica juncea l.) in a solar greenhouse. *Plant and Soil*. 2022;**479**:185-205 <https://doi.org/10.1007/s11104-022-05504-3>
 141. Blake C, Christensen MN, Kovács ÁT. Molecular aspects of plant growth promotion and protection by bacillus subtilis. *Molecular Plant-Microbe Interactions*®. 2020;**34**:15-25 <https://doi.org/10.1094/MPMI-08-20-0225-CR>
 142. Hashem A, Tabassum B, Fathi Abd Allah E. *Bacillus subtilis*: A plant-growth promoting rhizobacterium that also impacts biotic stress. *Saudi Journal of Biological Sciences*. 2019;**26**:1291-97 <https://doi.org/https://doi.org/10.1016/j.sjbs.2019.05.004>

143. Michelsen CF, Stougaard P. Hydrogen cyanide synthesis and antifungal activity of the biocontrol strain *Pseudomonas fluorescens* in5 from Greenland is highly dependent on growth medium. *Canadian Journal of Microbiology*. 2012;**58**:381-90 <https://doi.org/10.1139/w2012-004> %M 22417387
144. Nandi M, Selin C, Brawerman G, Fernando WGD, de Kievit T. Hydrogen cyanide, which contributes to *Pseudomonas chlororaphis* strain pa23 biocontrol, is upregulated in the presence of glycine. *Biological Control*. 2017;**108**:47-54 <https://doi.org/https://doi.org/10.1016/j.biocontrol.2017.02.008>
145. Otieno N, Lally RD, Kiwanuka S, Lloyd A, Ryan D, Germaine KJ *et al.* Plant growth promotion induced by phosphate solubilizing endophytic *Pseudomonas* isolates. *Frontiers in Microbiology*. 2015;**6** <https://doi.org/10.3389/fmicb.2015.00745>
146. Singh P, Singh RK, Zhou Y, Wang J, Jiang Y, Shen N *et al.* Unlocking the strength of plant growth promoting *Pseudomonas* in improving crop productivity in normal and challenging environments: A review. *Journal of Plant Interactions*. 2022;**17**:220-38 <https://doi.org/10.1080/17429145.2022.2029963>
147. Kumar A, Singh J Biofilms forming microbes: Diversity and potential application in plant–microbe interaction and plant growth. In: Yadav AN, Singh J, Rastegari AA *et al.* (eds.). *Plant microbiomes for sustainable agriculture*, Cham: Springer International Publishing. 173-97. Retrieved from https://doi.org/10.1007/978-3-030-38453-1_6
148. Heredia-Ponce Z, de Vicente A, Cazorla FM, Gutiérrez-Barranquero JA. Beyond the wall: Exopolysaccharides in the biofilm lifestyle of pathogenic and beneficial plant-associated *Pseudomonas*. *Microorganisms*. 2021;**9**:445
149. Shalev O, Karasov TL, Lundberg DS, Ashkenazy H, Pramoj Na Ayutthaya P, Weigel D. Commensal *Pseudomonas* strains facilitate protective response against pathogens in the host plant. *Nature Ecology & Evolution*. 2022;**6**:383-96 <https://doi.org/10.1038/s41559-022-01673-7>
150. Jameson PE. Zeatin: The 60th anniversary of its identification. *Plant Physiology*. 2023;**192**:34-55 <https://doi.org/10.1093/plphys/kiad094>
151. Kudoyarova GR, Melentiev AI, Martynenko EV, Timergalina LN, Arkhipova TN, Shendel GV *et al.* Cytokinin producing bacteria stimulate amino acid deposition by wheat roots. *Plant Physiology and Biochemistry*. 2014;**83**:285-91 <https://doi.org/https://doi.org/10.1016/j.plaphy.2014.08.015>
152. Sokolova MG, Akimova GP, Vaishlya OB. Effect of phytohormones synthesized by rhizosphere bacteria on plants. *Applied Biochemistry and Microbiology*. 2011;**47**:274-78 <https://doi.org/10.1134/S0003683811030148>
153. Andersen D, Renshaw JC, Wiebe MG. Rhodotorulic acid production by *Rhodotorula mucilaginosa*. *Mycological Research*. 2003;**107**:949-56 <https://doi.org/https://doi.org/10.1017/S0953756203008220>
154. Atkin CL, Neilands JB, Phaff HJ. Rhodotorulic acid from species of *Leucosporidium*, *Rhodospiridium*, *Rhodotorula*, *Sporidiobolus*, and *Sporobolomyces*, and a new alanine-containing ferrichrome from *Cryptococcus melibiosum*. *Journal of Bacteriology*. 1970;**103**:722-33 <https://doi.org/10.1128/jb.103.3.722-733.1970>
155. Georgescu A-M, Corbu VM, Csutak O. Molecular basis of yeasts antimicrobial activity—developing innovative strategies for biomedicine and biocontrol. *Current Issues in Molecular Biology*. 2024;**46**:4721-50

156. Jeong H, Choi S-K, Ryu C-M, Park S-H. Chronicle of a soil bacterium: *Paenibacillus polymyxa* e681 as a tiny guardian of plant and human health. *Frontiers in Microbiology*. 2019;**10** <https://doi.org/10.3389/fmicb.2019.00467>
157. Olishavska S, Nickzad A, Déziel E. *Bacillus* and *paenibacillus* secreted polyketides and peptides involved in controlling human and plant pathogens. *Applied Microbiology and Biotechnology*. 2019;**103**:1189-215 <https://doi.org/10.1007/s00253-018-9541-0>
158. Daud NS, Mohd Din ARJ, Rosli MA, Azam ZM, Othman NZ, Sarmidi MR. *Paenibacillus polymyxa* bioactive compounds for agricultural and biotechnological applications. *Biocatalysis and Agricultural Biotechnology*. 2019;**18**:101092 <https://doi.org/https://doi.org/10.1016/j.bcab.2019.101092>
159. Rybakova D, Cernava T, Köberl M, Liebming S, Etemadi M, Berg G. Endophytes-assisted biocontrol: Novel insights in ecology and the mode of action of *paenibacillus*. *Plant and Soil*. 2016;**405**:125-40 <https://doi.org/10.1007/s11104-015-2526-1>
160. Monier J-M, Lindow S. Frequency, size, and localization of bacterial aggregates on bean leaf surfaces. *Applied and environmental microbiology*. 2004;**70**:346-55
161. Tecon R, Leveau JHJ. The mechanics of bacterial cluster formation on plant leaf surfaces as revealed by bioreporter technology. *Environmental Microbiology*. 2012;**14**:1325-32 <https://doi.org/https://doi.org/10.1111/j.1462-2920.2012.02715.x>
162. Danhorn T, Fuqua C. Biofilm formation by plant-associated bacteria. *Annu Rev Microbiol*. 2007;**61**:401-22
163. Ryffel F, Helfrich EJN, Kiefer P, Peyriga L, Portais J-C, Piel J *et al*. Metabolic footprint of epiphytic bacteria on *arabidopsis thaliana* leaves. *The ISME Journal*. 2015;**10**:632-43 <https://doi.org/10.1038/ismej.2015.141>
164. Kusari S, Lamshöft M, Kusari P, Gottfried S, Zühlke S, Louven K *et al*. Endophytes are hidden producers of maytansine in *putterlickia* roots. *Journal of Natural Products*. 2014;**77**:2577-84 <https://doi.org/10.1021/np500219a>
165. Tyc O, van den Berg M, Gerards S, van Veen JA, Raaijmakers JM, de Boer W *et al*. Impact of interspecific interactions on antimicrobial activity among soil bacteria. *Frontiers in Microbiology*. 2014;**5** <https://doi.org/10.3389/fmicb.2014.00567>
166. DeFilippi S, Groulx E, Megalla M, Mohamed R, Avis TJ. Fungal competitors affect production of antimicrobial lipopeptides in *bacillus subtilis* strain b9–5. *Journal of Chemical Ecology*. 2018;**44**:374-83 <https://doi.org/10.1007/s10886-018-0938-0>
167. Babu AG, Shea PJ, Sudhakar D, Jung I-B, Oh B-T. Potential use of *pseudomonas koreensis* agb-1 in association with *miscanthus sinensis* to remediate heavy metal(loid)-contaminated mining site soil. *Journal of Environmental Management*. 2015;**151**:160-66 <https://doi.org/https://doi.org/10.1016/j.jenvman.2014.12.045>
168. Goswami M, Deka S. Biosurfactant production by a rhizosphere bacteria *bacillus altitudinis* ms16 and its promising emulsification and antifungal activity. *Colloids and Surfaces B: Biointerfaces*. 2019;**178**:285-96 <https://doi.org/https://doi.org/10.1016/j.colsurfb.2019.03.003>
169. Ikram-UI-Haq HU, Mahmood Z, Javed MM. Solid state fermentation for the production of α -amylase by *paenibacillus amylolyticus*. *Pak J Bot*. 2012;**44**:341-46
170. Li P-D, Zhu Z-R, Zhang Y, Xu J, Wang H, Wang Z *et al*. The phyllosphere microbiome shifts toward combating melanose pathogen. *Microbiome*. 2022;**10**:56 <https://doi.org/10.1186/s40168-022-01234-x>

171. Nowak MA. Five rules for the evolution of cooperation. *Science*. 2006;**314**:1560-63 <https://doi.org/doi:10.1126/science.1133755>
172. Ji N, Liang D, Clark LV, Sacks EJ, Kent AD. Host genetic variation drives the differentiation in the ecological role of the native miscanthus root-associated microbiome. *Microbiome*. 2023;**11**:216 <https://doi.org/10.1186/s40168-023-01646-3>
173. Yousefi B, Melograna F, Galazzo G, van Best N, Mommers M, Penders J *et al*. Capturing the dynamics of microbial interactions through individual-specific networks. *Frontiers in Microbiology*. 2023;**14** <https://doi.org/10.3389/fmicb.2023.1170391>
174. Kot AM, Kieliszek M, Piwowarek K, Błażej S, Mussagy CU. Sporobolomyces and sporidiobolus – non-conventional yeasts for use in industries. *Fungal Biology Reviews*. 2021;**37**:41-58 <https://doi.org/https://doi.org/10.1016/j.fbr.2021.06.001>
175. Ren D, Madsen JS, Sørensen SJ, Burmølle M. High prevalence of biofilm synergy among bacterial soil isolates in cocultures indicates bacterial interspecific cooperation. *The ISME Journal*. 2014;**9**:81-89 <https://doi.org/10.1038/ismej.2014.96>
176. Ansari FA, Ahmad I. Fluorescent pseudomonas -fap2 and bacillus licheniformis interact positively in biofilm mode enhancing plant growth and photosynthetic attributes. *Scientific Reports*. 2019;**9**:4547 <https://doi.org/10.1038/s41598-019-40864-4>
177. Murillo-Roos M, Abdullah HSM, Debbar M, Ueberschaar N, Agler MT. Cross-feeding niches among commensal leaf bacteria are shaped by the interaction of strain-level diversity and resource availability. *The ISME Journal*. 2022;**16**:2280-89 <https://doi.org/10.1038/s41396-022-01271-2>
178. Mataigne V, Vannier N, Vandenkoornhuysen P, Hacquard S. Microbial systems ecology to understand cross-feeding in microbiomes. *Frontiers in Microbiology*. 2021;**12** <https://doi.org/10.3389/fmicb.2021.780469>
179. Kümmerli R, Santorelli LA, Granato ET, Dumas Z, Dobay A, Griffin AS *et al*. Co-evolutionary dynamics between public good producers and cheats in the bacterium pseudomonas aeruginosa. *Journal of Evolutionary Biology*. 2015;**28**:2264-74 <https://doi.org/10.1111/jeb.12751>
180. Seth EC, Taga ME. Nutrient cross-feeding in the microbial world. *Frontiers in Microbiology*. 2014;**5** <https://doi.org/10.3389/fmicb.2014.00350>
181. Tabbene O, Slimene IB, Djebali K, Mangoni M-L, Urdaci M-C, Limam F. Optimization of medium composition for the production of antimicrobial activity by bacillus subtilis b38. *Biotechnology Progress*. 2009;**25**:1267-74 <https://doi.org/https://doi.org/10.1002/btpr.202>
182. Sánchez S, Chávez A, Forero A, García-Huante Y, Romero A, Sánchez M *et al*. Carbon source regulation of antibiotic production. *The Journal of Antibiotics*. 2010;**63**:442-59 <https://doi.org/10.1038/ja.2010.78>
183. Duerkop Breck A, Varga J, Chandler Josephine R, Peterson Snow B, Herman Jake P, Churchill Mair EA *et al*. Quorum-sensing control of antibiotic synthesis in burkholderia thailandensis. *Journal of Bacteriology*. 2009;**191**:3909-18 <https://doi.org/10.1128/jb.00200-09>
184. Miller MB, Bassler BL. Quorum sensing in bacteria. *Annual Review of Microbiology*. 2001;**55**:165-99 <https://doi.org/https://doi.org/10.1146/annurev.micro.55.1.165>
185. Christians U, Klawitter J, Hornberger A, Klawitter J. How unbiased is non-targeted metabolomics and is targeted pathway screening the solution? *Current pharmaceutical biotechnology*. 2011;**12**:1053-66

186. Ribbenstedt A, Ziarrusta H, Benskin JP. Development, characterization and comparisons of targeted and non-targeted metabolomics methods. *PLOS ONE*. 2018;**13**:e0207082 <https://doi.org/10.1371/journal.pone.0207082>
187. Saw NMMT, Suwanchaikasem P, Zuniga-Montanez R, Qiu G, Marzinelli EM, Wuertz S *et al*. Influence of extraction solvent on nontargeted metabolomics analysis of enrichment reactor cultures performing enhanced biological phosphorus removal (ebpr). *Metabolites*. 2021;**11**:269
188. Mushtaq MY, Choi YH, Verpoorte R, Wilson EG. Extraction for metabolomics: Access to the metabolome. *Phytochemical Analysis*. 2014;**25**:291-306 <https://doi.org/https://doi.org/10.1002/pca.2505>